# Specific Protein Interactions with the 5'- and 3'-Untranslated Regions of Coxsackievirus B3 RNA

By

PAUL Kim-ming CHEUNG

B.Sc., The University of British Columbia, 1997

A THESIS SUBMITTED IN PARTIAL FULFILMENT OF THE REQUIREMENTS FOR THE DEGREE OF

DOCTOR OF PHILOSOPHY

In

THE FACULTY OF GRADUATE STUDIES

Department of Pathology and Laboratory Medicine; Faculty of Medicine

We accept this thesis as conforming to the required standard

THE UNIVERSITY OF BRITISH COLUMBIA

JANUARY 2004

## ABSTRACT

In recent years, studies of the molecular pathogenesis of coxsackievirus B3 (CVB3) have revealed that the viral 5' and 3' untranslated regions (UTRs) contain determinants of viral tissue tropism, translation efficiency, and cardiovirulence. However, the mechanism that links the UTRs to these phenotypic observations remains unknown. Thus, the study of protein-UTR interactions is important to understand the underlying mechanism of functions mediated by the CVB3 UTRs. My dissertation addresses this subject by the identification and characterization of cellular proteins that bind to the CVB3 UTRs. To achieve these goals, I sub-cloned the CVB3 5' and 3'-UTR by a PCR-based strategy. The 5'-UTR sequences of nt 1-209, 210-529 and 530-630 were cloned in consideration of their respective structural and functional significance. At the same time, the 3'-UTR wild type sequence of nt 7299-7399 [+ poly(A) tail] and five mutated 3'-UTR clones were generated. Mutations in these 3'-UTR clones were previously reported to cause tertiary (but not secondary) structural changes in the 3'-UTR, leading to specific inhibition of viral replication. By using radiolabeled RNA transcripts of these UTR sequences in gel mobility shift and competitive UV cross-linking assays, fifteen specific CVB3 5'-UTR-binding proteins in the HeLa cell were identified. The molecular weight of six important 5'-UTR-binding proteins resembled those of the eukaryotic translation initiation factors (eIF4A, 4B, 4G), the death associated protein-5, La autoantigen and the polypyrimidine tract binding proteins. Using the same method, protein interactions with the 3'-UTR and its various mutants were also investigated. Two small proteins (22 and 24 kDa) that bound specifically to the mutated 3'-UTRs were observed. As these corresponding mutations were previously shown to inhibit viral replication, a functional role of these two protein-3'-UTR interactions was inferred. Also, the poly(A) tail of the 3'-UTR was found to be important in mediating HeLa cell protein

interactions. As the poly(A) tail can interact with the 3'-UTR sequence to maintain a stable secondary RNA structure, my data suggests an important role of the stem-loop RNA structures in mediating protein-3'-UTR interactions. In the A/J mouse model, by using *in situ* hybridization and UV cross-linking assays, the correlation between CVB3 tissue tropism and protein-5'-UTR interaction was investigated. Among the various UTR-binding proteins in different tissues, a 28 kDa kidney protein was found to bind to the antisense 5'-UTR sequence of nt 210-529 and correlated well with the low viral infectivity in the kidneys, thereby suggesting a possible inhibitory function of this 28 kDa protein.

Moreover, a specific 5'- and 3'-UTR-binding protein that shares the same molecular weight (52 kDa) with the La autoantigen, was chosen for further investigation. Using recombinant GST-La fusion protein from purified from *E. coli*, interactions between the La protein and the 5' or 3'-UTR radiolabeled probes was verified. Specificity of interaction was determined from competitive UV cross-linking experiments. It was observed that the La protein had the highest affinity towards nt 210-529, followed by the nt 530-630 (internal ribosomal entry site, IRES) and then nt 1-209. The lack of primary sequence consensus among these 5'-UTRs suggests that the La protein recognizes secondary RNA structures during interaction. This is also supported by the observation that the La protein interacted with both the wild type and mutated 3'-UTR RNAs, both of which share identical secondary structures. Analysis of the data suggests that each La protein may bind either one of the 5' and 3'-UTR at a time.

## TABLE OF CONTENTS

## LIST OF TABLES

## LIST OF FIGURES

## ABBREVIATIONS

| | |
|---|---|
| AIF | Apoptosis Inducing Factor |
| BIP | Immunoglobulin Heavy-Chain Binding Protein |
| CAR | Coxsackievirus Adenovirus Receptor |
| CPE | Cytopathic Effect |
| CREB | Cyclic-Amp-Response-Element-Binding-Protein |
| CVA9 | Coxsackievirus A9 |
| CVB3 | Coxsackievirus B3 |
| CVB4 | Coxsackievirus B4 |
| DAF | Death Accelerating Factor |
| DAP 5 | Death Associated Protein 5 |
| DCM | Dilated Cardiomyopathy |
| eIF | Eukaryotic Translation Initiation Factor |
| eIF4G | Eukaryotic Translation Initiation Factor 4G |
| EMCV | Encephalomyocarditis Virus |
| ER | Endoplasmic Reticulum |
| FGF-2 | Fibroblast Growth Factor 2 |
| FMDV | Foot And Mouth Disease Virus |
| GAD | Glutamate Decarboxylase |
| GPI | Glycophosphatidylinositol |
| GSK-3 | Glycogen Synthase Kinase-3 |
| HAV | Hepatitis A Virus |
| HCV | Hepatitis C Virus |
| HIV | Human Immunodeficiency Virus |
| HRV 14 | Human Rhinovirus 14 |
| HTLV-1 | Human T-Cell Lymphotropicvirus Type 1 |
| IGTP | Interferon-Gamma-Inducible Guanosine Triphosphatase |
| IL2 | Interleukin 2 |
| INF-$\gamma$ | Interferon $\gamma$ |
| IPTG | Isopropyl-$\beta$-D-thiogalactopyranoside |

| | |
|---|---|
| IRES | Internal Ribosomal Entry Site |
| ISH | In Situ Hybridization |
| Kd | Dissociation constant |
| MAPK | Mitogen Activated Protein Kinase |
| MHC | Major Histocompatibility Complex |
| MKK 6 | Map Kinase Kinase 6 |
| MOI | Multiplicity Of Infection |
| mRNA | Messenger RNA |
| NTP | Nucleoside Triphosphate |
| OCT-1 | Octomer Binding Transcription Factor -1 |
| ODC | Ornithine Decarboxylase |
| ORF | Open Reading Frame |
| P.I. | Post Infection |
| PABP | Poly-A Tail Binding Protein |
| PARP | Poly-Adp Ribose Polymerase |
| PCBP | Poly-Rc Binding Protein |
| PKB | Protein Kinase B |
| PTB | Poly-Pyrimidine Tract Binding Protein |
| PV | Poliovirus |
| RdRP | RNA dependent RNA polymerase |
| RNP | Ribonucleo-Protein Complex |
| RRM | RNA Recognition Domain |
| rRNA | Ribosomal RNA |
| RT-PCR | Real Time Polymerase Chain Reaction |
| SCID | Severe Combined Immunodeficiency Disease |
| SCR | Short Consensus Repeat |
| SD | Shine-Dalgarno |
| SN RNA | Small Nuclear RNA |
| TNF-α | Tumor Necrosis Factor α |
| tRNA | Transfer RNA |
| TUNEL | Terminal Deoxynucleotidyl Transferase Mediated Nick End Labeling |

| | |
|---|---|
| UTR | Untranslated Region |
| VEGF | Vascular Endothelial Growth Factor |
| WHO | World Health Organization |

## LIST OF PUBLICATIONS, ABSTRACTS AND PRESENTATIONS

1. **Cheung, P.**, Zhang, M., Yuan, J., Chau, D., Yanagawa, B., McManus, B and Yang, DC. Specific interactions of HeLa cell proteins with coxsackievirus B3 RNA: La autoantigen binds differentially to multiple sites within the 5' untranslated region. (2002). ***Virus Research 90, 23-26***

2. **Cheung, P.**, Yanagawa, B., Zhang, H., Wang, A., Luo, H., Esfandiarei, M., Saurez, A., Wilson, J., Carthy, C., McManus, B. and D. Yang. Molecular Mechanisms of Cardiovirulence and Host Cell Responses in Coxsackievirus B3 induced Myocarditis. (2002). ***Recent Research Developments in Virology 3, 427-454.***

3. **Cheung, P.**, Zhang, M., Yuan, J., Chau, D., Yanagawa, B., McManus, B. and Yang DC. Specific binding of La protein within the Coxsackievirus B3 3' UTR and the significance of the poly-(A) tail in mediating HeLa cell protein interactions. ***Under revision.***

4. **Cheung, P.**, Yuan, J., A. Suarez, McManus, B. and Yang, DC. Correlation between pathology of CVB3 infection in A/J mouse and interactions of cellular proteins with the viral 5' untranslated sequence. ***Under revision.***

5. Yang, DC., **Cheung, P.**, Sun, Y., Yuan, J., Zhang, H., Carthy, C.M., Anderson, D.R. Bohunek, L., Wilson, J.E., McManus, B.M. A Shine-Dalgarno-like sequence mediates in vitro ribosomal internal entry and subsequent scanning for translation initiation of coxsackievirus B3 RNA. (2003). ***Virology 305, 31-43***

6. Yang, D., **Cheung, P.**, Yanagawa, B., Cheung, Caroline, Chow, D., and McManus, B. Picornaviral proteases in viral replication and pathogenesis. (2003). **Current Topics in Virology 3, 17-31.**

7. Zhang, H. M., **Cheung, P.**, Yanagawa, B., McManus, B. M. and Yang, D.. BNips: A group of pro-apoptotic proteins in the Bcl-2 family. (2003). **Apoptosis. 8:229-236**.

8. Zhang, H. M., Yuan, J., **Cheung, P.**, Luo, H., Yanagawa, B., Chau, D., Tozy, N. S., Wong, B., Zhang, J., Wilson, J.E., McManus, B.M. and Yang, D.. Over-expression of interferon-gamma - inducible GTPase inhibits coxsackievirus B3-induced apoptosis through the activation of the PI3-K/Akt pathway and inhibition of viral replication. (2003). **J. Biol. Chem. 278:33011-19.**

9. Yanagawa, B., Spiller,O.B., Choy,J., Luo,H., **Cheung,P.**, Zhang,H.M.; Goodfellow,I.G.; Evans,D.J.; Suarez,A.; Yang, D. Coxsackievirus B3-associated myocardial pathology and viral load reduced by recombinant soluble human decay-accelerating factor in mice. (2003). **Lab Invest. 83: 75-85.**

10. Zhang, H. M., Yanagawa, B., **Cheung, P.**, Luo, H., Yuan, J., Chau, D., Wang, A., Bohunek, L., Wilson, J. E., McManus, B. M. and Yang, D. Nip21 gene expression reduces coxsackievirus B3 replication by promoting apoptotic cell death via a mitochondria-dependent pathway. (2002). **Circ. Res. 90, 1251-1258**.

11. Yanagawa, B., Esfandiarei, M., Carthy, C., **Cheung, P.**, Luo, H., Granville, D., Yang, D., Choy, J., Lui, A., Dabiri, D., Wilson, J.E., Wang, A., Zhang, M, Sinn, S., McManus, B., Wei, K., and

Laher, I. Life and death signaling pathways in CVB3 induced myocarditis. (2002). In **"Myocarditis: Bench to the Bedside"** Ed. LT Cooper (Rochester, MN). Humanan Press. August, 2002. **ISBN: 1-58829-112-X.**

12. Wang, A., **Cheung, P.K.,** Zhang, H., Carthy, C. M., Bohunek, L., Wilson, J. E., McManus, B. M. and Yang, D. Specific inhibition of coxsackievirus B3 translation and replication by phosphorothioate antisense oligodeoxynucleotides. (2001). **Antimicrob. Agents Chemother. 45:1043-1052.**

13. Liu, Z., Carthy, C. M., **Cheung, P.,** Bohunek, L., Wilson, J. E., McManus, B. M. and Yang, D. Structural and functional analysis of the 5' untranslated region of coxsackievirus B3 RNA: In vivo translational and infectivity studies of full-length mutants. (1999). **Virology 265:206-217.**

14. Taylor, L. A., Carthy, C. M., Yang, D., Saad, K., Wong, D., Schreiner, G., Stanton, L. W. and McManus, B. M. Host gene regulation during coxsackievirus B3 infection in mice: assessment by microarrays. (2000). ***Circ. Res.* 87: 328-334.**

## Highlights of Abstracts and Presentations

1. **Cheung, P.,** Zhang, M., Yuan, J., Chau, D., Yang, D. La autoantigen interacts with multiple sites in the 5'-UTR of Coxsackievirus B3. Annual Conference 2002, American Society of Virology, University of Kentucky, Lexington, US.

2. **Cheung, P.,** Yanagawa B, Chau, D., Zhang M, Lai, J., Yuan, J., McManus BM and Yang D. 2002. Differential Interactions of La autoantigen with the 5' untranslated region of coxsackievirus B3 RNA. Annual Pathology Day, 2002, Department of Pathology and Laboratory Medicine, UBC, Vancouver, Canada

3. **Cheung, P.,** Yanagawa B, Wang, A., Zhang, M., Lai, J., Carthy C, Bohunek L, Luo H, Wilson JE, McManus BM, Yang D. (2001) Host-proteins-coxsackievirus B3 RNA interactions. Frontiers in Cardiovascular Research Conference, 2001, Seattle, Washington, US.

4. **Cheung, P.,** Yanagawa, B., Wang, A., Zhang, M., Lai, J., Carthy, C.M., Bohunek, L., Luo, H., Wilson, J.E., McManus, B.M., Yang, D. Host proteins-coxsackievirus B3 RNA interactions: implications for systemic pathogenesis. Annual Pathology Day 2001, Department of Pathology and Laboratory Medicine, Faculty of Medicine, UBC Vancouver, Canada.

5. **Cheung, P.,** Yanagawa, B., Wang, A., Zhang, M., Lai, J., Carthy, C.M., Bohunek, L., Luo, H., Wilson, J.E., McManus, B.M., Yang, D. Specific interactions of HeLa cell proteins with the internal ribosome entry site and the 3' untranslated region of coxsackievirus B3 RNA. Annual Pathology Day 2001, Department of Pathology and Laboratory Medicine, UBC, Vancouver, Canada.

6. **Cheung, P.,** Carthy, C., Yanagawa, B., Wang, A., Zhang, M., Bohunek, L., Wilson, J.E., McManus, B.M., and Yang, D. Specific interactions of HeLa cell proteins with the 5' and 3' untranslated regions of coxsackievirus B3 RNA. Annual Pathology Day 2000, Department of Pathology and Laboratory Medicine, UBC, Vancouver, Canada.

7. **Cheung, P.,** Yanagawa, B., Wang, A., Zhang, M., Lai, J., Carthy, C.M., Bohunek, L., Luo, H., Wilson, J.E., McManus, B.M., Yang, D. Host protein interactions with the 5' and 3' untranslated regions of coxsackievirus B3. Annual Pathology Day 1999, Department of Pathology and Laboratory Medicine, UBC, Vancouver, Canada.

8. **Cheung, P.,** Carthy, C.M., Watson, K., Bohunek, L., Wang, A., Wilson, J.E., McManus, B.M. Host protein interactions with the 5' and 3' untranslated regions of coxsackievirus B3. Annual Conference 1999, American Society of Virology, Boston, USA. Oral Presentation.

9. **Cheung, P.,** Carthy, C.M., Watson, K., Bohunek, L., Wang, A., Wilson, J.E., McManus, B.M. Differential interaction of organ specific proteins with the 5'' untranslated region of coxsackievirus B3 RNA. Annual Meeting 1998, American Society of Microbiology, Vancouver, Canada.

10. McManus, B., Luo, H., Yanagawa, B., Esfandiarei, M., Carthy, C., Yang, D., Wilson, J.E., **Cheung, P.,** Wang A. Structural and biochemical basis of cardiac myocyte survival and death: A dynamic tension. Published for the 2nd International Congress on Heart Disease, Washington, DC (2001).

11. Yang, D., Zhang, M., **Cheung, P.,** Chau, D., Yuan, J., Yanagawa, B., Luo, H., Zhang, J., Wilson, J.E., McManus, B.M. Coxsackievirus B3 2A and 3C proteases induce cell death through apoptosis. Annual Conference 2002, American Society of Virology, University of Kentucky, Lexington, US.

12. Zhang, M, Yanagawa, B., Luo, H., **Cheung, P.,** Wang, A., Yuan, J., Yen, C., Granville, D., Choy, J., Luo, Z., Bohunek, L., Sinn, S., Wilson, J.E., McManus, B.M., Yang, D. Nip 21 is a pro-apoptotic gene and its product inhibits virus replication by promoting cell death. Keystone symposia, Colorado, USA, 2001.

13. Zhang, M., Yanagawa, B., **Cheung, P.,** Yuan, J., Esfandiarei, M., Chau, D., Luo, H., Zhang, J., Dabiri, D., Wilson, J.E., McManus, B.M. and Yang, D. Functional Roles of IP10 and IGTP Expression in Coxsackievirus B3 (CVB3) Replication. 2002. Providence Health Research Symposium, Vancouver, Canada.

14. Yang, D., Zhang, M., **Cheung, P.,** Chau, D., Yuan, J., Yanagawa, B., Luo, H., Dabiri, D., Toma, M., Wilson, J.E., McManus, B.M. Coxsackievirus B3 2A and 3C proteases induce cell death through apoptosis. Frontiers in Cardiovascular Research Conference, Oct 2001, Seattle, WA.

15. Zhang, M., Yanagawa, B., Yuan, J., Esfandiarei, M., Dabiri, D., Luo, H., **Cheung, P.,** Wang, A., Wilson, J.E, McManus, B.M., and Yang D. Functional role of IP10 and IGTP in cell survival, fetal gene re-expression and coxsackievirus B3-induced disease. Frontiers in Cardiovascular Research Conference, Oct 2001, Seattle, WA.

16. Spiller, O.B., Yanagawa, B., Choy, J., Luo, H., **Cheung, P.,** Zhang, M., Suarez, A., Yang, D., McManus, B.M. Soluble DAF abrogates CVB3-induced myocarditis in mice. Presented at the XIX International Complement Workshop, September 2002, Palermo, Italy

17. Yanagawa, B., Choy, J., Luo, H., **Cheung, P.,** Suarez, A., Esfandiarei, M., Zhang, M., Wang, A., Spiller, O.B., and McManus, B.M. A Potential Soluble Virus Receptor Therapeutic Agent for Early CVB3 Infection. Annual Research Day, Department of Pathology and Laboratory Medicine, UBC., Vancouver, May 2001. Also selected as a finalist (1 of 12) and for Presentation at CIHR/Biocontact, Quebec City, Quebec, October 2001 Presented at Frontiers in Cardiovascular Research Conference, Oct 2001, Seattle, WA.

18. Zhang, M., Yanagawa, B., Luo, H., **Cheung, P.,** Wang, A., Yuan, J., Yen, C., Granville, D., Choy, J., Luo, Z., Bohunek, L., Sinn, S., Wilson, J.E., McManus, B.M. and Yang, D.C. Nip21 Is a Pro-apoptotic Gene and Its Product Inhibits Virus Replication by Promoting Cell Death. Frontiers in Cardiovascular Research Conference, Oct 2001, Seattle, WA

19. Yanagawa, B., Luo, H., Rezai, N., Buckley, J., Triche, T., Zhang, J., Zhang, M., **Cheung, P.,** Yuan. J., Yang, D., and McManus, B.M. Gene profiling in CVB3-infected mouse hearts. La Jolla-Rome-Yamaguchi Research Conference, "Therapeutic Horizons in Heart Failure", San Diego, CA, December 2002.

20. Yanagawa, B., Spiller, O.B., Proctor, D.G., Goodfellow, I.G., Choy, J., Luo, H., **Cheung, P.,** Zhang, M., Suarez, A., Yang, D., and McManus, B.M. Are Soluble CAR and DAF Magic Bullets to Treat Coxsackievirus B3 Infection? CIHR National Poster Competition, Winnipeg, MA, Canada. June 2002. (one of four abstracts chosen to represent UBC in national competition - Award for Excellence: Silver)

21. Yanagawa, B., Luo, H., Carthy, C., Cheung, C., Choy, J., Walinski, H., Zhang, M., **Cheung, P.,** Zhang, J., Chau, D., Yang, D.C., and McManus, B.M. The Role of Apoptosis in Myocarditis. Presented at Providence Health Research Symposium. March, 2002 and the Department of Pathology and Laboratory Medicine, Faculty of Medicine, University of British Columbia, Annual Research Day, Vancouver, Canada.

22. Yanagawa, B., Spiller, O.B., Proctor, D.G., Choy, J., Luo, H., Walinski, H., **Cheung, P.,** Zhang, M., Suarez, A., Zhang, J., Yang, D.C., and McManus, B.M. CAR-Fc To Treat Early CVB3-Induced Myocarditis. Presented at Providence Health Research. Symposium. March, 2002, and the Department of Pathology and Laboratory Medicine, Faculty of Medicine, University of British Columbia, Annual Research Day, Vancouver, Canada

23. Yang, D., **Cheung, P.,** Carthy, C., Bohunek, L., Wilson, J.E., McManus, B.M. HeLa cell proteins interact with the 5' untranslated region of coxsackievirus B3 genomic RNA. International conference on medical virology, Beijing, China. 1999.

**Highlights of Awards**

1. Doctoral Research Award, year 2001-2003, Heart and Stroke Foundation, BC and Yukon.

2. Research Traineeship Award, year 1999-2001, Heart and Stroke Foundation, BC and Yukon.

3. Student Travel Grant, 1999, American Society for Virology,
   - for oral presentation of research findings at the Annual Meeting of American Society for Virology, University of Massachusetts, Boston, USA.

4. Student Travel Award, 1999, Faculty of Medicine, UBC.,
   - for poster presentation at the American Society for Virology, University of Massachusetts, Boston, USA.

5. Student Travel Award, 2001, Faculty of Medicine, UBC.,
   - for poster presentation at the Frontier in Cardiovascular Research Meeting, Seattle, WA., US.

## ACKNOWLEDGEMENTS

Over the past few years, there have been tremendous changes in the landscape of virus research. New technologies and novel publications are rapidly released every month, accelerating advances in the field of viral pathogenesis. It would be impossible to keep up with these new knowledge and technologies without the help of my mentors, collaborative scientists, laboratory technicians, fellow graduate students, computing and other laboratory support staff at the MRL/iCAPTUR$^4$E centre. Thus I would like to express my sincere gratitude to all of these people. In addition, I would like to express my sincere appreciation to the funding agencies, the **Heart and Stroke Foundation of B.C. and Yukon** and the **St. Paul's Hospital Foundation**. Their financial assistance has ensured the continuation of my program.

Of particular importance to my academic development is **Dr. Decheng Yang**. I am most grateful for his mentorship and his willingness to accept me as his first graduate student. His leadership, patience, and attention have been most crucial to my academic development. His encouragement and his support have helped me endured difficult times. I thank him for the countless hours of dedications in my projects, in refining my manuscripts and in the improvement of my research methods and strategies.

As well, I am deeply thankful to my mentor **Dr. Bruce McManus**. As director of the cardiovascular laboratory, Dr. McManus has always encouraged and challenged me to be creative in thinking, be precise in experimental work, be insightful in analysis and be strong in undertaking difficult assignments. Dr. McManus has also provided me with opportunities to explore new techniques and collaborations with other excellent research personnel. Dr. McManus is highly dedicated to the progress of science and the nurture of young apprentices.

I am also most thankful to my supervisory committee members, **Dr. Gregory Bondy** (chairman), **Dr. Shirley Gillam** and **Dr. Caroline Astel**, who have generously provided me with inputs and guidances. Throughout my program, their advice and criticisms have been much appreciated and most essential to the incorporation of new ideas into my work, to the refinement of my research skills and to the generation of the thesis. At the same time, I would like to thank other scientists and collaborators: **Dr. Mary Zhang, Dr. Ed Pryzdial, Dr. Aikun Wang**, and **Dr. Zewei Liu**, who were visiting scientists to the laboratory and provided me with help and guidance in various aspects of my research; **Dr. Delbert Dorscheid** who has provided me with expertise in laser capture microdissection; **Dr. Derek Smith, Dr. Bob Olafson** and other staff at the Genome B.C. center, who have enlightened my eyes to the science of proteomics analysis.

A special person whom I would like to mention in my acknowledgement is **Ms. Patricia Sham** who has been an understanding and altruistic friend during my years of graduate studies. I am indebt to all her support and companionship, during all difficult times and especially my recovery period from the surgical repair of my broken Achilles' tendon.

Last but not the least, I would like to thank my parents for their infinite love and their patience with the time it took to complete my graduate studies. I am deeply grateful for their dedication to my upbringing, their sacrifice and their willingness to put my education ahead of their interests. Since childhood, they have planted in my heart the concept of becoming a better person everyday, and to be courageous in defeating challenges. All these have been the source of my energy to excel in research and to overcome all hardships and challenges.

# CHAPTER I BACKGROUND

The concept of viruses was first described by Jacob Henle of Gottingen in 1840, as "extremely small infectious agents". Eventually, these agents were characterized as "non-filterable" and "toxin-like", eventually leading to the recognition that 'viruses' as pathogenic materials that are significantly smaller in size than bacteria [31]. In 1900, the United States Army presented the first report on a human pathogenic virus: the yellow fever virus; and established the link to patients with acute febrile illness [1]. An important landmark in the study of viruses as causative agent of diseases was the development of unified diagnostic criteria by A. S. Evans in 1982 [104].

At the present day, viruses are understood as parasitic organisms that can only replicate within cellular environments. Viruses utilize enzymes and other metabolic machineries of a host to complete their life cycles. Consequently, interactions of cytoplasmic proteins and viral genetic material are important in the pathogenesis of many viruses. Knowledge of these interactions helps understand the process of disease development. In this dissertation, I shall present findings of my investigations on the interactions between host proteins and the untranslated region (UTR) of the coxsackievirus B3 (CVB3).

## 1.1 Discovery of Coxsackieviruses

Coxsackievirus was discovered in 1948 by Dalldorf and Sickles [91] when a filterable agent was isolated from children suffering paralysis that resembled poliomyelitis in the village of Coxsackie, New York. At the present time, coxsackieviruses are divided into two main groups based on the types of pathology that they cause in murine models. Group A coxsackieviruses

(serotypes 1-22, 24) infect mostly striated muscles causing flaccid paralysis [91], while the group B (serotypes 1-6) viruses cause local myositis as well as meningitis, pancreatitis, myocarditis and hepatitis [118]. Genetically, coxsackieviruses are very similar to the poliovirus (PV) and other *enteroviruses* (**Figure 1a**), all of which display highly similar physical and chemical properties: single stranded positive sense genomic RNA, commonly with a length of 7,500 nucleotides (nts) and that is flanked by UTRs on both the 5' and 3' ends.

*Enterovirus* is a genus in the family of *Picornaviridae*. *Picornaviridae* is a family of small, icosahedral, non-enveloped viruses with a single-stranded RNA genome of positive polarity. To date, more than 230 serotypes of picornaviruses have been recognized and they are classified into six genera [176,307] : *enteroviruses* (e.g. PV and coxsackievirus), *rhinoviruses* (the most important etiological agent of the common cold), *parechoviruses* (e.g. human echovirus 22), *hepatoviruses* (e.g. hepatitis A virus, HAV), *aphthovirus* (e.g. foot-mouth-disease virus, FMDV), *cardiovirus* (e.g. encephalomyocarditis virus, EMCV) (**Table 1**). Together, these viruses cause numerous human syndromes, ranging from fatal paralysis, encephalitis, meningitis, myocarditis, diabetes, hepatitis and the foot-and-mouth disease.

The name "*enterovirus*" originates from the ability of these viruses to infect human and animals via the alimentary tract. *Enteroviruses* share high degree of sequence homology, and it has been postulated that the whole genus of *enteroviruses* resemble more a pool of genetic variants than genetically discrete species [246,339]. The rise of genetic variations in this group of viruses is likely a consequence of the inaccurate RNA transcription performed by the enteroviral RNA polymerase which has an error rate of roughly $10^{-3}$ to $10^{-4}$ substitutions per base [246]. Such an error rate translates into an average of one mutation incorporated per genome-replication: a rate that is almost detrimental to the continued existence of the species [246]. Yet, this nearly fatal

error rate contribute to the evolutionary advantage of the enteroviruses: to diversify into strains that can thrive in a wide range of host environments [246].

## 1.2 Epidemiology of viral myocarditis and CVB3

In numerous studies, CVB3 is characterized as a major viral agent causing acute myocarditis and its late phase dilated cardiomyopathy (DCM) [114,166,167,218,226,340]. Various studies, using real time-polymerase chain reaction (RT-PCR) and *in situ* hybridization (ISH) of enteroviral RNA have demonstrated the presence of an enteroviral genome in as much as 70% of myocarditis patients [251]. In a global surveillance conduced by the World Health Organization (WHO) from 1975 to 1985, the group B coxsackieviruses have been diagnosed as the most common causal agent, with 34.6 cardiovascular diagnoses per 1,000 documented virus infections [126] (**Figure 1b**). This is followed by the influenza B virus (17.4 per 1,000 infections), influenza A virus (11.4 per 1,000 infections), coxsackie A virus (9.1 per 1,000 infections) and cytomegalovirus (8.0 per 1,000 infections). Other viruses such as coxsackievirus B4 (CVB4), adenoviruses [216], hepatitis C virus (HCV) [221], and human immunodeficiency virus (HIV) [28] are also implicated in causing myocarditis or myocardial decompensation, although their contributions may not be as dominant as that by the CVB3 [158,321,333].

**Figure 1a. Phylogenetic relationship of major enteroviruses.**

The dendrogram is constructed by comparing nucleotide alignments of coat protein sequences for the polioviruses, coxsackieviruses, enterovirus 70, and bovine enterovirus (BEV). Percent nucleotide identity is given by the vertical bar connecting virus pairs (Fitch et.al. 1977, Rico-Hesse 1987). High homology is defined as more than 50% sequence identity. Thus, poliovirus and coxsackievirus share high homologies in the virion capsid sequences (60~70%), while the enterovirus 70 (EV70) and the bovine enterovirus (BEV) are more distally related (50-60%). (Adapted from B.N. Fields et. al. (ed)., Fields Virology Lippincott-Raven Publishers, Philadelphia, Pa., 1996)

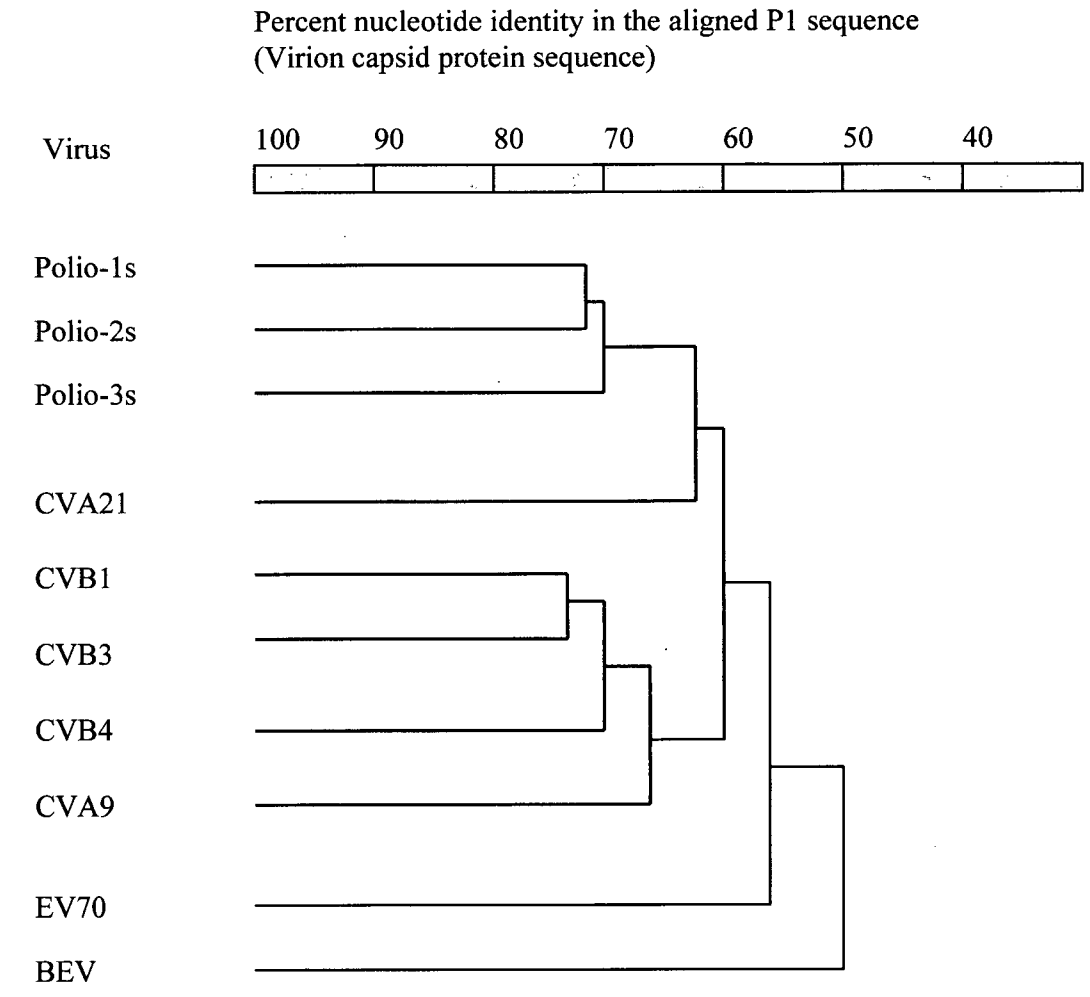

**Table 1. The family of Picornaviruses**

Adapted from B.N. Fields et. al. (ed)., Fields Virology (Lippincott-Raven Publishers, Philadelphia, Pa., 1996 and from The International Committee on Taxonomy of Viruses http://www.ncbi.nlm.nih.gov/ICTVdb/

| Genus | No. Serotypes | Members |
|---|---|---|
| Rhinovirus | 102 | Human rhinoviruses 1A-100, 1B, "Hanks" |
| | 3 | Bovine rhinoviruses 1,2,3 |
| Enterovirus | 3 | Human polioviruses 1,2,3 |
| | 23 | Human coxsackieviruses A1-22, 24<br>*Coxsackieviruses A23 = echovirus 9* |
| | 6 | Human coxsackieviruses B1-6 |
| | 28 | Human echoviruses 1-7, 9, 11-21, 24-27, 29-34<br>*Echovirus 1 = echo 8*<br>*Echovirus 10 = reovirus type 1*<br>*Echovirus 28 = rhinovirus 1A* |
| | 4 | Human enterovirus 68-71 |
| | 1 | Vilyuisk virus |
| | 18 | Simian enterovirus 1-18 |
| | 2 | Bovine enterovirus 1,2 |
| | 8 | Porcine enterovirus 1,2 |
| Aphthovirus | 7 | Foot-and-mouth disease virus 1-7 (serotypes A,C,O, SAT-1,2,3, Asia-1) |
| Cardiovirus | 2 | Encephalomyocarditis virus, theiler's virus murine encephalomyelitis |
| Hepatovirus | 1 | Human hepatitis virus A |
| Parechovirus | 2 | Human parechoviruses 1, 2<br>(*Formerly human echoviruses 22 and 23*) |

**Figure 1b. CVB3 epidemiology (*Rate of cardiovascular diagnosis per 1000 viral infections*).**
This figure shows the result of global surveillance by the World Health Organization of viral infections related to cardiovascular disease. The coxsackie B group of viruses is the major causative agent of myocarditis. (Adapted from Grist and Reid, 1993)

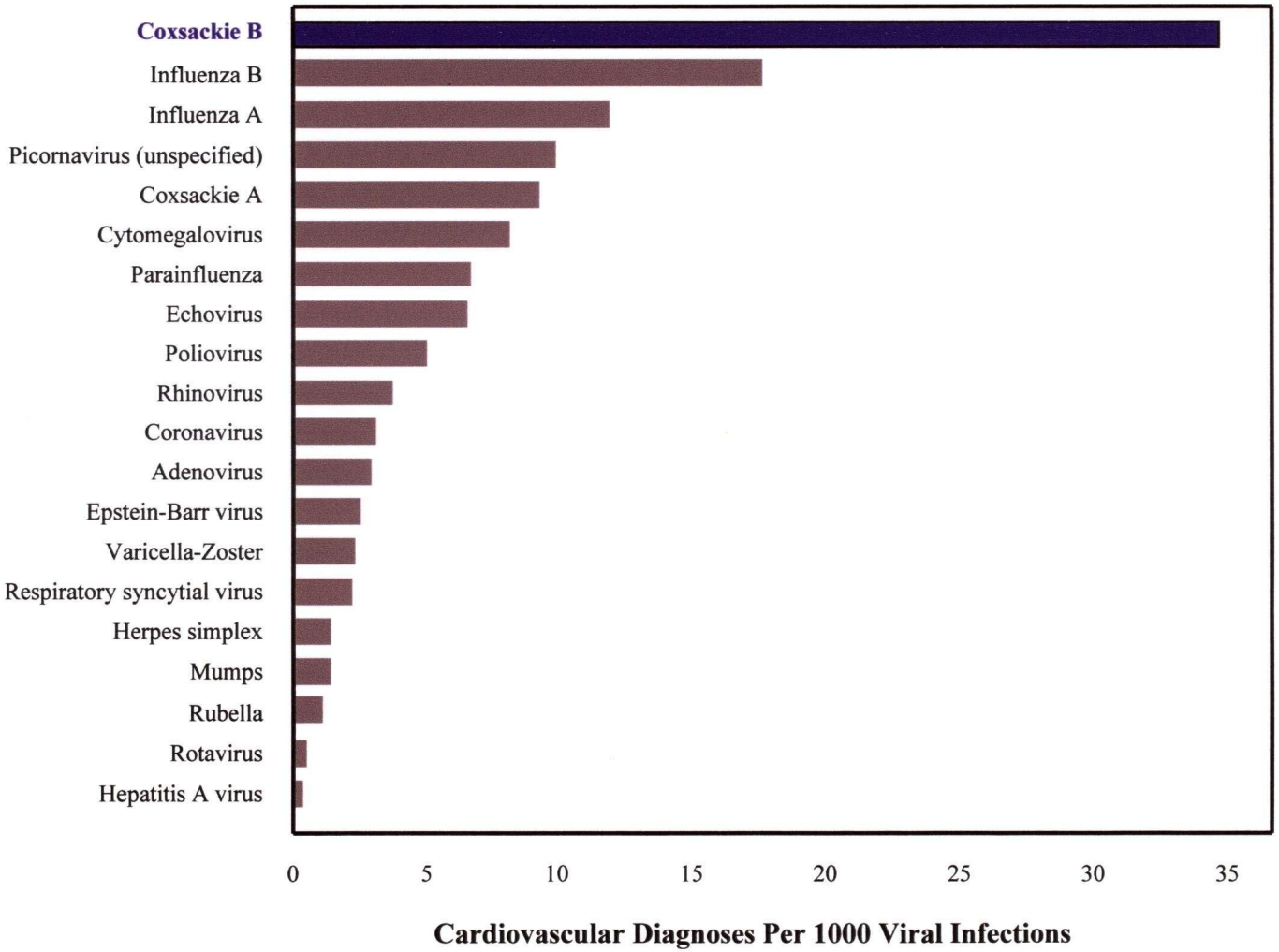

## 1.3 CVB3-induced myocarditis

Direct CVB3 involvement in the injury of cardiomyocytes has been proven by histological analysis of murine hearts and the observation of myocardial death and destruction in virus infected myocytes at early post-infection (p.i.) time points [64,68,184,226]. Pathologic effects are common before the infiltration of immune cells. The host inflammatory response then causes further injuries to the organ [206,219,282]. CVB3-induced myocarditis is a poorly understood disease because it progresses through different stages with distinctly different mechanisms and manifestations. Recent analysis [206] of available data has concluded that the disease can be summarized by a triphasic model: Phase 1) Direct viral injury by viral replication in the heart muscles and subsequently the triggering of immune responses; Phase 2) Activation of immune responses to achieve viral clearance and recovery but possible development of immune and autoimmune injuries; Phase 3) Remodeling of the myocardium by mechanisms that eventually lead to dilated cardiomyopathy (**Figure 2**).

During phase I of the infection, CVB3 enters host via the alimentary tract. The virus is harbored in immune cells of lymphoid organs, temporarily escapes immune clearance and is then transported to target organs such as the heart and pancreas [144]. Viral replication and direct cellular injury occurs rapidly in infected cells, causing cell lysis and viral dissemination. The viral mediated injury may not be as damaging to the myocardium as are the secondary immune responses that serve to eliminate viruses. Specifically, T-cells are activated by the classic cell-mediated pathway: via presentation of viral peptide fragments by the major histocompatibility complex (MHC) at the cell surface. This results in the destruction of the infected cell by cytokine and or perforin-mediated cell cytolysis. In the heart, the rapid cytolytic effect causes significant reduction in the number of effective myocytes in the contractile units. At the same

time, molecular mimicry by viral peptides to host antigens on the myocyte surface will result in persistent T-cell activations, TH-2 responses and CD8 killer cells that are directed against healthy cardiomyocytes. Such is commonly described as CVB3-induced autoimmune injury and further amplifies the structural injury of the myocardium [144,206]. The significance of autoimmune injury in the course of CVB3-induced myocarditis has been demonstrated by the data that survival-rate of CD4/CD8- or p56lck-knockout animals is significantly better than that of the wild type mice during a CVB3 challenge [152,205,255]. On the other hand, while autoimmune injury is a pathogenic consequence of CVB3 infection, the benefit of an intact host immune system in clearing CVB3 infection can not be ignored: CVB3 infection can result in higher mortality when the host is immunocompromised [181]. Events such as T-cell activation [178], nitric oxide synthesis [211,293,354] and immunoglobulin production [177,179,180] are also important in reducing disease severity and viral dissemination. In summary, a delicate balance between immune reactivity and viral clearance is essential to limit the severity of a CVB3 infection.

**Figure 2. Triphasic disease development of CVB3 induced myocarditis.**

CVB3 is the prime agent in causing myocarditis. Acute infection, as well as cell death as a result of host inflammatory responses and autoimmune responses contribute to the injury inflicted upon the myocardium. is followed by which can progress to autoimmune injury (phase II) despite viral clearance. Autoimmune injury is often diagnosed by endomyocardial biopsy and serological markers. Death of myocytes and possible activity of proteases induce the remodeling of the myocardium, eventually leading to the condition of dilated cardiomyopathy (phase III). Repeated exposure to the virus can enhance the likelihood of developing dilated cardiomyopathy. (Model adapted from Liu, P. P. and J. W. Mason. 2001. Circulation 104:1076-1082.)

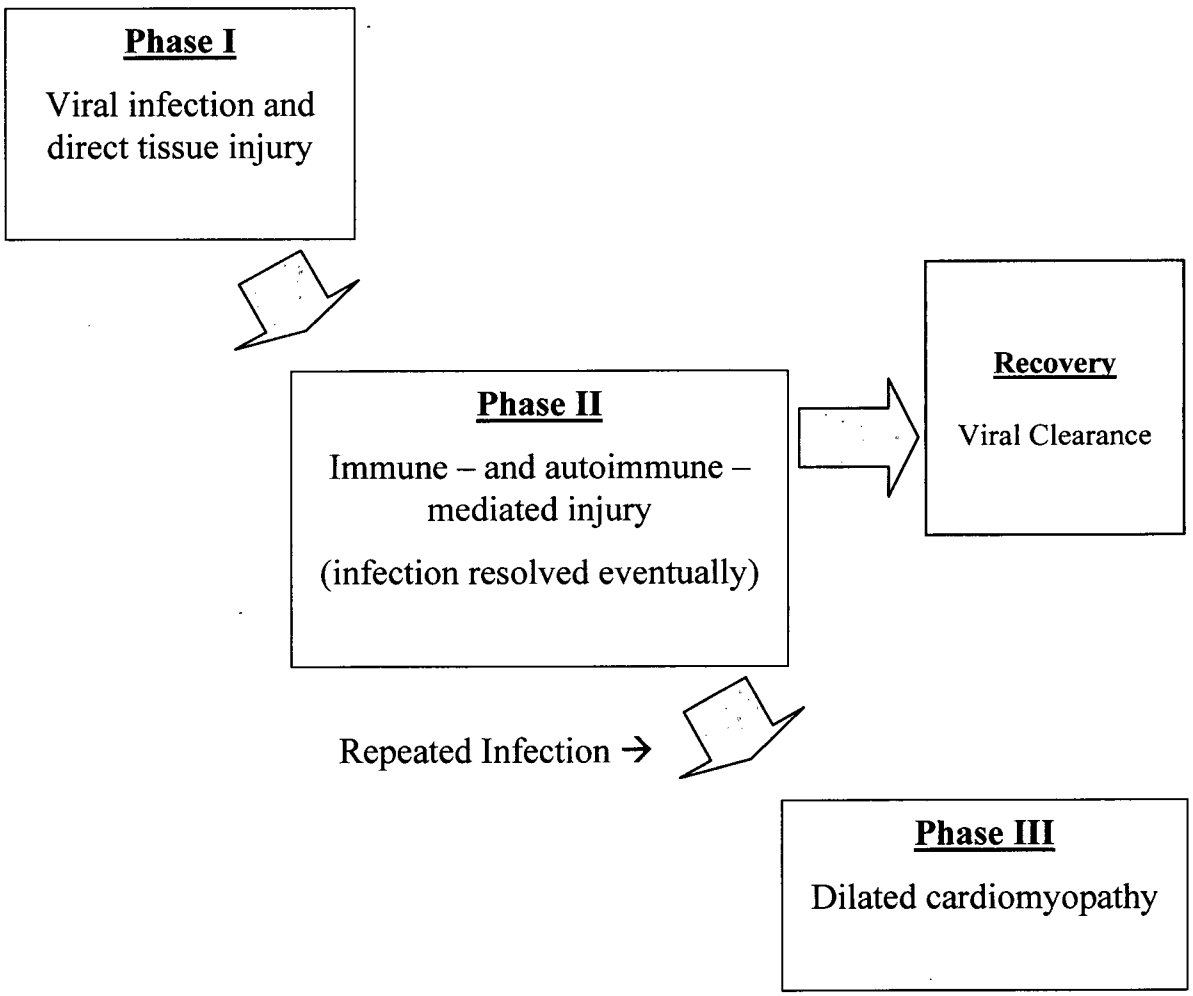

## 1.4 Chronic infection by CVB3

Typically, CVB3 infection of murine models resolves rapidly after immune clearance and the initial phases of infection. However, there are isolated instances when viral RNA can persist in myocytes for as long as 42 days post infection, in immune-competent mice [185]. Using sensitive diagnostic methods such as PCR, CVB3 RNA has been detected at 90 days p.i. without significant levels of inflammation [282,333]. Such are interesting observations as CVB3 is a single-stranded RNA and cytopathic virus that requires continuous RNA-dependent RNA replication in order to persist. Persistence of viral replication without cytopathic effect and apparent pathogenic markers in immune-competent animals suggests that there are yet other undiscovered reservoirs or mechanisms of viral persistence.

### *1.4-1 Myocarditis and dilated cardiomyopathy*

Extended periods of myocarditis will lead to the condition of dilted cardiomyopathy. During myocarditis, the CVB3 protease $2A^{pro}$ can directly cleave the cytoskeletal proteins such as the dystrophin and sarcoglycan complexes in myocytes [23,26], causing myocardial remodeling and ventricular dilation, which are often observed soon after viral infection [24-26,199]. Compounded to other events such as the activation of matrix metalloproteinases (gelatinase, collagenases, and elastases) [254] and repeated viral infections [243,336], persistent heart muscle injury is resulted. Extended periods of tissue damage will lead to the condition of dilated cardiomyopathy [243,254,336]. Cardiomyopathy is a term that describes the general illness of the heart muscles which can lead to clinically significant dysfunction. Heart muscle diseases due to infarcts from coronary atherosclerotic diseases are excluded from such a definition. The dilated, hypertrophic and restrictive forms of cardiomyopathy can be responsible for heart failure [97,109].

Phenotypic pathology of dilated cardiomyopahty includes observations of significant calcification, fibrosis, myocardium remodeling and ventricular dilation [166,226]. Murine models are often chosen to study the molecular mechanism of CVB3 induced myocarditis and dilated cardiomyopathy *in vivo* because the pathology observed in the mouse model is strikingly similar to those of the human conditions. Typically in CVB3-infected A/J mice, prominent changes to the myocardium occur within 2 days of infection, including coarse granularity and multivesicular vacuolation [183,184,226]. From days 3 to 5, large areas of myocytes would appear damaged, with signs of calcifications [68,183,226]. The use of terminal deoxynucleotidyl transferase mediated nick end labeling (TUNEL) and ISH for viral RNA reveals that the presence of viral RNA can be associated with the pathology of cellular injury [64,68]. Data from TUNEL-staining has been regarded as a general indicator of cells that are apoptotic, necrotic or proliferating [78,125,186]. At this stage of disease, significant changes in gene expression in the tissue can be detected by the method of differential mRNA display [350]. As well, remodeling of the heart tissue begins in order to compensate for the reduced contractile capability. On day 7 and beyond, inflammatory infiltrates are common [68,81]. Often, necrotic myocytes are indicative of the presence of viral mediated cellular destruction as well as the presence of auto-immune injury. For mice that survive past this point, infection should be resolved on day 9 and onwards.

## 1.5 Life cycle of CVB3

The virion of CVB3 is extremely compact and the structure is simple in that a single molecule of a 7,399 nt long positive sense RNA, coupled to a 22 amino-acids protein (VPg), is enclosed in a 30 nm hexagonal protein coat. Similar to other picornaviruses, the CVB3 virion structure is composed of sixty protomer subunits. The process of CVB3 virion binding to host receptor has not been verified but is believed to be highly similar to that of other picornaviruses

[240] (**Figure 3**). Upon cellular entry, the genomic RNA is immediately expressed by the mechanism of internal ribosomal entry, producing a poly-protein of ~250 kDa. Autolytic cleavage of this poly-protein results in the generation of the individual virion capsid proteins and the viral proteases. The viral proteases are mostly responsible for "reprogramming" the cellular environment to achieve three major goals:

1. Exclusive translation of the viral genome RNA;
2. Inhibition of the majority of host protein translation;
3. Replication of viral genome RNA and the subsequent packaging of viral RNA into infectious virions.

Replication of the viral genome and packaging of the new virions occur in the late stage of infection but before the lysis of the host cell. The life cycle of CVB3 is highly similar to that of other enteroviruses, such as the poliovirus, and a schematic representation of the cycle is illustrated in **Figure 4**.

**Figure 3. The picornaviral virion structure and viral entry**
(Adapted from B.N. Fields et.al. (ed)., Fields Virology, Lippincott-Raven Publishers, Philadelphia, Pa., 1996)

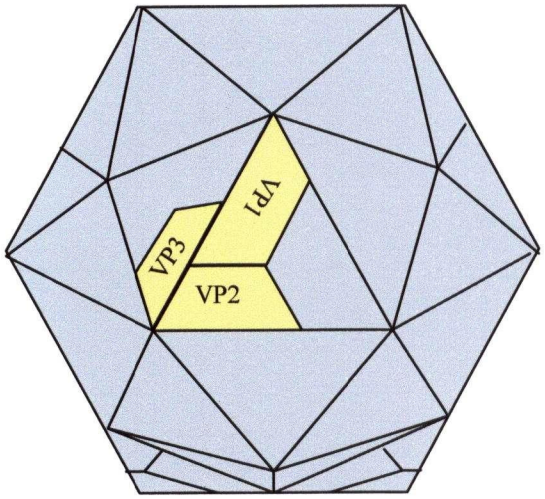


**Arrangement of VP1, 2, 3 on the surface of a picornaviral virion.**
VP4 is buried beneath the surface. Each asymmetric face of the virion is illustrated by a triangle. Each molecule of P1 is autocleaved to generate one set of VP1,2,3,4 asymmetric triangular units (yellow). A total of 60 asymmetric subunits integrate to form a complete virion. The structure and organization of the CVB3 virion is expected to be highly similar.

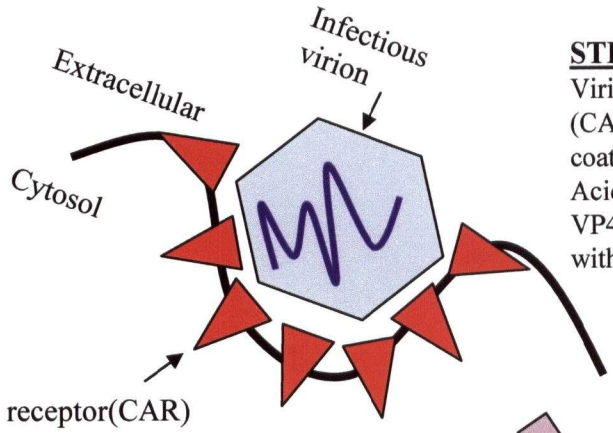


**Entry of viral genome**

**STEP 1:**
Virion binding to coxsackie-adenovirus receptor (CAR) internalization receptor (red triangle). A coated pit on the cellular membrane is formed. Acidic conditions inside the coated pits result in VP4 release and the fusion of lipid membrane with hydrophobic patches inside the virion.

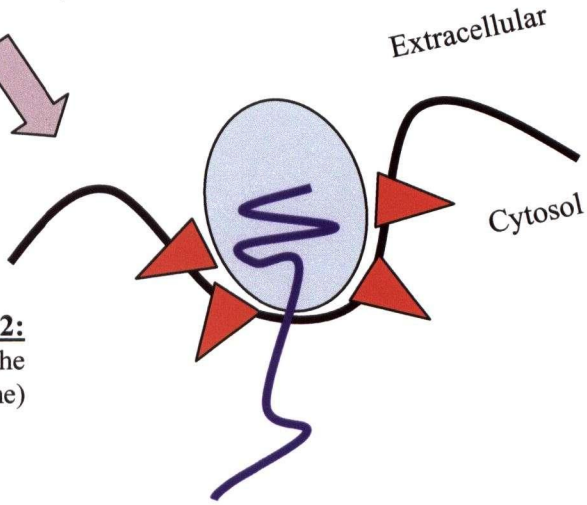


**STEP 2:**
Fused virion and membrane permits the injection of the RNA genome (blue line) into the cytoplasm.

**Figure 4. The life cycle of CVB3.**

Virion particles attach to the CAR and DAF receptors (1). Conformational changes in the virion results in injection of the RNA genome into the cytoplasm (2), which is directly translated to yield the 250 kDa polyprotein (3). Autocatalytic cleavage of the polyprotein produces the various structural and non-structural proteins (4) which participate in replication as well as modification of host environments. Virions are assembled together with progeny RNA (5) and released by cytolysis (6). (Adapted from B.N. Fields et.al. (ed)., Fields Virology, Lippincott-Raven Publishers, Philadelphia, Pa., 1996)

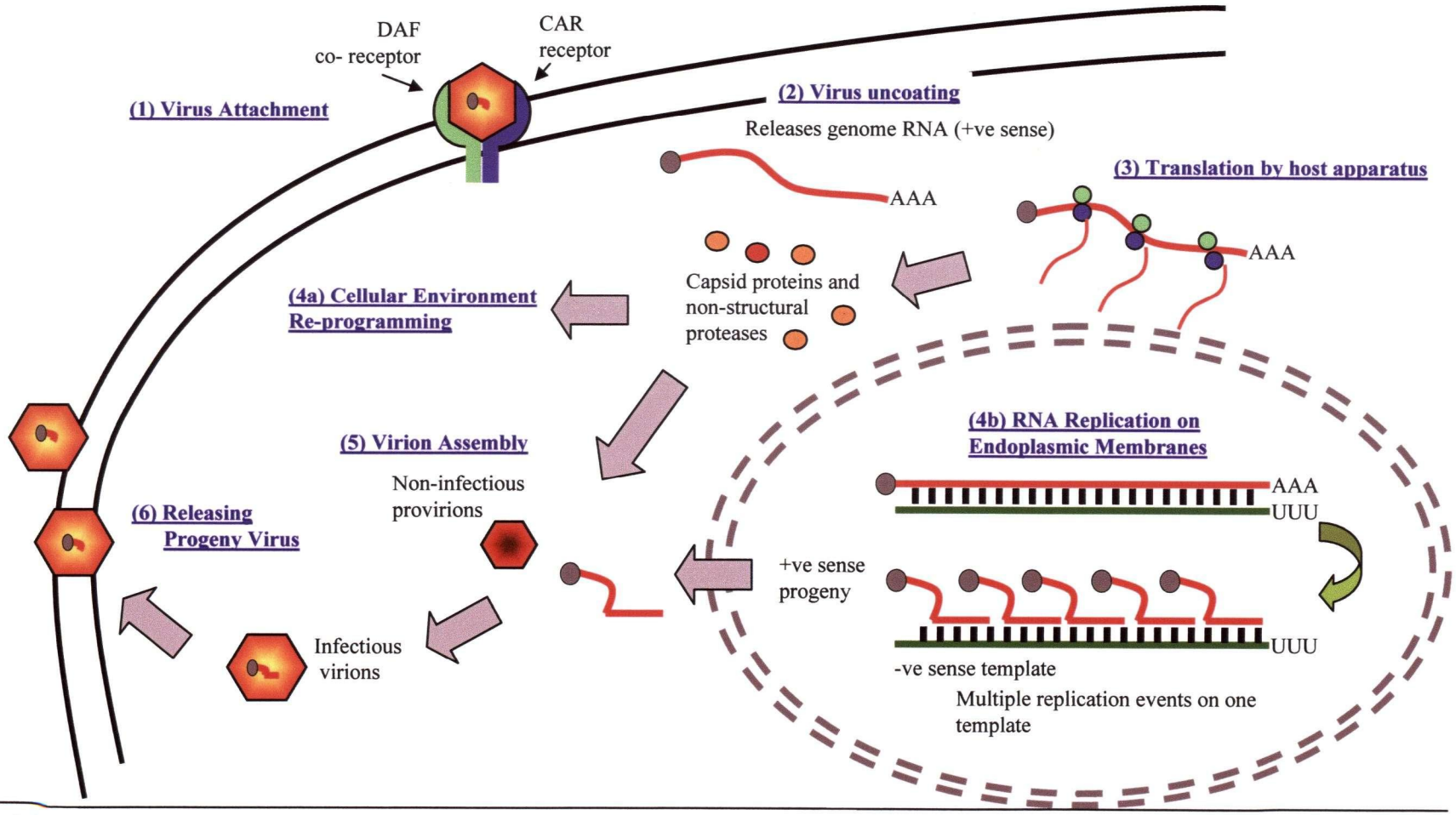

## 1.6 Cellular receptors

Generally speaking, the study of cellular receptors of a virus is important to the understanding of pathogenesis and tissue tropism. For picornaviruses, at least nine receptors and attachment proteins have been identified [36,105,318]. For CVB3, two specific receptors have been discovered and studied in detail: the 46 kDa coxsackie-adenovirus receptor (CAR) and the ~70 kDa decay accelerating factor (DAF).

### *1.6-1 The Coxsackievirus-Adenovirus Receptor*

Both the human and mouse CAR were demonstrated to mediate attachment and infection of coxsackie B group viruses and adenovirus 2 and 5 [35,220,285]. The importance of CAR in mediating infection has been demonstrated by studies that show that chinese hamster ovary cells become susceptible to all six serotypes of coxsackie-B group viruses only after they are transfected by the CAR mRNA [220]. The murine CAR protein is 91% similar in sequence to the human CAR [36]. CAR is a transmembrane adhesion molecule of the immunoglobulin superfamily [36] (**Figure 5**). The trans-membrane domain does not play a role in the internalization of the virus [332], and the endogenous function of CAR is uncertain, as are the downstream signaling events following the binding of extracellular substrates (and virus). The extracellular domain of the receptor is sufficient for virus binding and internalization.

Current knowledge of the relationship between CAR expression and CVB3 infection is not sufficient to fully understand the cardiovirulence of the virus. For instance, the use of an anti-CAR monoclonal antibody does not attenuate the binding of CAR to some isolates of CVB3 [220]. This suggests the presence of co-receptors or chaperone molecules that may participate in virus binding and presentation to the CAR receptor. The CAR receptor has been cloned and

sequenced by various methods [35,61,62,318,342,343]. Northern-blot analysis of the RNA expression indicates that the CAR mRNA is strongly expressed in human (and mouse) heart, brain, and pancreas, but is below the level of detection in the placenta or skeletal muscle [35,318]. The patterns of mRNA expression correlate in part with the patterns of CVB3-induced pathology in mouse, with pancreas and heart being the most susceptible organs [230]. Yet, high levels of CAR expression in the kidney do not correlate with the general resistance of the organ towards CVB3. It is possible that transcription of the CAR mRNA may not truly reflect the amount of functional protein. At present, there is no definitive data regarding receptor protein expression and CVB3 tissue tropism. In light of other findings on the cardiovirulence determinants of CVB3 in the viral genomic RNA sequence (**Section 1.7-3**), it is reasonable to assert that the expression of CAR may only partially determine the tissue tropism of CVB3.

**Figure 5. The CAR and DAF receptors**

Schematic representation of the CAR and DAF receptors. DAF (also named CD 55) is anchored to the surface of the cellular membrane by a glycophosphoinositol (GPI) linkage (red line). The CAR receptor (green) is attached to the membrane via a transmembrane domain. The C-terminal sequence of the CAR receptor extends into the cytoplasm. Immunoglobulin-like domains of the receptors are shown as circles. SCR 2 and 3 on the DAF receptor are responsible for CVB3 virion attachment. The SCR 2,3 and 4 of the DAF protein are required for proper conformation of the active SCR3 site which is involved in complement regulation. Domains of the receptors that can bind CVB3 virion are shaded in yellow. (Adapted from Matino, T.A. et.al., Virology 244:302-314 and 271:99-108).

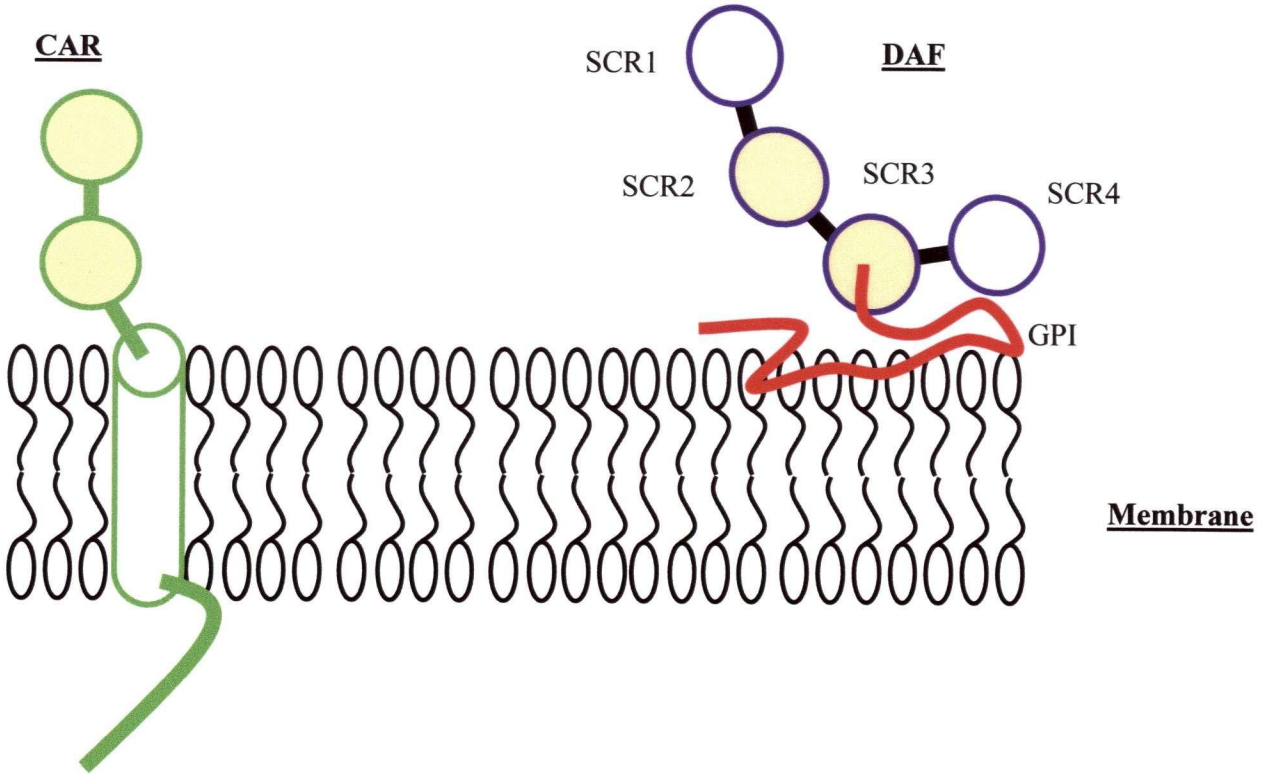

### *1.6-2 The Decay-Accelerating Factor*

DAF is a membrane-bound glycoprotein, which is also known as CD55. It serves as an attachment protein for a number of different human enteroviruses including enterovirus type 70 and coxsackievirus A21 [83,168,224,296,299]. Interaction of CVB3 with DAF appears to occur with the short consensus repeat (SCR) sequence 2 and 3 on the DAF protein [34] (**Figure 5**). The normal physiological function of this protein is to inhibit complement-mediated cellular damage at the C3 convertase level, thus preventing the generation of the membrane attack complex and other cytopathic molecules such as anaphylotoxins and opsonins [212]. The expression of DAF on the cell surface is an important mechanism to protect cells from complement-mediated lysis [248].

DAF is expressed in most human cells types, including the blood cells and the vascular endothelium [248]. Human and mouse DAF are both functionally and genetically similar [93,175,304,305], although CVB3 only interacts with the human DAF and not with the mouse counterpart. The glycosylphosphotidylinositol (GPI) moiety on the DAF is critical for its attachment to the cellular membrane [224,227] but not for interaction with CVB3. The GPI moiety also allows the DAF molecule to interact with other membrane bound glycoproteins. For instance, dimerization of DAF or interaction with other unidentified proteins via the phosphatidylinositol domain can lead to interleukin 2 (IL2) secretion and T cell activation [93,300]. The GPI domain of DAF is a post translational modification that occurs in the SCR 3 region. The mature form of DAF is about 70 kDa, although the MW of DAF can vary with the extent of glycosylation. Interestingly, while the GPI and SCR 3 are involved in initiating T-cell activation [86], the same domain is also involved in interaction with the CVB3 virion (**Figure 5**). Thus, it is believed that CVB3 binding with DAF can have immunological consequences.

The role of DAF in the pathogenesis of CVB3 is now believed to be that of a co-receptor: membrane-bound DAF captures a CVB3 virion from the extracellular environment and delivers the virion to the transmembrane CAR, which then mediates the internalization of the virus [299]. Shafren et al. showed that DAF expression in rhabdomyosarcoma cells does not permit viral infection unless CAR is co-expressed. Monoclonal antibodies against DAF are required to protect permissive cell lines against high input multiplicities of infection (MOI) [37,299]. A similar mechanism of viral entry has also been reported in the lytic infection by coxsackievirus A21, which utilizes ICAM-1 and DAF as receptor molecules [297,298]. The use of soluble DAF in preventing CVB3 infection was demonstrated by our research group [347].

## 1.7 Genetics of CVB3

Like other enteroviruses, the entire coding region of CVB3 is a single open reading frame (ORF) encoding one polyprotein. The coding region of CVB3 starts from nt 741 to 7299. This single polyprotein is organized into three regions: P1, P2 and P3 (**Figure 6**). Structural proteins (VP1-VP4) are encoded in P1, and non-structural proteins (2A-2C and 3A-3D) in domains P2 and P3, respectively. P1 is encoded at the N-terminus of the polyprotein and the 2A protease ($2A^{pro}$) is located immediately downstream of P1. Upon translation, the $2A^{pro}$ *cis*-cleavage activity occurs between the C-terminus of capsid protein VP1 and the N-terminus of the $2A^{pro}$ itself, which then releases the P1 precursor peptide (capsid proteins) from the P2-P3 precursor peptide. Most of the remaining cleavages of the picornaviral polyprotein are mediated by the viral enzyme, 3C protease ($3C^{pro}$) (**Figure 6**). The "primary" cleavage event by protease $2A^{pro}$ occurs very rapidly while the polyprotein chain is still nascent. In some polioviruses, protease

**Figure 6. Genome organization (P1-P3) and proteolytic cleavage of polyprotein.**

The P1 region encodes structural proteins VP1-4 (yellow boxes), which is followed by the P2 and P3 region (pink boxes). Autocatalytic cleavage (cis) by 2A of the polyprotein separates the structural proteins from the proteases. Subsequent $3C^{pro}$ cleavages release the rest of the proteases / capsid proteins. VP0 is cleaved by $3C^{pro}$ into VP4 and Vp2 upon packaging of genomic RNA into mature virion.

(Adapted from: Yang et al., 2002 Picornaviral proteaeses in viral replication and pathogenesis. Current Topics in Virology, 3,17-31).

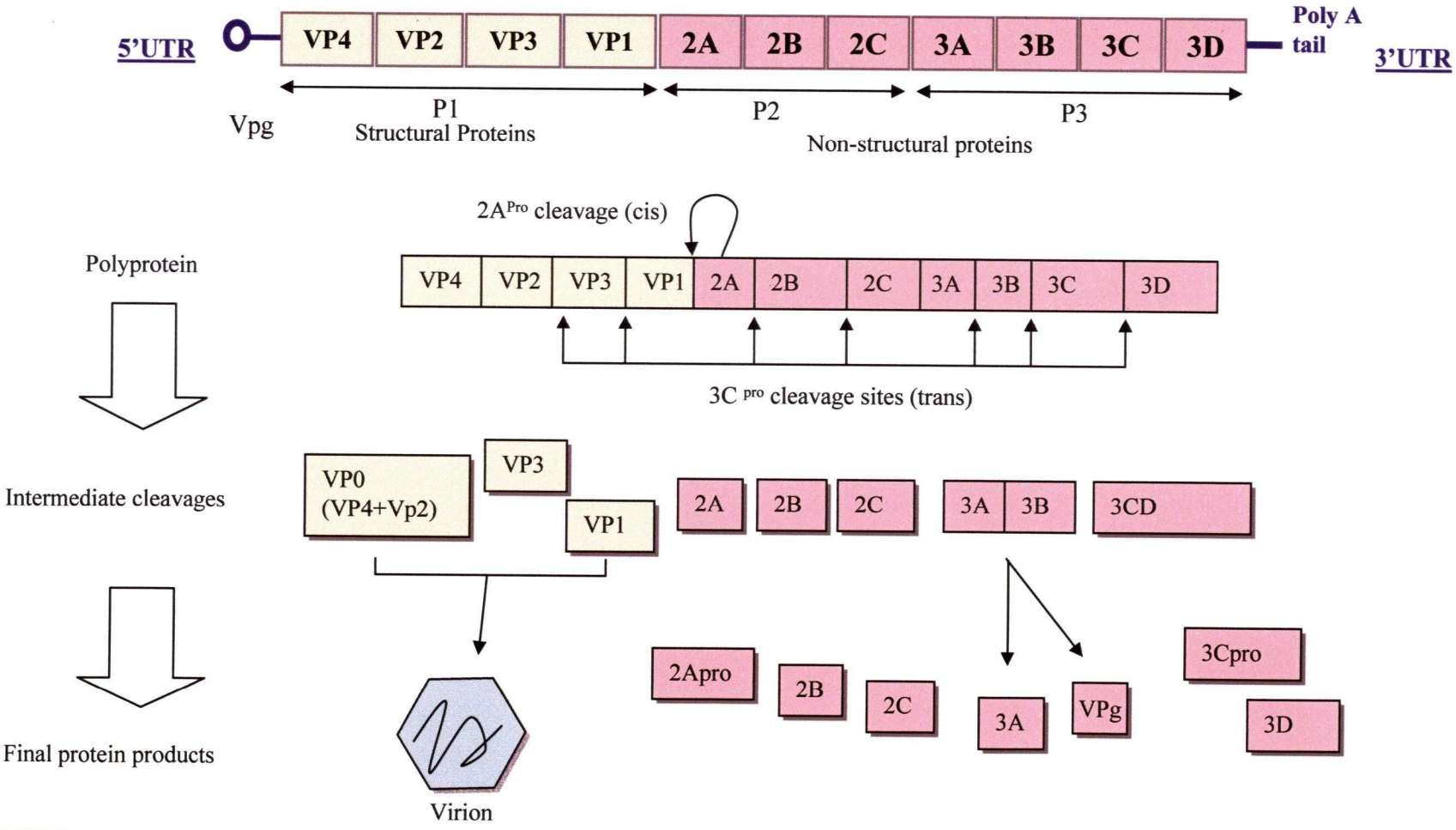

$2A^{pro}$ recognizes another cleavage site on the 3CD-precursor protein, producing non-functional products 3C' and 3D' proteins instead of the viral protease $3C^{pro}$ and polymerase $3D^{pol}$. These alternative cleavages of the 3CD protein by protease $2A^{pro}$ appears to be strain-specific and the cleavage products are not essential for viral replication [190,289]. Thus, the "secondary" cleavage and formation of the 3C' and 3D' proteins were speculated to modulate the ratio of functional capsid proteins and viral enzymes in an infected cell [190].

The P1 region of the genome encodes four virion proteins, known as VP1, 2, 3, and 4. Each of the 60 subunits of the virion is constructed from these four viral proteins. Data from X-ray crystallography indicates that the structure of the viral capsid proteins VP1, VP2 and VP3 is highly conserved among CVB3 and other picornaviruses [239]. Structural differences in the capsids between CVB3 and other enteroviruses are located mostly on the virion surface. The canyon and major surface depressions of the virion are predicted to be the primary and secondary receptor-binding sites, respectively. Assembly of the virion capsid from VP1-4 occurs by the following process [108,288,339] : the P1 capsid precursor is myristoylated to form 5S promoters, which are then cleaved by the protease $3CD^{pro}$ to result in VP0, VP3, and VP1 proteins [161]. The VP0 protein is the combined form of VP4 and VP2 proteins. Repeating units of 5S promoters are then assembled into 14S pentamers. The 14S pentamers are further assembled into 75S hexagonal empty capsids. Packaging of the genomic RNA into the capsid forms the 160S provirions. The VP0 protein in the pro-virion is then cleaved by the protease 3Cpro to produce VP4 (inside virion) and VP2 (on the surface), effectively closing the capsid and forming a mature progeny virus.

The P2 region of the genome encodes three polypeptides: $2A^{pro}$, 2B and 2C proteins. $2A^{pro}$ is a major protease that is responsible for many pathogenic events, and the functionality of

this protease will be discussed in detail in **section 1.7-2a**. The 2B protein modifies the permeability of cellular membranes, by creating amphipathic pore structures which disrupt cellular $Ca^{2+}$ concentrations. This modification can lead to the release of viral progeny from infected cells [95,326,327]. The 2C protein is postulated to participate in viral replication [274,275]. It contains three motifs that are characteristic of an RNA transcription function: an amino-terminal amphipathic helix [261], a putative zinc finger [137] , and a nucleoside triphosphate (NTP)-binding site [98]. Other possible functions of the 2C protein may include RNA encapsidation [201] and molecular mimicry. Sequence homology between the 2C protein (amino acids. 32-47) of several members of CVB and the glutamate decarboxylase (GAD, amino acids. 247-279), which is a major diabetes antigen, has been observed [15,169]. These cellular immunological findings suggest an inductive role for Coxsackie B viruses in autoimmunity [15,169].

The P3 region of the enterovirus genome encodes the 3A protein, 3B (Vpg) protein, protease $3C^{pro}$, and 3D polymerase. Stable intermediates of 3AB protein and protease $3CD^{pro}$ are also present and functional during infection. The functional 3AB protein and protease $3CD^{pro}$ localize in membranous replication complexes [40,314,315]. Based on data from mutational studies [38], the 3A and 3AB proteins are postulated to mediate viral replication. Also the 3AB protein and 3D polymerase cooperate to initiate the activity of RNA polymerase [192,193,260]. The protease $3CD^{pro}$ polypeptide is a proteinase that is responsible for RNA transcription as well as cleaving the polyproteins [133,134,161]. $3C^{pro}$ is also a major CVB3 proteinase and its functionality is discussed in **section 1.7-2b**. The 3B (Vpg) protein is a short, 22 amino acid residue protein that is attached to the 5' end of the genomic RNA. The Vpg is proposed to be an essential feature in forming the replicative complex of the virus. It is present on genomic RNA of the virus, while viral RNA that is undergoing translation does not necessarily possess the Vpg.

### *1.7-1 VPg protein*

A unique feature of the picornaviral genomic RNA is the covalent linkage of a twenty-two amino acid Vpg protein at its 5' end. This is in contrast to the host mRNA which contains the 7-methylated guanosine triphosphate cap-structure. The functional role of the Vpg remains unclear, but it may serve as an anchor for the formation of a replication complex [30,315,317]. The viral Vpg protein, however, cannot substitute the function of the 7-methylated guanosine triphosphate cap structure. Without the 7-methylated cap structure, the CVB3 RNA cannot be recognized and translated by the normal method of host translation initiation, the ribosomal scanning mechanism. Instead, translation of the CVB3 RNA occurs by direct ribosomal entry into a specific viral sequence known as the internal ribosomal entry site (IRES). The general mechanism of internal ribosomal entry has also been observed in many other RNA viruses and in a small number of eukaryotic mRNAs.

### *1.7-2 CVB3 proteases $2A^{pro}$ and $3C^{pro}$*

The proteases $2A^{pro}$ and $3C^{pro}$ are crucial in the life cycle of CVB3. In addition to processing the viral polyprotein, they also cleave major host proteins and result in the severe loss of cellular homeostasis. So far, identified targets of cleavage include translation proteins [3], anti-apoptotic proteins [119], caspases [29], and structural proteins such as dystrophin [26] (**Figure 7**). Beyond causing immediate cell death, such cleavages are also related to the remodeling of the infected target organs such as the myocardium, wherein dilated cardiomyopathy can be a consequence of acute CVB3 infection [90,245]. The structures and functional significances of these two proteases, $2A^{pro}$ and $3C^{pro}$, are discussed below in detail.

**Figure 7. Major cellular cleavage events mediated by the $2A^{pro}$ and $3C^{pro.}$**

The coxsackievirus protease $2A^{pro}$ (pink) and $3C^{pro}$ (blue) are responsible for the cleavage of various major host proteins. Cleavage of structural proteins (thin arrows) includes dystrophin, cytokeratin 8 and MAP4 and leads to remodeling of the myocardium. Other proteins of the transcription and translation apparatus, such as Oct-1, CREB and eIF4G are also cleaved. Activation of caspases and apoptotic pathways is also induced by the $3C^{pro}$, possibly involving other intermediate cleavage substrates. (Adapted from: Yang et al., 2002 Picornaviral proteaeses in viral replication and pathogenesis. Current Topics in Virology, 3,17-31).

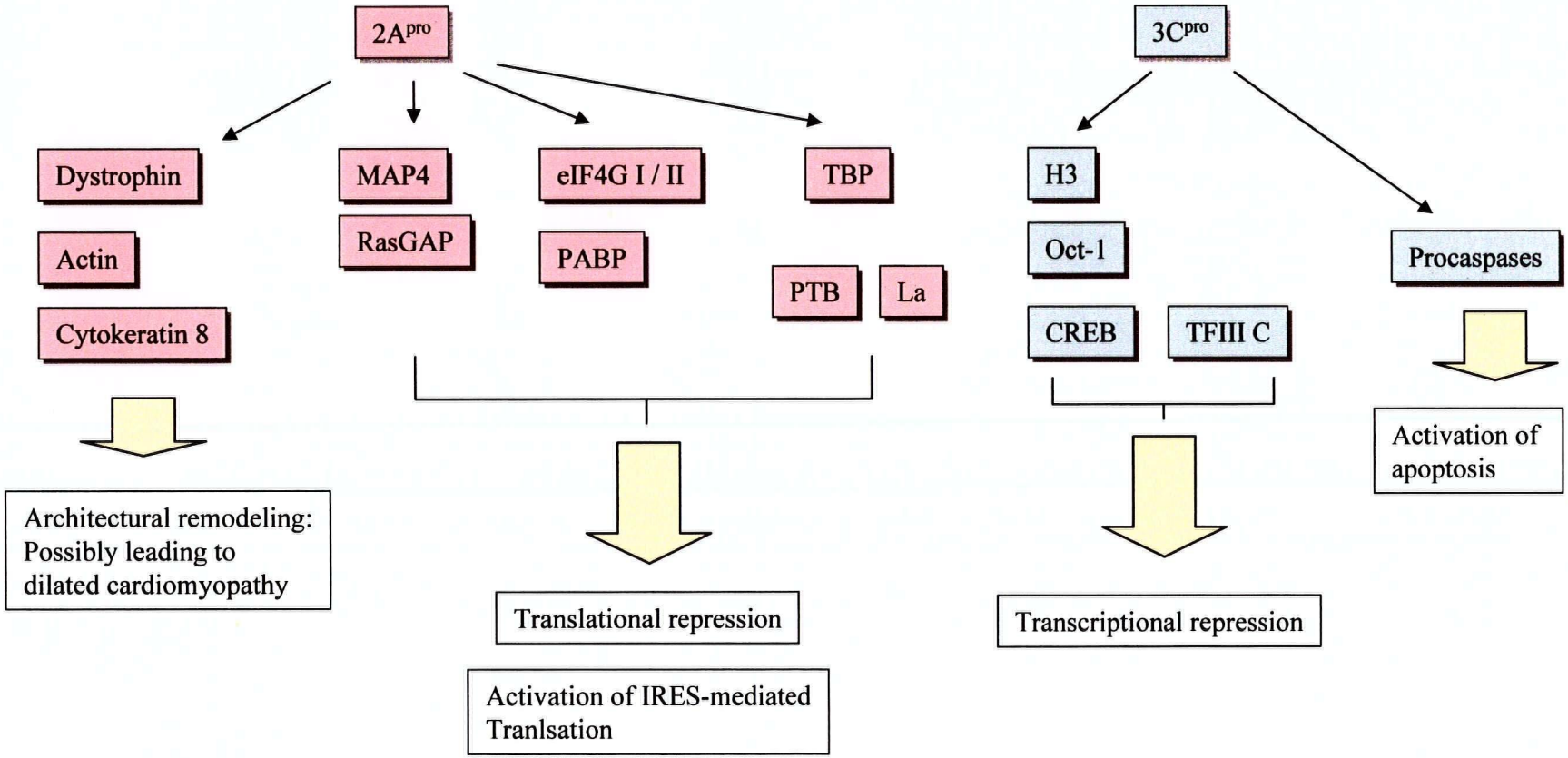

### 1.7-2a Protease 2A ($2A^{pro}$)

Coxsackievirus protease 2A ($2A^{pro}$) is a small cysteine protease, about 17 kDa, which shares sequence homology with bacterial trypsin-like serine proteases [289,353]. In the case of the entero- and rhinoviruses, the catalytic triad of protease $2A^{pro}$ was identified as His-20, Asp-38 and Cys-109 [289,353]. The thiol group of the cysteine residue acts as a nucleophile and its catalytic activity can be strongly inhibited by thiol alkylating reagents [289,331], as shown by inhibitor studies using iodoacetamide and *N*-ethylmaleimide, compounds that are known to be active against thiol proteases [289]. The role of these residues in catalysis was confirmed by site-directed mutagenesis. These data also suggests that protease $2A^{pro}$ is structurally more related to a small trypsin-like serine protease than to a typical papain-like cysteine protease [289,353]. A proposed model of the protease $2A^{pro}$ of human rhinovirus type 2 suggested that the overall structure of viral protease $2A^{pro}$ is similar to that of *Streptomyces griseus* protease A: both proteases were found to share the same components in the domains of the catalytic center [295]. Recent data has characterized the protease $2A^{pro}$ as a zinc-containing enzyme, in which the metal ion, $Zn^{2+}$ stabilizes the protein rather than being directly involved in catalyzing proteolysis [289,295,302].

As mentioned earlier, the *cis*-cleavage activity of protease $2A^{pro}$ takes place between the C-terminus of capsid protein VP1 and the N-terminus of $2A^{pro}$ itself. T*rans*-cleavage by protease $2A^{pro}$ also occurs in an increasing list of cellular factors. Over the past decade, a major focus of studies on protease $2A^{pro}$ has been its cleavage of eukaryotic translation initiation factor 4G (eIF4G). The focus on eIF4G cleavage is due to the probable association of this activity with picornaviral-induced inhibition of translation of host proteins. Investigations have demonstrated that purified recombinant protease $2A^{pro}$ of CVB4 and human rhinovirus type 2, as well as PV, can cleave eIF4G between amino acid residues Arg485-Gly486, *in vitro* [54,195]. Given the known

functional role of eIF4G as a bridge between the ribosome and mRNA, the cleavage of eIF4G is believed to inhibit normal host protein synthesis. During viral infection, cleavage of eIF4G occurs very rapidly, in an average of two hours post-infection [195]. Timing of this cleavage event coincides with that of the reduction of cap-dependent translation of cellular mRNA and the rise of cap-independent translation of viral mRNA. On the other hand, studies of PV infection in cell culture environments have shown that host protein translated by the cap-dependent mechanism is suppressed by only 50% or less despite the complete cleavage of eIF4G [208,269]. Hence, the general inhibition of host protein synthesis during a picornaviral infection may require proteolysis of factors in addition to eIF4G.

Recently, a novel human homologue of eIF4G, called eIF4GII (while the original eIF4G was renamed as eIF4GI), has been reported as the second event required for the complete inhibition of host protein synthesis [123,124]. eIF4GII appears to be functionally equivalent to eIF4GI, but is only 46% identical at the amino acid level [123] (**Figure 8**). Both poliovirus and human rhinovirus protease $2A^{pro}$ were found to cleave eIF4GII, with slower kinetics as compared to the cleavage of eIF4GI. The cleavage can result in the greater inhibition of host protein synthesis [119,310]. These data may explain several earlier reports documenting the lack of correlation between eIF4GI cleavage and the partial inhibition of cellular mRNA translation after enterovirus infections [208,269]. More significantly, the cleavages of both eIF4GI and eIF4GII may trigger host cell apoptosis, either directly by inhibiting the cap-dependent expression of proteins required for maintaining normal cell viability or by enhancing the cap-independent expression of important regulatory proteins such as c-Myc [159] and death associated protein (DAP5) [138], which may play roles in the activation of cell death responses.

**Figure 8. Homology between eIF4G I and 4G II.**

Both proteins are functionally similar, with an overall 46% a.a. sequence homology. Sequence homology in the eIF3 binding domain (blue) is 79%. The eIF4GII is 1585 a.a. long and the eIF4G I is 1560 a.a. long. Both can be cleaved by picornaviral $2A^{pro}$ and the cleavage of both eIF4G variants correlates with the general inhibition of host protein synthesis during an infection. Other protein-interaction domains are also indicated.

(Adapted from Gingras, A. C., B. Raught, and N. Sonenberg. 1999. Annu. Rev. Biochem. 68:913-963).

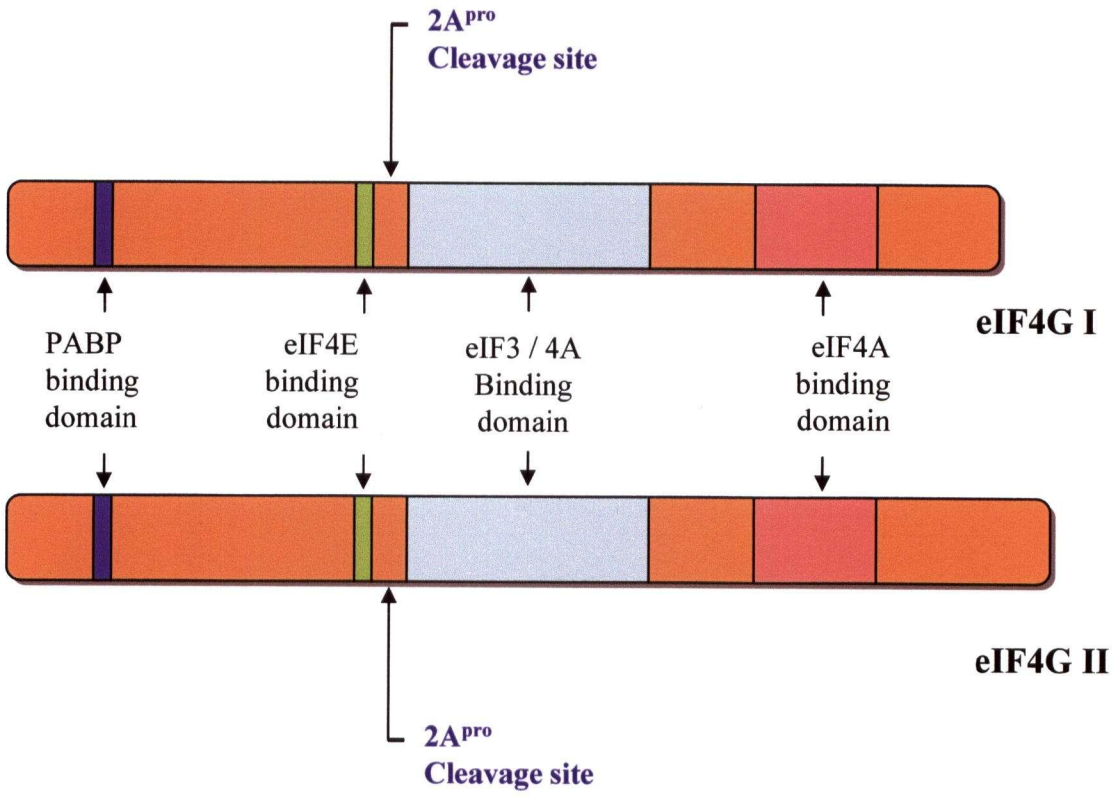

1.7-2b Protease 3C ($3C^{pro}$)

The protease $3C^{pro}$ is a 20 kDa cysteine protease that is phylogenetically conserved among picornaviruses. Protein cleavage mediated by the poliovirus protease $3C^{pro}$ occurs exclusively at glutamine and glycine bonds, although in other picornaviruses the glycine residue may be substituted by other amino acids such as serine and alanine [14,257,258,278]. The viral protease has been cloned and characterized as a cysteine protease that can be inhibited by N-ethylmaleimide and iodoacetamide [265]. The histidine and cysteine residues are believed to form the active site, as confirmed by X-ray crystallography of protease $3C^{pro}$ from the HRV14 and HAV [6,215,222].

The protease $3C^{pro}$ is generated from the autolytic cleavage of 3CD (**Figure 6**). Alternative cleavage of 3CD by the polio protease $2A^{pro}$ can give rise to 3C' and 3D' [182], which is not required for the generation of infectious virus particles [170]. It is suggested that the alternate cleavage of 3CD serves as a possible regulatory mechanism for the replication and maturation of pro-virions [190]. The protease $3C^{pro}$ is capable of cleaving a number of host proteins (**Figure 7**). The 3D domain is an RNA-dependent RNA polymerase but in the uncleaved form (3CD), the presence of the 3D domain serves to alter the substrate specificity of protease $3C^{pro}$ in the processing of capsid precursors [161].

Recombinant protease $3C^{pro}$ [42] has been used to study its effect on host protein cleavages [155,237,238]. Of note, a number of translationally important host proteins are affected by the protease $3C^{pro}$. Although a significant body of evidence suggests that cleavage of the eIF4G family is mainly executed by the protease $2A^{pro}$ , there is also evidence that protease $3C^{pro}$ induces cleavages of eIF4A and 4G in the FMDV system [33]. Our research group has also observed cleavages of eIF4G by the CVB3 protease $3C^{pro}$ [351] . Another important target protein

of the protease $3C^{pro}$ is the La autoantigen, a 408-amino acid residue. cellular protein that has been demonstrated to stimulate internal ribosomal entry [16,110,156,287]. The normal physiological functions of the La protein includes tRNA folding, synthesis of polymerase II transcripts and formation of snRNP complexes as well as ribosomal binding [121,122,264,266]. Cleavage of La by the poliovirus protease $3C^{pro}$ occurs in the C-terminal region, between Gln358 and Gly359 [301]. This protease modification of the nuclear-bound La protein can cause it to relocate into the cytoplasm, and such relocation is observed in a number of other independent studies [17-21] (also discussed in section 1.9-2). The Picornaviral translation take place mostly in the cytoplasm, and thus the cleavage of the La autoantigen is believed to improve the translational efficiency of the virus.

The poly-pyrimidine tract binding protein (PTB) is another major nuclear protein cleaved by the protease 3Cpro. The PTB is pertinent to picornaviral translation initiation because it has been shown to bind viral 5'-UTR sequences and cooperate with the La autoantigen in stimulating translation initiation of the viral genome [147,164,165]. Interestingly, cleavage of the PTB by poliovirus protease $3C^{pro}$ occurs in 3 different positions, at amino acid residues Ala-X-X-Gln/Ala, generating multiple peptides which appear to inhibit IRES-dependent translation in a cell-based assay system [22]. The cleavage results in inhibition of its capability to bind to another translation stimulatory molecule : poly-rC-binding protein (PCBP) [171]. The RNA-recognition motiff (RRM) of PTB resides in RRM-3 and RRM-4 [268]. The protease $3C^{pro}$ can cleave all forms of the PTB protein (including isoforms: PTB1, PTB2, and PTB4), and the cleaved products are redistributed to the cytoplasm from the nucleus [22]. The fragments of PTBs are hypothesized to interfere with the binding of intact PTBs to the PV IRES. Analysis of the cleavage event reveals that the cleaved PTB protein can stimulate replication of the viral RNA genome [22]. Consequently, the cleavage event has been suggested as a molecular switch from viral protein

expression to viral genome replication [22]. However, the molecular mechanisms signaling the appropriate time of transition remain unknown. In a picornaviral infection, successful expression of viral proteins increases the amount of functional protease $3C^{pro}$ (along with other viral structural and non-structural proteins) in the cytoplasmic environment, and the rising cellular concentration of protease $3C^{pro}$ may increase the overall likelihood that the protease will cleave proteins that are already bound to the viral 5'-UTR RNA (such as the La, PTB and other proteins). Thus, the overall transition from the stage of viral protein translation to the stage of genome replication may be achieved in a gradual manner [22]. This assertion requires further studies and verification. Nonetheless, it underscores the significance of the viral protease $3C^{pro}$ in the pathogenesis of the picornaviruses.

1.7-2c Cytopathic effects induced by the proteases

Activity of the CVB3 proteases can directly lead to cytopathic effects (CPE). The term CPE is used in multiple models of virus infection when significant cell death is observed in lieu of morphological changes. In the case of CVB3, rapid CPEs are observed in HeLa cell cultures, typically resulting in the severe loss of cellular homeostasis, rupturing of mitochondrial or plasma membranes and the alteration in cellular morphology. These observations occur usually from 7-9 hrs post infection in HeLa cell cultures [66,68]. These CVB3-specific CPEs are consistent with the classical definition of necrotic cell death [214,322]. In the picornaviral family, the first and best studied viral protease causing CPE is the protease $2A^{pro}$ .

Over-expression of recombinant protease $2A^{pro}$ alone in a cell line is sufficient to induce cell death [119]. Structural damage by the protease $2A^{pro}$ in a cellular environment can be related to the cleavage of intermediate filament family members, dystrophin and cytokeratin 8, leading to cell lysis [23,25,26]. These structural proteins may also have scaffolding or docking functions

that are especially important in the formation of intricate signaling pathways [25]. Furthermore, depletion of the dystrophin-glycoprotein complex is the primary cause of Duchenne muscular dystrophy [11,55], and has been identified in patients with viral myocarditis leading to DCM [26]. Hence, there is evidence of the causal effect of the CVB3 protease activity in remodeling of the myocardium, which eventually leads to the condition of dilated cardiomyopathy.

Equally significant in causing cell death is the protease $3C^{pro}$. The PV protease $3C^{pro}$ induces drastic morphological alterations and apoptotic cell death by a caspase-dependent mechanism [29]. The protease $3C^{pro}$ has been demonstrated to cleave the cyclic-AMP-response-element-binding-protein (CREB/ATF) [344], transcription activator octomer-binding-transcription-factor (OCT-1) [346], the TATA-binding protein and TFIIIC [82,345], and the histone protein (H3) [106,316] (**Figure 7**). The cleavage of these major transcription factors and host proteins reduces the efficiency of host mRNA expression and hence, leads to eventual cell death by inhibition of host protein expression.

In addition to the protease $2A^{pro}$ , and 3C pro, the viral protein 2B can modify the permeability of the plasma membrane, mitochondria and endoplasmic reticulum (ER) [4,292,326]. This will disrupt the delicate balance between selective membrane permeability and cellular homeostasis. Damage to the ER will release calcium into the cytosol, and contributes to further cellular injury [4]. Ukimura et al. [324] have provided electron microscopic evidence of mitochondrial swelling and rupture in infected mouse hearts. The direct consequence of losing mitochondrial membrane integrity is the release of calcium and death pathway "trigger molecules" such as cytochrome C, AIF, and caspase-2 and -9 [39,65,66], leading to apoptotic responses. This is in contrast to other protease activity that leads to rapid cell lysis. Of note, the cap-independent translation of some host proteins continues (discussed in **section 1.8-3**). The

apoptotic response of the CVB3-infected host is both interesting and important in the course of disease development. Detailed discussion of the relationship between apoptotic responses and CVB3 infection can be found in recent articles that our group has published [67,355,356].

### *1.7-3 Molecular determinants of CVB3 cardiovirulence*

Among the six serotypes of the coxsackievirus B group viruses, there are high homologies in the genomic RNA sequences. In spite of these similarities, each of the six viruses exhibits very different tissue tropism. For instance, CVB4 is a well studied agent in diabetes, while CVB3 is notorious for its cardiovirulence. Within the CVB3 serotype, several strains exist that demonstrate specific differences in cardiovirulence. For example, the CVB3/0 is a noncardiovirulent strain and unable to induce inflammatory heart diseases, while CVB3/m is cardiovirulent and can cause severe myocarditis. Persistent infection with CVB3/m may also result in the development of dilated cardiomyopathy [56,319]. Upon close inspection, the coding sequences of all CVB3 strains are very similar. This raises the question as to what determines the specific cardiovirulence and pathogenicity of coxsackieviruses.

#### 1.7-3a Relationship between virulence and IRES

Studies from the tissue tropism of PV has provided some insights into the molecular mechanisms of CVB3 cardiovirulence. One of the remarkable properties of the PV is its capability to infect motor neuronal cells (as opposed to sensory cells) in specific areas of the neural system, namely the spinal cord of the cervical and lumber regions while the cerebral cortex, the olfactory and the thoracic regions are spared [149,249,341]. The attenuated PV vaccine strains have provided possible explanations for this tissue tropism. In this attenuated strain of PV, mutations were mapped to a specific region in the 5'-UTR of the viral RNA [150]. This region was subsequently identified as the domain V of the IRES [339]. Within this domain, nts 480, 481

and 472 were mutated in PV types 1, 2 and 3, respectively [128]. Point mutations in domain V significantly reduced translation efficiencies of the corresponding viral RNA as compared to wild-type templates. This is the first evidence that the translation efficiency of a viral genome is directly related to its virulence. Recently, in order to determine the structures responsible for neurovirulence, Gromeier et al [100,127] used a chimeric virus strategy to dissect the PV and human rhinovirus-2 IRES elements. They found that both domains IV and V of the PV 5'-UTR are required to produce a neurovirulent phenotype. It appears that specific UTR sequences are coordinately responsible for the neuropathogenicity (neurovirulence) of PV.

Following the work in the PV system, molecular determinants of the tissue tropism of CVB serotypes were also discovered within the 5'-UTR. CVB1, a less pathogenic strain than CVB3, has virulence determinants in nts 117 to 161 of its 5'-UTR [284]. Also, Tu et al [75,323] found that an U to C mutation at nt 234 within the CVB3 5'-UTR results in attenuation of the cardiovirulent phenotype in mice. Replacement of the cardiovirulent CVB3/m or CVB3/20 5'-UTR with that of avirulent strain CVB3/0 attenuates the ability of the resultant viruses in causing myocarditis [197,198]. These investigators subsequently analyzed multiple clinical CVB3 isolates as well as other enteroviruses and demonstrated that nt 234 is always U regardless of the cardiovirulence phenotype of the virus [74,75]. Thus, they concluded that the previously reported U-C mutation at nt 234 is most likely the result of a rare artificial mutation, as opposed to a naturally occurring genetic variation. However, their findings do imply the likelihood of discovering other sites in the CVB3 5'-UTR that can account for the variations in virulence as seen in the natural isolates of CVB3.

In the search for these determinants, Gauntt and Pallansch [115] performed partial sequence analysis of the 5'-UTR (nts 300-599) of 15 CVB3 wild-type strains and found that nt 565 was A

in cardiovirulent strains and U or C in avirulent strains. These data suggest that translation efficiency is related to CVB3's tissue tropism because this position is located at the center of the CVB3 IRES [349]. Recently, Dunn et al. [102] used two phenotypically and genotypically different clinical isolates to examine the genetics of CVB3 cardiovirulence. By constructing of a chimeric virus and testing it in a mouse model, these investigators finally confirmed that the 5'-UTR harbors natural genetic elements which regulate the cardiovirulent phenotype of CVB3: a chimeric virus, constructed by replacing the entire 5'-UTR of a cardiovirulent CVB3 strain with that of the PV strain, cannot induce heart disease in young mice. However, inoculation of this non-virulent chimeric virus does stimulate protective immunity against inflammatory heart and pancreatic diseases that are triggered by subsequent virulent CVB3 challenge [73]. Further work has also identified the high order secondary structures in the 5'-UTR as possible determinants of cardiovirulence [101]. These findings are very interesting and strongly highlight the fact that CVB3 cardiovirulence is related to the functions of the 5'-UTR. The functions mediated by the 5'-UTR are in turn dependent on interactions of host proteins with the UTR sequence. Currently, there are no data on such interactions. It is thus an objective of my dissertation to discover and characterize these host protein- CVB3 UTR interactions.

### 1.7-3b Virion capsid proteins and CVB3 virulence

In general, the efficiency of interaction between virion and receptor is a determinant of virulence. For enteroviruses, the conformation and structure of the capsid proteins contain determinants contributing to the pathogenic phenotypes of PV [53], CVB4 [280], and FMDV [217]. In the study of CVB3, specific virulence of the virus towards cardiomyocytes is of particular interest due to its clinical consequences. Early studies on this subject were focused on the interaction between capsid proteins and the viral receptor. Zhang et al. [358] derived an attenuated

strain of CVB3 from a highly cardiovirulent parental strain in cell culture. Characterization of this attenuated strain using a chimeric virus system demonstrated that sites other than the CVB3 5'-UTR were responsible for the attenuation. The search for determinants in the coding region of the viral genome was performed by passaging the attenuated CVB3 strain in the heart of SCID (Severe combined immunodeficiency disease) mice and eventually a revertant with wild type cardiovirulence was isolated [60]. Sequence analysis and comparison of the revertant virus with the wild-type cardiovirulent CVB3/Nancy strains suggested that amino acid 155 in the VP1 region might play a role in attenuation [102].

By comparing the near-atomic-structures of the CVB3 virion of different isolates, Couderc et al and Dunn et al [85,102] found that tissue tropism determinants of PV and CVB3 could be mapped to amino acids exposed on the surface of the virion, on sites of the VP1 and VP2 subunits which are known to form an important neutralizing antigenic domain of the PV virion [256]. The CVB3/AS (cardiovirulent) and CVB3/CO (non-cardiovirulent) strains differ from each other in the major surface protrusion region of VP3 [102]. However, neither of these capsid surface differences appears to affect the tropism of the cardiovirulent strain CVB3/20 when its capsid proteins are replaced by those of either CVB3/CO or CVB3/AS [102]. Therefore the relationship between the capsid protein sequences and cardiovirulence remains at best a strong correlation.

Besides CVB3 virion proteins, the CVB3 5'-UTR can also determine cardiovirulence. Current knowledge with respect to the determinants of CVB3 cardiovirulence resemble findings in the poliovirus system: the primary determinant of PV neurovirulence is localized in the 5'-UTR, while variations within the capsid protein sequence may also influence the full expression of the overall tissue tropism [53,85].

## 1.8 Expression and replication of viral genome

Expression of the CVB3 genome occurs by the mechanism of internal ribosomal entry. This is also known as the cap-independent mechanism of translation initiation, as the viral RNA does not possess a methylated 5' guanosine structure which is present in eukaryotic mRNAs. Similarities between the prokaryotic translation system and the viral internal ribosomal entry mechanism have been discussed in several recent publications [348] [247,270,272,306] . Recent work in our laboratory has defined the structures of the IRES in the 5'-UTR of CVB3 (**Figure 9**) [349]. By mutational analysis and *in vitro* translation using a bi-cistronic plasmid containing a CVB3 P1 reporter gene, the minimum IRES-sequence has been determined to be located within the 5'-UTR stem-loops F, G and H [349]. Further analysis by mutations of the full-length CVB3 cDNA and transfection of HeLa cells has defined the 5' and 3' boundaries of the IRES as spanning nts 309-432 and 639-670, respectively [207] . In addition, a 46-nt polypyrimidine tract was found to be critical for viral translation and infectivity [207].

An interesting property of the IRES mechanism is the continuum of translation initiation during the G2/M phase of the cell cycle. This is opposite to the expression of host mRNAs by the cap-dependent method [47]. As well, recent studies on HCV using a bicistronic RNA with the HCV IRES at the intercistronic space demonstrated that in synchronized cultures of stably transfected cells, the IRES activity varied in relation to the cell cycle: the IRES activity was the greatest during the M phase and the lowest during the quiescent ($G_0$) phase [143]. It appears that HCV translation is regulated by the cellular IRES binding proteins that vary in abundance during

**Figure 9. The CVB3 5' UTR secondary structures and IRES homology**

A schematic of RNA secondary structures in the 5'UTR of CVB3 (Yang *et al.,* 1997). The predicted base-pairing model between the pyrimidine-rich tract sequence of the viral 5'UTR and the 3' terminal sequence of human 18S rRNA is indicated. Complementary nucleotide interactions are represented by dots. The ranges of the numbers indicate the nucleotides of respective stem-loop structures, which are labeled A through K. The IRES, authentic initiation codon AUG, and conserved polypyrimidine/AUG tract are marked. Dots between two sequences denote base pairing. (Adapted from Yang, et al., 2003)

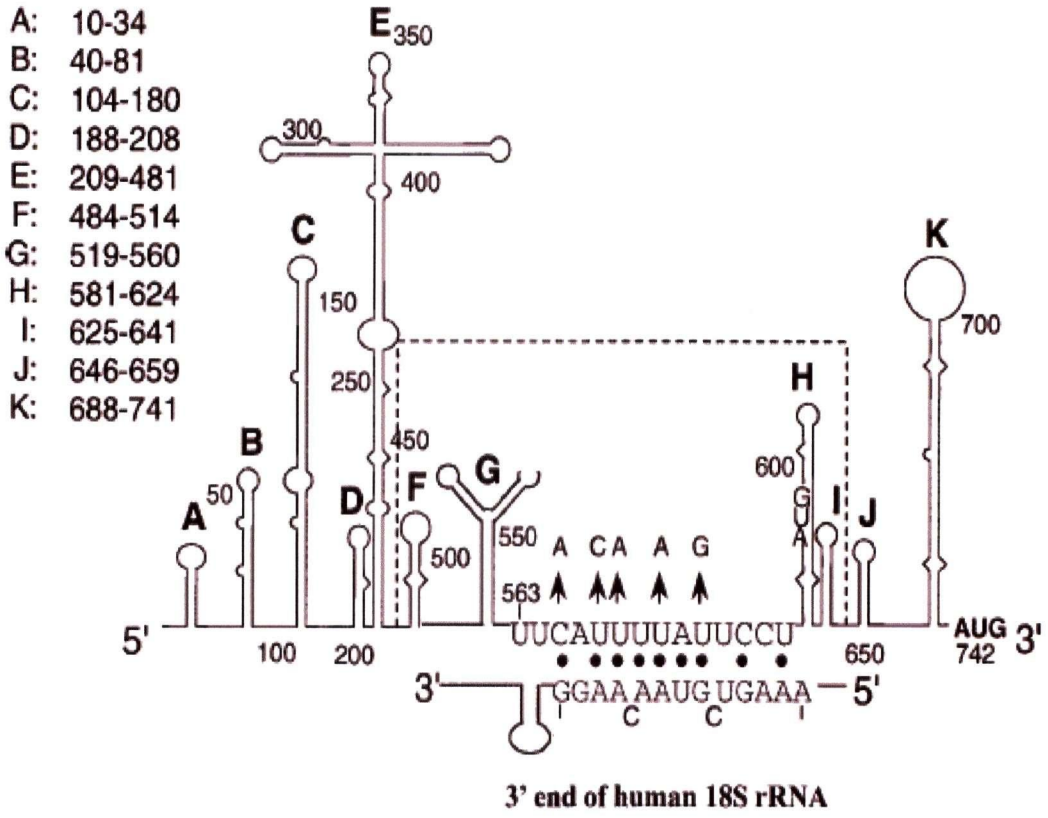


**3' end of human 18S rRNA**

the cell cycle [143]. Further, the variation of IRES activity during different cell cycles suggests that the IRES mechanism is a tightly regulated function of the host and requires specific cytoplasmic conditions for maximal efficiency. Thus, investigating host proteins that promote such conditions is important to understand how the expression of viral genes can be intervened.

### *1.8-1 Classification of picornaviral IRES*

Extensive work has been performed to classify IRES elements based on their functional roles and / or their sequence homologies. A summary of the three types of IRES is presented in **Table 2**. Current data support the classification of all picornaviral IRES into three major categories. Results of classification based on IRES sequence homology [49] agrees well with the results that are based on the functionality of IRES in specific environments [51]. Borman et al. performed transfection studies and analyzed the activities of six different picornaviral IRES in six different cell lines [51]. From those analyses, it was proposed that type I IRES include those of the enteroviruses and the rhinoviruses. These IRES direct internal initiation efficiently only in specific human and mouse cell lines [51]. They are inefficient in driving translation initiation in rabbit reticulocyte lysates (RRL) unless HeLa cell lysates are added. *In vitro* translation reactions with type I IRES are sensitive to changes in concentrations of KCl and $MgCl_2$ in the reaction. Also, the *in vitro* activity of type I IRES can be enhanced by addition of the picornaviral 2A protease [202,359]. In contrast, type II IRES are generally efficient in most human and mouse cell lines [51]. Type II IRES include those of the cardiovirus, apthoviruses, and the non-picornaviral HCV. Unlike the type I IRES, they are neither sensitive to the fluctuation of salt concentrations nor the presence of protease 2A [252,360]. Finally, type III IRES appear incapable of directing efficient internal translation initiation in most cell lines and their *in vitro*

**Table 2. Classification of three types of IRES**

Adapted from B.N. Fields et. al. (ed)., Fields Virology (Lippincott-Raven Publishers, Philadelphia, Pa., 1996 and from The International Committee on Taxonomy of Viruses. http://www.ncbi.nlm.nih.gov/ICTVdb/

| IRES | Representative virus/genus | IRES length | Efficiency | Other variables |
|---|---|---|---|---|
| Type I | Enterovirus (CVB3)<br>Rhinovirus | 30-150nt upstream authentic AUG | Highly restricted in RRL and in other human or mouse cell lines | Sensitive to KCl, $MgCl_2$, Stimulated by $2A^{pro}$ |
| Type II | Cardiovirus<br>Apthovirus | Can extend beyond the authentic AUG | Generally efficient in most cell lines | Insensitive to KCl, $MgCl_2$, and $2A^{pro}$ |
| Type III | Hepatovirus (HAV) | Can extend beyond the authentic AUG | Not efficient in natural cell lines | Mutations in IRES may help efficiency. |

activity cannot be rescued by the addition of HeLa cell lysates. So far, the only type III IRES reported is that of the HAV. The extremely low activity *in vitro* [51] of the HAV IRES is also correlated to the poor replication of HAV seen in cell culture environments [200]. The unusually low efficiency of this type of IRES in cell lines can be alleviated by accumulating mutations in the IRES during repeated culture-adaptations [94], implicating the importance of RNA structure in mediating efficient interaction with the translation apparatus.

The general RNA sequences of both the type II and type III IRES appear to extend up to, include, or even continue beyond the authentic start site for translation [117,148,163,283]. In contrast, the type I IRES (enteroviruses) typically lies between 30 and 150 nt upstream of translation initiation [48,191,247]. Experiments conducted in our laboratory showed that a type I IRES exists in the CVB3 5'-UTR: in vitro translation of the CVB3 P1 gene is restricted in the RRL system, but such a restriction can be relieved by the addition of HeLa cell extracts [349]. Thus, trans-acting factors that are specific for the CVB3 IRES must be abundant in HeLa cell extracts but not in the RRL cytoplasmic environment. To date, studies from other RNA viruses have revealed several HeLa cell factors that participate in viral translation and or replication via interactions with the UTRs, such as the PTB and La protein. The 5'-UTR binding locations of these proteins appear to be dependent on individual viruses [5,136,228,294]. The protein interactions with picornaviral UTRs are further discussed in the **section 1.9**

### *1.8-2 Cap-independent translation initiation of eukaryotic mRNA*

Internal ribosome binding is not restricted to uncapped picornaviral RNA as IRES also exist in viruses whose RNAs are capped at the 5' end. These viruses include the HCV [250] and the pestivirus [277]. Interestingly, increasing number of reports have indicated that a certain number of cellular mRNAs also employ the internal initiation mechanism for translation. To date, such

mRNAs include the immunoglobulin heavy-chain binding protein (Bip) [159,213], eIF4G [113], death-associated-protein-5 (DAP5, also called p97 or NAT1) [138], fibroblast growth factor-2 (FGF-2)[13,325], the proto-oncogene product c-Myc [244], ornithine decarboxylase (ODC) [279], Rbm3 (a cold stress response mRNA) [77] and vascular endothelial growth factor (VEGF) [145]. A summary of genes that are translated by the IRES mechanism is listed in **Table 3**. The 5'-UTRs of these host genes have short IRES: Bip includes a 220 nt IRES [213] and eukaryotic translation initiation factor 4G (eIF4G) has a 101 nt IRES [113] . Note that the presence of a 50-100 nt 5'-UTR is commonly observed in host mRNAs [231,232], but the IRES is a specific sequence element that, if present, can facilitate cap-independent translation initiation of the respective mRNA. Interestingly, translation of these host proteins may also be stimulated or inhibited by proteins (such as La autoantigen and the PTB) that play specific roles in the translation of picornaviral RNA [172,173].

One important structural distinction between host mRNA IRESes and picornaviral IRESes is the lack of a polypyrimidine tract in the 5'-UTR of host mRNAs [116]. However, this difference may not be critical for the functionality of mRNA IRESes because the activity of the cardiovirus IRES is also independent of such sequences [273]. Recently, an 9-nt segment in the 5'-UTR of the homeodomain protein Gtx has been reported to function as an IRES, and multiple copies of this 9-nt sequence increase its activity synergistically [76]. This 9-nt sequence is 100% complementary to the 18S rRNA at nts 1132-1124. Ten linked copies of this 9nt sequence can increase IRES activity up to 570-fold in neuro-2a cells. The level of this Gtx IRES activity is up to 63-fold greater than that obtained by using the well characterized EMCV IRES when tested in the same assay system. The synergism of the linked 9-nt copies is reduced when spacingTable 3

between the linked copies are increased, suggesting that higher order RNA structures may play determinant roles in the IRES activity, in a way similar to how a transcriptional enhancer element functions [76].

**Table 3** Summary of host genes that are translated by the IRES mechanism. (adapted from Kozak et.al., 2001 [189])

| Gene | Changes in translation activity (by the respective IRES) vs controls | Reference |
|---|---|---|
| Apaf-1 | 8-10 fold increase | 84,236 |
| Bip | 2.6-15 fold increase, Synergism with La and PTB | 160,172,173 |
| DAP5 | 10 fold increase | 138 |
| FGF-2 | 5-35 fold depending on cell type | 13,325 |
| eIF4G | 5-42 fold increase | 113 |
| Gtx | 7-570 fold increase depending on IRES repeats | 76 |
| C-myc | 14-70 fold increase | 308,309 |
| VEGF | 4-60 fold increase | 145 |
| XIAP | 150 fold increase Possible synergism with La protein | 140-142 |

### *1.8-3 Apoptosis and IRES mediated translation initiation*

Apoptosis induction is an intriguing aspect of a CVB3 infection because it appears to be correlated to the process of viral gene expression. It is now accepted that coxsackievirus and other picornaviruses can induce apoptosis *in vitro* and *in vivo* [57]. Although previous investigation has found that this is in part due to the proteolytic cleavage of eIF4G (and its isoforms) by caspase 3 [356,357], the relationship between cap-independent translation initiation and the process of apoptosis was further demonstrated in three recently published papers concerning c-Myc, MKK6 and DAP5.

The c-Myc is a cellular proto-oncogene involved in very disparate cellular processes including proliferation, transformation and apoptosis [103]. The authors demonstrated that the c-Myc protein is still expressed by the cap-independent mechanism when more than 90% of cells are apoptotic [308,309]. The presence of the protein MKK6, which is a specific immediate upstream activator of p38 mitogen-activated protein kinase (MAPK), appears to increase the IRES-mediated translation of c-Myc. Thus, it is proposed that IRES-mediated translation initiation of the c-Myc during apoptosis is activated by the p38 MAPK pathway [335]. These data suggest that cap-independent translation initiation is an important and highly regulated alternative mechanism of protein expression.

In a related paper, a cellular IRES that functions specifically during apoptosis is observed in the translation initiation of DAP5 [138]. DAP5 is a 97 kDa protein which is homologous to eIF4G. It is cleaved during Fas-induced apoptosis, yielding an 86 kDa isoform. Interestingly, while the overall translation rate in apoptotic cells was reduced by 60-70%, the translation rate of DAP5 protein was selectively maintained. The authenticity of IRES-mediated translation initiation of DAP5 has been further confirmed by using a bicistronic plasmid construct

containing the 5'-UTR of DAP5 in the intercistronic space [138]. The experiments demonstrated that the translation initiation of DAP5 can depend on the cleavage status of the DAP5 protein in the cellular environment: the DAP5/p86 apoptotic form is more potent than the normal DAP5/p97 in stimulating IRES-mediated translation. Thus, a positive feedback mechanism is proposed for the translation of DAP5 during apoptosis [138]. Reflecting on our previous discussions, the process of CVB3 induced apoptosis and translation of the viral genome are probably interlinked and highly regulated. The cellular proteins that specifically bind to the IRES of CVB3 and mediate the regulation process remain to be discovered.

### *1.8-4 Transcription of Viral RNA*

Successful replication of the CVB3 virus involves synthesis of the viral capsid proteins (translation) and the transcription of the viral RNA (genome replication). The packaging of the genomic RNA into virions occurs late in an infection cycle and is prior to the release of progeny virions into the intercellular environment. At the present time, there is very limited knowledge of the mechanism and requirements of the process by which the genomic RNA is transcribed.

#### 1.8-4a Tertiary RNA structure of the 3'-UTR and CVB3 replication

In the CVB3 system, data from a mutational study strongly implicate a functional role of the 3'-UTR in viral replication. The CVB3 3'-UTR is a 99 nt long sequence starting from nt 7300 to 7399, followed by a poly-(A) tail of variable length [229,330]. Work by Melchers et al. demonstrated that formation of tertiary structure from the secondary stem-loops in the 3'-UTR is important in viral replication [229]. This tertiary RNA structure in the 3'-UTR is maintained by interactions between two of the three stem-loops that are present in the 3'-UTR (**Figure 10**). Failure to form such tertiary structure results in the phenotype of reduced replication at non-physiological temperature while the translation of viral RNA is unaffected. The mechanism of

how the tertiary structure mediates viral replication has not yet been discovered. Similar findings of the 3'-UTR in determining viral replication have been reported for Coxsackievirus A9 (CVA9) [235] . Analysis of a CVA9 mutant containing a single-base mutation in the 3'-UTR indicates that faulty tertiary RNA structures are related to replication defects. The mechanism of how the tertiary structure interaction can mediate viral replication remains elusive.

1.8-4b Requirement of host proteins in picornaviral replication

A common strategy of replication is proposed for all picornaviruses [8]. Thus, findings in the PV system may help our understanding of the CVB3 replication process. In the PV system, a cloverleaf structure in the proximal 5'-UTR region of the poliovirus forms a ribonucleoprotein (RNP) complex with host proteins and the polio 3CD protease / polymerase [8-10,339] . The importance of other 5'-UTR regions in viral replication of the PV system has been reported [50]. The formation of the RNP complex in the 5'-UTR of PV appears to be essential for positive sense RNA replication by serving as a double stranded RNA primer [2]. The efficiency of RNA replication in turn determines the specific tissue tropism and pathogenicity of the virus [79,242]. During replication, the RNP may involve interactions between stem loop structures in the 3' and 5' ends of the viral genome [9,10]. Several daughter strands may be replicated at the same time from one template [27]. The time of replicating each RNA molecule is estimated at about 45 seconds [27] and is believed to take place on smooth membranes [41,58,59,196]. Crude cellular extracts from HeLa cells, which also include cellular membranes, can support the replication of

**Figure 10. 3'UTR tertiary structure and kissing pair interactions**

Secondary and tertiary structure formation in the CVB3 3' UTR (nt 7300-7399). Stem loops are formed by nucleotide-nucleotide pairings while interactions among the indicated nucleotides on loops X and Y result in the formation of a kissing pair interaction (dotted lines). These structures were verified by Melchers et al., 1997. Interaction between nt. 7352/3 (G/A) to nt 7392/1 (C/U) are joined by dashed lines and indicated by arrows. Interactions of the poly-(A) tail with the region of stem loop X are indicated. Nucleotide sequences in the loop regions of stems Z, Y and X are indicated. Nucleotide 7352/3 and 7391/2 have been demonstrated to be critical for maintaining the tertiary structure (interaction between X and Y) which is in turn critical for the replication efficiency of the virus.
(Adapted from Melchers et al., J. Virol. 71, 686-696).

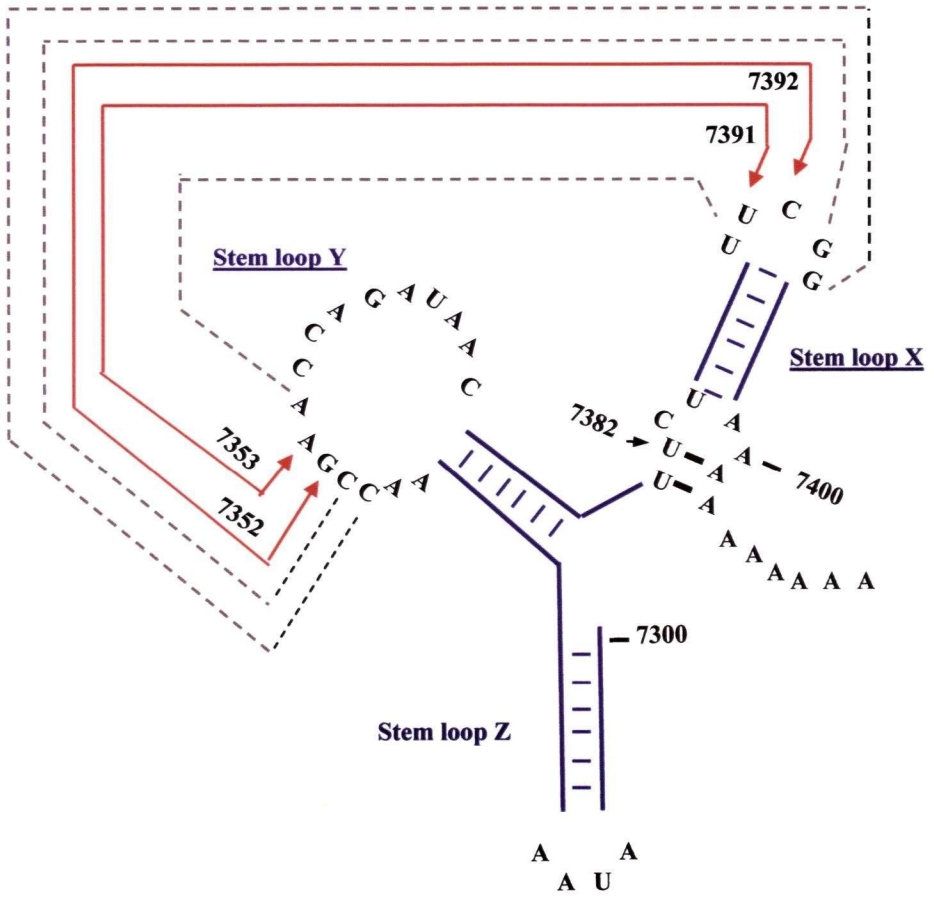

poliovirus in vitro [30]. Interestingly, fractionation of the extract will inhibit replication, and such inhibition can be overcome by addition of the soluble fraction from the extract [30]. Similarly, injection of a HeLa cell cytoplasmic extract into the oocytes of *X. laevis* is a pre-requisite for poliovirus replication in this otherwise non-permissive environment [111]. Therefore, it is believed that soluble host proteins in the cytoplasmic environment are critical to the process of RNA-dependent RNA transcription.

Using UV cross-linking techniques, three proteins have been observed to bind the PV 3'-UTR RNA: p105, p68 and p45 [328]. The 105 kDa protein appears to be nucleolin, which translocates into the cytoplasm upon infection. The functional significance of this interaction is unclear. The other two proteins remain unidentified. Together with data that implicate the tertiary structures of CVB3 3'-UTR in regulating replication, it is probable that the efficiency of the protein-3'-UTR RNA binding process may be a crucial determinant in viral replication. In the CVB3 system, there is currently no data reported for the host proteins that bind to the 3'-UTR.

## 1.9 Functional roles of host protein-CVB3 UTR interactions

As the infectious CVB3 virus particle carries no enzymatic molecules, host proteins and translational machineries will have to play an integral role in viral translation and or transcription. As discussed in the above sections, specific interactions between the host proteins and the CVB3 UTR sequences are most likely important in achieving the function of viral RNA translation and transcription. Although there is currently no data available with respect to the CVB3 system, studies in other RNA viruses have provided valuable data to understand the significance of interactions between host proteins and viral UTRs.

### *1.9-1 Participation of eukaryotic translation initiation factors*

Despite fundamental differences in the mechanisms of translation initiation that are utilized by the eukaryotic mRNA and picornaviral RNA, both processes are thought to be dependent on the well studied eukaryotic translation-initiation factors (eIF). Translation of EMCV RNA, for example, requires $tRNA^{met}$, 40S ribosome, eIF2 and 3, and eIF4F [271]. These eukaryotic translation factors are often modified by viral proteases during an infection, most likely in order to favor viral translation. At the present time, little is known about protein requirements in the translation of CVB3 RNA.

The translation initiation factors of interest can be summarized by the subunits that form the well studied eIF4F complex which includes eIF4A, B, E and G [120]. Binding of the eIF4F complex to the host mRNA is facilitated by the eIF4E subunit which recognizes the cap-structure [303]. The eIF4B is an mRNA binding protein [157,233] which also stimulates the helicase activity of the eIF4A [262]. Finally, eIF4G serves as the linker between eIF4A, B, E, and the 40S ribosomal subunit in the RNP-translation initiation complex [194,204,209,210]. A schematic representation of the translation initiation process in eukaryotic mRNA is presented in **Figure 11a**.

eIF4G is also an important molecule in the translation initiation of picornaviral RNA. eIF4G is a 175 kDa protein with multiple domains that bind other proteins and RNA molecules (**Figure 8**). Enterovirus proteases or FMDV leader proteases commonly sever the carboxyl-terminal domain, thus inhibiting interaction of eIF4E with the eIF4G complex [33,124,194,291]. Since there is no cap structure on picornaviral RNA, the function of eIF4E should not be necessary in the translation initiation of picornaviral RNA. Severing the eIF4E binding domain of the eIF4G has been suggested to directly cause inhibition of host protein synthesis during an infection [124,194].

**Figure 11a. Summary of steps in Cap-dependent translation initiation.**
Typical capped mRNA interact with eIF4E (step 1). Secondary mRNA structures are unwound by eIF4A. Formation of eIF4F complex occurs between the eIF4G, 4A, 4B, 4E with eIF4G as the central docking module (step 2). Pre-initiation complex includes the eIF3 unit which can bind eIF4G. Interaction with the 60S ribosomal subunit (not shown) forms the final 80S complex which scans the mRNA for the AUG start codon (step 3). (Adapted from Gingras, A. C., B. Raught, and N. Sonenberg. 1999. Annu. Rev. Biochem. 68:913-963).

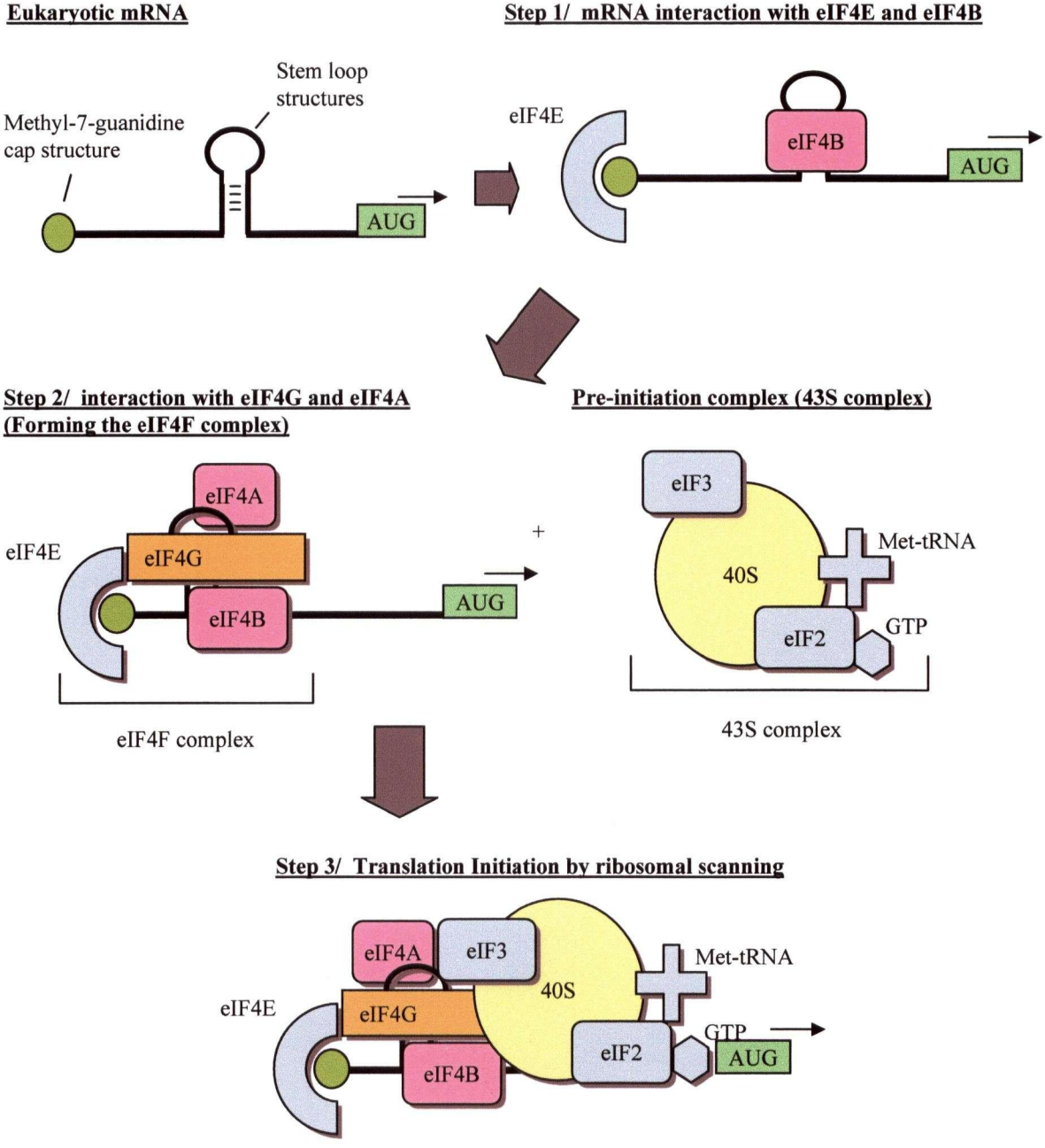

Binding of the central domain of eIF4G to the IRES of EMCV has been demonstrated [188]. Of note, eIF4A also exhibits binding to the EMCV IRES at a location close to the eIF4G binding site, indicating the importance of co-operation among the eIF4F subunits in mediating translation initiation of the picornaviruses. A schematic representation of the eIF4 factors in mediating picornaviral RNA translation via the internal ribosomal entry mechanism is presented in **Figure 11b**.

In addition to eIF4G, recent reports have indicated the role of the poly-(A) tail and poly-(A) tail binding protein (PABP) in enhancing the efficiency of translation initiation by interacting with the translation machinery [52,87,151,234,311]. It has been suggested that circularization of the EMCV RNA can occur by interaction of the 5'-UTR-IRES-eIF4G complex with the PABP-3'-UTR complex [290]. However, the contribution of the PABP protein to the model of circularized translation initiation in picornaviral system requires further investigation, as the eIF4G cleavage by viral proteases can also separate the PABP binding site (which is also located in the carboxyl-terminal domain) of eIF4G from its RNA binding domain. For the coxsackievirus system, interaction of eIF4 factors and the PABP proteins with the CVB3 RNA has not been verified.

### *1.9-2 Functional roles of the La autoantigen and PTB*

Besides the above mentioned translation initiation factors and other possible RNA binding proteins [46,146,147], two host proteins appear to play functional roles in the cap-independent translation of picornaviruses. The PTB and La autoantigen were among the first proteins characterized to bind to the picornaviral 5'-UTR and to stimulate the translation of a variety of RNA viruses [32]. Of note, interactions of these proteins with the viral RNA do not require

**Figure 11b. Current model of picornaviruses' IRES-mediated translation initiation.** Without a cap structure, the viral RNA requires the participation of other UTR binding proteins, such as La, PTB, PCBP and eIF4G (step 2). This protein-viral RNA complex can then interact with the ribosomal subunit, directly over its IRES location, possibly involving sequence complementation with the 18S rRNA (step 3). In type I IRESes (CVB3), the spacing between the authentic AUG and the IRES may be important in translation initiation, whereas the authentic AUG in type II and III IRES is often located inside the IRES sequence. The ribosomal scanning mechanism is not at play. Other less well characterized host proteins that bind to the 5' UTR are not demonstrated.

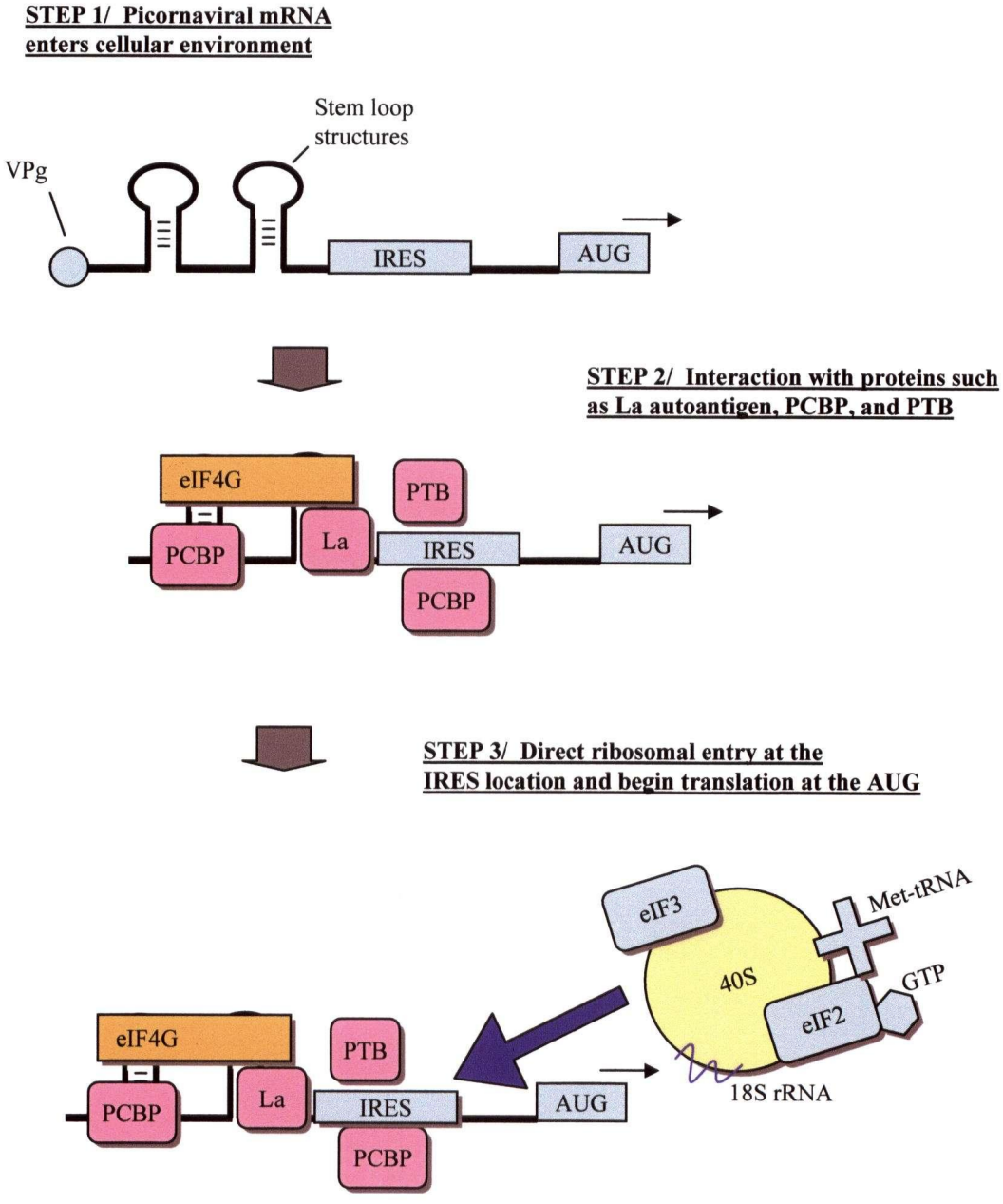

modifications by viral proteases. Thus, their natural presence in a cellular environment may be important to the initial stages of CVB3 translation and / or replication, before the successful expression of the viral proteases.

The La autoantigen is first discovered as a target of autoimmune recognition in patients with systemic lupus erythematosus and Sjorgren's syndrome [69,70]. It is a 408 amino acid protein that participates in a variety of RNA transcription activities including maturation of RNA pol III transcripts [121,122,253]. La protein contains an RNA recognition motif (RRM) within amino acids 1-194. The protein domain involved in the stimulation of translation was mapped to amino acids 1-293 [88]. Dimerization of La protein occurs in the physiological cellular environment which enhances its translation efficiency [88]. The domain spanning amino acids 293-348 has been shown to facilitate dimerization, suggesting that the function of dimerization can be independent of RNA interaction. During infection by PV, La protein is cleaved by the protease $3C^{pro}$ and is transported from the nucleus to the cytoplasm [301]. The cleaved La protein still contains amino acids 1-358 and thus the cleaved protein remains functional in RNA binding, translation stimulation and dimerization [301].

La protein is capable of interacting with the RNA of a variety of viruses, including the HCV [5], EMCV [174], sindbis virus [259], rubella virus [276], human parainfluenza virus-3 [96], HIV [72], and PV [312]. The La protein has also been reported to bind a variety of viral and non-viral RNAs, with a generally stimulatory effect on translation [89,96,153,266,313,320]. Pertinent to the study of CVB3, binding of La to the HCV RNA stimulates translation activity in a dose-dependent manner [153], while an optimal stoichiometric cooperation of La with PTB can enhance the activity of the EMCV IRES [174]. These data strongly suggest synergism among protein molecules and viral RNAs to form an optimal UTR-protein complex in order to mediate IRES-based translation

initiation. Differences in UTR sequences among different enteroviruses may require a different set of host chaperone proteins for their specific systems of translation initiation [92]. The expression of La autoantigen may be tissue-specific and dependent on cellular conditions [63]. Hence, the availability of the La protein in CVB3 infected cells may also play a role in determining the rate of expression of viral proteins and consequently the occurrence of cellular injury.

PTB is a cellular protein that normally functions as a splice regulator [203,267]. There are four RRMs in this protein. Like the La autoantigen, PTB can also exist as a dimer. Interaction of PTB with viral UTRs has been verified in poliovirus [131,135,136], EMCV [164], and FMDV [187], HCV [5,154], HIV [43] and Human T-cell leukemia virus -2 [44]. In general, PTB is capable of interaction with type I and type II IRESes [32]. Interaction with PV occurs in multiple locations including sites that contain determinants of neurovirulence [129]. There are numerous observations of the stimulatory effects of the non-cleaved PTB in IRES-mediated translation. The activity is often observed in cooperation with secondary protein or RNA molecules [130,131,147,174,187,320]. There is also a suggestion that the PTB activity may be virus-specific, as illustrated by the differential effect of PTB on the entero-/rhinovirus IRES elements (strong activity) [146,147] and the FMDV IRES (moderate activity) [329]. These observations further reinforce the assertion that an optimal complex of host proteins and viral UTRs specific to individual viruses are required for efficient translation initiation. As discussed earlier, the role of PTB in the pathogenesis of PV has been characterized as a possible switch between viral translation and genome replication [22]. The effect of PTB on the overall translation-stimulation decreases over time due to the cleavage of PTB by $3C^{pro}$ which increases with time, resembling a process that is governed by a negative feedback mechanism. Naturally, in a picornaviral system, the saturation of viral translation

products (virion proteins and various proteases) signals the need for the virus to focus on genome replication and to proceed towards viral packaging / dissemination. Thus, the overall functions of the PTB in picornaviral pathogenesis may be in both the translation and transcription of the viral genome [22]. Whether this applies to the CVB3 system remains to be studied.

### *1.9-3 Role of protein-RNA interaction in stimulating RNA transcription*

During the replication of PV, the RNA replicative complex contains several host proteins in addition to the viral 3CD protease/polymerase. These include the EF-1α [134], possibly poly(rC)-binding protein (known as PCBP or hnRNP E) [112] and Sam68 [225]. Sam68 is a host protein involved in cellular mitosis and this protein is transported to the cytoplasm during infection by PV. However, there is no firm evidence suggesting a functional role of Sam68 interaction with the replicative complex. On the other hand, EF-1α and hnRNP E appear to participate in positive strand RNA synthesis. Interestingly, EF-1α interacts with the UTR of two positive strand RNA viruses: west nile virus [45] and turnip yellow mosaic virus [162], although its exact role in RNA replication remains to be further investigated. Of interest, the hnRNP E binds to both the 5' end of the cloverleaf structure[112] and the IRES of the PV RNA [46]. Because the PV 3CD complex binds to a different location of the 5' cloverleaf structure and the hnRNP E is part of the complex, interaction of the hnRNP E at multiple sites in the PV 5'-UTR is thus proposed to serve as a bridge that brings together other protein complexes at distal regions of the 5'-UTR [46]. As discussed in the previous sections, proteins such as La and PTB either possess dimerization domains or bind to multiple sites of the PV 5'-UTR. Further work is needed to verify if these proteins also participate or affect the process of RNA transcription by the 3CD complex in a manner similar to that of the hnRNP E protein. Interestingly, La protein interacts with HIV RNA in the TAR region (tat-binding site), an RNA sequence of the HIV that binds

multiple cellular proteins and serves to regulate the switching between transcription and translation of the HIV RNA [72,313].

### *1.9-4 Characterization of other UTR binding proteins*

Using biochemical methods, such as UV cross-linking and mobility shift assays, several other cellular proteins have been reported to bind to viral IRES. These proteins include a 97 kDa protein 'unr' (for upstream of N-ras) and a 38 kDa protein (known as unrip, unr-interacting proteins), both of which can stimulate the activity of the rhinovirus IRES [146]. The unr-unrip complex can also correct aberrant translation initiation in PV [146]. Interestingly, recombinant unr acts synergistically with recombinant PTB to stimulate translation initiation by the rhinovirus IRES, but the same unr-PTB synergism can not be observed with the PV IRES [146]. Thus, the observation highlights the co-operative nature of UTR-binding proteins and specific RNA sequences in effecting translation and or transcription.

In summary, several important host proteins appear to play major roles in the regulation of picornaviral translation and transcription by interacting with the UTR sequences. There is very limited knowledge of other additional host proteins that participate in the processes. Besides the limited number of identified host proteins, one inadequacy of the current knowledge on protein – picornaviral UTR interactions is the lack of data on the specificity and affinity of the interactions. Upon cellular entry, the few copies of viral RNA will have to compete against the vast majority of cellular mRNA for interaction with RNA-binding proteins. In this respect, the affinity and specificity of interactions between the viral RNA and the host proteins are two critical factors in evaluating the functional importance of the observed interactions. A high specificity of interaction between the host and the viral RNA (UTR sequences) is required to ensure successful competition against host mRNA for protein translation. On the other hand, a

high affinity of interaction will contribute to the stability of the RNA-protein complex to allow for the initiation of translation and or transcription events. From this logic, interactions that have low specificity and affinity are less likely to be significant in the pathogenesis of the virus. At present, most studies that characterize UTR binding proteins do not quantify or address the questions of specificity or affinity.

### *1.9-5 Research Focus*

As discussed above, the 5' and 3'-UTR of the CVB3 mediates the expression and replication of the viral genome. The efficiency of these two processes can determine the extent of cellular injuries and overall tissue tropism of the virus. Among all enteroviruses that cause myocarditis, CVB3 has evolved to be specifically virulent in cardiomyocytes. Several lines of studies strongly implicate that the 5'-UTR sequence of the virus contains determinants of cardiovirulence, although the mechanism is still a mystery. As well, the tertiary structures of viral 3'-UTR are critical to the replication of the virus. RNA sequences alone can not effect phenotypic observations. Rather, it is their interactions with host proteins that result in the processes of translation initiation (via the IRES mechanism) and genome transcription (via the host-viral protein RdRP complex). The significance of these processes have been studied for CVB3 and other related enteroviruses. However, the specific interactions of host proteins with the CVB3 5' and 3'-UTR sequences and their potential correlations with the virulence of the virus remain to be discovered. In particular, there is no studies that focus on the presence or absence of these UTR-interacting proteins in CVB3-susceptible and non-susceptible cell types. Further, these UTR-interacting proteins can potentially interact with various localized RNA structures of the UTRs to result the various phenotypic observations of tissue tropism and infectivity. Therefore, in my dissertation, I focused on the study of three major issues:

1. Verification of specific interaction between host protein-viral UTR sequences.
2. Characterization of these interactions in the context of tropism, viral protein translation, and genome transcription.
3. Assessment of the significance of these protein – UTR interactions in the process of viral pathogenesis.

# CHAPTER II HYPOTHESIS AND SPECIFIC AIMS

The central hypothesis of this work is that the ***interactions of host proteins and coxsackievirus B3 untranslated regions are specific and correlate with the viral tissue tropism, replication and translation initiation.***

The following **specific aims** are addressed experimentally:

Aim 1. To demonstrate the presence of specific interactions between cellular proteins and CVB3 UTRs.

Aim 2. To determine whether specific interaction(s) can correlate with the tissue tropism of CVB3 in the A/J mouse model.

Aim 3. To determine the molecular weights of UTR-binding-HeLa cell proteins.

Aim 4. To determine whether HeLa cell protein-UTR interaction(s) can correlate with the CVB3 mutations that inhibit viral replication.

Aim 5. To determine the biochemical characteristics of the interaction between the 5' and 3'-UTR sequences and the La autoantigen.

# CHAPTER III RESEARCH QUESTIONS AND STRATEGY

The ***questions*** relevant to the hypothesis and specific aims are:

1) How specific are the interactions between host proteins and viral UTR sequences? Are the mobility shift / UV cross-linking assays effective in determining the nature of the interactions? (e.g. the sensitivity in distinguishing different specificities and the resolution in the MWs of the binding proteins.)

2) By using the UV cross-linking technique, is it possible to identify a reasonable number of unique targets that correlate to the determinants of tissue tropism and the processes of viral translation and replication?

3) How can biochemical characterizations be used to infer functional and mechanistic information of a protein-UTR interaction?

To answer these questions, I have conducted my research with the strategy described in **Figure 12a**. Results and discussion of the experiments are organized into two chapters: *Identification of UTR Binding Proteins* (**Chapters IV**) and *Biochemical Characterization of the La Protein–UTR interactions* (**Chapter V**). Details of the materials and methods utilized in these experiments are presented in **Chapter VII**.

**Figure 12a The overall strategy employed in my dissertation**

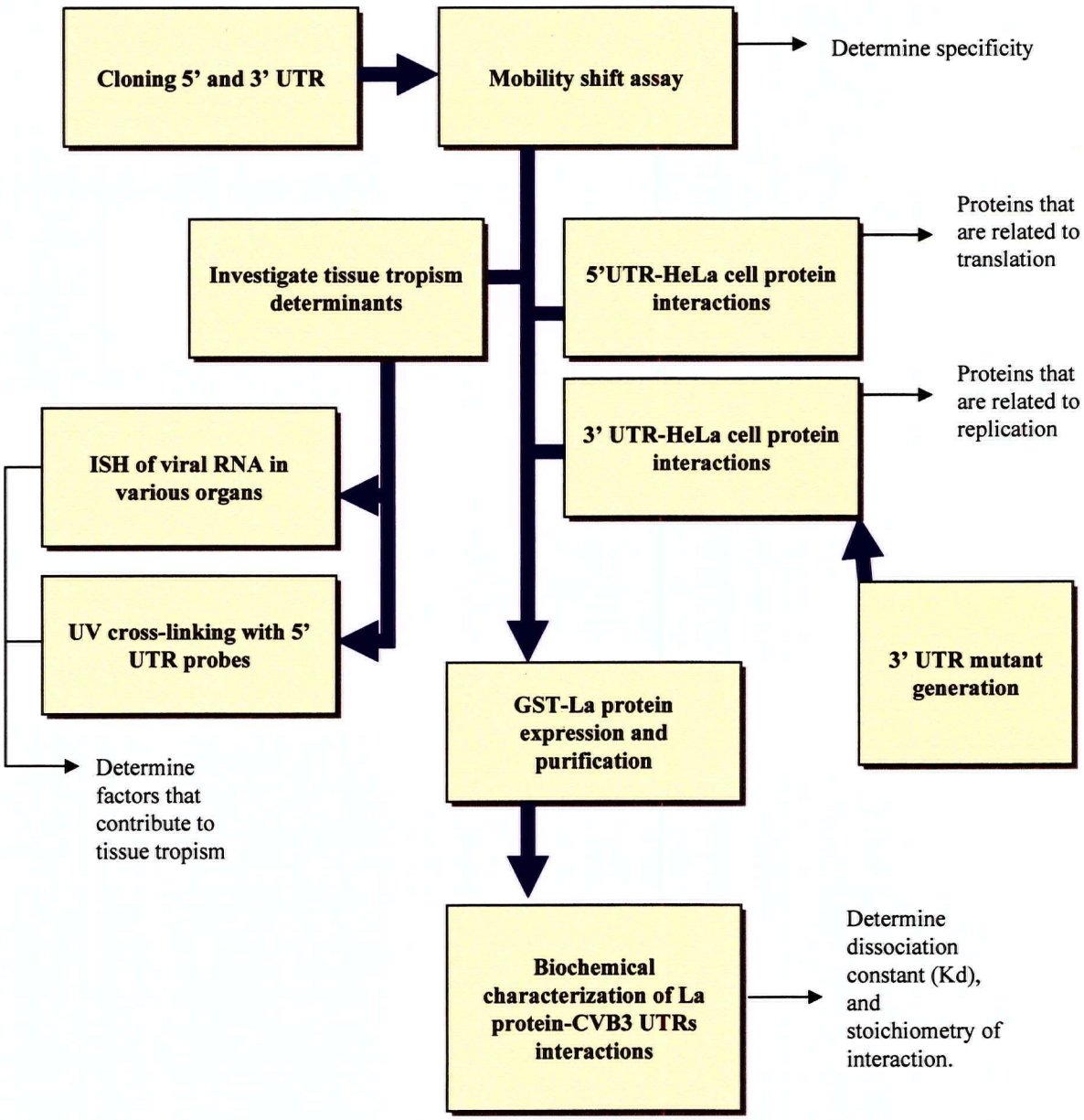

# CHAPTER IV

# IDENTIFICATION OF SPECIFIC CVB3 UTR-BINDING PROTEINS

Prior to my studies, there was no report on the subject of host protein - CVB3 UTR interactions. Also, the use of UV cross-linking and mobility shift assays in the detection of RNA-binding proteins had met with limitations in two aspects: the determination of specificity and the resolution of MW. Further, the different sequences of the 5' UTR appear to be differential in their functional significances. The proteins that bind to such sequences and possibly mediate the specific functions have not been investigated. Thus, in my studies, I began by sub-cloning the viral UTR sequences. The overall goal is to identify specific CVB3 UTR-binding proteins in HeLa cells and A/J mouse tissues, and to correlate some of these interactions with pathogenic attributes of the virus.

## 4.1 EXPERIMENTAL STRATEGIES

***Mobility shift assay and probe synthesis***

Mobility shift assays were conducted to demonstrate the presence of specific interactions between cellular proteins and CVB3 5' and 3'-UTRs (Aim 1). Proteins from non-infected HeLa cell lysates (nuclear and cytoplasmic) were prepared following procedures described in **Chapter VII** (Materials and methods). The concentration of proteins was determined by standard Bradford assays, and lysates were stored at -80 °C in 1 ml aliquots (~ 2.5 mg/ml). RNA molecules of the viral UTRs were synthesized from linearized plasmid templates by *in vitro*

transcription. Plasmid templates carrying sequences of the CVB3 5'-UTR were created by PCR cloning. Detail of the primers and PCR conditions are listed in **Chapter VII**. In brief, the CVB3 5'-UTR sequences of nt 1-209, 210-529, 530-630 were sub-cloned, based on the 5'-UTR secondary structures (**Figure 9**). As discussed, extensive secondary stem-loop structures have been predicted for the 5'-UTR. Secondary RNA structures are often domains of recognition in protein interactions. As a result of this consideration, sequence nt 1-209 was sub-cloned to preserve the first four stem loops (**Figure 9**) and nt 210-529 was sub-cloned to preserve the major stem loops E and F. On the other hand, the functional significance of the sequence nt 529-630 was considered more important than the preservation of complete stem loop structures. Previous mutational studies revealed that this is the minimal sequence required for the CVB3 IRES activity [349]. Thus, this exact sequence was sub-cloned.

DNA fragments of these 5'-UTR sequences were produced by PCR reactions and directly cloned into T/A vector (PCR 2.1, *Invitrogen*). Positive (sense) and negative (antisense) sequences of the 5'-UTR RNA were produced from linearized recombinant T/A vectors by *in vitro* transcription reactions, with the appropriate restriction and transcription enzymes (**Figure 12b**). In a similar fashion, the 3'-UTR of the CVB3 was sub-cloned into the T/A vector. The sequence nt 7299-7399+ 33 bases of adenosine [poly-(A) tail, artificially included into the PCR primer)] was sub-cloned (total 133bp). Again, sense and antisense RNA sequences were produced from this recombinant vector. **Figure 12b** illustrates the cloning scheme for the 5'-UTR and **Figure 12-c** illustrates the cloning scheme for the 3'-UTR.

**Figure 12b. Sub-cloning of the CVB3 5' UTR.**

Secondary stem-loop structures of the 5' UTR is shown, with nucleotide sequences indicated by numbers (not drawn to scale). DNA fragments of the three 5' UTR regions (nt 1-209, 210-529 and 530-630) were generated by PCR and inserted into the T/A vectors*. Orientations of inserts with respect to the transcription promoters were determined by DNA sequencing. Restriction enzyme sites utilized for linearization of the plasmids are also indicted.

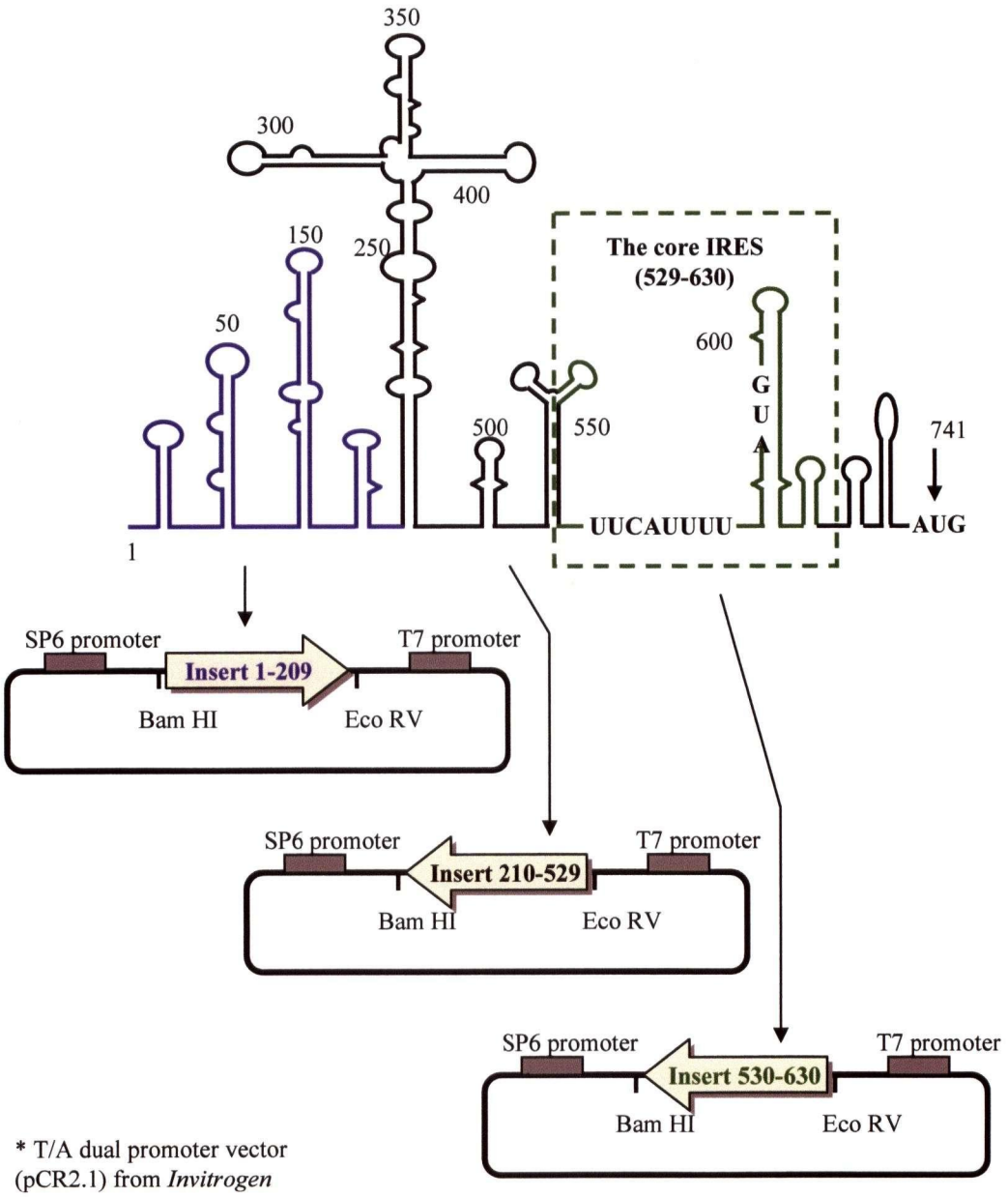


* T/A dual promoter vector (pCR2.1) from *Invitrogen*

**Figure 12c. Sub-cloning of the CVB3 3' UTR.**

Secondary structure of the 3' UTR is shown, with nucleotide sequences indicated by numbers (not to scale). PCR products of the respective 3' UTR sequences are ligated into PCR II vectors (*Invitrogen*). Orientation of the inserts with respect to the transcription promoters was determined by DNA sequencing. Restriction enzyme sites utilized for linearization of the plasmids are indicted. Mutations (mt) was indicated at the specific nucleotide sequences.

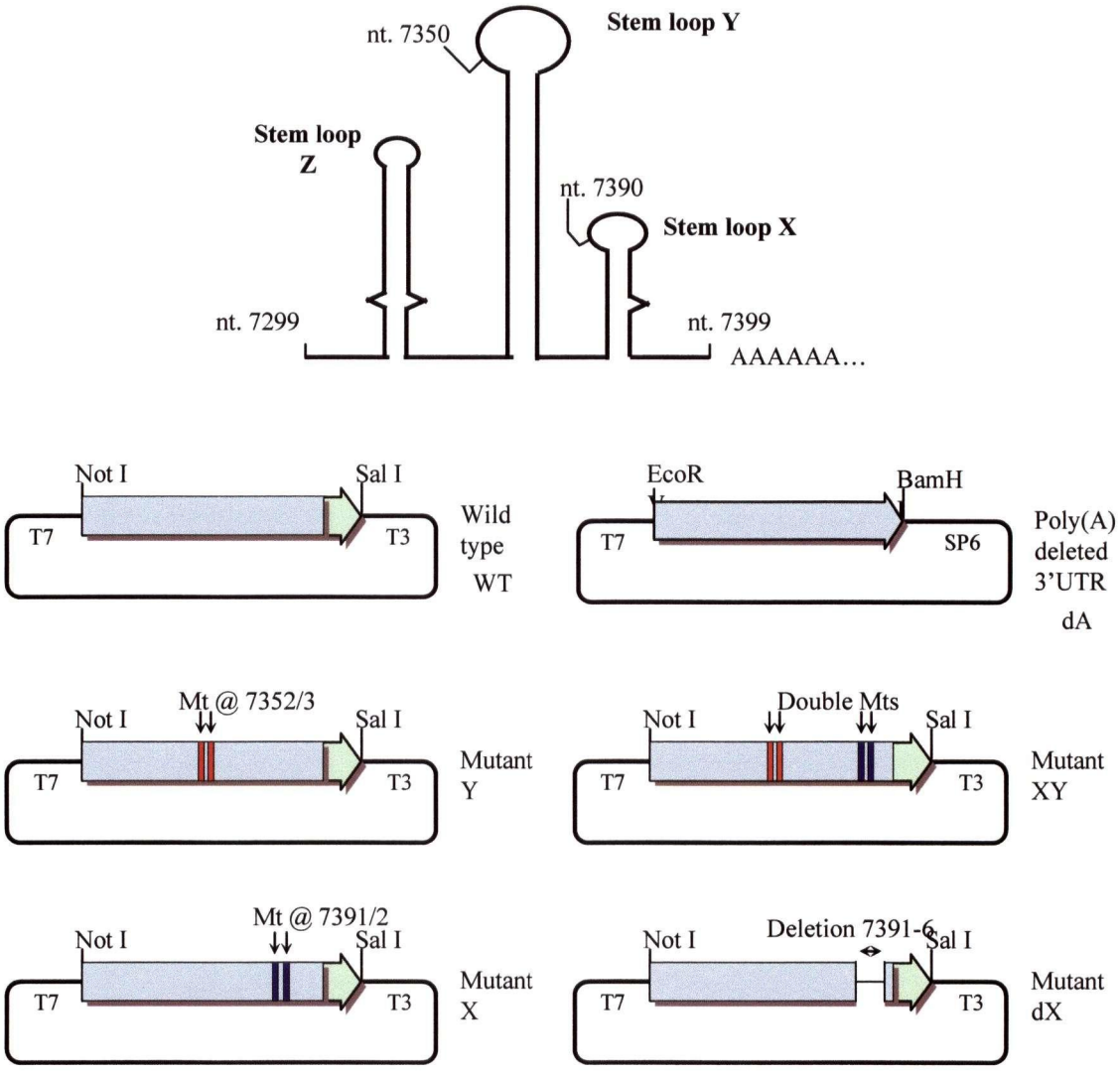

In the mobility shift assays, a radiolabeled RNA transcript (probe) of each UTR sequence was mixed with HeLa cell protein lysates in reaction buffer (**Chapter VII**), and incubated at 37°C for 10 min. The host proteins in the HeLa cell lysate that bound to the UTR were expected to form protein-radiolabeled-RNA complexes. To determine the specificity of interactions, non-labeled RNA of the same sequence to each of the corresponding probes was added at high molar excess ratios (20-250x) prior to addition of the respective probe. In addition, as a negative control, yeast tRNA was added to the reaction at the same molar excess ratios as the non-labeled RNA. Yeast tRNA was chosen because its secondary structures resemble those predicted for the CVB3 5' and 3'-UTRs, and interaction of yeast tRNA with HeLa cell proteins should not be physiologically significant.

The reaction products were analyzed by a non-denaturing poly-acrylamide gel electrophoresis (PAGE). The gel was fixed, dried and examined by autoradiography. Thus the distribution of the probes in its free form (fast migrating) or in protein complexes (slow mobility, 'mobility shift') could be distinguished. The presence of specific interaction would be concluded when the mobility shift of the probe was dependent on the amount of non-labeled competitor RNA of the same sequence but not the yeast tRNA. **Figure 12d** summarizes the strategy applied in the mobility shift experiments.

**Figure 12d. Determination of specific interaction.**
Radiolabeled RNAs (probes) and protein lysate were allowed to interact (**1**). Interactions resulted in RNA-protein complex formation that exhibited a slower electrophoretic mobility (**2**) than the free non-interacting probes (**3**). Non-denaturing gels and autoradiography were used to analyze the interactions. Addition of non-labeled RNA of the same sequence served as specific competitor, while yeast tRNA was used as negative control (**4**).

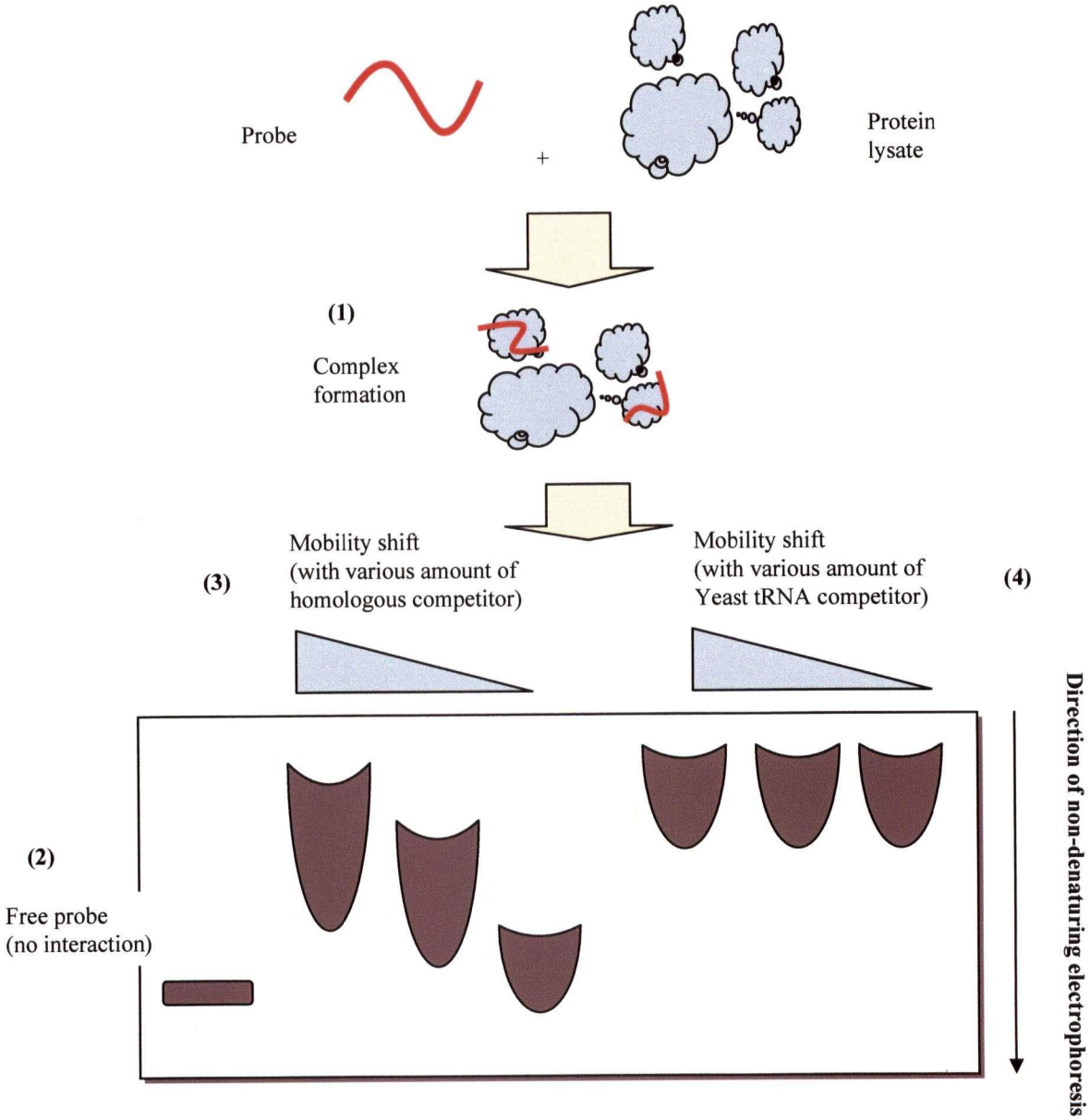


Autoradiograph of radioactivity
(Mobility shift/ complex formation is rescued only by homologous RNA)

***Correlation between protein-UTR interactions and viral infectivity in A/J mouse organs.***

To determine whether specific protein-UTR interactions correlate with tissue tropism of CVB3 in the A/J mouse model (Aim 2), I investigated correlations between the following two observations:

1) the *in situ* hybridization (ISH) of viral genome in organs of A/J mouse;

2) the respective patterns of protein-5'-UTR interactions in the organs.

The A/J mouse was chosen because it has been a well established model from which much data of CVB3-induced myocarditis was derived. Various A/J mouse organs also display significantly different but often interesting patterns of susceptibility to the CVB3 virus. The patterns of protein interactions between organ proteins of the A/J mouse and the 5'-UTR was a focus of my study because:

1) CVB3 5'-UTR has been demonstrated to stimulate viral translation by the IRES mechanism.

2) cardiovirulent determinants have been mapped to the 5'-UTR.

The background assumption was that the efficiency of CVB3 translation initiation was dependent on protein-UTR interactions, and the presence of these interactions in different cellular environments can lead to the specific patterns of CVB3 tissue tropism in A/J mice. Thus, the goal of this investigation is to identify targets that are important in the regulation of the CVB3 translation initiation and at the same time relevant to the development of disease in specific cellular environments. A schematic representation of the experimental design is shown in **Figure 12e**

**Figure 12e. Correlation between viral infectivity and protein-RNA interaction.**
The pattern of viral load in each organ of infected A/J mice is detected by *in situ* hybridization. Corresponding lysate of the organ from uninfected mouse is tested for interaction with the 3 probes of the 5' UTR via UV cross-linking method. Possible correlation of viral titre and protein interactions were thus investigated.

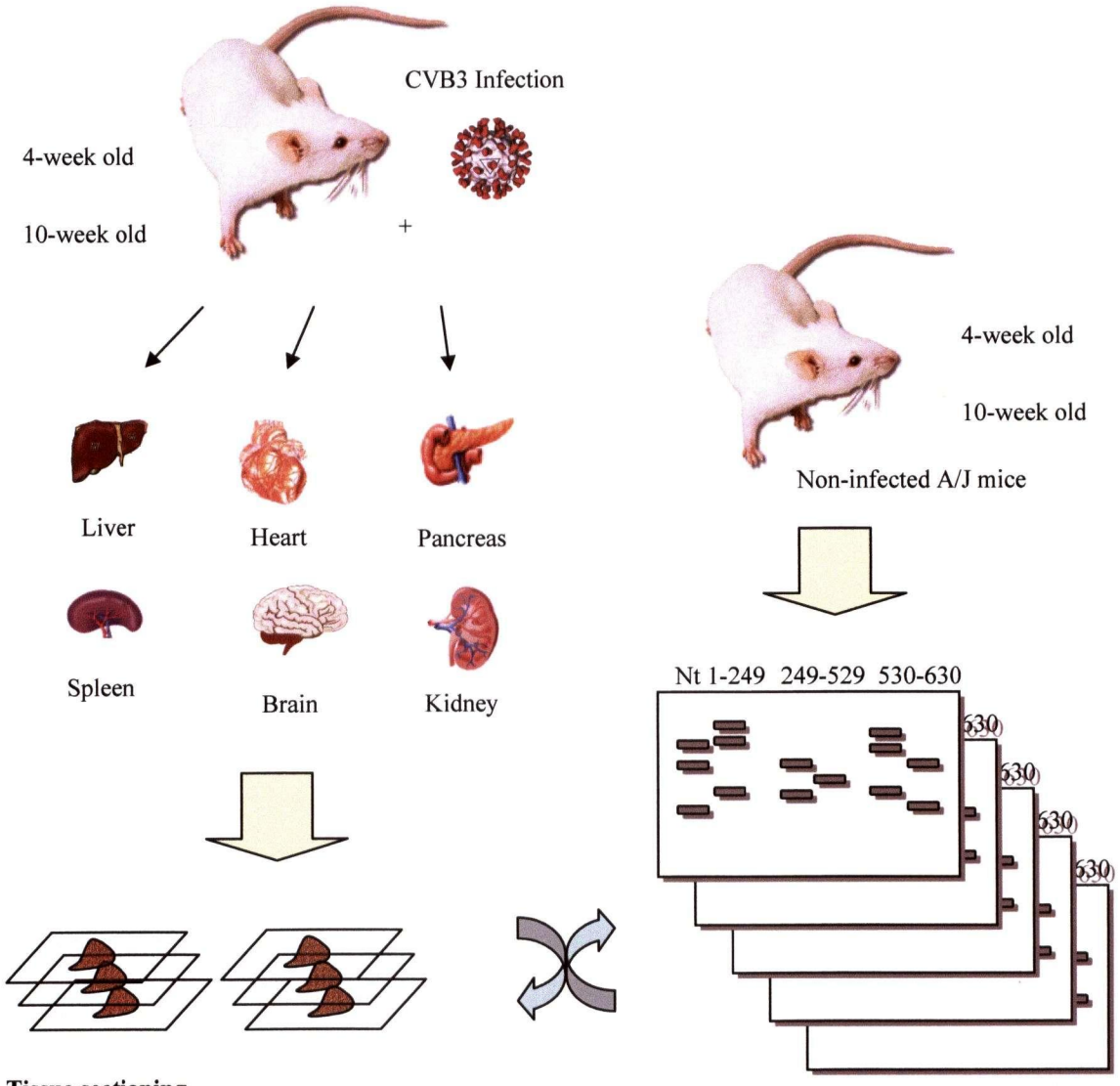


**Tissue sectioning**
ISH of viral genome
One representative image per organ per age group

**UV Cross-link profile**
*Non-infected Lysate* vs three pairs of 5' UTR probes (sense and antisense)
One profile per organ per age group

***In situ hybridization of viral genome.***

To acquire data on viral infectivity in various mouse organs, adolescent (4-week-old) and adult (10-week-old) A/J mice were infected by intraperitoneal injection of $1x10^5$ plaque forming unit (pfu) of myocarditic CVB3 (Kandolf) and euthanized on day 4 post infection (p.i.). The heart, liver, kidney, pancreas, brain and spleen were fixed and frozen in 4% paraformaldehyde. Organ lysates were obtained by a standard method (**Chapter VII**) and 8 μm sections of the fixed organs were used for ISH. Viral negative sense probe sequence was labeled with digoxigenin-11-uridine-5'-triphosphate DIG-11-UTP and signals were detected with BCIP /NBT substrate / Carmalum (SIGMA). Representative images of the sections under light microscopy were captured.

***UV cross-linking between radiolabeled 5'-UTR RNA and its binding proteins.***

To determine the MW of UTR binding proteins, the method of UV cross-linking was applied. Radiolabeled sense and antisense 5'-UTR RNA of sequences nt 1-209, 210-529 and 530-630 were synthesized by *in vitro* transcription. Protein lysates from the respective mouse organs were incubated with the radiolabeled probes under conditions as described in the mobility shift assay. After the interaction, the reaction was exposed to UV light which induced chemical bond formation between UTR binding proteins and probe RNA, thus covalently linking radioactive RNA to the UTR-binding proteins. Following UV exposure, unbound probe and non-interacting regions of the probe were digested by RNase A so that subsequent analysis of the reaction by denaturing SDS-PAGE would separate proteins according to their native MWs. A schematic representation of the UV cross-linking procedure is presented in **Figure 12f**. Each SDS PAGE was fixed, dried and analyzed by autoradiography. One profile of protein-UTR

interaction for each lysate was therefore generated. Specifically, I searched for differences that could correlate with the infectivity (ISH of viral genome) in the respective organs.

**Figure 12f. UV cross-linking methodology.**
Radiolabeled RNA of the UTR (probe) were incubated with protein lysates under standard conditions (**1**). Interactions are covalently linked by UV exposure (**2**). Excess and non-interacting probes of the probe is digested by RNaseA (**3**). Thus, only UTR-binding proteins are labeled. Protein mix is analyzed by SDS PAGE and autoradiograph (**4**). Molecular weights were estimated by a concurrently loaded marker.

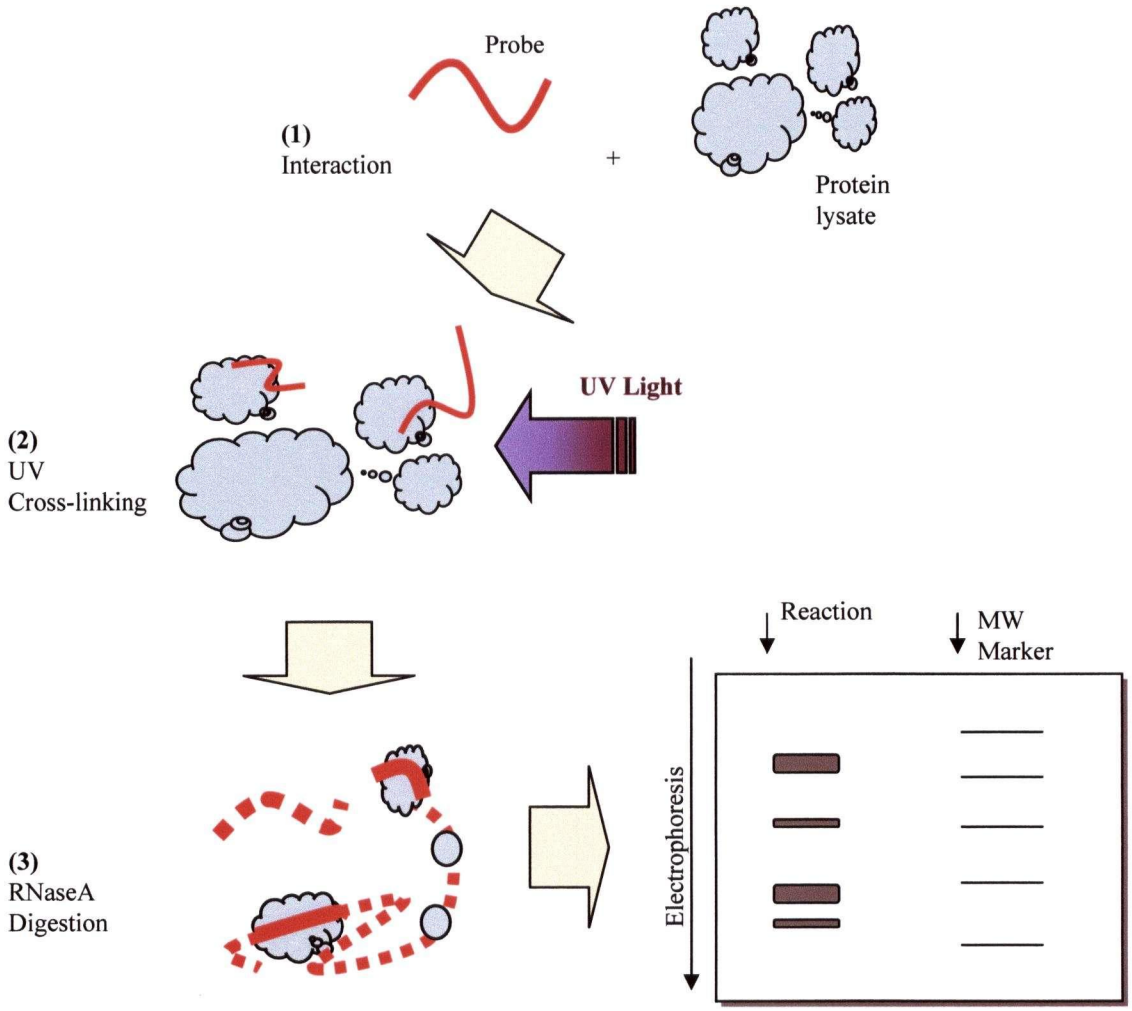

***Competitive UV cross-linking.***

Competitive UV cross-linking was performed to determine the specificity of UTR binding protein. Clones from aim 1 were used to produce 5'-UTR RNA transcripts. Both radiolabeled (probe) and non-labeled RNA (competitor) of the respective sequences were produced by *in vitro* transcription. The pattern of UV cross-linking between radiolabeled probe and HeLa cell proteins were compared to the reactions in which non-labeled RNA (of the same sequence) were added as competitors. Non-labeled competitor RNA was added to the reactions at various molar excess ratios prior to the addition of the radiolabeled probe. The non-labeled RNA would thus compete specifically against the radiolabeled probe for interactions with the same set of UTR-binding proteins. (note: It was experimentally determined that the order of the addition of non-labeled/ labeled probe to the reactions had no observable effect on the final protein complex formation). For interactions that are specific and not random or weak RNA associations, significant reduction in the radioactivity of the protein complex would be expected with increasing amounts of non-labeled competitor. Thus, this method can differentiate the specific and non-specific 5'-UTR-protein interactions that are detected in the normal UV cross-linking experiments.

***Construction of the 3'-UTR mutants.***

As mentioned earlier, mutations at the 3'-UTR inhibit viral replication. This may be due to the disruption of protein-RNA interactions which play important roles in translation and / or transcription. To confirm this speculation, protein-RNA interaction assays using the wild type and mutated 3'-UTR probes were performed (Aim 4). The 3'-UTR mutants were constructed based on previous reports regarding the crucial nucleotides in the 3'-UTR which maintain the

wild type tertiary structures (between stem loops Y and X, **Figure 10**). Mutations in those sequences led to disruption of tertiary structures and subsequently, inefficient replications [229]. The primers and conditions with which the cloning was performed are listed in **Table 7 (Chapter VII)**.

In addition to the tertiary structural mutations, I have created a new 3'-UTR clone to investigate the functionality of the viral poly-(A) tail sequence. In this clone, the wild type 3'-UTR sequence was preserved without the poly-(A) tail. In summary, six different CVB3 3'-UTR sequences were generated:

1) wild type with poly-(A) tail, **Clone WT.**
2) wild type without poly-(A) tail, **Clone dA.**
3) mutation in stem loop X (nt 7391/2), **Clone X.**
4) mutation in stem loop Y (nt 7352/3), **Clone Y.**
5) compensatory mutations (replication efficiency was partially rescued), **Clone XY.**
6) deletion mutation of loop X (nt 7391-6), **Clone dX.**

**Figure 12c** illustrates the strategy of constructing the 3'-UTR mutants. The plasmid templates of these mutants were used in the preparation of RNA probes for the UV cross-linking assays.

## 4.2 RESULTS

***Specificity of HeLa protein-CVB3 UTR interactions (aim1).***

We measured mobility shifts of the $^{32}$P-labeled 5'-UTR probes in the presence of HeLa cell proteins and various competitor RNAs. Data for the mobility shift assays are presented in **Figure 13a-d**. In each of these figures, the integrity and mobility of the free probe is shown in lane 1. Formation of protein-probe complex (**Co**) results in changes of the electrophoretic mobility of the probes under non-denaturing conditions. The specificity of the complex formation was tested by adding various amounts of non-labeled RNA of the same sequence (competitor RNA). Competitor RNAs at the indicated molar excesses were effective in inhibiting protein-probe interactions: In all the experiments (**Figure 13a-d**), competitor RNAs reduced the amount of protein-probe complex (**Co**) (lane 2-4), and progressively restored the normal mobility of the labeled RNA probes in a dose dependent manner. This contrasted to the findings where yeast tRNA was used: at the same molar excess ratios, the mobility and amount of protein-probe complex remained unaffected by the yeast tRNA. This suggests that the interactions between the HeLa cell proteins and the CVB3 UTR regions are specific.

In the case of the 5'-UTR nt 530-630 (**Figure 13c**), adding competitor RNA at high molar excess (lane 5) resulted in the detection of two major bands of protein-complexes. Similar band-like patterns were also observed in the case of the 3'-UTR sense probe (**Figure 13d**, left panel). A possible cause of this aggregation like phenomenon may be related to mode of interactions: While some protein-UTR interactions are reversible and competitive, specific

UTR-interacting proteins may exhibit a mechanism of co-operative binding to the RNA molecules, such that when the presence of additional competitor RNA enhances the formation of the specific protein-RNA complex, leading to observation of major bands.

**Figure 13a. Mobility shift of labeled 5' UTR probe nt 1-209.**
The probe (**P**) alone is shown in lane 1. Significant mobility shifts of the protein-probe complexes are observed in lane 2, indicated by (**Co**). Such protein-probe interactions could be competed when identical non-labeled RNA was added to the incubation, at 20x, 50x and 100x molar excess (lane 3, 4 and 5 respectively). Yeast tRNA molecules was added in lane 6, 7 and 8 as non-specific competitors, at 10x, 50x and 100x mass excess ratios. Complex formation was competed for only by the use of homologous non-labeled RNA.

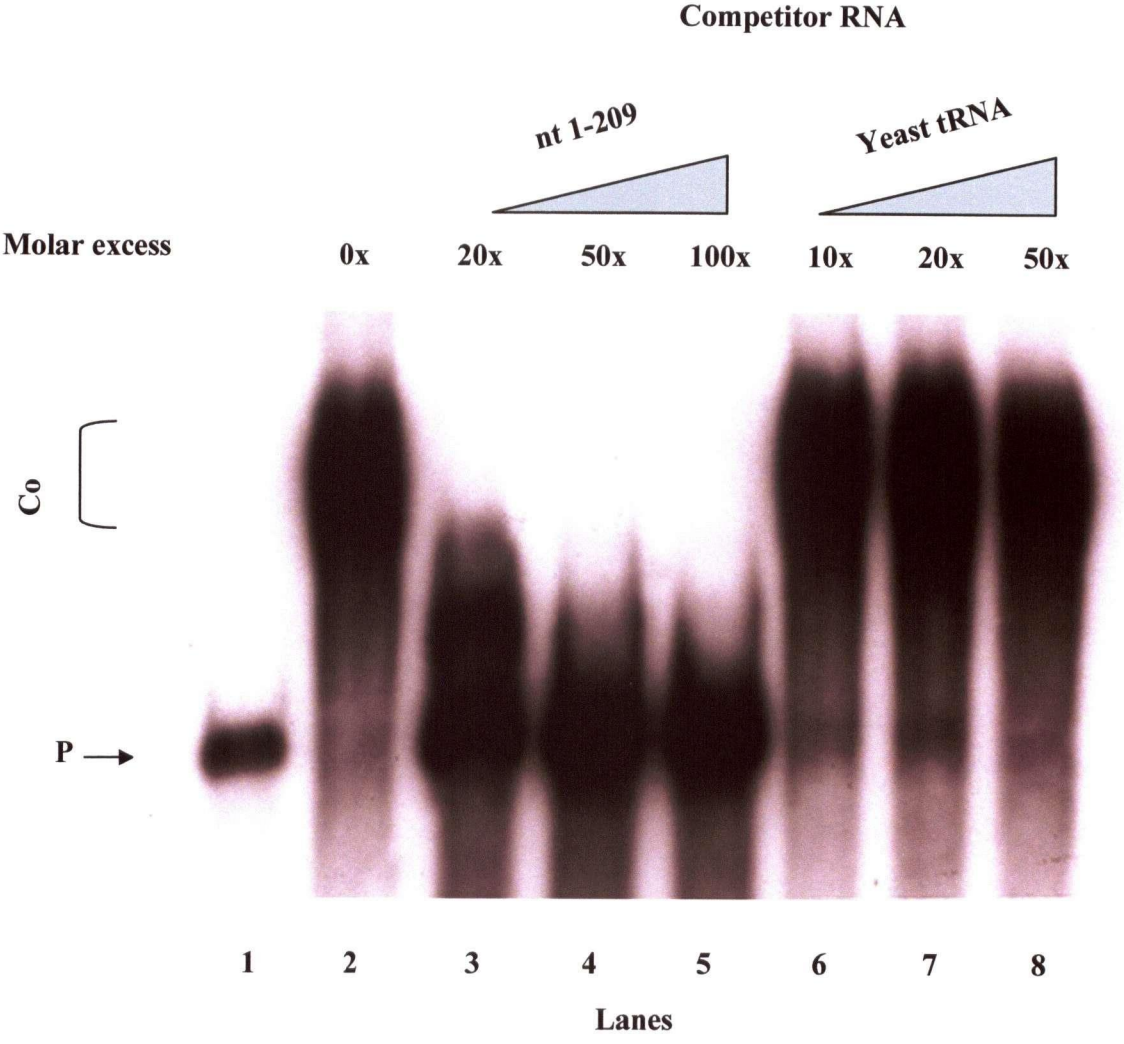

**Figure 13b. Mobility shift of labeled 5' UTR probe nt 210-529.**
The probe (**P**) alone is shown in lane 1. Significant mobility shifts of the protein-probe complexes are observed in lane 2, indicated by (**Co**). Such protein-probe interactions could be competed when identical non-labeled RNA were added to the incubation, at 20x, 50x and 100x molar excess (lane 3, 4 and 5 respectively). Yeast tRNA molecules was added in lane 6, 7 and 8 as non-specific competitors, at 10x, 50x and 100x mass excess ratios. Complex formation was competed for only by the use of homologous non-labeled RNA.

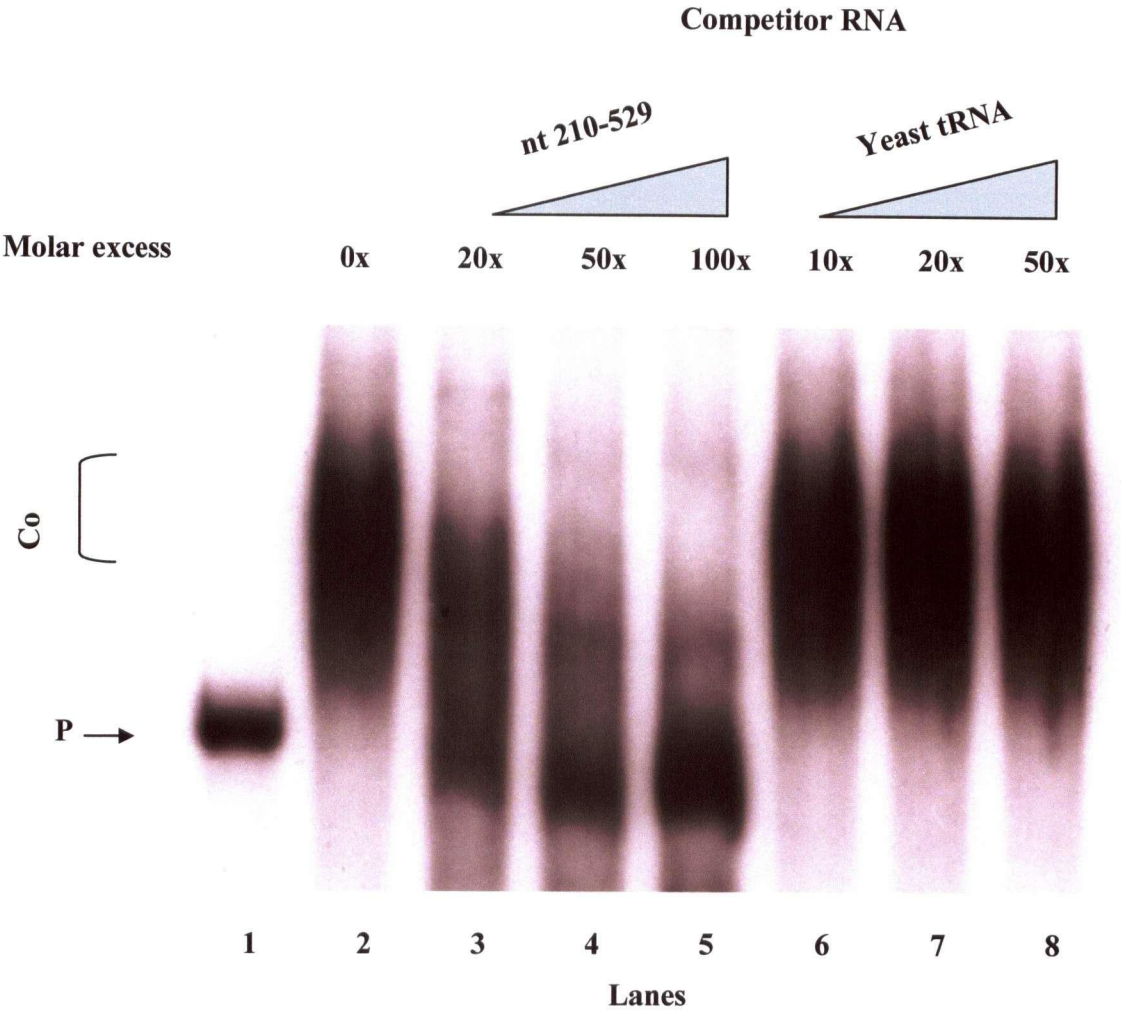

**Figure 13c. Mobility shift of labeled 5' UTR probe nt 530-630 (IRES).**
The probe (**P**) alone is shown in lane 1. Significant mobility shifts of the protein-probe complexes are observed in lane 2, indicated by (**Co**). Such protein-probe interactions could be competed when identical non-labeled RNA were added to the incubation, at 20x, 50x and 100x molar excess (lane 3, 4 and 5 respectively). Yeast tRNA molecules was added in lane 6, 7 and 8 as non-specific competitors, at 10x, 50x and 100x mass excess ratios. Complex formation was competed for only by the use of homologous non-labeled RNA.

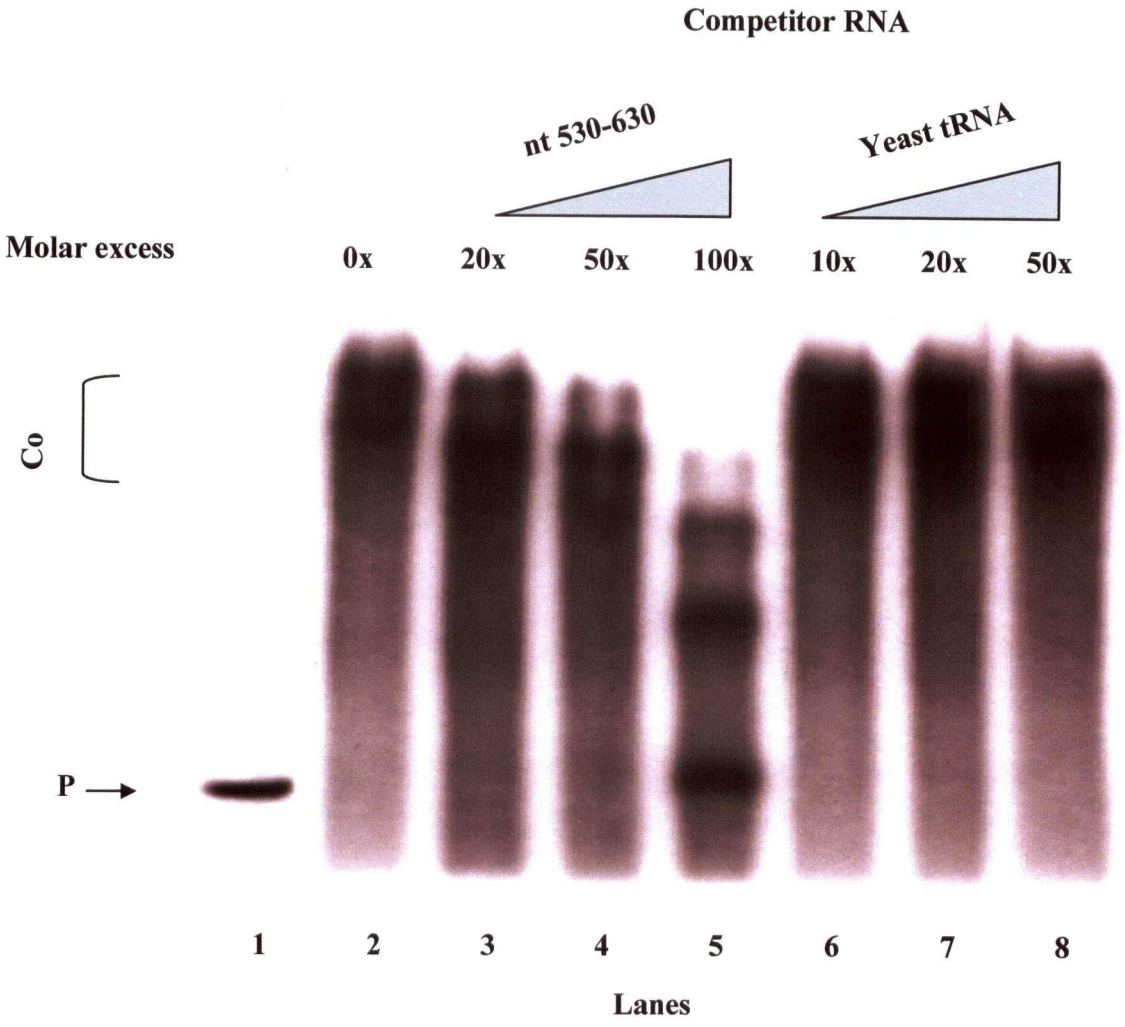

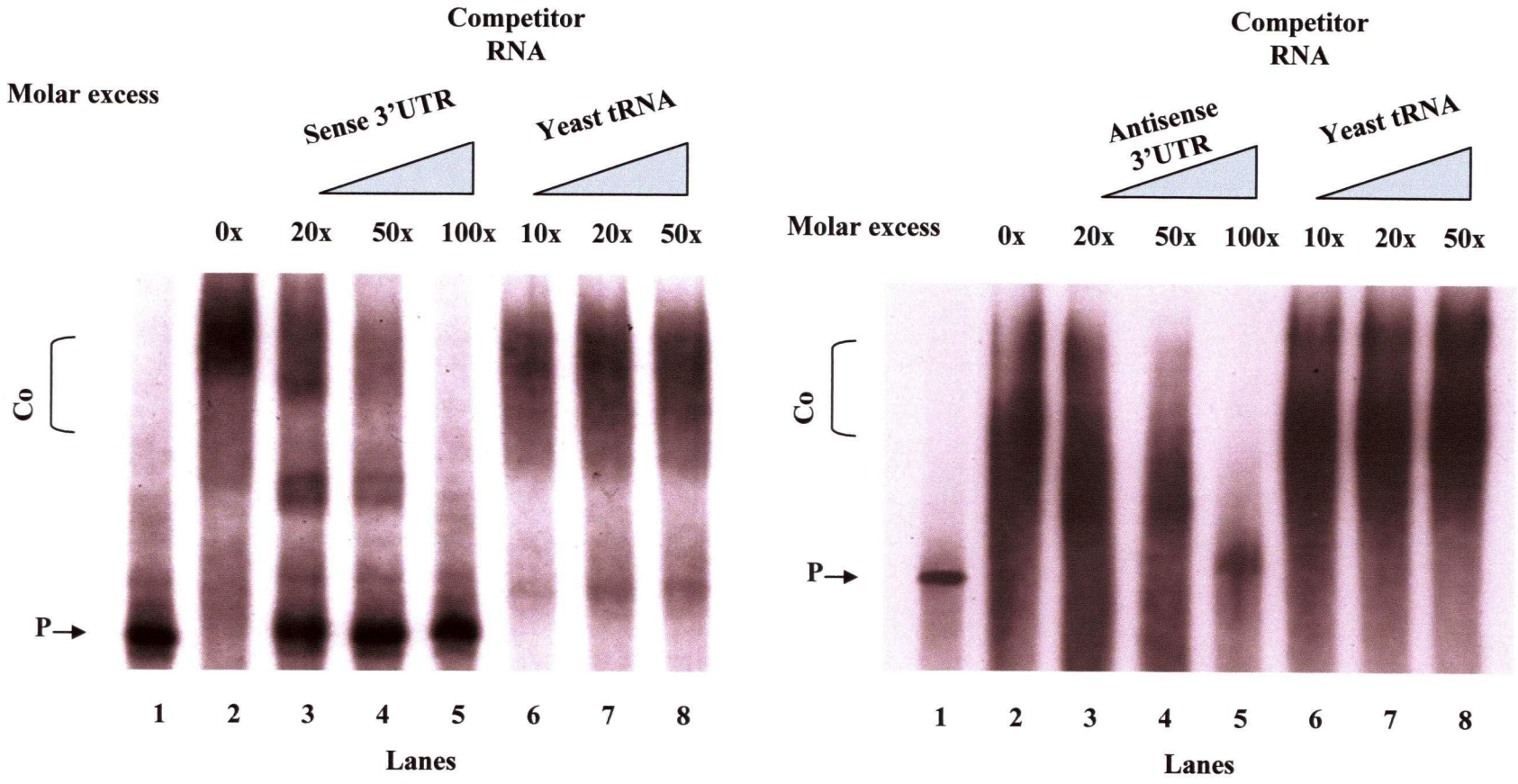


**Figure 13d. Mobility shift of labeled 3' UTR probe nt 7299-7399.**

Data for the sense 3' UTR sequence is shown on the left panel. Data for the antisense sequence is shown on the right panel. Lane 1 demonstrates the free hot probe (**P**) without protein interactions. Significant mobility shifts of the hot probes are observed in lane 2, indicated by the protein-probe complex (**Co**) formations. Such protein-RNA interactions can be competed when identical non-labeled RNA are added to the incubation, at 20x, 50x and 100x molar excess (lane 3, 4 and 5 respectively). Yeast tRNA molecules was added in lane 6, 7 and 8 as non-specific competitors, at 10x, 20x and 50x mass excess ratios. Mobility shift was only countered by the use of homologous non-labeled RNA.

***Tissue tropism of CVB3 in A/J mice by ISH (Aim 2).***

The specific infectivity of the virus in each mouse tissue is revealed by the ISH observations, which is then compared to the pattern of interaction between the 5'-UTR and the respective protein lysates.

*In situ hybridization of viral genome in CVB3 infected A/J mice.*

In this experiment, I performed *in situ* hybridization of the viral genome to determine the extent of infection in different organs of the immunocompetent A/J mice. The antisense (negative) strand of the viral RNA genome (nt 888-7399), labeled with digoxigenin-11-5'-triphosphate (DIG-11-UTP), was used as the RNA probe. Thus ISH positivity on day 4 p.i. is a strong indicator of successful viral entry, translation and replication. **Figure 14** summarizes typical images of ISH observation of the various 4- and 10-week-old A/J organs during the acute phase of infection (4 days p.i.). Positive sense viral RNA genome in the tissues was hybridized to the DIG-11-UTP labeled probes and stained by Sigma BCIP / NBT (blue black) in the tissue sections. I have chosen day 4 p.i. to perform ISH because CVB3 viral replication in systemic organs, including that of the heart and liver, typically reaches a maximum. In general, CVB3 infection of A/J mice begins to exhibit increased viral replication in most organs at day 2 p.i.. Specific immune mediated viral clearance begins at day 4 and beyond [64,66,68].

*Age dependent susceptibility of the heart.*

CVB3 infection of the heart muscles was random and dispersed, without specific localized sites of replication. From experience, the atrial tissue demonstrated limited CVB3 infection when compared to ventricular cardiomyocytes. My tissue sections thus were obtained from the left ventricular free wall. From the ISH observations, young mice appeared more susceptible to CVB3 than older mice, and such contrast is illustrated by the representative images in **Figure 14a**.

*Contrasting susceptibility of the pancreatic cell types.*

Pattern of CVB3 infection of the pancreas tissue was intriguing (**Figure 14b**). High levels of viral replication and cellular injury was observed in the exocrine cells. However, the neighboring endocrine acinar and ductal cells were contrastingly resistant to viral replication and appeared healthy. Occasional interstitial and endocrine cells contained some viral genome. It is unclear if the resistance of the endocrine cells was due to the lack of the CVB3 receptor or the presence of intracellular inhibitors of the viral replication. Both the 4-week and 10-week-old mice appear to be similarly susceptible to infection in the pancreas.

*Increased susceptibility of the liver with age.*

Liver cells of the A/J mice exhibited a generally susceptible phenotype to the CVB3. The pattern of infection appeared random and non-localized (**Figure 14c**). The level of genomic viral RNA was lower than that observed for the cardiomyocytes. Overall, cellular injury and viral replication in the livers of older A/J mice were similar to that in the younger A/J mice, in contrast to the decreased viral replication with age that was observed for the cardiomyocytes.

**Figure 14a. ISH detection of viral genome in A/J hearts.**

The CVB3 viral genome is stained with blue black. There appears to be an age-dependence on the susceptibility to CVB3 infection: the 4-week-old mouse heart (right panel) has more viral infection than the 10-week-old heart.

**4-week-heart**

- comparatively more susceptible

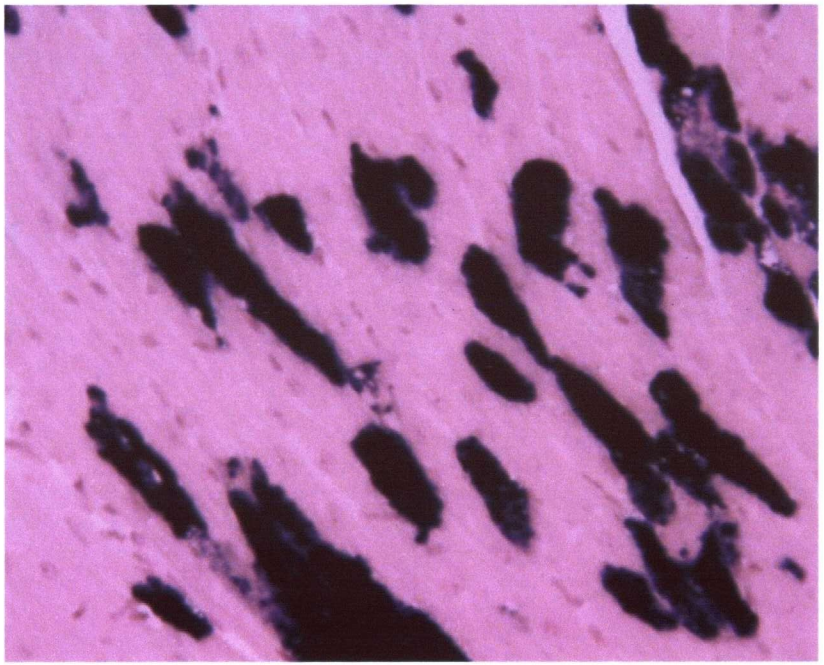

**10-week-heart**

- lower viral titre

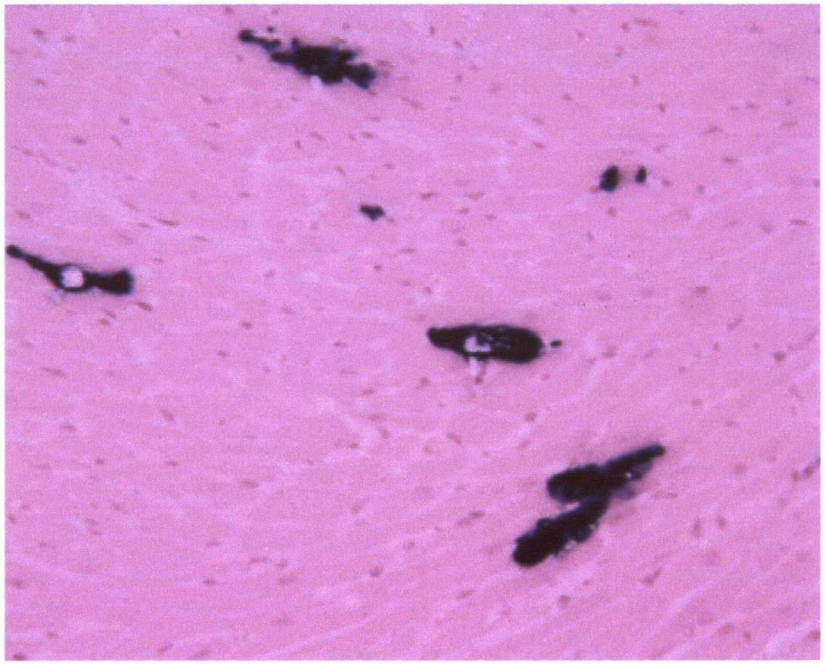

**Figure 14b. ISH detection of viral genome in A/J pancreas.**
The CVB3 viral genome is stained with blue black. The exocrine pancreas is hybridized with large amounts of antisense RNA probes while the endocrine pancreas remains non-infected. Sporadic genome detection on the endothelial cells and in the endocrine cell types was occasionally observed.

**4-week-old pancreas** **10-week-old pancreas**

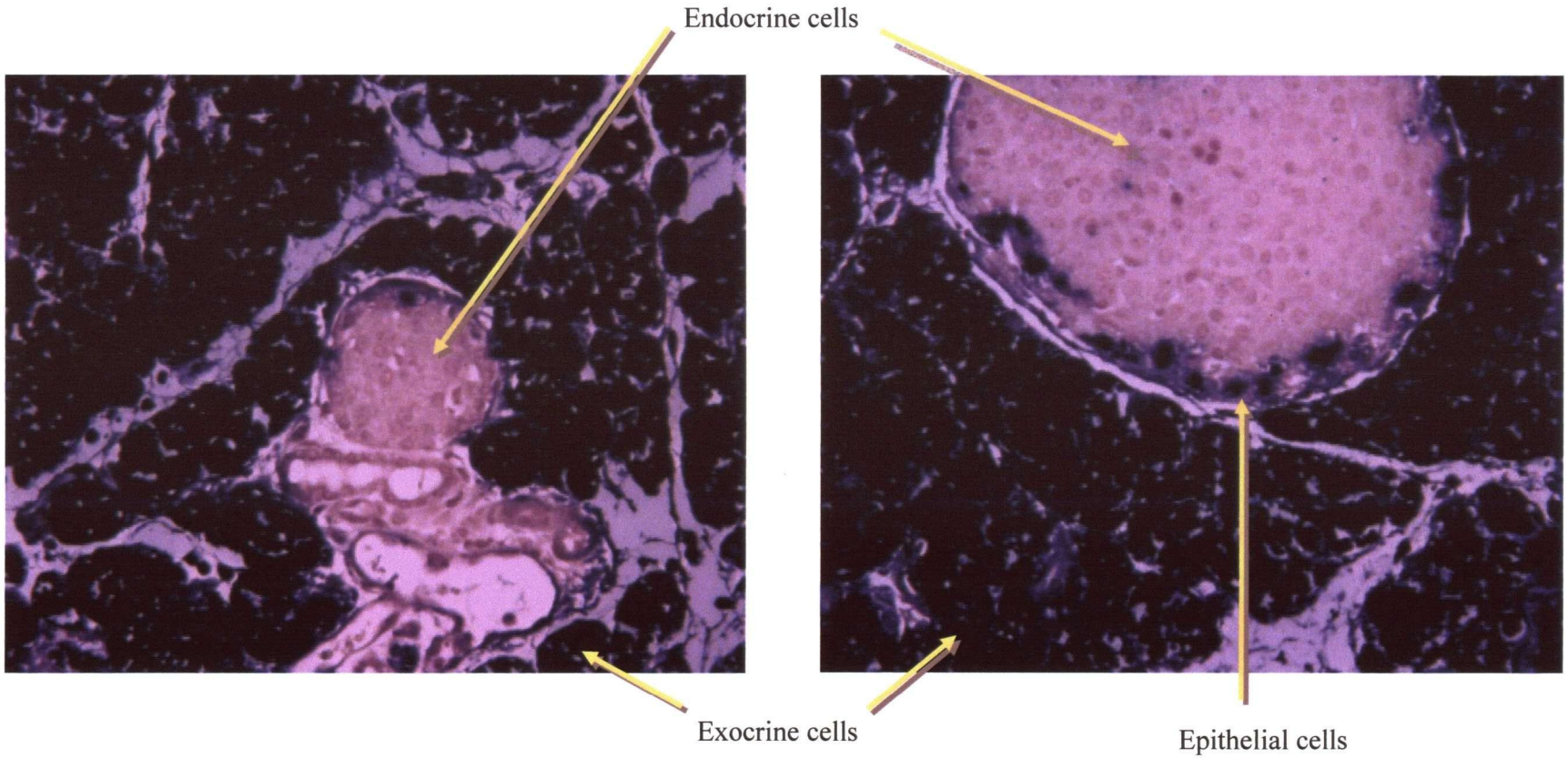

**Figure 14c. ISH detection of viral genome in A/J Livers.**
The CVB3 viral genome is stained with blue black. The 10-week-old liver appears more susceptible than the 4-week-old liver. This age dependent susceptibility is reversed in the heart.

**4-week-old Liver**

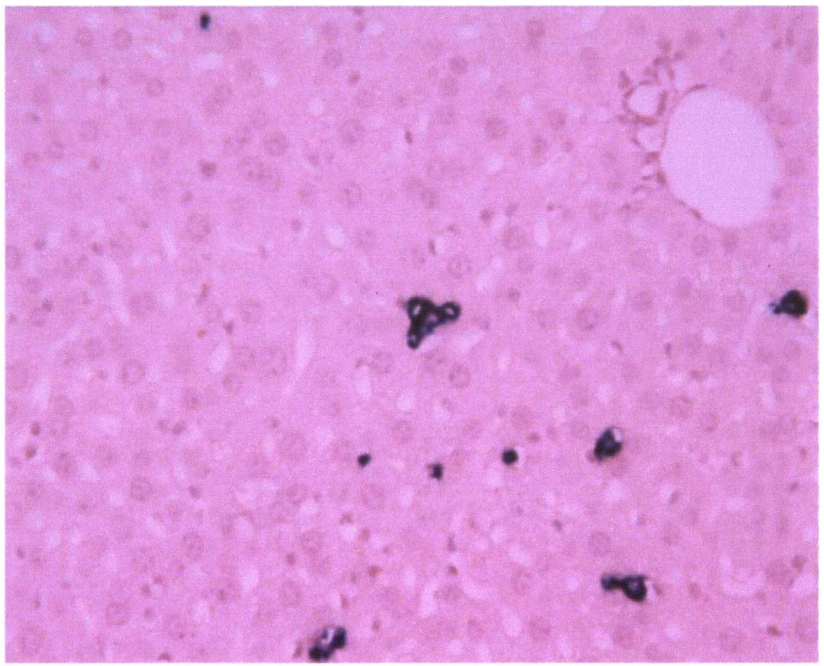

**10-week-old Liver**

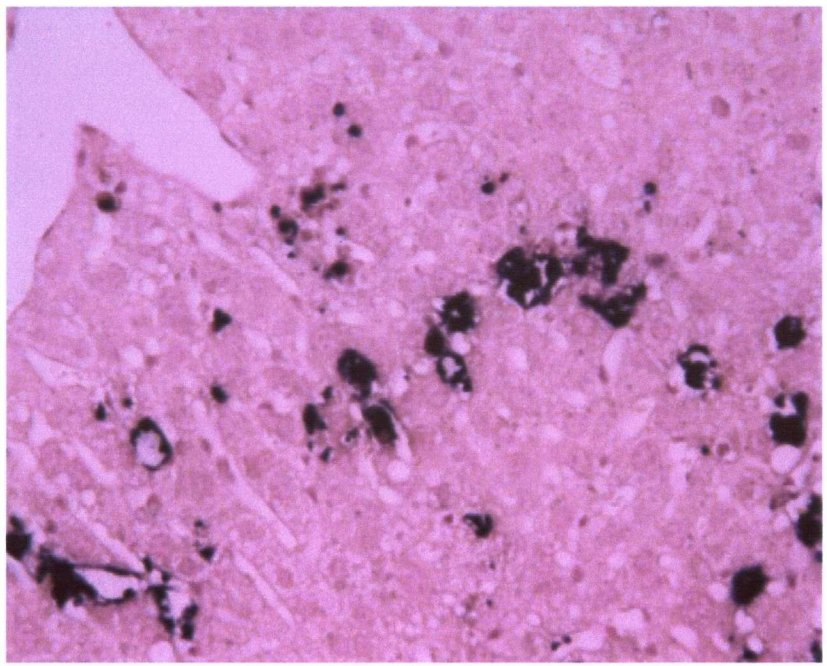

*CVB3 infectivity in the brain, spleen and kidney.*

In general, CVB3 injury in the brain and spleen was not as severe as in the heart, pancreas, or liver. However, it is interesting to observe that in the brain and spleen, CVB3 replication appears to localize in specific regions of the tissue (**Figure 14d-e**). There was no age dependence of tissue injury or significantly different levels of viral titre in these organs. However, the reduced level of viral genome in the spleen of A/J mice on day 4 pi may be a result of rapid viral clearance by the immune cells in the organ. Finally, ISH observation of the kidney was in contrast to all the other organs. Almost no virus genome could be detected in the kidney cells (**Figure 14f**). The tissue also appeared healthy and was highly resistant to the CVB3 replication regardless of age.

**Figure 14d. ISH detection of viral genome in A/J brain.**
The CVB3 viral genome is stained with blue black. Infection is modest in brain. Only localized regions of the brain demonstrate viral replication.

**4-week-old brain**

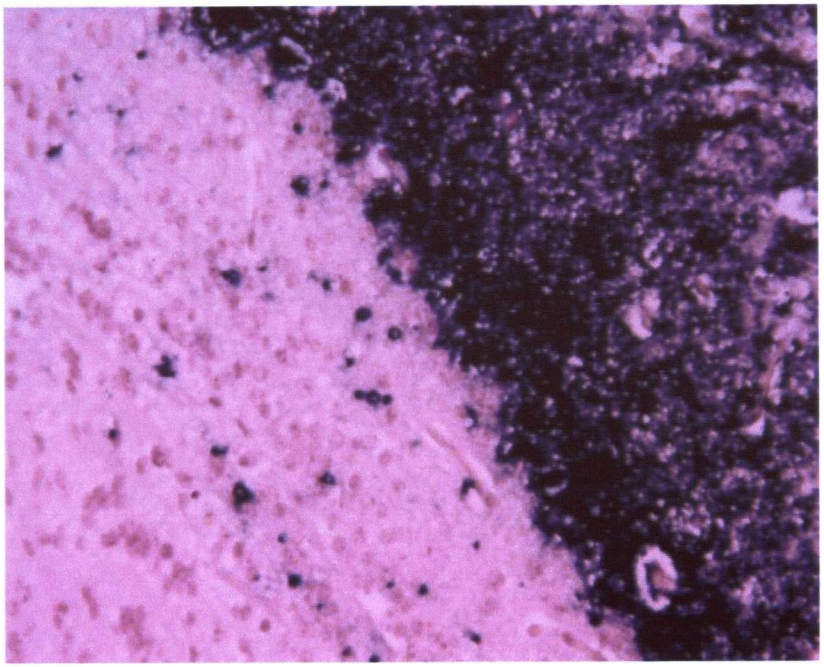

**10-week-old brain**

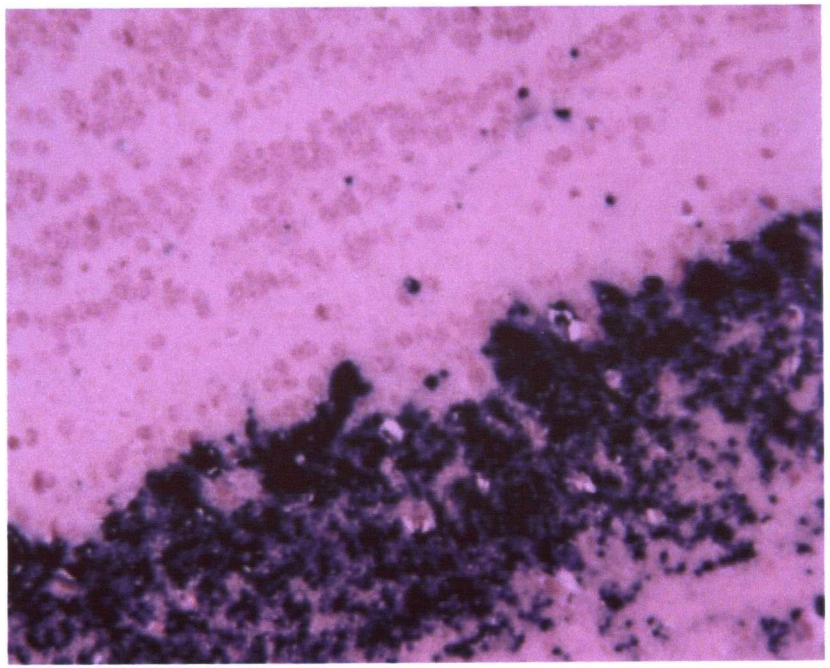

**Figure 14e. ISH detection of viral genome in A/J spleens.**
The CVB3 viral genome is stained with blue black. Virus genome appears to be more localized in geminal centers.

**4-week-old spleen**

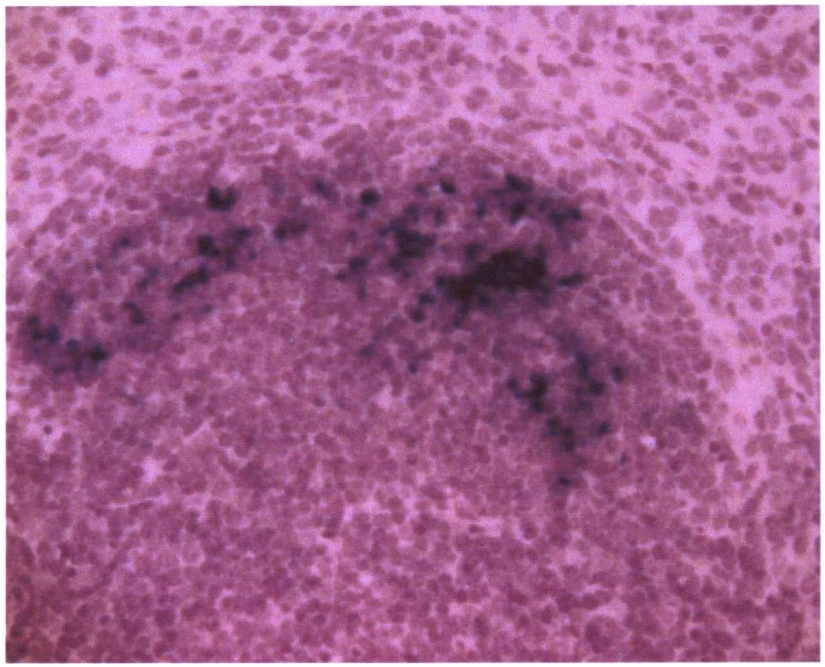

**10-weekold spleen**

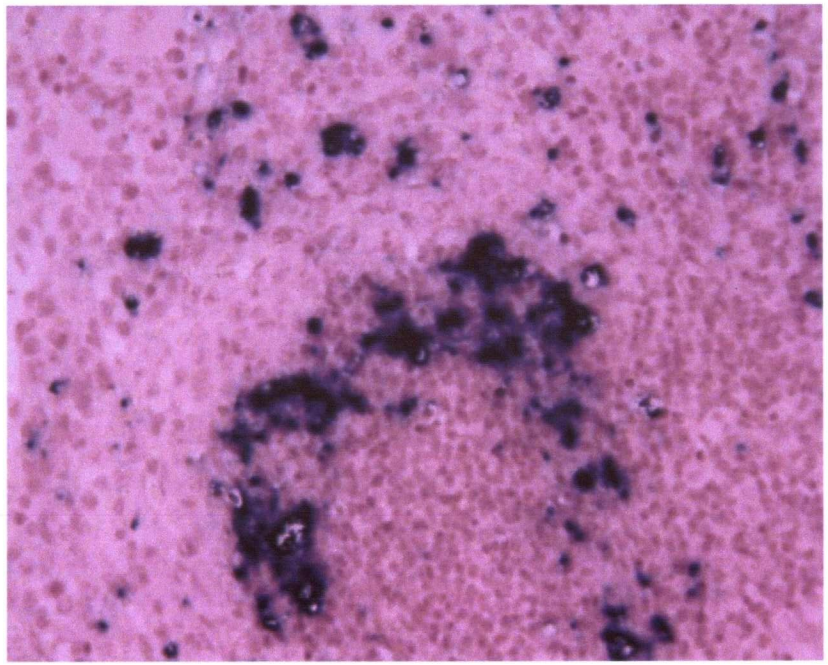

**Figure 14f. ISH detection of viral genome in A/J kidney.**
Both 10-and 4-week-old kidneys are resistant to CVB3 infection. Viral genome is barely detected by the *in situ* hybridization.

**4-week-old kidney**

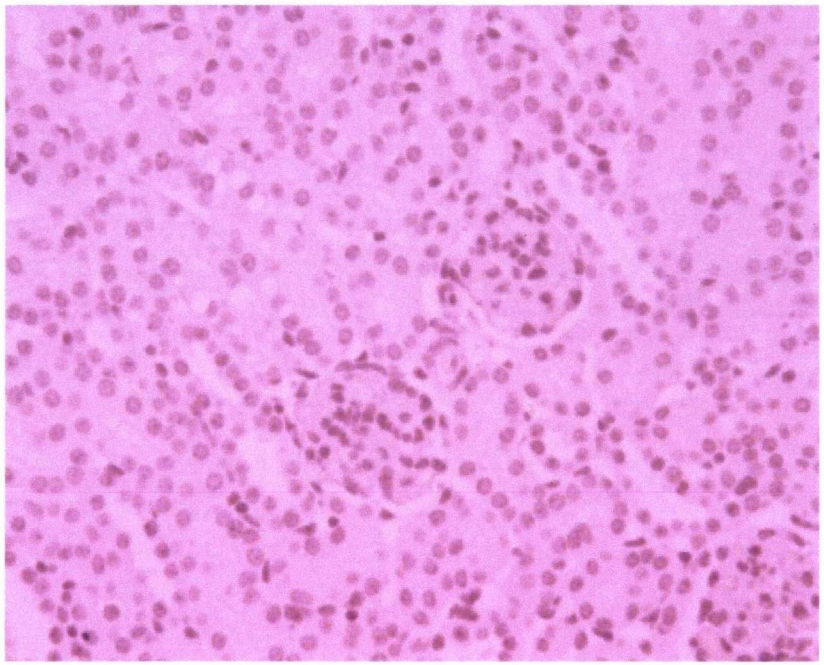

**10-week-old kidney**

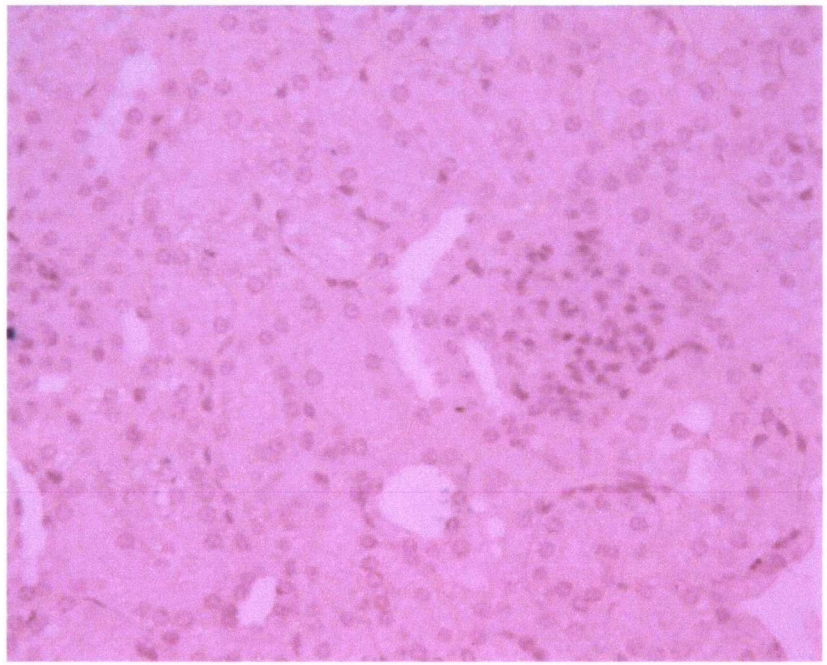

***Profiles of the protein-5'UTR interactions (Aim 2)***

UV cross-linking reactions were performed using protein lysates of the various A/J mouse tissues and the radiolabeled probes of the 5'-UTR regions (nt 1-209, nt 210-529, and nt 530-630) . The pattern of protein-UTR interaction of each protein lysate is presented in one autoradiograph, in the format described in **Figure 15**. Each experiment was repeated at least 3 times to verify the reproducibility of the pattern and estimations of the molecular weights.

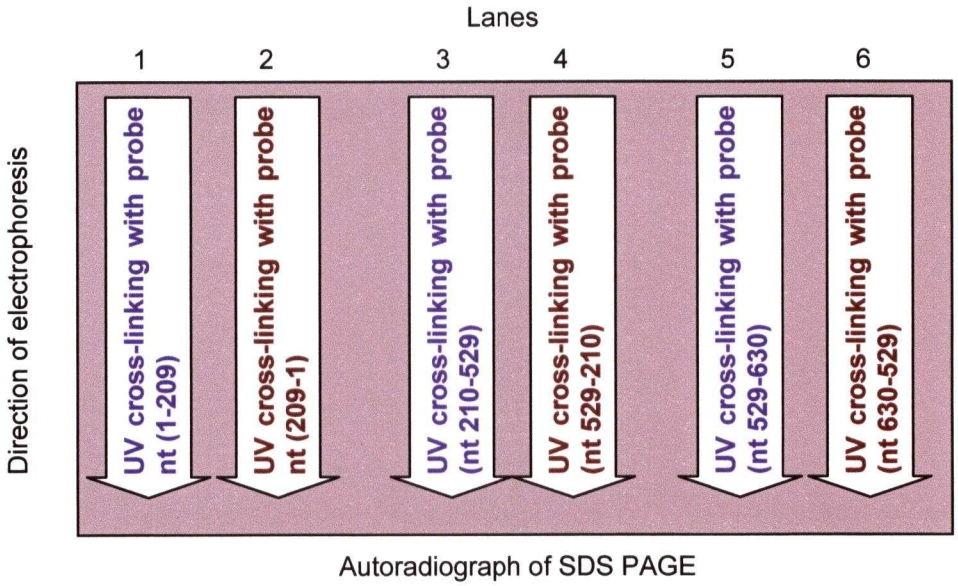


**Figure 15. Layout of each profile of tissue protein-5'-UTR interaction.**

Labeled probes of the 5'-UTR regions were added to tissue lysates. The sense and antisense sequences of each 5'-UTR region were paired up (lane 1,2 for nt 1-209; lane 3,4 for nt 210-529;

and lane 5,6 for nt 530-630). MWs of the protein-UTR complex were determined by a concurrently loaded MW marker.

UV cross-linking analysis was performed for protein lysates from each of the A/J mice organs. Two autoradiographs were generated per organ: using 4-week-old lysate and 10-week-old lysate. Thus, a total of 12 autoradiographs were produced. The results are presented in **Figure 16**. A comprehensive list of identified protein-UTR complexes in each profile is presented in **Table 5**. In the following section, I shall summarize important observations from these profiles of interaction.

*Intense interactions in the IRES region (nt 530-630).*

The 100 nt long IRES region displayed the most intense protein-RNA interaction in each of the profile (lanes 5 and 6 in each panel of **Figure 16**). The intensity of bands was generally stronger in comparison to protein-RNA interactions within other regions (nt 1-209, lanes 1 and 2; nt 210-529, lanes 3 and 4). The prominence of bands of the IRES-interacting proteins indicates abundance of these factors, or the capability of these factors to bind multiple copies of the IRES. The patterns of the interacting bands were not as discrete as others, possibly due to complex aggregations among the various UTR-binding proteins. This may reflect the functional importance of the IRES, in which multiple molecules such as the ribosomal proteins, rRNAs and the eIF4 factors interact and form the translation initiation complexes. This interpretation is in line with our previous observation that the short 100 nt IRES core sequence is essential for the initiation of viral translation [349].

*Four unique interactions with the sense sequence of nt 210-529.*

There are four UTR binding proteins that are consistently observed in all profiles, in a configuration that resembles two sets of doublets, with molecular weights 29 kDa / 31 kDa (**Marked A in all of Figure 16**) and 43 kDa / 45 kDa (**Marked B**). In the 10-week pancreas, the 29 kDa / 31 kDa band is not very distinctively resolved under standard exposure time, but using longer exposure the doublets at the anticipated position could be observed (data not shown). Differential intensity of such interactions among the tissue extracts reflects the differential expression / availability of the UTR-binding proteins in the tissues, since the overall protein- and probe-quantities in each UV cross-linking experiment and the time of autoradiograph exposure were standardized.

*Lack of UTR-binding proteins in the pancreas.*

The intensity of protein-CVB3 RNA interactions in the pancreas appeared weaker than in other organs, despite the use of identical experimental conditions. Particularly in the antisense region of nt 1-209 and 210-529 (lane 2 and 4, **Figure 16c**), I have observed little significant protein interaction. This is in contrast to other profiles. This weakness in band intensity can be due to two major reasons:

1) Proteases in the pancreatic lysate began digestion of the UTR-binding protein during the incubation with hot probes.

2) Nucleases in the pancreatic lysate began digesting the radiolabeled UTR probes during the incubation with proteins.

I would also like to emphasize that it was not possible to isolate the endocrine and exocrine cell types by the methods that were available at the time of experiments. Thus, the

lysate was in fact a combined lysate from the endocrine and exocrine cell types which were, from my in situ hybridization data, contrasting in susceptibility. This short-coming in my experiment is recognized and possible resolution to this issue is discussed in the future directions (Chapter VII).

*The p28 interaction correlates with kidney's resistance.*

Perhaps the most intriguing result from this set of UV cross-linking experiments is the intense 28 kDa protein interaction with the antisense sequence of nt 250-529 (**marked C in the respective profiles in Figure 16a**). As illustrated by *in situ* hybridizations, kidney is the **only** organ that remains consistently resistant to CVB3 infection. To compare protein-probe interactions of the lysates in this UTR probe, **Figure 17** displays a summary of lane 4 of **Figure 16** from the brain, pancreas, kidney and heart. Both the 4-week and 10-week profiles of the kidney demonstrated the p28 interaction at very similar intensities. In addition, the p28 band was detected in the 10-week-old heart profile, but not in the 4-week-old profile. This p28 interaction in the heart corresponds strongly to ISH observation wherein older mice have less viral infection in the heart as compared to younger mice. Moreover, no such p28 interaction was observed in the severely infected pancreas. Minimal p28 interaction was also observed in the liver and brain, which can be correlated to the overall lower level of infection in these organs (**Figure 14**). Thus, the intense p28 interaction with the kidney lysates correlates well with the ability of different organs to limit viral titer during a CVB3 challenge.

**Figure 16a. Profile of kidney protein interaction with CVB3 5'-UTR.**
Protein lysate of the A/J mouse kidney was UV cross-linked to the three 5'-UTR probes (nt 1-209, nt 210-529 and nt 530-630). Protein interactions with the sense (s) and antisense (s) probes are observed as bands. The UTR-binding proteins are observed as bands. The doublets labelled A and B are consistently observed in all profiles. The strong 28 kDa interaction (C) correlates with the kidney's resistance to CVB3 infection at both ages.

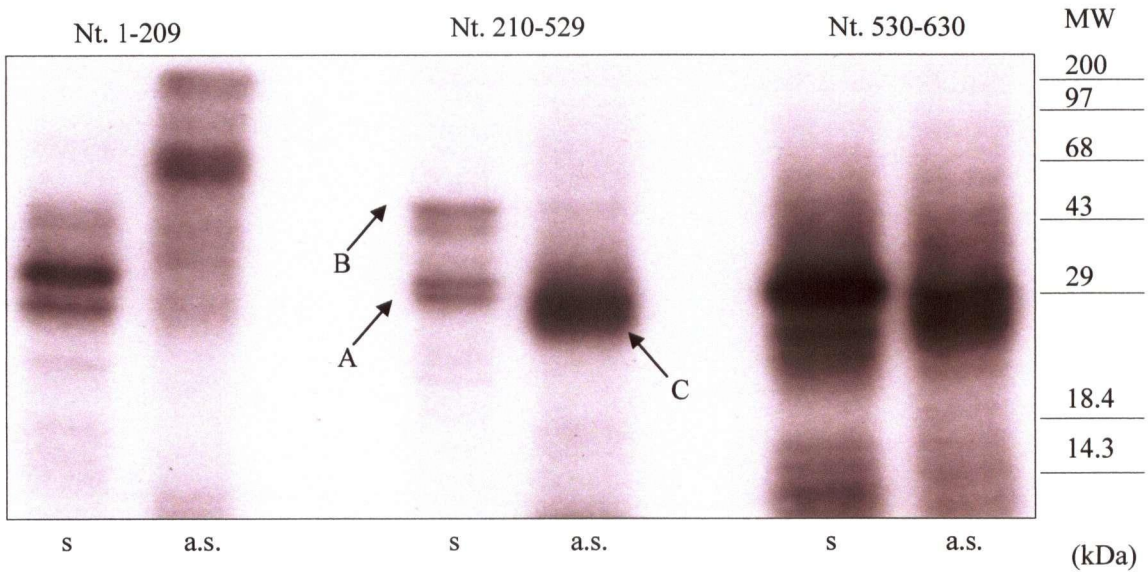


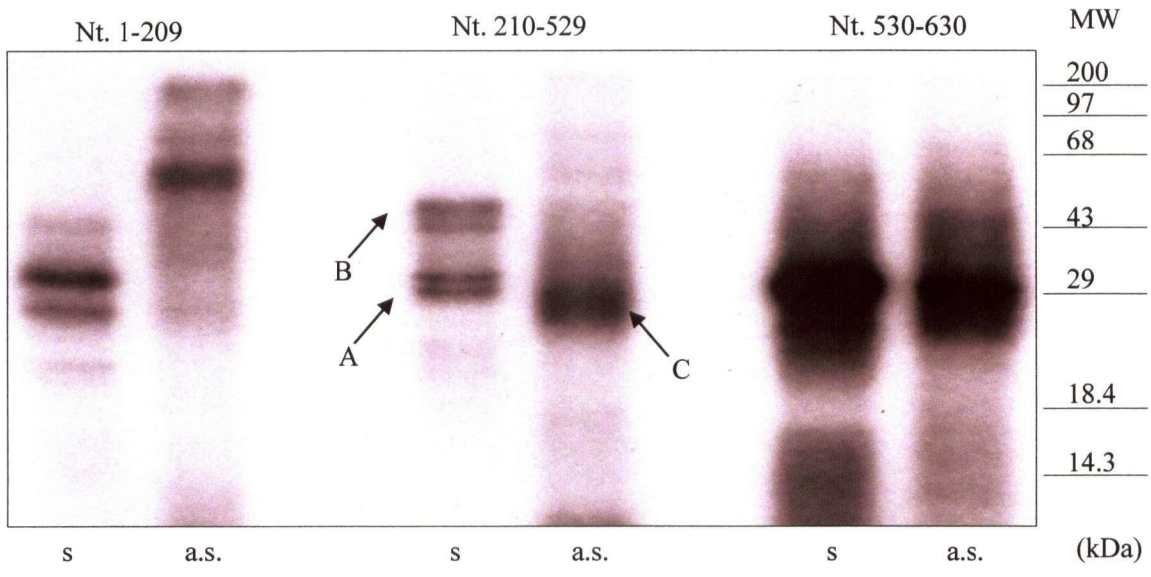

**Figure 16b. Profile of heart protein interaction with CVB3 5'-UTR.**
Protein lysate of the A/J mouse heart was UV cross-linked to the three 5'-UTR probes (nt 1-209, nt 210-529 and nt 530-630). Protein interactions with the sense (s) and antisense (s) probes are observed as bands. The UTR-binding proteins are observed as bands. The doublets labelled A and B are consistently observed in all profiles. The 28 kDa interaction (C) in the 10-week-old heart correlates with the age-dependence susceptibility of the organ as revealed by the *in situ* hybridization observation.

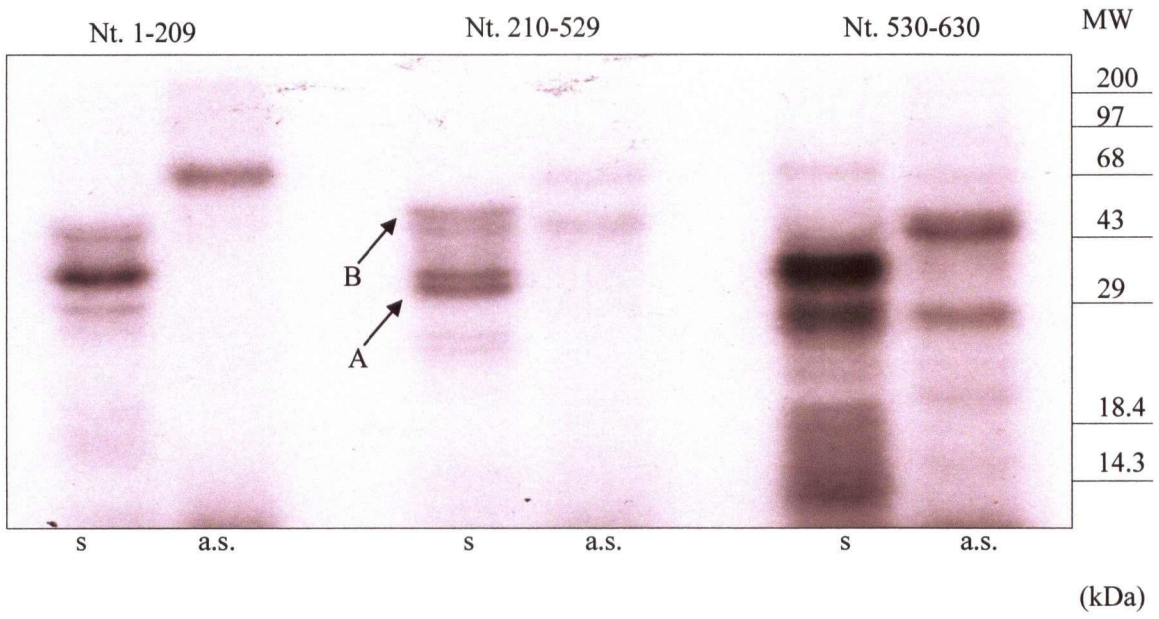


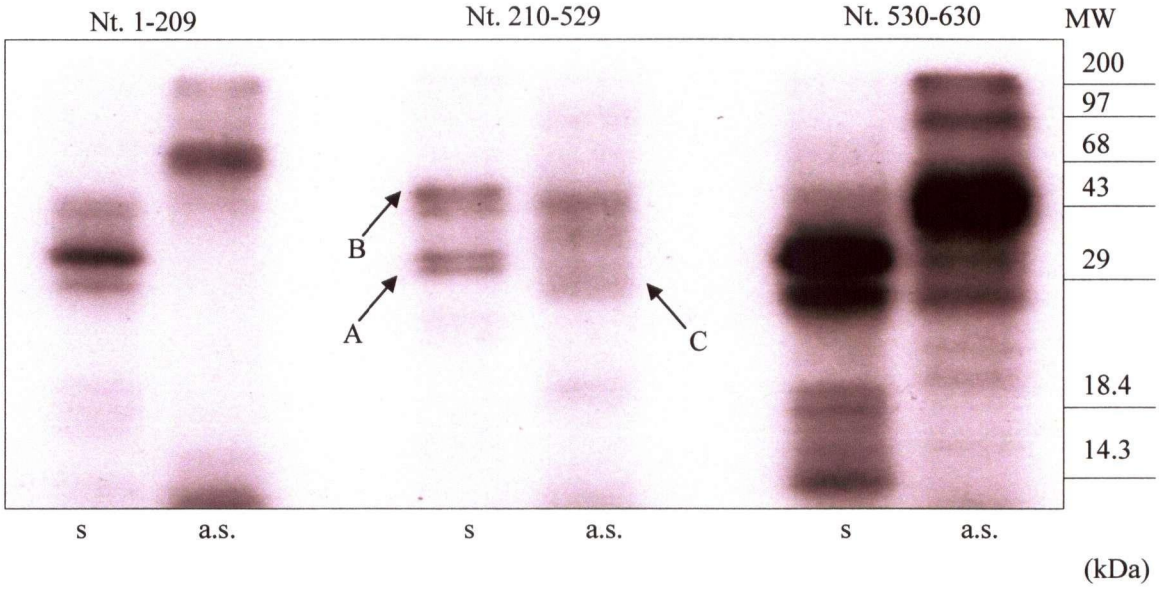

**Figure 16c. Profile of pancreas protein interaction with CVB3 5'-UTR.**
Protein lysate of the A/J mouse pancreas was UV cross-linked to the three 5'-UTR probes (nt 1-209, nt 210-529 and nt 530-630). Protein interactions with the sense (s) and antisense (s) probes are observed as bands. The UTR-binding proteins are observed as bands. The doublets labelled A and B are consistently observed in all profiles. The absence of the p28 interaction in lane 4 is correlated to the intense viral genome detection by the *in situ* hybridization, supporting the postulation that p28 may be a potential inhibitor of infection.

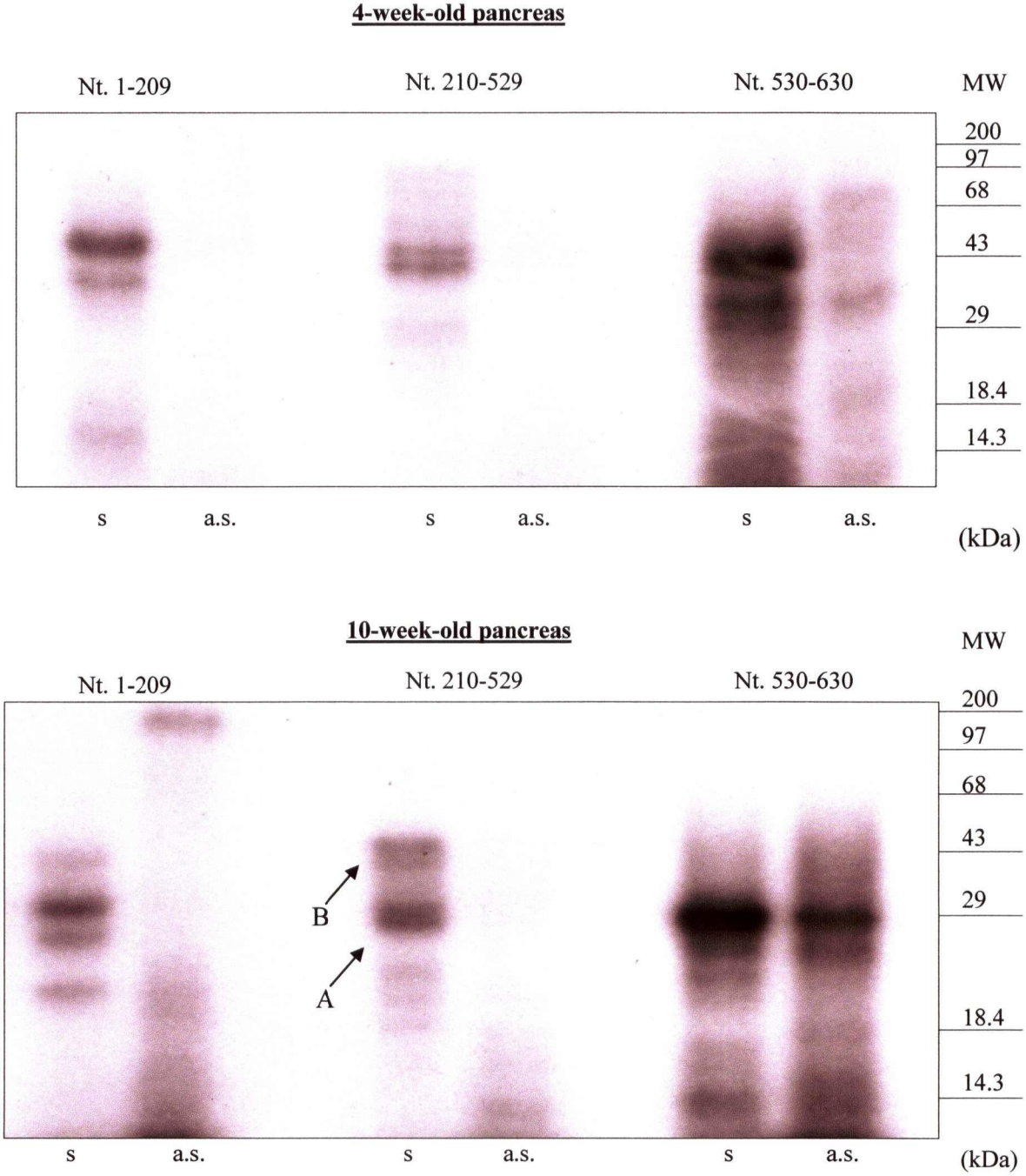

**Figure 16d. Profile of brain protein interaction with CVB3 5'-UTR.**

Protein lysate of the A/J mouse brain was UV cross-linked to the three 5'-UTR probes (nt 1-209, nt 210-529 and nt 530-630). Protein interactions with the sense (s) and antisense (s) probes are observed as bands. The UTR-binding proteins are observed as bands. The doublets labelled A and B are consistently observed in all profiles. However, the p28 was weakly detectable in lane 4.

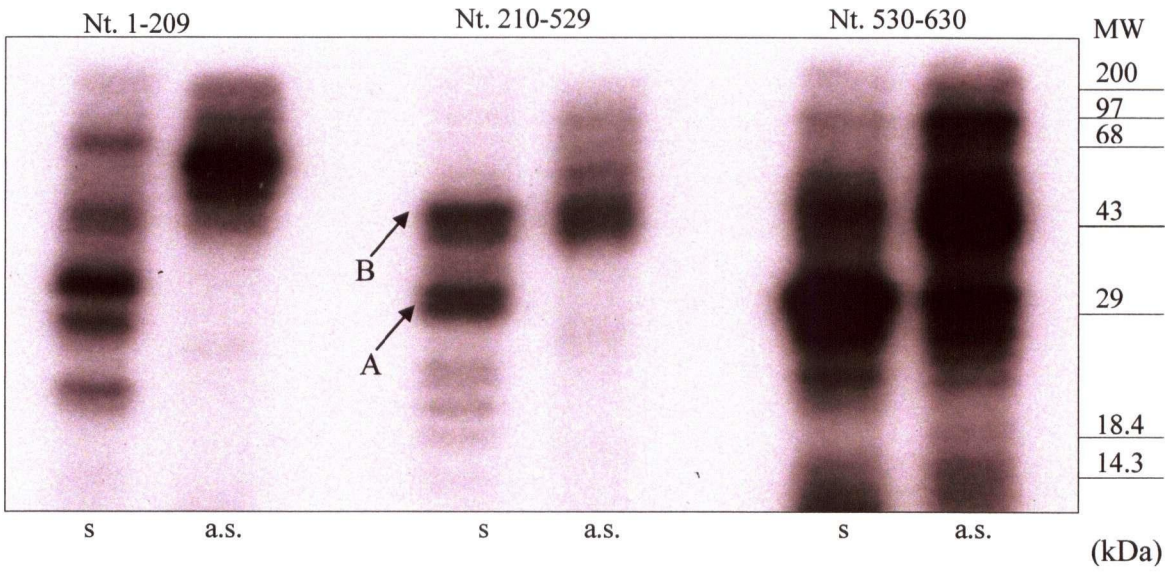


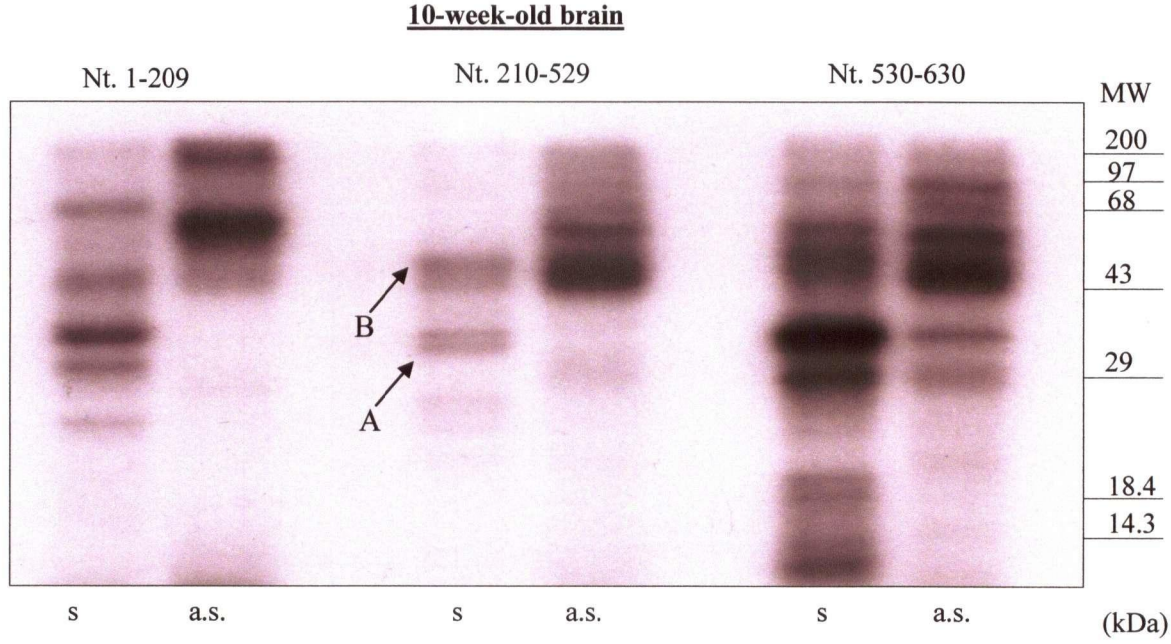

**Figure 16e. Profile of spleen protein interaction with CVB3 5'-UTR.**
Protein lysate of the A/J mouse spleen was UV cross-linked to the three 5'-UTR probes (nt 1-209, nt 210-529 and nt 530-630). Protein interactions with the sense (s) and antisense (s) probes are observed as bands. The UTR-binding proteins are observed as bands. The doublets labelled A and B are consistently observed in all profiles. However the p28 was not observed in lane 4.

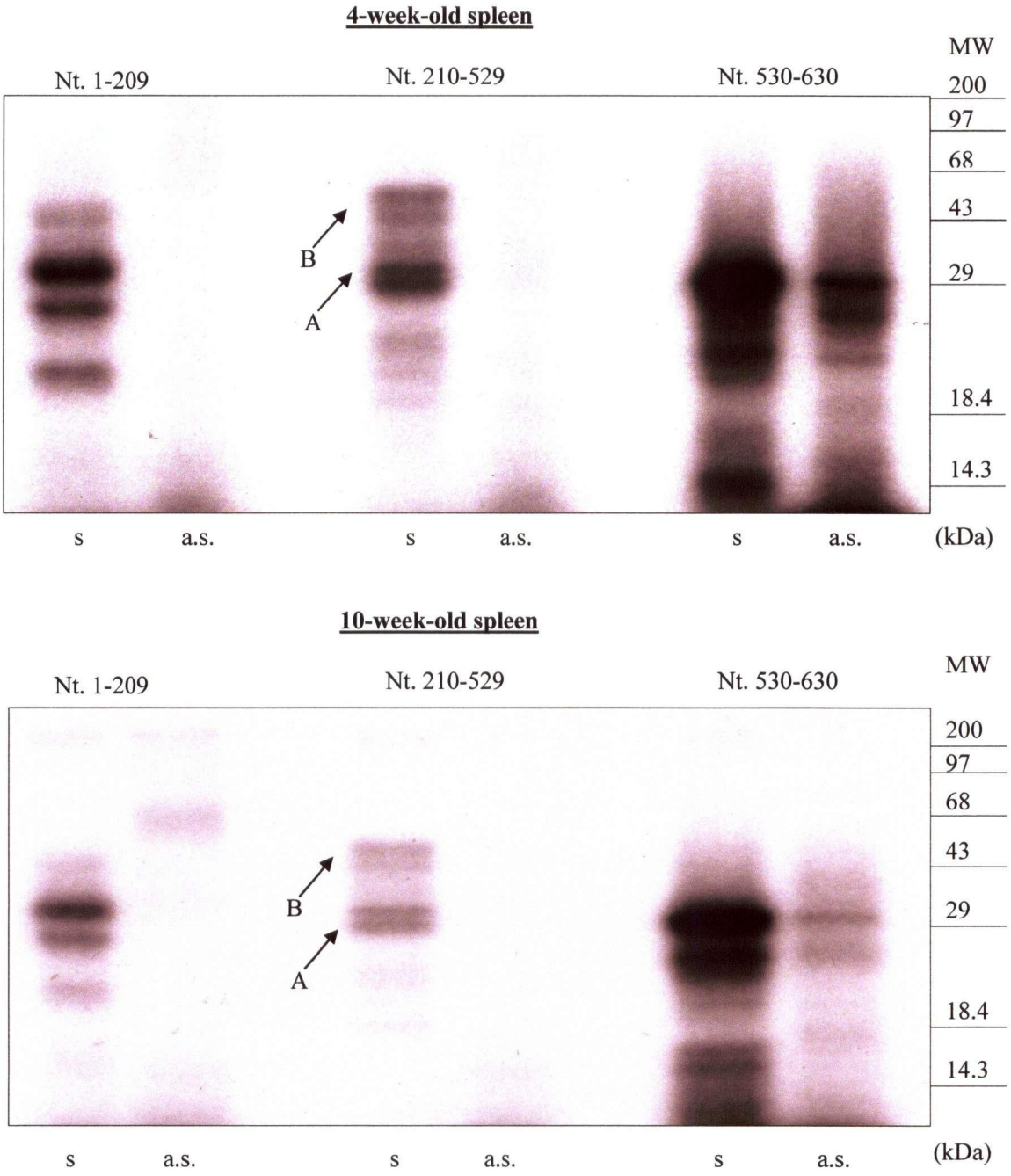

**Figure 16f. Profile of liver protein interaction with CVB3 5'-UTR.**
Protein lysate of the A/J mouse liver was UV cross-linked to the three 5'-UTR probes (nt 1-209, nt 210-529 and nt 530-630). Protein interactions with the sense (s) and antisense (s) probes are observed as bands. The UTR-binding proteins are observed as bands. The doublets labelled A and B are consistently observed in all profiles. The 28kDa interaction (C) is also observed and such correlates to the reduced viral load as observed by the *in situ* hybridization.

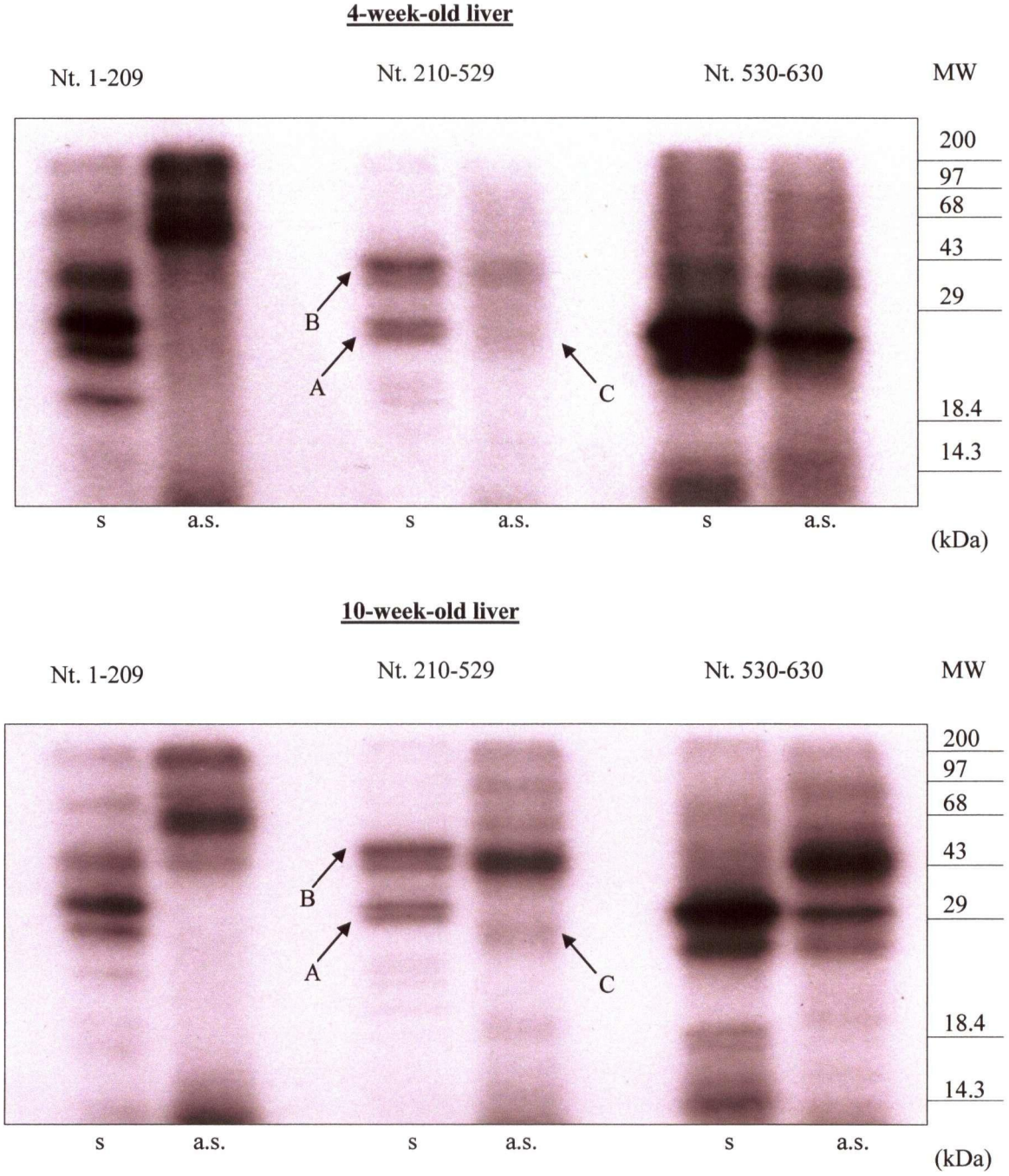

**Figure 17. Comparison of the p28-antisense nt 210-529 interactions observed in different A/J organs.**
The p28-probe interaction is most strongly observed in the kidney. The liver and the 10 week-old-Heart exhibit some degree of interaction, which correlates with lowered viral infection. The absence of the protein-probe interaction in the pancreas also corresponded to the high level of infection.

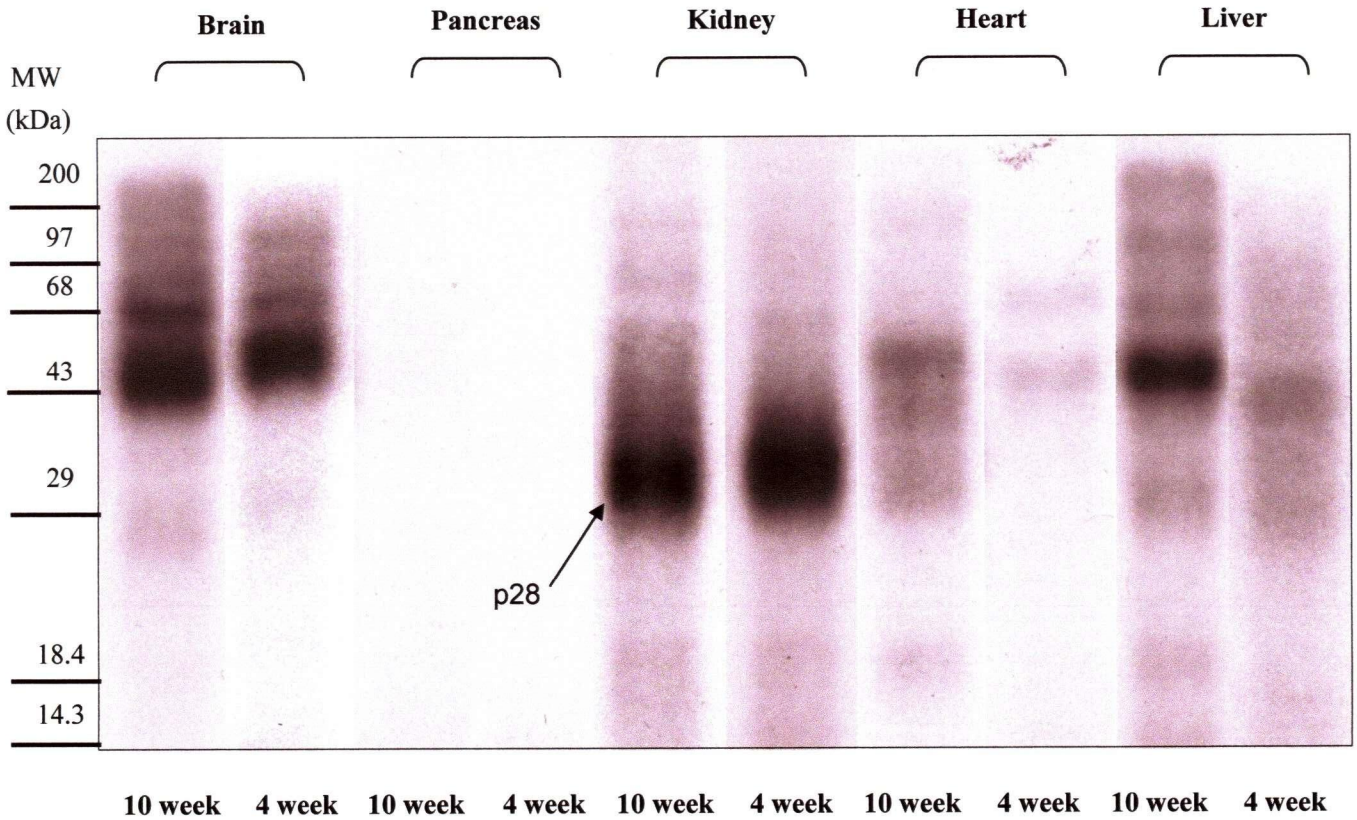

In order to quantify the descriptive correlation (ISH and p28 protein) as much as possible, observation CVB3 viral genome by ISH staining of the CVB3 genome in the kidney, heart and pancreas is subjectively scored from 1 to 5 (1 being the lowest level of infection and 5 the highest). The scoring was averaged from myself and two fellow laboratory technicians, and the results are listed in **Table 4.0** below.

**Table 4**. Summary of the correlation between ISH observations and the p28 interactions. The detection of CVB3 genome by the ISH observation and the intensity of the p28 interaction were listed. The amount of viral titre is subjectively scored from 1 to 5 and represented by the number of '+' in the table. No observable viral genome was detected from the kidney.

| Organ and age | Viral infectivity by ISH | Intensity of p28 interaction |
|---|---|---|
| 10-week kidney lysate | No virus genome observed | STRONG |
| 4-week kidney lysate | No virus genome observed | STRONG |
| 10-week Heart lysate | +++ | MODERATE |
| 4-week heart lysate | +++++ | WEAK |
| 10-week-old Liver lysates | ++ | MODERATE |
| 10-week-old Pancreas lysates | +++++ | NONE |

*Unique p43 interaction with the antisense sequence in the brain.*

From **Figure 17** and **Figure 16**, a strong 43 kDa protein from the brain lysate is observed to bind to the antisense nt 210-529 (lane 4). Although this may not be correlated to a specific pattern of infectivity, it appeared to be only strongly observed in the brain lysate. A modest 43 kDa interaction has been observed in the 10-week-old heart and the 10-week-old liver. The intensity of the p43 interaction may indicate possible abundance of this specific factor in the brain lysate. Whether this interaction plays a specific role in the replication of the virus and correlates with the apparent localized infection of the virus in the organ requires further investigation.

*Other important protein interactions*

In comparing the pattern of protein-UTR interactions from the 10-week-old heart to the 4-week-old heart, there is a major difference in the protein interactions with the anti-sense sequence of the nt 529-630 (lane 6, **Figure 16b**). The ~200, ~100kDa protein bands were observed in the 10-week-old profile while the intense 43 kDa protein band was only weakly observed in the 4-week-old profile. These bands correlate with the differences in susceptibility of the two age groups. Thus, these bands of proteins are interesting targets that are worth further identifications and studies.

To summarize other UTR-binding proteins, **Table 5a and 5b** presents the molecular weights of the protein complexes that are observed in each of the profiles.

**Table 5a** Summary of cellular protein interactions with viral 5'-UTR sequences for multiple organs of the 4-week-old animals.

| Organ/ polarity of RNA probe | Protein (kDa) binding to nt 1-249 | nt 250-530 | nt 530-630 |
|---|---|---|---|
| Heart (+ve) | 29,38,45 | 29,31,43,45 | Under 18<br>28,38 |
| (-ve) | 68 | 43 | 28,43 |
| Pancreas (+ve) | 18,43,57 | 29,31(both weak), 43,45 | Under 29<br>38,43 |
| (-ve) | --- | --- | 35 |
| Liver (+ve) | 22,29,38,45,68,170 | 29,31,43,45 | Under 18<br>28,29,43 |
| (-ve) | 68, 80,170, | 28,43 (weak) | 29,43 |
| Brain (+ve) | 22,29,38,43,85 | 29,31,43,45 | 10,22,29,43 |
| (-ve) | 57,68 | 43 | under 14<br>29,43,97 |
| Spleen (+ve) | 22,29,38,43 | Under 22<br>29,31,43,45 | 14,22,29 |
| (-ve) | --- | --- | 22,28,29 |
| Kidney (+ve) | 29,38,43 | 29,31,43,45 | Under 28<br>29 |
| (-ve) | 68,200 | 28 | 28 |

**Table 5b.** Summary of cellular protein interactions with viral 5'-UTR sequences for multiple organs of the 10-week-old animals.

| Organ/ polarity of RNA | Protein (kDa) binding to nt 1-249 | nt 250-530 | nt 530-630 |
|---|---|---|---|
| Heart (+ve) | 29,35,43 | 29,31,43,45 | Under 18 , 28,35 |
| (-ve) | 70 | 28,→ 43 | 28,43,97,200 |
| Pancreas (+ve) | 22,29,35,43 | 29,31,43,45 | Under 29 , 29 |
| (-ve) | 170 | --- | 29 |
| Liver (+ve) | 28,35,43,85,170 | 29,31,43,45 | Under 18<br>28,29 |
| (-ve) | 68, 170 | 28,43 | 29,43 |
| Brain (+ve) | 22,29,35,57,85 | 29,31,43,45 | Under 18<br>28,35,43,57 |
| (-ve) | 57,170 | 28,43,57 | 28,35,43,57,85 |
| Spleen (+ve) | 22,28,35 | 29,31,43,45 | Under 18<br>28,35 |
| (-ve) | --- | --- | weak signals |
| Kidney (+ve) | 28,29,43 | 29,31,43,45 | Under 29<br>29 |
| (-ve) | 57,170 | 28 | 29 |

***HeLa cell protein-5'-UTR interactions (Aim 3).***

Identification of 5'-UTR binding HeLa cell proteins was achieved by competitive UV cross-linking assays. Specifically, the sense sequences of the 5'-UTR were tested because of their functional significances in tissue tropism and viral translation initiation. Non-labeled homologous RNA of each probe sequence was used as competitors to assess the specificity of the protein-UTR complex formation observed in the autoradiograph. In each of **Figure 18a-c**, Lane 1 illustrates probe-protein complexes without competitor. Lane 2 is a negative control which includes samples that were not treated with UV radiation. No cross-linking took place and thus no protein-RNA complex could be detected after the RNase A treatment. This is a negative control for the protein-probe complexes that were observed in other lanes. Homologous competitor of the corresponding probe sequence was added in lanes 3, 4, and 5 at the indicated molar ratios relative to the probe. As in the mobility shift experiments, specific interactions were concluded when the increase in band intensity corresponded to the decrease in competitor ratios.

*Specific interactions.*

**Figure 18a** demonstrates a total of five proteins that specifically interacted with the probe nt 1-209. The MWs of these proteins were 200, 80, 62, 52, and 45 kDa. Similarly, a total of six proteins were observed to bind the nt 210-529 sequence (**Figure 18b**). These proteins had MWs of 200, 100, 57, 52, 45, and 39 kDa. Four major proteins were observed to bind the IRES (**Figure 18c**). The MWs of these proteins are 170, 95, 57, and 52 kDa. All these proteins appeared to specifically interact with the core IRES sequence.

**Figure 18a**

HeLa cell protein interactions with the 5' UTR nt 1-209. HeLa cell lysate is UV cross-linked to the radiolabeled RNA, in the presence of non-labeled RNA at the indicated molar excess ratios. UTR-binding proteins are visualized as bands, and their respective MW estimate is indicated on the right. Lane 2 is a negative control of interaction without UV treatment. Non-specific protein interactions are marked NS1.

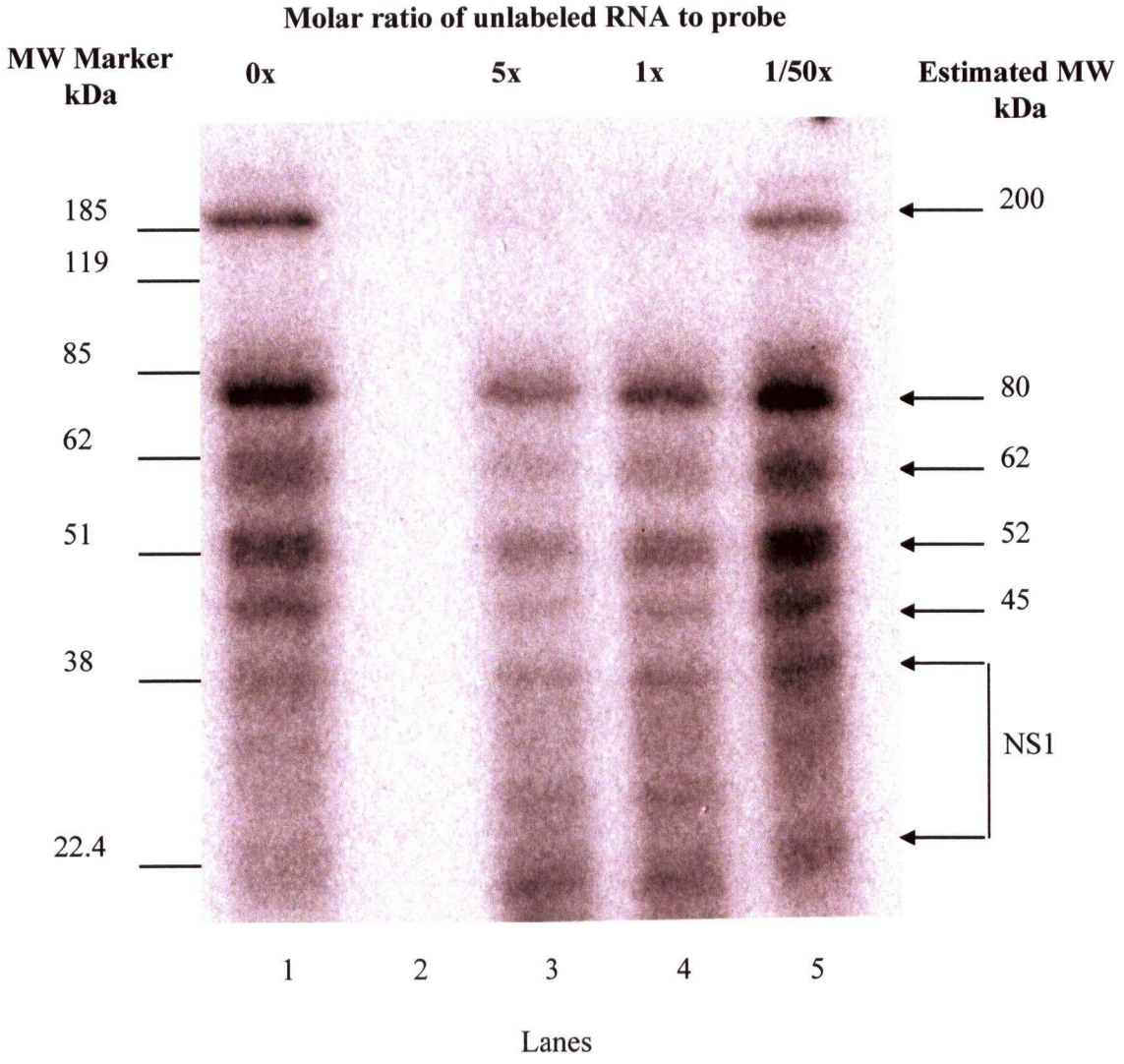

**Figure 18b**

HeLa cell protein interactions with the 5' UTR nt 210-529. HeLa cell lysate is UV cross-linked to the radiolabeled RNA, in the presence of non-labeled RNA at the indicated molar excess ratios. UTR-binding proteins are visualized as bands, and their respective MW estimate is indicated on the right. Lane 2 is a negative control of interaction without UV treatment. Non-specific protein interactions are marked NS2.

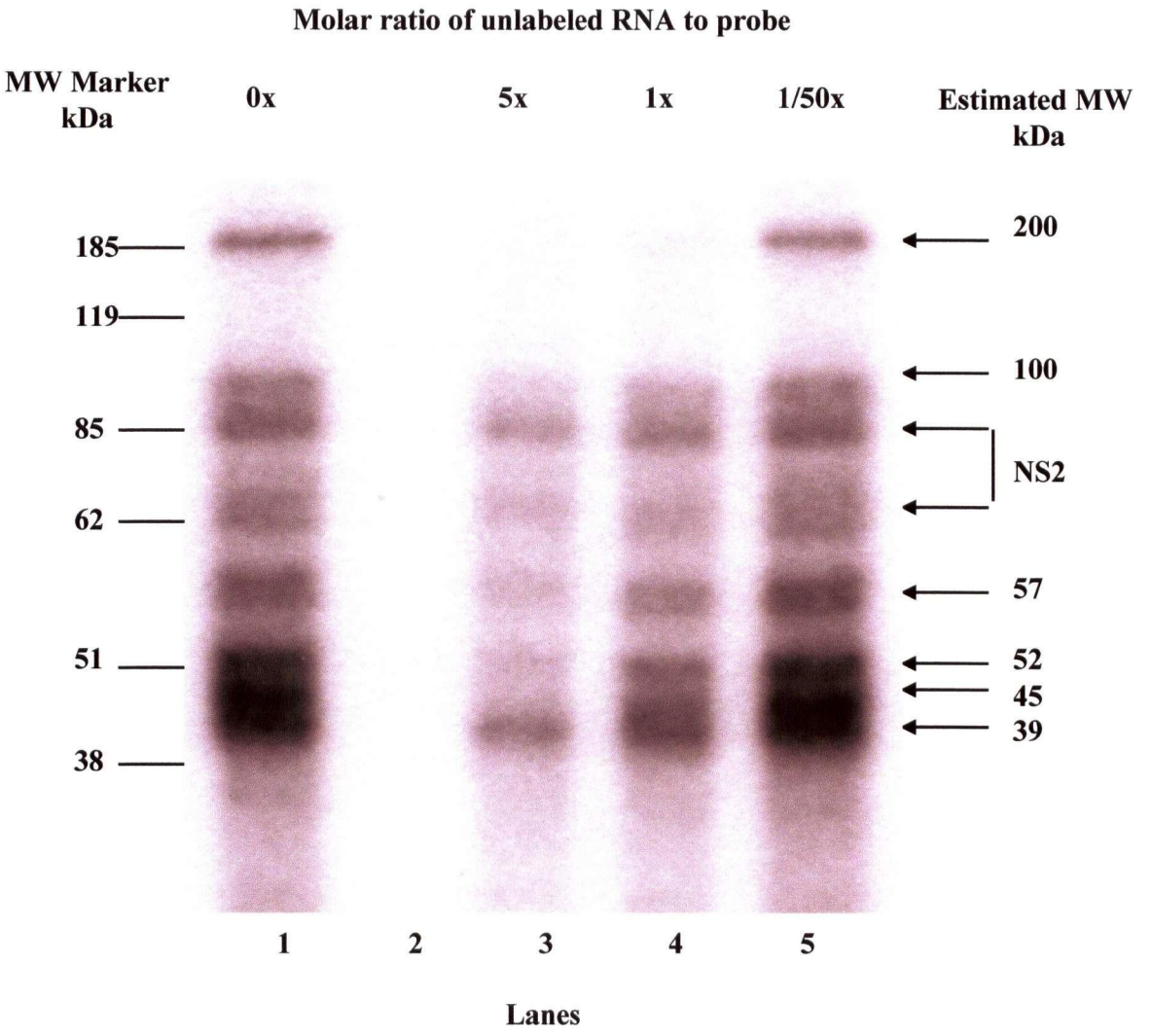

**Figure 18c**

HeLa cell protein interactions with the 5'-UTR nt 530-640. HeLa cell lysate is UV cross-linked to the radiolabeled RNA, in the presence of non-labeled RNA at the indicated molar excess ratios. UTR-binding proteins are visualized as bands, and their respective MW estimate is indicated on the right. Lane 2 is a negative control of interaction without UV treatment.

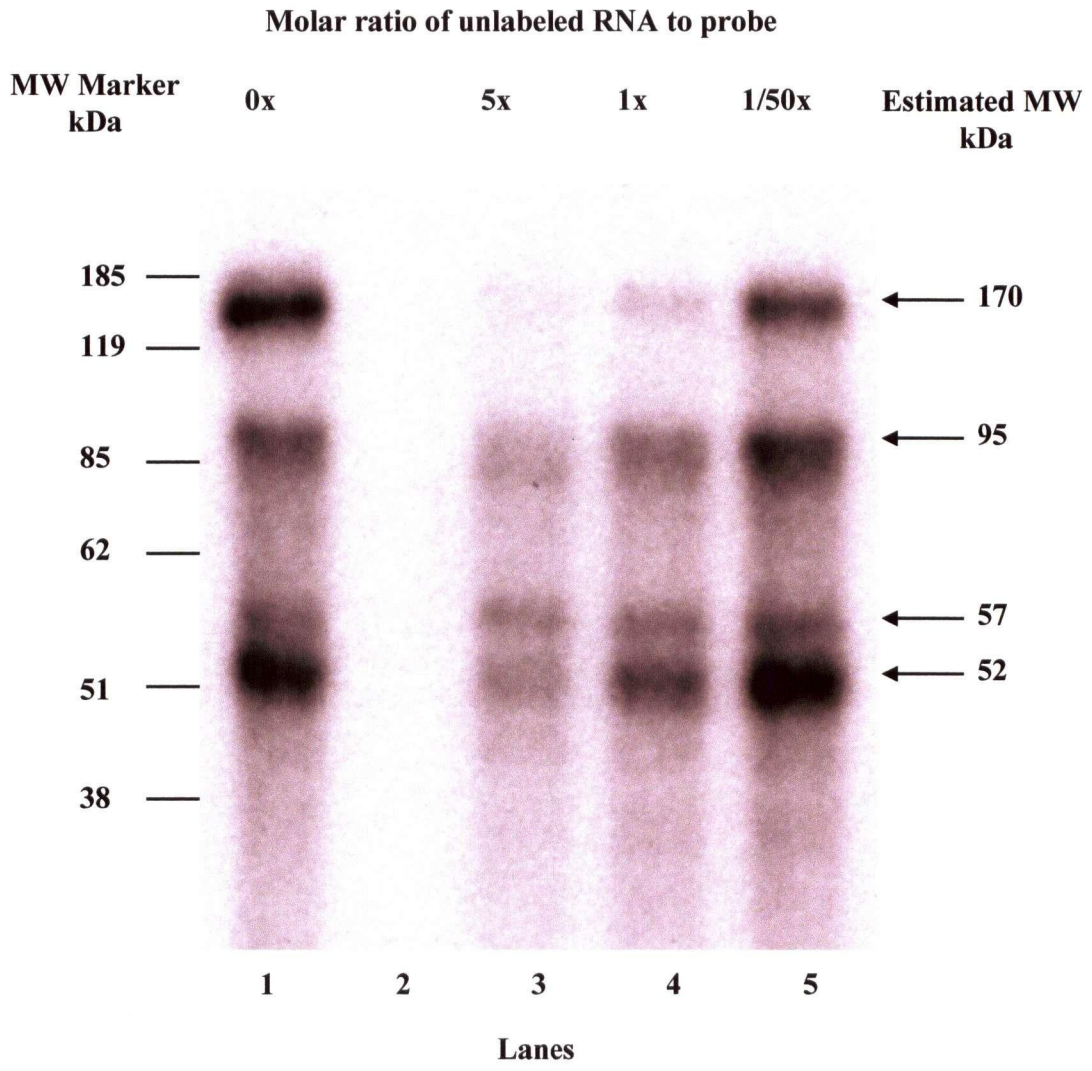

Some of these 5'-UTR binding proteins appeared to be differently susceptible to competition. For example, the 200 kDa protein band (**lane 1, Figure 18a and b**) was heavily competed by homologous RNA at the 5x (lane 3) and 1x (lane 4) molar excess ratios. It was restored only at the 1/50x molar excess (lane 5), while in contrast, the 45 kDa band was heavily competed at 5x excess but could be detected at 1x molar excess ratio (lane 4). These differences in susceptibility to competition reflected the differential binding specificities or differential quantities of the respective proteins towards the probe sequence.

*Non-specific interactions.*

Several HeLa cell protein-5'-UTR interactions were concluded to be non-specific. These include the complexes (**NS1**) in the nt 1-209 experiment (**Figure 18a**) in the MW range below 38 kDa and the 65/ 85 kDa bands in the nt 210-529 experiment (**marked NS2**). These proteins were not reported as specific interactions for two reasons:

1) the intensity of these bands did not vary significantly in response to the changes in the amount of homologous RNA competitor (lane 3-5);

2) the band intensities were weak and the bands were poorly defined.

Non-specific or very low affinity associations of labeled RNA to protein can occur, and due to the non-specific nature of these interactions, increasing the amount of homologous RNA competitor would not have resulted in competition for probe binding.

A summary of protein molecular weights that bound to the three 5'-UTR sequences is presented in **Table 6**. Of interest, the MW of 170 kDa, 80 kDa and 45 kDa resemble eIF4G,

eIF4B, and eIF4A respectively (bold type in the table). Functional roles of the eIF4A and B in resolving RNA secondary structures were discussed in **Section 1.6.1**. Proteins with MWs that corresponds to PTB (57 kDa) and La autoantigen (52 kDa) were also observed. Of note, the 52 KDa protein was observed to bind all three probes.

**Table 6.** Summary of Protein-RNA interactions between CVB3 5'-UTR sequences and the HeLa cell Lysate. Among these, the p200, p57, p52, p45 can bind to more than one 5'-UTR probe. Each of them may be the same protein binding to multiple sites in the 5'-UTR or different proteins that exhibit the same MW.

| **5'-UTR sequence** | **Molecular weight** | **Comment** |
|---|---|---|
| Nt 1-209 | 200, **80**, 62, **52**, **45** | Non-specific bands not included in list.<br>Possible ID:<br>eIF4B (80 kDa), eIF4A (45 kDa); La protein (52 kDa) |
| Nt 210-529 | 200, 100, **57**, **52**, **45** | This 5'-UTR region contains cardiovirulence determinants.<br>Possible ID:<br>eIF4A (45 kDa); PTB (57 KDa); La protein (52 kDa) |
| Nt 529-630 | **170**, **95**, **57**, and **52** | Possible ID:<br>eIF4G (175 kDa); DAP 5 (95 kDa); PTB (57 KDa); La protein (52 kDa) |

***HeLa cell protein-3'-UTR interactions (Aim 4).***

I have tested six different 3'-UTR clones for their ability to interact with the HeLa cell proteins. As before, UV cross-linking experiments were performed. The pattern of protein-RNA interaction with each probe was compared side by side in **Figure 19**. Data for the sense and antisense sequence was presented in the left and right panel, respectively.

Significant complex formation in the range of 70-100kDa (C1) and 36-45kDa (C2) were observed for both the sense and antisense probes (**Figure 19a** and **b**). The intense signals were observed with smear-like band patterns. Repeated experiments with reduced amount of probe and / or protein lysate did not improve the resolution of bands in these areas. This smear but intense signal suggests possible aggregations of the 3'-UTR-binding proteins in those ranges of MWs.

In general, the poly-(A) intact probes of the sense and antisense sequences demonstrated a visibly different pattern of protein-RNA interactions (comparing lanes 1, 3-6 of the left and right panel). For example, a 32 kDa (marked **Q**) protein complex was noted to bind to the antisense sequences specifically (comparing **Figure 19a** and **19b**). The corresponding area of the sense sequence did not show any comparable complex. There were fewer complexes observed in the C1 and C2 region of the antisense probes than in the sense probe. On the other hand, a common feature of the two probes was the interaction with a 52 kDa protein (marked **L**). This MW resembles that of the La autoantigen.

**Figure 19. HeLa cell protein interactions with the CVB3 3' UTR sense and antisense sequences.**

HeLa cell lysate is UV cross-linked to the radiolabeled 3' UTR RNA. The UTR-binding proteins are visualized as bands. The wild type 3'UTR probe is presented in lane 1, followed by the poly (A)-deleted 3' UTR (lane 2), stem loop X mutant (nt 7391/2, lane 3), stem loop Y mutant (nt 7352/3, lane 4), complementary mutant (stem loops XY mutated, lane 5), and deletion mutant (lane 6). The 52 kDa protein is observed to bind to both the sense (panel A) and antisense (panel B) 3' UTR probes. The 32 kDa protein **(Q)** is unique to the antisense profile. The AS1/AS2 are two small proteins (22 and 24 kDa) that bind exclusively to the 3' UTR mutants.

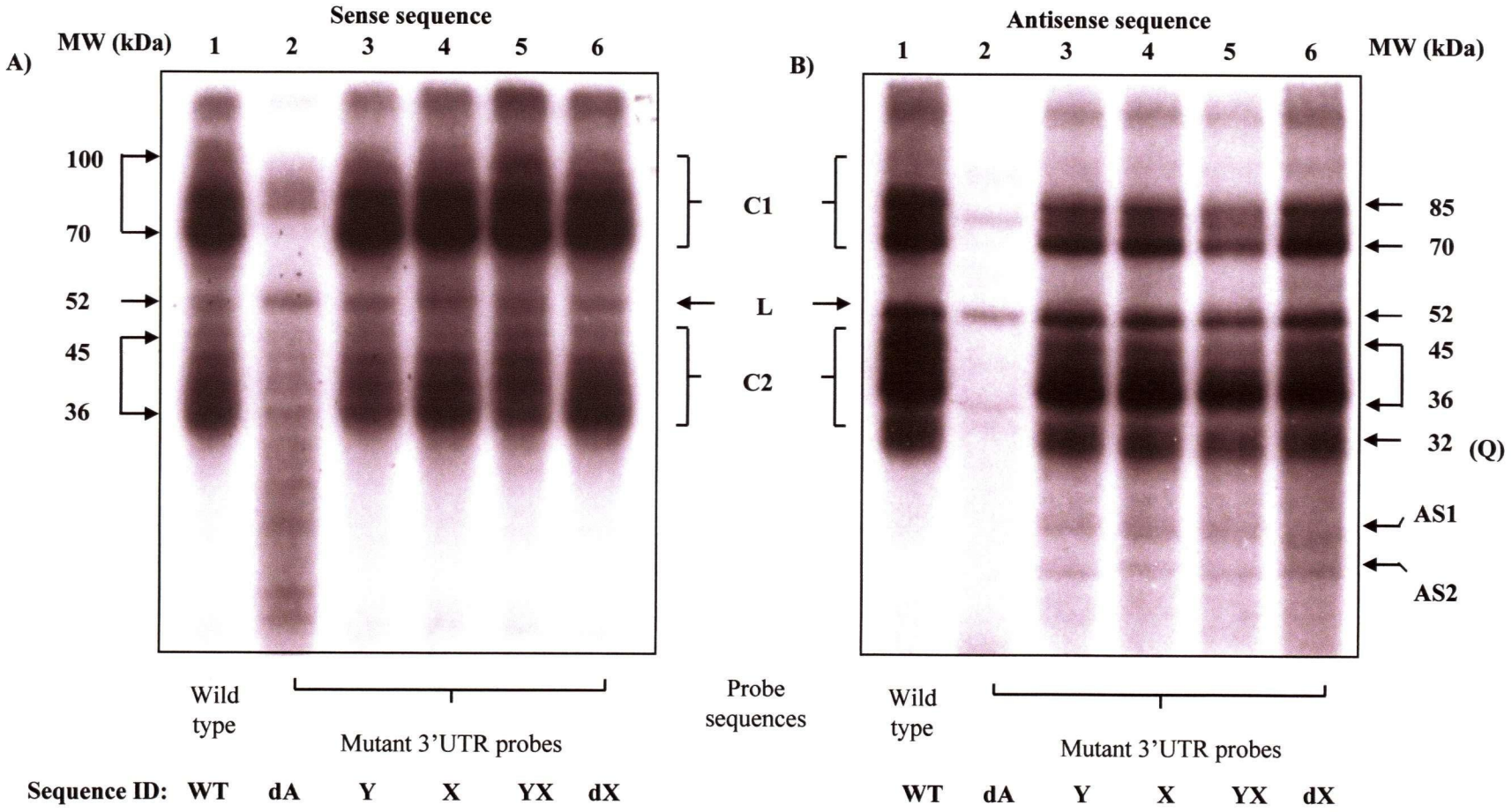

*Unique protein interactions with the mutated 3'-UTR sequences.*

When comparing the patterns of the protein interaction of the wild-type 3'-UTR sense sequence to that of the mutated 3'-UTR sense sequences (**Figure 19a**, lane 1 vs lane 3-6), no significant differences were observed. The extent of intense complex formations (area **C1** and **C2**) were highly similar, and the 52 kDa band appeared to be similar. Thus, mutations in the stem loop X and Y, which led to tertiary structural instability of the 3'-UTR, appeared **not** essential for inhibiting protein interactions with the sense 3'-UTR sequence.

When inspecting complex formation with the antisense probes (**Figure 19b**), the majority of the protein-RNA interactions were similar between the wild type probe (lane 1) and the stem-loop mutants (lane 3-6). However, for the mutants, two interaction bands (labeled **AS1** and **AS2**, **Figure 19b**) appeared exclusively with the antisense mutants (lane 3-6). Such complexes were estimated to be approximately 22 and 24 kDa in size. The interactions were not as intense as other protein bands, suggesting either a low abundance of such proteins in the lysate or the low efficiency in the formation of such complexes. These two interactions were unique to the mutated 3'-UTR antisense probes, including that of the complementary mutant. Since the wild-type tertiary structure of the 3'-UTR is partially restored in the complementary mutant [229], this observation strongly implies that the two additional interactions occurred by recognition of the mutated RNA sequences at nt 7352/3 and or nt 7391/2. The interactions of these two proteins with the mutated sequences, however, do correlate with the defective replication which is due to the mutations. In other words, the interaction of **AS1** and **AS2** can be related to the observation of impaired viral replication.

*Significance of the poly-(A) tail in mediating protein interaction.*

By comparing lane 1 to lane 2 in each of **Figure 19a** and **19b**, we have observed that the poly-(A) tail of the sense 3'-UTR and (poly(U) for the antisense 3'-UTR) were crucial for complex formations. In the sense sequence of the poly-(A) deleted probe (lane 2, **Figure 19a**), the 52 kDa band was discretely observed, while smear -like bands were detected in the ranges of 85- to 90 kDa and also from 15- to 45 kDa. In the antisense probe, only the 52 kDa and the 75 kDa were strongly distinguished, while bands in the 35- and 90 kDa range were weakly observed. In general, these poly-(A)/poly-(U) deleted probes demonstrated highly reduced protein binding capabilities.

## 4.3 DISCUSSION

Specific interactions between host proteins and CVB3 UTR RNA probes were shown by the use of mobility shift assays and UV cross-linking experiments. Data from Aim 1 demonstrates the feasibility of detecting protein-RNA complexes by *in vitro* methods. In the following sections, I shall focus on the discussion of the findings that are significant and related to the pathogenesis of CVB3 infection.

***Interactions of A/J mouse proteins with the viral 5'-UTR.***

In my study, the differential susceptibility of A/J mouse tissues has been further established by data from the ISH experiments. Three major observations are:

1) Endocrine and exocrine pancreas cells had contrasting susceptibilities to CVB3;
2) Kidney cell types were resistant to infection despite previously reported high-level of receptor expression;
3) Cardiomyocytes had an age-dependent susceptibility to infection.

Currently, these phenotypic observations are not adequately explained by any known molecular mechanisms. To investigate these issues, I have focused on the identification of host proteins that may be responsible for viral translation or transcription via interactions with the CVB3 5'-UTR. However, a draw-back in these UV cross-linking experiments of the A/J organ tissues was the variability in the content of the lysates, as organs contain variable amounts of fibrous material, DNA / RNA, lipid and salt. As a result of these variations, resolution of protein-UTR complex bands by the standard SDS PAGE was less than ideal. The nature of autoradiograph imaging has limited the ability to perform quantitative comparisons of the UTR

binding proteins. Thus, my data analysis is focused on the identification of unique proteins that relate to the susceptibility of organs to CVB3 infection.

In all the profiles of tissue protein-UTR interactions, a high degree of sequence specificity was observed. This is concluded from the significant differences in the number, intensity and MW of the proteins-UTR complexes formed by each of the 5'-UTR sense and antisense probes (comparing lane 1 to lane 2, lane 3 to lane 4 and lane 5 to lane 6 of each profile, **Figure 16**). Since the antisense sequence of the CVB3 5'-UTR does not serve as an mRNA template for translation, my initial intent was to exploit the results using the antisense probe as controls to verify the specificity of bands detected by the UV cross-linking method. To this purpose, the patterns of protein-probe interactions of the sense and anti-sense were indeed contrasted and thus demonstrated the probe-sequence-dependent nature of the protein-RNA interaction. The same can be concluded when comparing the protein interactions of the three regions of the 5'-UTR (nt. 1-209, nt. 210-529 and nt. 530-630).

***Common-UTR binding proteins in cell lysates of A/J mouse tissues.***

Despite these sequence-dependent differences in protein-UTR interactions, the overall profiles of interaction among all the A/J organ-lysates appeared similar (comparing the complete profile of UV cross-linking from one lysate to another). This overall similarity in the patterns of protein-probe interactions suggests that some UTR-binding proteins are universally present in all cell lysates. For example, four proteins, the 29 kDa / 31 kDa (Marked A) and 43 kDa / 45 kDa (Marked B; lane 3 in each panel of Figure 16), were found to bind to the sense sequence of nt 250-529, which were commonly observed in all profiles. As discussed in the Introduction, translation initiation of the viral or host RNA requires the eIF4 family factors (and other host

proteins). These factors are universally present in all cell types, and considering the role of the CVB3 5'-UTR in translation initiation, those UTR-binding proteins that are commonly observed in all profiles are possibly involved in the process of viral RNA translation initiation. In light of the extensive secondary 5'-UTR structure in the sequence of nt 210-529 (**Figure 9**), I further speculate that the above mentioned four proteins may be involved in the stabilization of higher-order RNA structures. In this respect, the eukaryotic translational initiation factor 4A (eIF4A) can be a potential candidate. The eIF4A is a 45 kDa RNA dependent helicase protein. The eIF4A molecule functions by ATP hydrolysis to unwind secondary structures within the 5' leader of host mRNA, thereby facilitating the 40S ribosomal binding and scanning for the initiation codon. The affinity towards single strand RNA of the ATP bound eIF4A can vary significantly depending on phosphorylation status [263,286]. Thus, interaction of this protein to the CVB3 UTR sequence may be observed as closely migrating doublets of the phosphorylated/ dephosphorylated forms. Of note, a 45 kDa protein complex is also observed to bind this 210-529 sequence in the experiments using the HeLa cell protein lysate (**Table 6**). Whether the eIF4A is indeed one of the four proteins that bind to the nt 210-529 region remains to be verified by other methods, such as immunoprecipitation and / or the use of recombinant proteins. These proteins are also interesting because the sequence of nt 210-529 is currently regarded as important in the determination of the cardiovirulence of the virus (see Introduction).

The UTR-protein complexes detected in my UV cross-linking experiments using the A/J mouse organ lysates are documented in **Table 5**. These proteins were not identified further than their apparent MWs due to technical limitations. At the time when the study was conducted, expertise and equipment for large scale protein purification and characterization was limited. This was compounded by the fact that the method of detection was dependent on radioactive

labeled RNA. Although this method, in contrast to other fluorescence or biotin-labeling techniques, has the advantage of being highly sensitive and preserving the chemical properties of the UTR sequence, it required the use of dedicated equipment and bench space to limit environmental contamination. To further identify these proteins, I have proposed the use of several recently emerging proteomics technologies, and some preliminary data is discussed in **Chapter VI.** At the present time, in order to remain concise in the discussion of the key results, I will focus on the potentially important p28 protein interaction.

***The 28kDa protein interaction with antisense nt 210-529.***

The objective of the UV cross-linking experiments with the A/J mouse organ lysate was to discover if specific protein interactions may be responsible for the tissue susceptibility as revealed by the ISH observations. To this end, the 28 kDa protein-UTR complex that is observed in the profiles of kidney, liver and 10-week-old heart is unique and correlates well with the organs' resistance to the virus.

The 28 kDa protein-RNA interaction occurs only in the 5'-UTR of nt 210-529, specifically to the antisense sequence (not observed in the sense sequence of this region). Considering the general rule of nucleotide base-pairings, It is expected that the sense and antisense probes would form similar (but mirror-imaged) secondary structures. Thus, the absence of such interaction in the corresponding sense sequence of nt 210-529 suggests that the p28 likely recognizes and binds to a specific single strand RNA sequence (e.g. loop regions), as opposed to secondary structures, of the antisense probe. As noted, CVB3 is a positive sense single-stranded RNA virus. Progeny RNA (sense RNA) is synthesized by transcription that is initiated from the 5'-UTR of the antisense template. If the p28 interaction does contribute to

resistance to viral replication in the kidneys, the mechanism could be due to the sequestration of the viral antisense template by p28, preventing effective production of progeny viral RNA: a transcription block at this location of the antisense template may prevent the genomic RNA synthesis beyond the 5'-UTR. During acute myocardial infection, the antisense strands of CVB3 are synthesized rapidly and reach a high concentration in a very short period of time. Thus, a large amount of p28 is possibly required to inhibit viral transcription. To this end, the high level of p28 expression in the kidney correlates to its high resistance to CVB3 replication. The moderate to low level of p28 interactions in the liver and 10-week-old heart also correlate with their respective viral titre. Further investigation on the cellular concentration, identity and function of the p28 is required to verify my postulate. Data from these further work may provide very important information on the molecular determinants of CVB3 infectivity and tissue tropism.

***HeLa cell protein vs 5'-UTR.***

In this study, I have demonstrated a number of proteins bound to the three different 5'-UTR sequences. Some of these UTR-binding proteins may be identical proteins that have multiple binding sites in the 5'-UTR; some of them may be different proteins with similar MWs. Since there is no previous report on protein-RNA interactions of the CVB3, I would compare my findings to other close relatives of CVB3.

Dildine and Semler [99] reported that HeLa cell proteins that interact with the poliovirus 5'-UTR can be cross-competed by the CVB3 5'-UTR, suggesting a conservation of both the RNA stem loop structures as well as the basic function of the RNA-protein interaction in the viral life cycles, especially in the IRES-directed translation initiation. Further work has identified a

number of known / unknown picornaviral-UTR binding-proteins [132] such as the hnRNP, PTB, La autoantigen and PCBP2 that bind to the IRES, with MW 68, 57, 52 and 39 kDa, respectively. Notably, the PTB can inhibit the activity of another host protein GAPDH [352], while GAPDH is also capable of IRES interaction [352]. This observation is contrasted to the synergistic effect between the PTB and the La autoantigen in stimulating the EMCV IRES activity [174]. From current knowledge, it appears that specific picornaviral UTR sequences may interact with a similar set of host proteins, but each viral UTR-protein interaction can occur by a unique mechanism to achieve optimal translation initiation in their respective target cellular environments. In my experiments, some of the CVB3 5'-UTR-binding proteins have MWs that are identical to the above mentioned five polio-UTR interacting proteins (**Table 6**). In addition, I have also observed similarities in MWs between the CVB3 5'-UTR-binding proteins and the eIF4 family of translation initiation factors. These host proteins include the eIF4A (45 kDa), eIF4B (80 kDa), and eIF4G (170-220kDa). The three eIF4 proteins are constituent molecules of the 220kDa eIF4F, which is also critical in the translation initiation of eukaryotic mRNA.

***The eIF4F family and CVB3 5'-UTR.***

The large 170 kDa protein complex bound to the CVB3 IRES sequence is similar to the MW of the well-characterized eIF4G (**Figure 18**). The eIF4G is occasionally detected as a 220 kDa protein when it combines with other eIF factors to form the eIF4F complex. The integral eIF4F is crucial for the host cap-dependent mRNA translation initiation [116]. Incidentally, UV cross-linking experiments detected a ~200 kDa complex for 5'-UTR probes nt 1-209 and 210-529. The normal cellular functions of eIF4A and eIF4B are to resolve complex secondary structures of the mRNA prior to binding of eIF4G and ribosome. The binding of these factors to

nt 1-209 and nt 210-529 of the CVB3 5'-UTR would not be surprising since extensive stem-loop structures have been predicted within these sequences (**Figure 9**) and the eIF4A and eIF4B could resolve the secondary structures prior to internal ribosomal entry and translation initiation. Pertinent to viral pathogenesis, eIF4G alone has been reported to bind the IRES of the EMCV; the eIF4E binding domain of the eIF4G is cleaved by CVB3 protease $2A^{pro}$ during active infection, leading to the inhibition of host mRNA translation while viral uncapped RNA remains unaffected (**Chapter I**). As a side note, a protein of MW that is similar to the eIF4E (25 kDa) is not observed in the UV cross-linking experiments with the HeLa cell lysates (**Table 6**). Reflecting on these findings, I propose that eIF4 family of proteins may also bind the IRES of CVB3 and play important roles in the translation initiation of the viral RNA, while eIF4A and eIF4B can be involved in the resolution of secondary structures in the 5'-UTR and facilitate the binding of eIF4G and ribosomes.

***Significance of the Poly-(A) tail in mediating protein-interaction.***

The existence of the poly-(A) tail sequence (in the sense 3'-UTR probes) or the poly-(U) tail (in the antisense 3'-UTR probes) was found critical to protein interactions with the 3'-UTR. This suggests two possible roles of the poly-(A) tail in the interactions: 1) the poly-(A) tail directly interact with the observed complexes; 2) the poly-(A) tail maintains a stable secondary structure that favours protein binding to the 3'-UTR. Based on the predicted stem loop X formation by base-pairing between the poly-(A) (or poly-(U) of the negative sense) and nt 7380-4 (**Figure 10**), deletion of the poly-(A) tail could disrupt base-pairing in the X-stem loop and thus lead to changes in the 3'-UTR secondary structures. In contrast, mutations in other 3'-UTR mutants did not result in changes in secondary structures [229] as mutations in the loop region only

affect tertiary interactions (**Figure 10**). In other words, the absence of the poly-(A) or -(U) sequence resulted in altered secondary structure which in turn reduced the ability of the 3'-UTR in binding host proteins. This is a possible explanation for why the 3'-UTR mutants exhibit protein interaction patterns that are identical to the wild type, while the patterns of the poly-(A) or poly-(U)-deleted mutants were dramatically different. Further identification of the 3'-UTR binding proteins will thus be important to the understanding of the mechanism of poly-(A) tail on the viral pathogenesis.

***Protein interactions unique to the replication defective mutants.***

A major objective in the investigation of 3'-UTR mutants is to identify protein–UTR interactions that correlate with the inhibition of viral replication. To this end, the interactions between 22 / 24 kDa (AS1 and AS2) and the antisense mutant 3'-UTR probes were identified. The antisense sequence of the 3'-UTR is a template for the synthesis of the positive sense viral genome. As mentioned in the results, these two proteins are likely recognizing the primary (linear) RNA sequence on the 3'-UTR at the mutation site, since no 22 / 24 kDa proteins were observed binding to the sense mutant 3'-UTRs. While the low level of the 22 / 24 kDa protein complexes are suggestive of inefficient complex formation, it may also be due to a lack of these proteins in the HeLa cell lysate. Since, these two bands were not observed in the wild type probe (lane 1), it is likely that such interactions are specific. It is important to note that the complementary mutations of the stem loops also exhibit interactions with these two proteins, which was not unexpected. Melchers et al. [229] demonstrated that in a cell culture environment, different complementary mutations in the 3'-UTR can lead to contrasting growth characteristics, from as low as 5% to non-wild type efficiency. The instability of the tertiary structures in the 3'-

UTR complementary mutants was evident from the temperature sensitive phenotypes of the mutants [229]. Hence, the tertiary structural stability of the 3'-UTR mutant RNA is possibly not sufficiently restored to prevent the interactions of the 22 and 24 kDa proteins. The 22 and 24 kDa interactions correlate well with the inhibitory function of the mutations and thus raise important issues for further studies. Investigating these proteins, along with the p28 kidney protein that was observed to bind the antisense sequence of nt 210-529, may greatly advance our understanding of the participation of host proteins in the CVB3 viral replication process.

# CHAPTER V

## Characterization of the La autoantigen - CVB3 UTR interactions.

Data from studies described in **Chapter IV** indicated that a 52 kDa protein bound to the 3'-UTR and all three regions of the 5'-UTR. In light of current knowledge of picornaviral systems, including literature that shows a stimulatory effect of La protein in translation initiation from an IRES, it is worth investigating if the La protein may bind to multiple regions in the 5' and 3'-UTRs, and whether the La protein is processed by CVB3 proteases in a fashion similar to that is observed in the poliovirus system.

### 5.1 EXPERIMENTAL STRATEGIES

A flow chart of the strategy employed in this series of experiments is presented in **Figure 20**. In addition to techniques described in **Chapter IV**, several other techniques were used. These include the expression and purification of the GST-fusion La protein in an *E.coli* system. The La autoantigen has been studied in other virus systems. The plasmid vector pGEX-La was a gift from Dr. Y. K., Kim / S. K. Jang, Pohang University of Science and Technology, Korea. Using this plasmid, recombinant La protein was produced and purified. Detailed modifications to the original purification procedure [174] are described in **Chapter VII**. Each batch of La protein production was performed with 100 ml of LB medium. A typical yield of 3.5 mg La protein was achieved. The functionality of this recombinant protein had been proven in a study of the IRES of the EMCV system [174]. The schematic structure of the pGEX-La plasmid and the process of protein purification is presented in **Figure 21** and **Figure 22**, respectively.

**Figure 20. Strategy for characterizing the interaction between La protein and the CVB3 5'- and 3'-UTR.**

The recombinant GST-La protein was expressed in *E.coli.* Purified La protein and GST-La fusion protein were used in competitive UV cross-linking assays to determine specific interaction. A saturation curve was generated by increasing the amount of RNA probe to further confirm the specificity of interactions. The corresponding data was transformed into a Scatchard plot to estimate the apparent dissociation constant (Kd). The concurrent / exclusive binding mode of the La protein with the 5'- and 3'-UTR was determined by two-stages UV cross-linking.

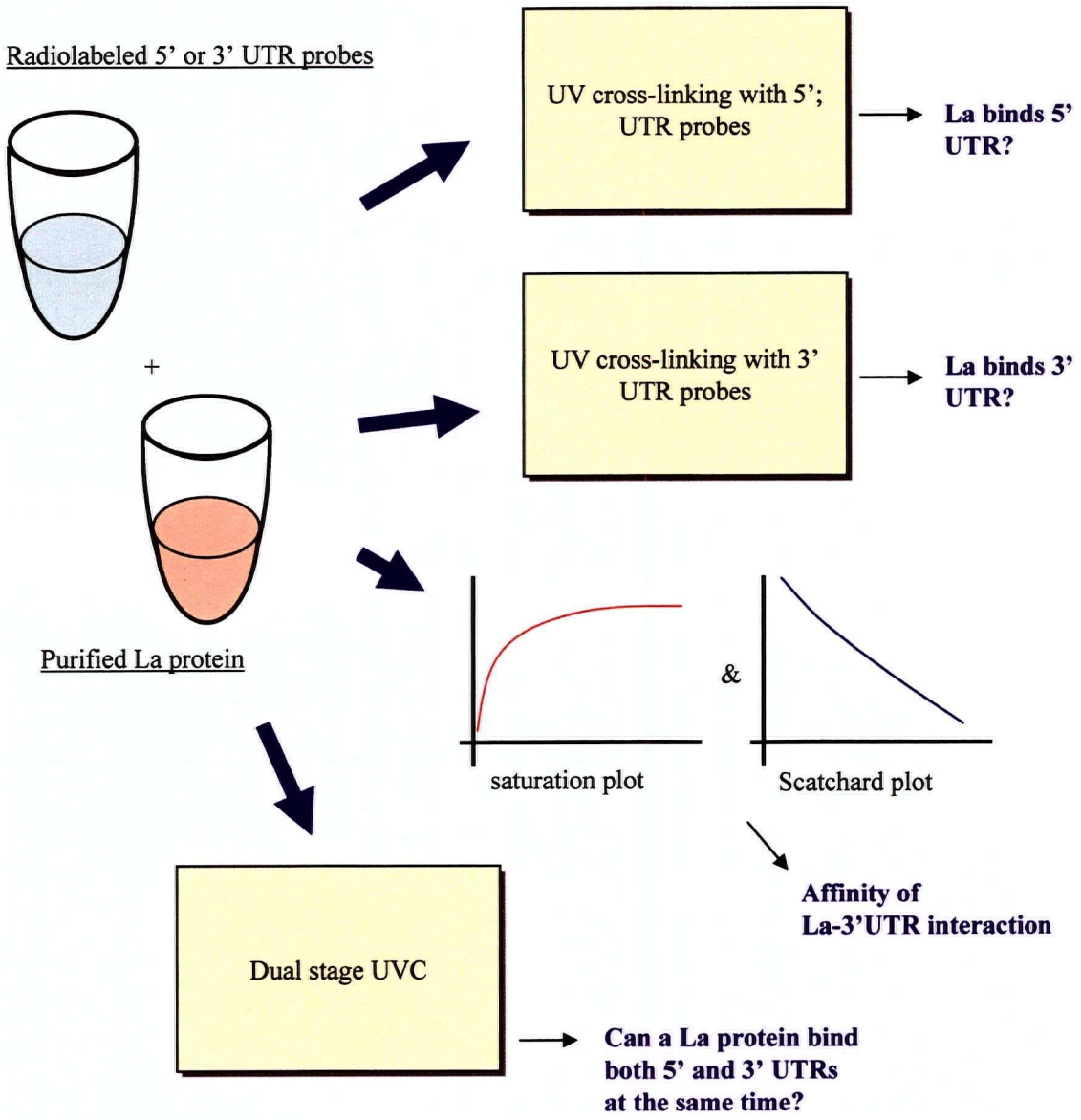

**Figure 21.** Structure of the pGEX-La protein plasmid.

Expression of the GST-fusion protein is mediated by the T7 promoter. The fusion protein can be cleaved by thrombin to separate the La protein from the GST domain.

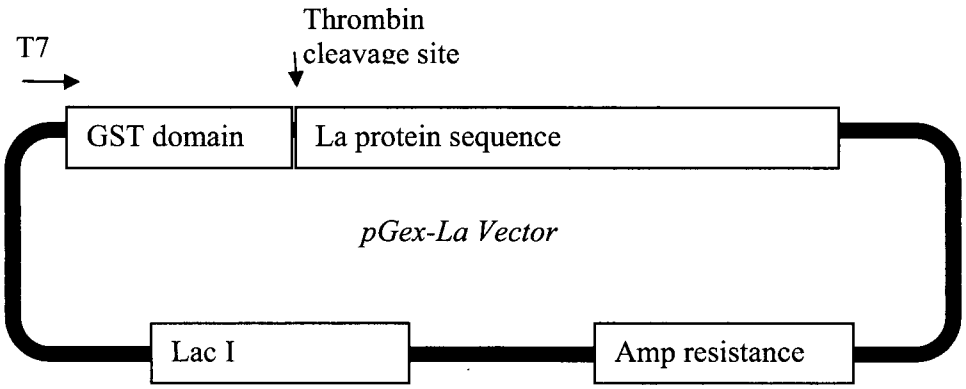

**Figure 22. Strategy for the expression of recombinant La protein.**
E.Coli BL21 is induced to produce the recombinant protein, which was then purified by the GST affinity method. Either the ~80 kDa GST-fusion La protein is eluted by 1M glutathione or the 52 kDa La protein is obtained from the matrix by thrombin protease digestion. The purity of the protein was verified by SDS PAGE and coomassie blue staining.

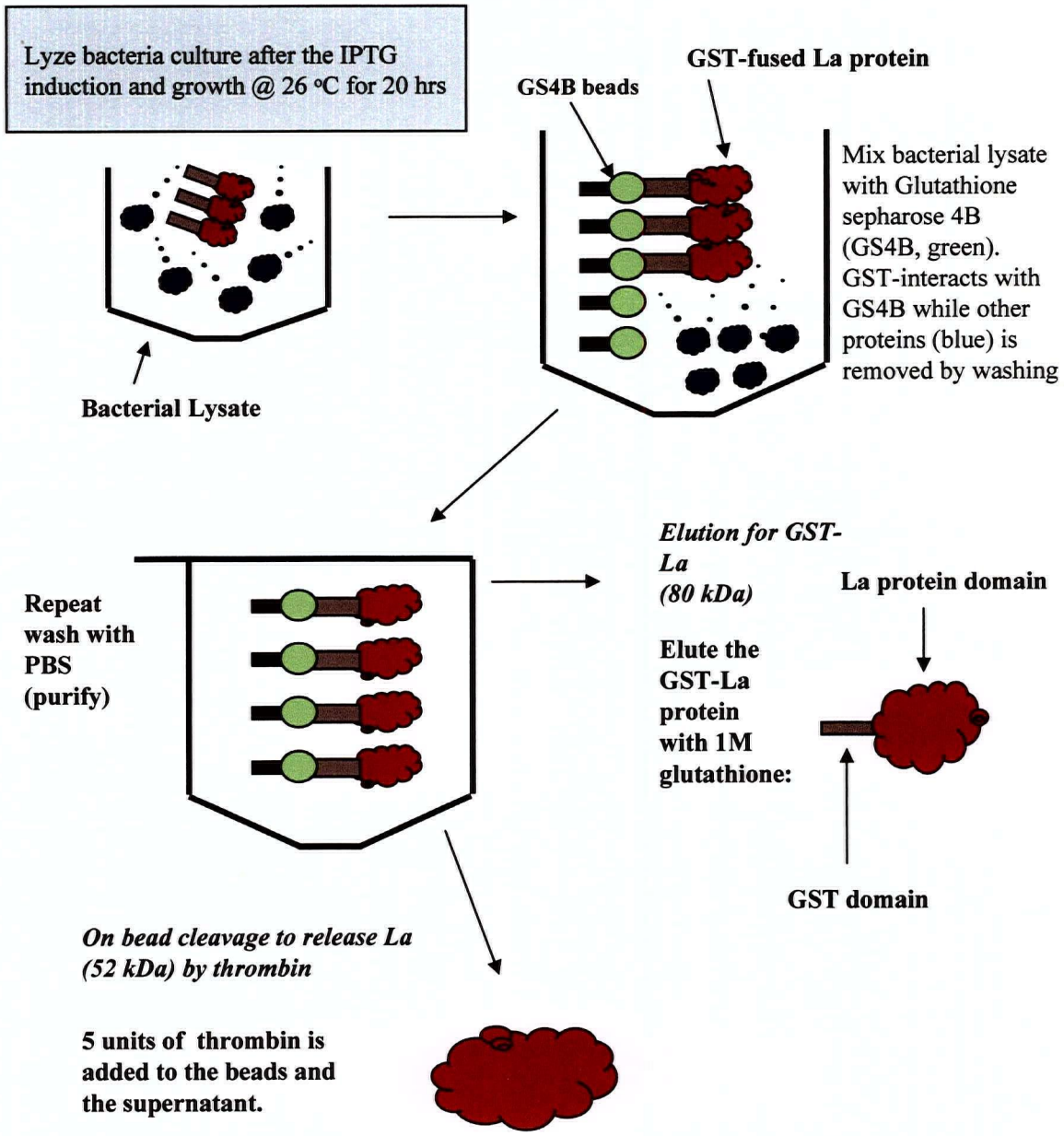

*Quantification of the La-UTR complex*

The purified recombinant La protein was used in competitive UV cross-linking assays to determine if the La protein interacts specifically with the 5' and 3'-UTRs. In addition, I have developed the use of scintillation counting to quantify the amount of Cherenkov radiation emitted by the La-UTR complex in 70% ethanol. In brief, the UV cross-linked La protein-probe complex in each reaction was analyzed on the SDS PAGE as described in **Chapter IV**. The SDS PAGE was dried on Whatman paper and the band of protein-probe complex was physically cut out from the dried acrylamide gel. The band was immersed in 5 ml of 70% ethanol (covering the entire strip) in a transparent scintillation count vial. The activity of each band was recorded as counts per minute (CPM). Final CPM counts were adjusted for radioactive decay ([$\alpha$-$^{32}$P]-UTP, ½ life of 14.3 days) based on the day of each experiment. This approach is advantageous over the use of autoradiography in demonstrating the specificity of interaction because the data is numerically quantified, reproducible, and does not depend on uncertainties such as exposure time and image processing, etc. The method is also necessary because the scintillation count (cpm) allows calculation of the extent of complex formation in the saturation experiments, which were designed to biochemically characterize the La-UTR interactions.

***Estimation of the apparent Kd and stoichiometry of La-UTR interaction***

The apparent dissociation constants of interaction between the La protein and the 5' or 3'-UTR labeled RNA were determined by saturation experiments and the subsequent scatchard plot transformation of data. The two quantities allow a biochemical assessment of the physiological significance of the La-UTR interactions. The equilibrium assumption is summarized by the following equation:

$$\text{La protein} + \text{RNA probe} \underset{\text{Kd}}{\overset{\text{Ka}}{\rightleftharpoons}} \text{Protein-RNA complex}$$

And using this equilibrium assumption, the interaction between La and the UTRs were characterized. Details of the method is described in Section 7.10. Similar Scatchard plot analyses have been used in other single substrate-interaction studies such as the poliovirus receptor-virion interactions [12]. By transforming the data of the saturation curve into a standard scatchard plot, I have determined the apparent dissociation constant (Kd) of the La protein- 3'-UTR interaction. All data was organized, processed and plotted using Microsoft Excel.

## 5.2 RESULTS

***Purification of the La autoantigen.***

The pGEX-La plasmid was successfully transformed into BL21DE3 (pLys) (Novagen). I have observed that induction of the transformed bacteria with IPTG at O.D. <0.6 will produce the maximum yield of La protein. Induction with IPTG beyond 0.5 mM (final concentration) did not result in significant gain in protein yield. There had been suggestion of using <0.3% glucose to stimulate expression of the recombinant protein. I have not observed significant improvement with this procedure.

Purity of the La protein was verified by Coomassie Blue staining (**Figure 23**). The purity of the recombinant protein was verified by the absence of other protein bands and was suitable for use in subsequent interaction experiments. Each batch of La protein was aliquoted and stored in -80°C freezer for a maximum of one week to avoid protein degradation.

**Figure 23.** Coomassie blue staining of the La protein preparation.

Recombinant expression of the La autoantigen in BL21 DE3 (pLys) and purification. Protein lysate of the IPTG induced bacteria is shown in lane 4. Over expression of the recombinant GST-La protein (~78 kDa) is observed among other proteins. Lane 3 is the final supernatant to check against protein loss during washes of glutathione-sepharose beads. Lane 1 and 2 are the purified protein products. Recombinant GST-la (~78kDa) is eluted with 1M glutathione pH7.0 (lane 2). Purified La is obtained by 5 units thrombin on-beads-cleavage for 3 hrs at 4'C. The 10% SDS PAGE is stained by Coomassie blue.

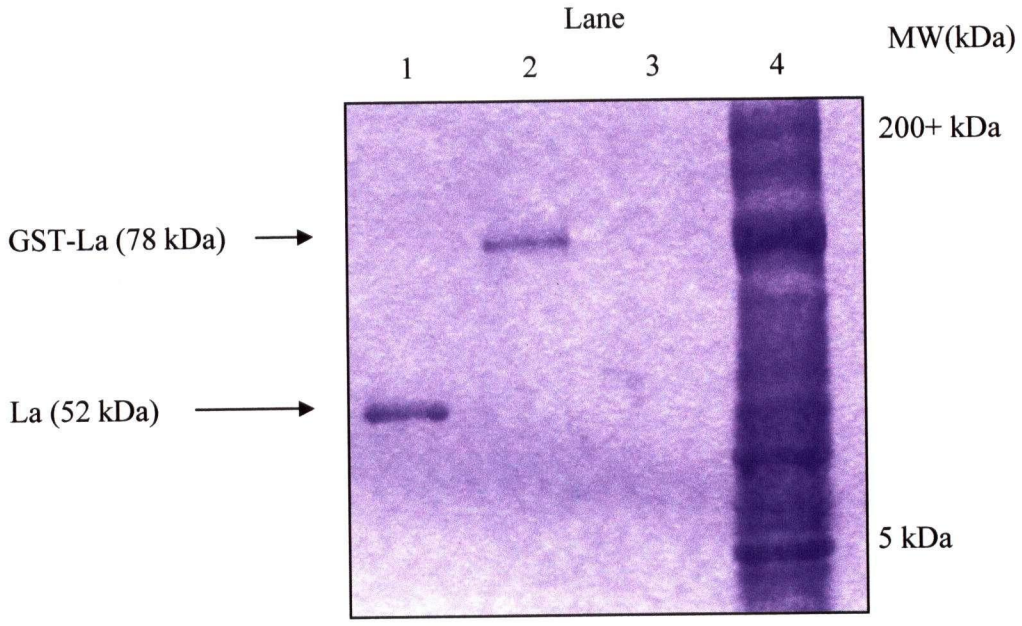

***Interaction of the 5'-UTR with the La protein.***

Purified La autoantigen was incubated with radiolabeled 5'-UTR probes and UV cross-linked. The results using probe sequences nt 1-209, nt 210-529, and 530-630 were shown in **Figure 24a, b, and c**, respectively. Interaction between labeled probe and La protein was observed by the 52 kDa band of complex on the autoradiograph (lane 3, all of **Figure 24**) . Homologous RNA and yeast tRNA were used as competitors to test for the specificity of interactions.

*Weak interaction of La protein and nt 1-209.*

Initial experiments did not detect complex formation between the La protein and the probe nt 1-209: No significant signal was observed in the autoradiograph. By trying different interaction procedures, I could observe the 52 kDa protein-probe complex when the labeled probes of nt 1-209 were preheated to 95 °C for 2 min prior to reaction with the La protein at 37 °C. Hence, it is likely that complex formation between the La protein and the sequence nt 1-209 was sub-optimal at 37 °C. Pre-heating of the RNA at 95 °C would have denatured secondary and tertiary structures. When added to the reaction, the temperature transition from 95°C to 37°C should have allowed formation of intermediate RNA structures that favored the binding of the La protein. Despite the requirement of pre-heating, the interaction between La and nt 1-209 appeared specific. In lane 1 (**Figure 24a**), the use of GST-La fusion protein resulted in a very weak interaction at the corresponding MW range (80 kDa). The use of 2x molar excess homologous non-labeled competitor (lane 2) resulted in a reduction in the amount of labeled complex. The use of non-labeled competitor of the nt 210-529, or nt 529-630, (lane 4, 5 respectively) also resulted in the reduction in complex intensity. Of note, intensity of the La

protein-probe complex in lane 4, in which non labeled nt 210-529 was added, is much weaker than that in lane 2. Thus the competition effect by the non-labeled RNA of nt 1-209 (self) was weaker than that of the nt 210-529, and as a result the intensity of the protein-probe complex in lane 4 was lower. In other words, affinity of the La protein towards nt 210-529 is considered to be stronger than that of the self-competitor (nt 1-209). Similarly, competitor of the IRES core sequence (lane 5) also appeared to have a stronger competition effect than the self competitor. The sequence specific nature of the La protein - nt 1-209 interaction is confirmed by the use of vector RNA at 2x molar excess, which did not result in reduction in band intensity (lane 6).

*Strong interactions of La protein with the nt 210-529 and the IRES.*

Strong La protein interactions with the probe nt 210-529 and the IRES core sequence were observed (lane 3, **Figure 24b and c**). For these probe sequences, no pre-heating was necessary and standard interaction conditions were applied. In **Figure 24b**, the intensity of the probe-protein complex in the presence of self competitor (lane 2) was much weaker than in lane 4 and 5. The band intensity in lane 5 was in turn weaker than that in lane 4. Strong competition from a homologous RNA resulted in less labeled probe being bound to the La protein, and hence a lower band intensity would be the consequence of a more effective competitor. Therefore, the data suggests that the La protein bound most strongly to the nt 210-529 (lane 2), less so to the 530-630 region (**Figure 24b**, lane 5), and the weakest to the nt 1-209 region (**Figure 24b**, lane 4).

In **Figure 24c**, this hierarchy of La-5'-UTR affinity was confirmed by the use of nt 529-630 as probe: the intensity of the IRES-La complex (**Figure 24c**, lane 5), in which non-labeled nt 210-529 was used as a competitor, was weaker than in lane 2, in which the IRES self

competitor was added. The nt 210-529 had a stronger affinity towards La protein than the IRES. Together with the observation in **Figure 24a**, the sequence nt 210-529 consistently demonstrated the strongest La-binding activity than other 5'-UTR sequences.

In **Figure 24b** and **c**, the GST-fusion La protein appears to result in moderate complex formation (lane 1). The GST domain on the recombinant protein can reduce the ability of the La protein in RNA interaction, as the band intensity was noticeably lower than the corresponding La-probe complex.

**Figure 24a. UV crosslinking of the La protein and the 5' UTR probe nt 1-209.**

Purified GST-La (lane 1) and La protein (lane 2-6) were UV cross-linked to the radioactive probe of sequence nt 1-209. Competitors were added in lanes 2-6 as described. Complex formation is observed using purified La autoantigen at the expected 52 kDa range (lane 3). GST-fused La protein-UTR complex is observed very weakly (lane 1). The use of vector RNA (PCR 2.1, Invitrogen) at 2x molar excess did not result in competition (lane 6).

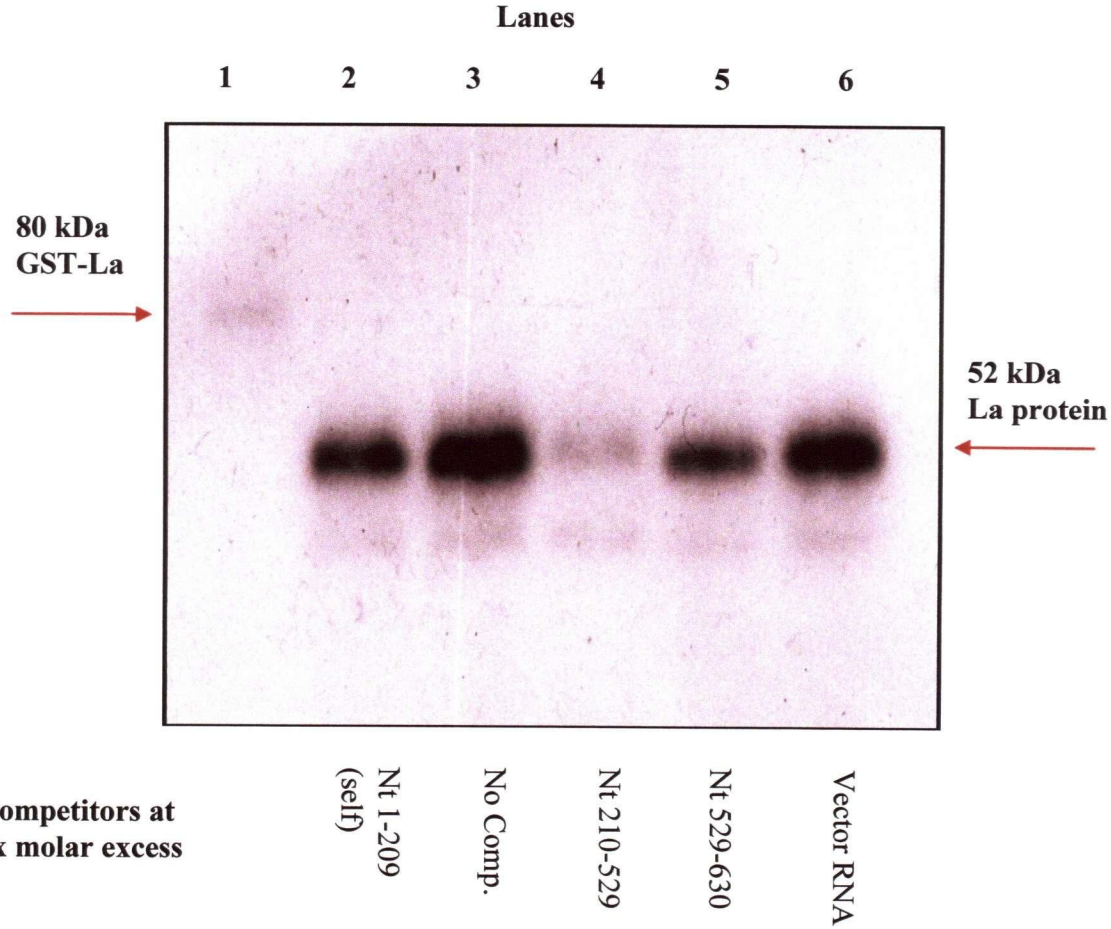

**Figure 24b. UV crosslinking of the La protein and the 5' UTR probe nt 210-529.**

Purified GST-La (lane 1) and La protein (lane 2-6) were UV cross-linked to the radioactive probe of sequence nt 210-529. Competitors were added in lanes 2-6 as described. Complex formation is observed using purified La autoantigen at the expected 52 kDa range (lane 3). GST-fused La protein-UTR complex is observed very weakly (lane 1). The use of vector RNA (PCR 2.1, Invitrogen) at 2x molar excess did not result in competition (lane 6).

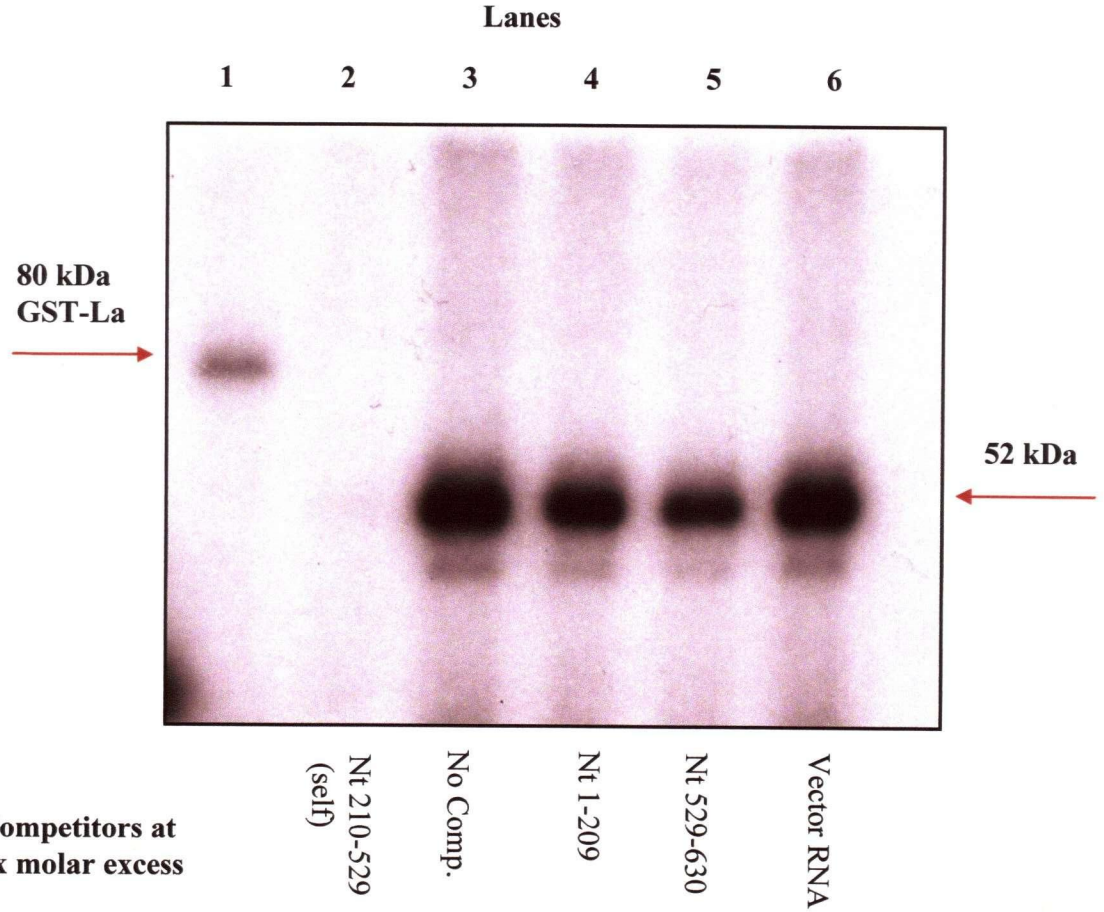

**Figure 24c. UV crosslinking of the La protein and the 5' UTR probe nt 530-630.**

Purified GST-La (lane 1) and La protein (lane 2-6) were UV cross-linked to the radioactive probe of sequence nt 530-630. Competitors were added in lanes 2-6 as described. Complex formation is observed using purified La autoantigen at the expected 52 kDa range (lane 3). GST-fused La protein-UTR complex is observed very weakly (lane 1). The use of vector RNA (PCR 2.1, Invitrogen) at 2x molar excess did not result in competition (lane 6).

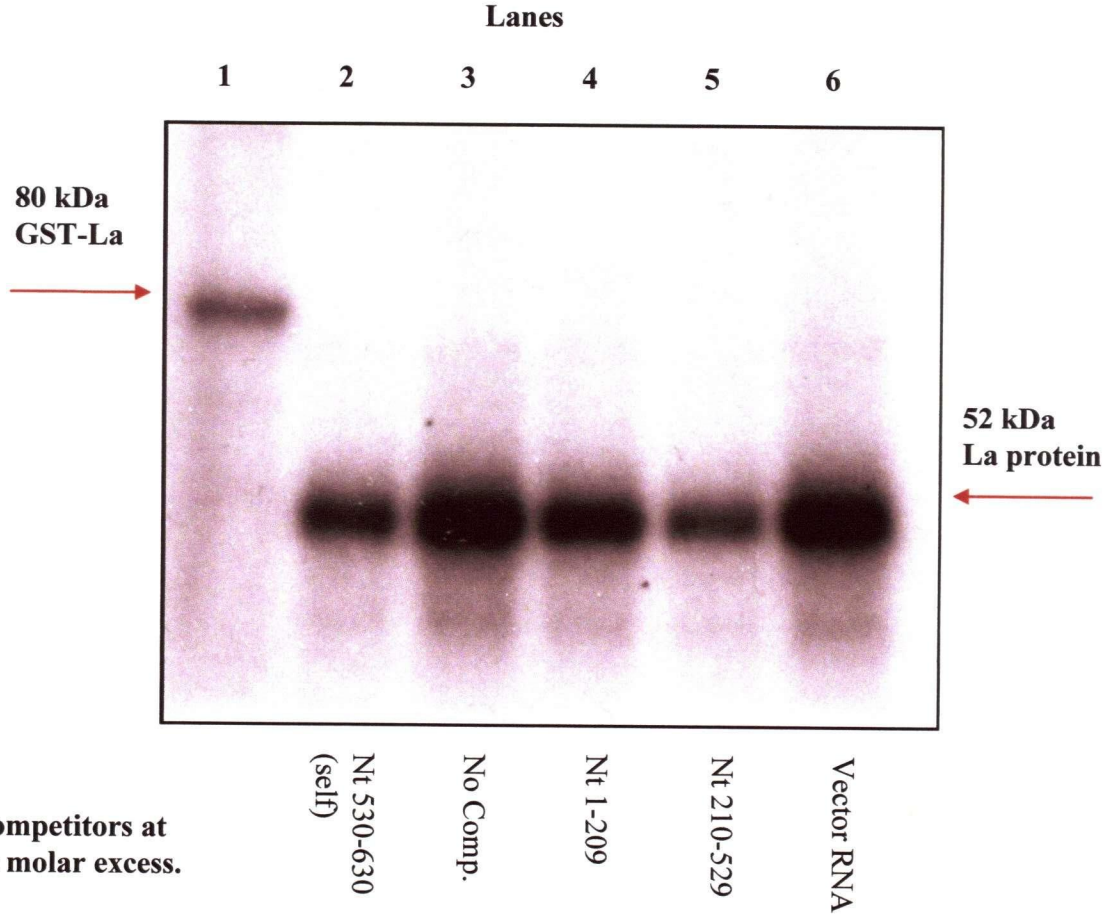

***Specific La protein - 3'-UTR interaction – hyperbolic saturation curve.***

Using the scintillation counting method, I demonstrated specific interaction between the La protein and the 3'-UTR by the saturation experiments. A fixed amount of La protein (3.27 x $10^{-7}$ M) was interacted with increasing amount of labeled 3'-UTR wild type probe (**Table 8, Appendix section 7.10**). Resulting radioactivity count of the complex increased until reaching a saturation level (**Figure 25**). The presence of specific protein-RNA interaction (as opposed to random / weak RNA association) was implied by the observation of the hyperbolic curve. The maximum saturation value in this experiment was estimated to be about 9600 cpm (marked by the line S). Of note, the cpm count of protein-probe complex was generally much lower than the specific activity of the labeled probe (~$10^8$ cpm / ug). This is because the procedure of RNase A digestion degraded non-interacting sequences of the RNA to nucleotides which were rapidly run off the SDS PAGE. The resulting cpm count of the complex reflected only the radioactivity of the sequence of the 3'-UTR RNA that was bound to the La protein.

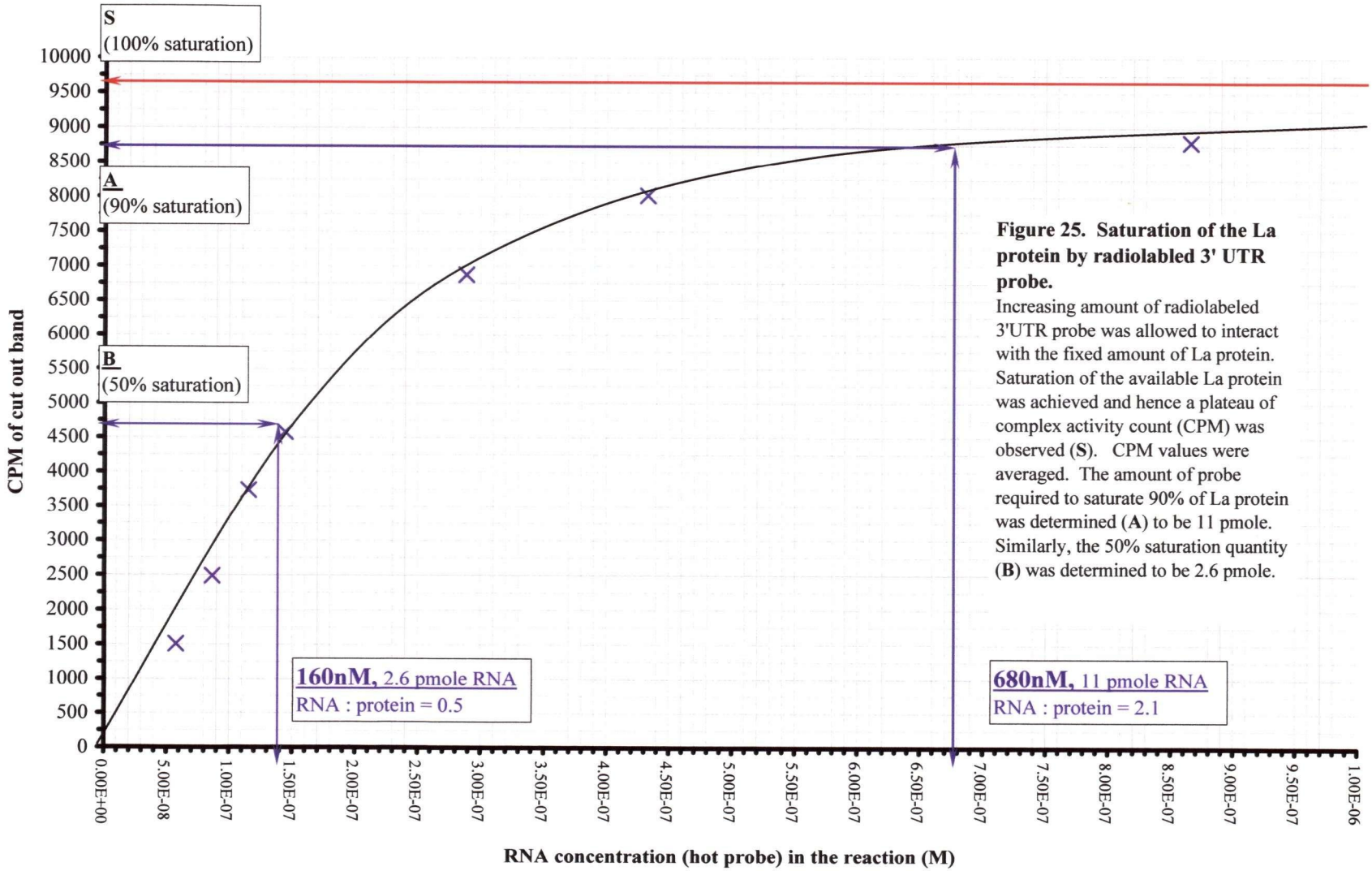


**Figure 25. Saturation of the La protein by radiolabled 3' UTR probe.**
Increasing amount of radiolabeled 3'UTR probe was allowed to interact with the fixed amount of La protein. Saturation of the available La protein was achieved and hence a plateau of complex activity count (CPM) was observed (**S**). CPM values were averaged. The amount of probe required to saturate 90% of La protein was determined (**A**) to be 11 pmole. Similarly, the 50% saturation quantity (**B**) was determined to be 2.6 pmole.

***Specific La protein - 3'-UTR interaction – hyperbolic saturation curve.***

Using the scintillation counting method, I demonstrated specific interaction between the La protein and the 3'-UTR by the saturation experiments. A fixed amount of La protein (3.27 x $10^{-7}$ M) was interacted with increasing amount of labeled 3'-UTR wild type probe (**Table 8**). Resulting radioactivity count of the complex increased until reaching a saturation level (**Figure 25**). The presence of specific protein-RNA interaction (as opposed to random / weak RNA association) was implied by the observation of the hyperbolic curve. The maximum saturation value in this experiment was estimated to be about 9600 cpm (marked by the line S). Of note, the cpm count of protein-probe complex was generally much lower than the specific activity of the labeled probe (~$10^8$ cpm / ug). This is because the procedure of RNase A digestion degraded non-interacting sequences of the RNA to nucleotides which were rapidly run off the SDS PAGE. The resulting cpm count of the complex reflected only the radioactivity of the sequence of the 3'-UTR RNA that was bound to the La protein.

***Stoichiometry of interaction (1:1) and the 90% saturation quantity.***

From the saturation curves (**Figure 25**), two important observations are noted.

First, the curve indicates that at 4,800 cpm (50% of the maximum 9,600 cpm), the corresponding molar ratio of RNA to protein was approximately 0.5 (point **B**). This value is the ratio of RNA and protein at the start of reaction (not at equilibrium). A ratio of 0.5 indicates that for every 2 molecules of protein in the reaction, one 3'-UTR probe was present at the start of reaction. The 4800 cpm is the 50% saturation point of the maximum amount of La protein-complex achievable (which was limited at 3.27 x $10^{-7}$ M) under that particular experimental conditions. Together, the data indicates that 1.64 x $10^{-7}$ M of the La protein (50%) was saturated

by 1.6 x $10^{-7}$ M of probe RNA (from **Figure 25**): this is consistent with an interaction stoichiometry of 1:1. This observation suggests a simple one to one molecular interaction between the La protein and the probe RNA, thus supports the use of the Scatchard plot transformation to estimate the value of the apparent Kd.

Second, at the 90% saturation point (0.9 x 9,600 cpm), the initial concentration of the 3'-UTR probe in the reaction was 680 nM ($6.8x10^{-7}$ M) (**Figure 25**, point **A**). This concentration of probe corresponded to ~11 pmole ($1.1 x10^{-11}$ mole) of the 3'-UTR RNA. Therefore, under the experimental conditions, 11 pmole RNA was required to saturate 90% of the available La protein. I defined this 11 pmole as the 90%-pre-blocking quantity. In the subsequent competition experiments, this amount of competitor non-labeled RNA was added to reaction to simulate a 90% saturation effect. By the same approach, the 50%-blocking quantity was determined to be 2.5 pmole ($2.5x10^{-12}$ mole) at the 50% cpm point (**Figure 25**, Point **B**).

***Mutations in the 3'-UTR do not affect interaction with the La protein.***

To determine if interaction between the La protein and the 3'-UTR mutant exists, competitive UV cross-linking assays were performed. The La protein was first incubated and UV cross-linked with a non-labeled RNA prior to adding the radiolabled wild-type-3'-UTR probe. As both radiolabeled and non-labeled RNA are chemically identical, UV cross-linking non-labeled competitors at the 90%-blocking-quantity would thus significantly inhibit the subsequent complex formation with radiolabeled probes. Thus, if the pre-blocking non-labeled RNA competed specifically against the 3'-UTR probe for interaction, the amount of radioactive complex would be significantly reduced.

The reactions were carried out under standard conditions (5.2 pmole, 245 ng of La protein), pre-incubated with different non-labeled 3'-UTR RNA or vector RNA at the 90%-pre-blocking quantity, followed by UV cross-linking with 11 pmole radiolabeled wild type 3'-UTR RNA. Radioactivity of the corresponding band was determined from two independent experiments and plotted on the bar chart (**Figure 26**). A representative autoradiograph of the complex formation was included at the bottom of the bar chart to demonstrate the actual band patterns. Intensity of the La protein-3'-UTR complex under no competition was demonstrated in lane 1, with an averaged cpm count of ~9,600. The use of non-labeled self RNA (wild-type-3'-UTR) at the 50%-blocking quantity resulted in a corresponding decrease in cpm count of the complex to ~5,600 cpm (lane 2). When using the 90%-blocking quantity of cold self RNA, the complex count was reduced to ~2,150 cpm (lane 3). Thus, the use of self RNA as competitor at the 50%- and 90%-blocking quantity demonstrated the specific nature of the La-3'-UTR interaction. This was contrasted to the use of non-labeled vector RNA (100 nt) at the 90%-blocking quantity, which did not result in noticeable changes of the cpm count of the complex (lane 10). Therefore the sequence specific nature of the interaction between the 3'-UTR wild type sequence and the La protein has been clearly demonstrated.

The mutations in the 3'-UTR RNA did not affect the La protein-binding. When using the 90%-pre-blocking quantity of the 5 different non-labeled mutant 3'-UTR RNAs (**Figure 26**, lane 4-9), the resultant cpm counts were essentially identical to that observed when the non-labeled wild type RNA was used as competitor (lane 3). Thus, the corresponding 3'-UTR mutations as well as the poly-(A) deletion did not affect the ability of the 3'-UTR to interact with the La protein. This interpretation is consistent with the observation of the 52 kDa protein band in my previous 3'-UTR UV cross-linking experiments (**Chapter IV**).

**Figure 26.**

**Two-stage UV cross-linking of La protein to 3'-UTR RNAs.**

Radiolabeled RNA probes of the 3'-UTR clones were interacted with the La protein. In lane 1, the wild type probe interacted with 5.2 pmole of La protein without competitor. CPM of the complex in this lane indicates maximum complex formation under non-competed conditions. In lane 2 and 3, wild-type non-labeled RNA were added at the indicated pre-blocking quantity. These non-labeled RNAs were UV cross-linked ($1^{st}$ UV crosslink) to the protein prior to the incubation and UV cross-linking ($2^{nd}$ UV cross-link) of the radiolabeled probe. The corresponding decrease in complex observation (reduction in yield) indicates specific competition. RNAs from the mutated 3'-UTR sequences (**Chapter 4**) (lane 4-8) also demonstrates similar competition, suggesting that the mutations did not affect the La protein interaction. Lane 9 is a non-labeled vector RNA control that did not compete for La protein binding. Radioactivity count of the respective complexes was averaged from two independent experiments.

**Figure 26. UV crosslinking of 3'-UTR wild type probe under various 3'-UTR competitors.**

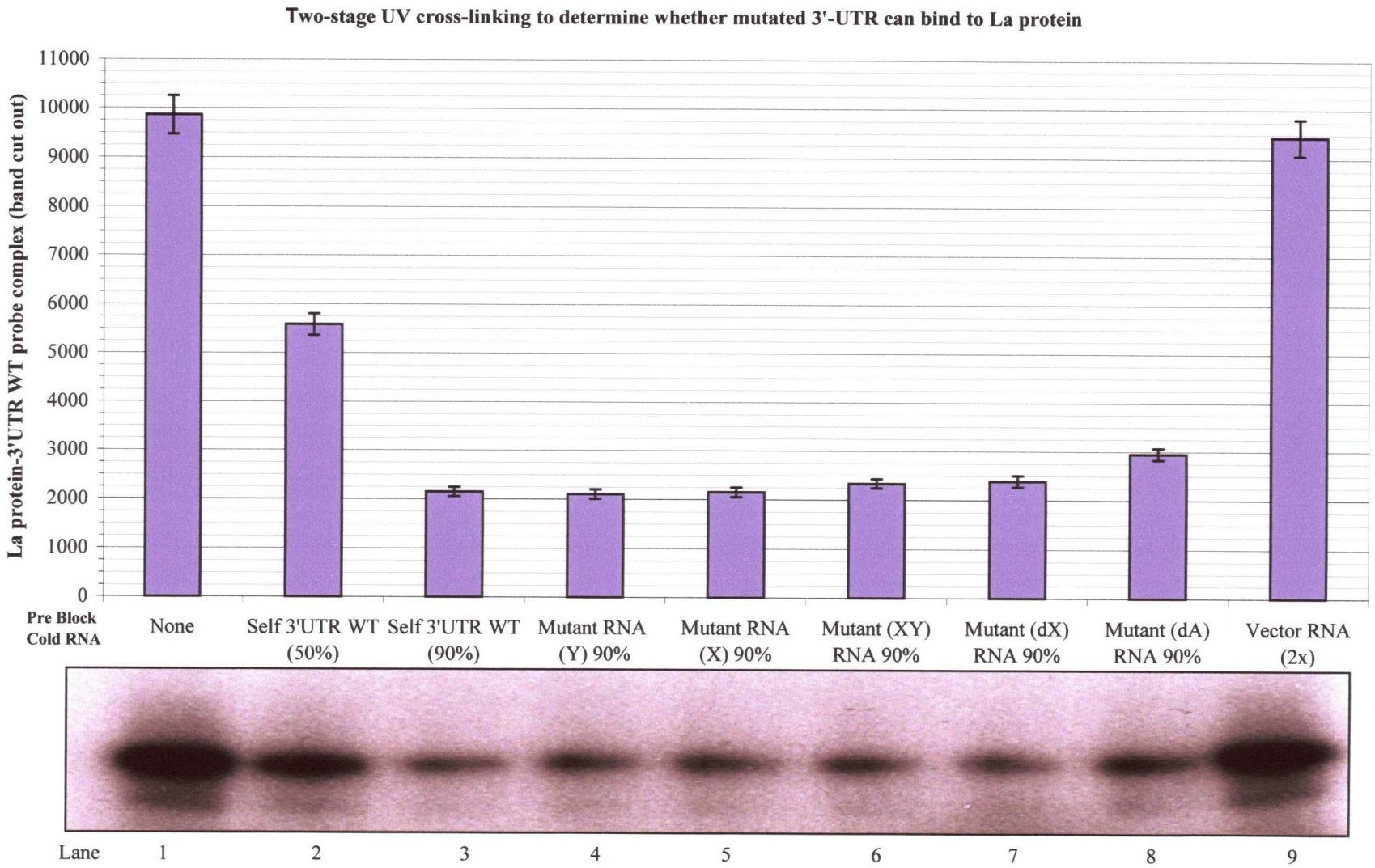

***Each La protein molecule can only bind to either one of the 5' / 3'-UTR at a time.***

To investigate whether the La protein could bind both the 5'-UTR and the 3'-UTR concurrently, I performed the experiment with the use of three different 5'-UTR RNAs at the 90%-blocking quantity. The results are shown in **Figure 27**. In lane 1 the non-competed La protein–3'-UTR interaction was measured with a radioactivity of ~ 12000 cpm. This is slightly higher than the maximum radioactivity as observed in the saturation experiment, possibly a result of a different batch of radiolabeled probes with higher specific activity (more $^{32}P$ labels incorporated per molecule of RNA during transcription). Using 3'-UTR wild type non-labeled RNA at the 90% and 50% pre-blocking quantity (lane 2 and 3, respectively), I demonstrated the pattern of competitive complex formation under an exclusive binding scenario. This was because the cold 3'-UTR RNA was chemically identical to the radiolabeled 3'-UTR RNA and thus must have occupied the same binding site on the La protein as the labeled probe. In lane 4 to 6, pre-blocking by the 5'-UTR non-labeled RNAs also resulted in significant reduction of the cpm count of complex. In fact, the radioactivity counts appeared lower than that of the 3'-UTR wild-type competitor at the 90%-pre-blocking quantity (lane 2). This observation (competitions from the 5'-UTR non-labeled RNA) would not be expected if there were two different binding sites on the La protein for the 5' and 3'-UTR RNA.

**Figure 27**

**Two-stages UV cross-linking of La protein to 3' and 5'-UTR RNA.**

Radiolabeled RNA probes of the 3'-UTR Wild type RNA were interacted with the La protein. In lane 1, the wild type interacted with 5.2pmole of La protein without competitor. CPM of the complex in this lane indicated maximum complex formation under non-competed conditions. In lane 2 and 3, homologous (WT) non-labeled RNA were added at the indicated pre-blocking quantity. The corresponding decrease in complex observation (reduce in cpm count) indicated specific competition. In lanes 4- 6, non-labeled 5'-UTR RNAs were UV cross-linked to the La protein prior to interaction with the 3'-UTR probe. Competition from the 5'-UTR RNA appeared stronger than that presented by the homologous 3'-UTR RNA. Overall, the result suggests that the La protein can only interact with one UTR molecule at the time, and thus the model of concurrent 5' and 3'-UTR binding was not supported. Lane 9 is a control: non-labeled vector RNA did not compete for La protein binding. Radioactivity count of the respective complexes was averaged from three independent experiments.

**Figure 27. UV crosslinkig of La protein and 3'-UTR probe under competition from various 5'-UTR RNA.**

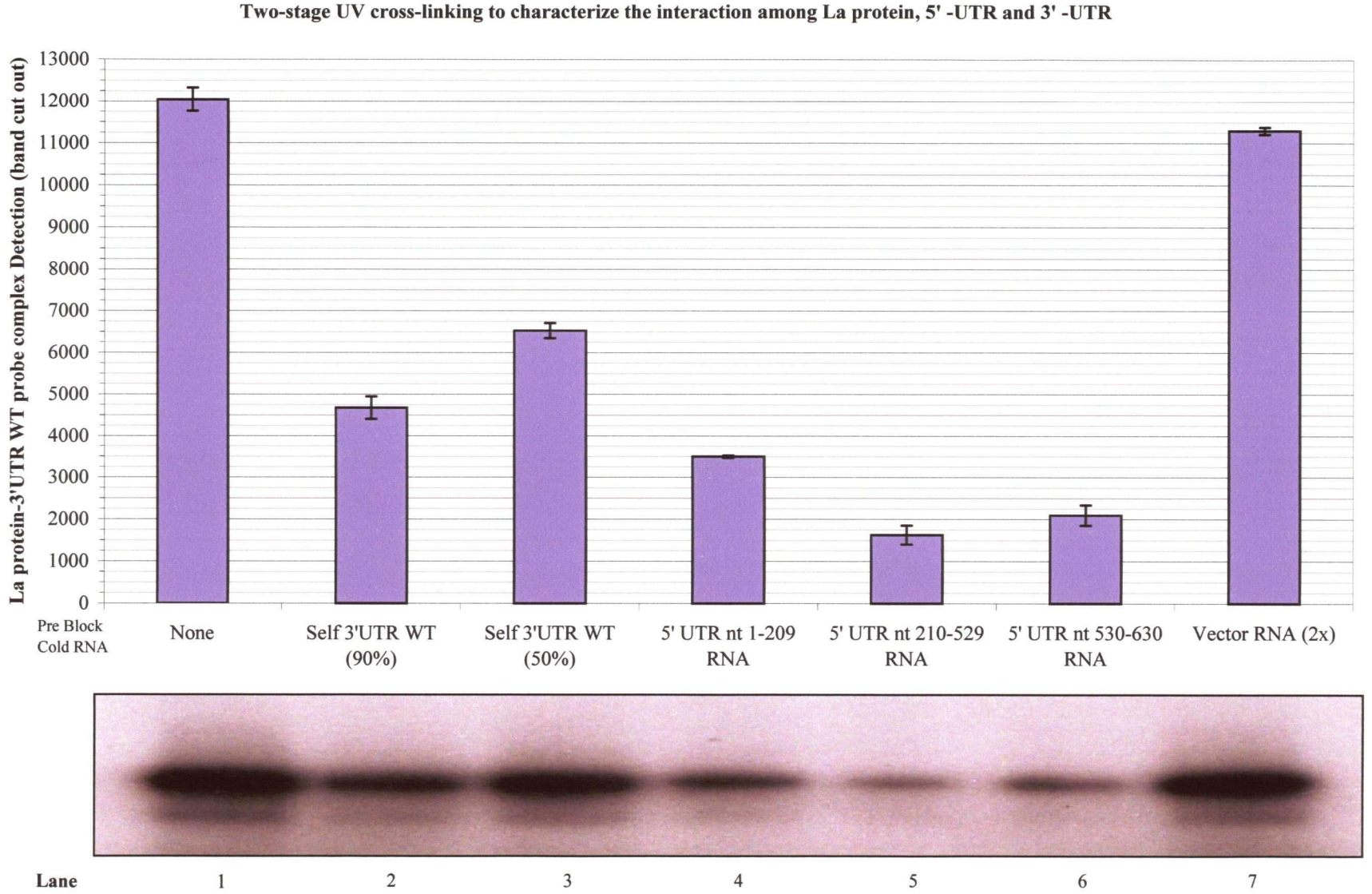

An important observation during my experiment was the apparently stronger competition effects of the 5'-UTR non-labeled RNAs than the 3'-UTR self RNA at the 90%-pre-blocking quantity. During the experiments, in order to obtain a more visually distinct band pattern of the La-3'-UTR probe under competitions (lane 4-6), the autoradiograph in **Figure 27** was exposed with ~50% longer time than the one presented in **Figure 26**. The data seem to suggest that the same quantity of the pre-blocking 5'-UTR RNA can result in more reduction in the protein-probe complex formation, than the 3'-UTR competitor RNAs. Hence the 5'-UTR RNA may have stronger affinity towards the La protein than the 3'-UTR. Further experiments to quantify the difference may be useful in understanding the functional significance of the interactions.

***Apparent dissociation constants of the La - UTR interactions***

In order to compare the affinity of the 5'-UTR and the 3'-UTR towards the La protein, I have determined the apparent Kd between the La protein and the 3'-UTR by transforming data of the 3'-UTR saturation curve (**Figure 25**) into the variables described by the standard scatchard plot (**Figure 28**). Standard equations of the transformation was programmed into a Microsoft excel work sheet and the results of each steps of the calculations were listed in **Section 7.11, Table 9**. In the scatchard plot (**Figure 28**), the quantity of **[Protein Bound] / [RNA total] [Protein Free]** was plotted against **[Protein Bound] / [RNA total]** (all items in concentrations, M).

**Figure 28.**

**3'-UTR Scatchard plot**

Data from the La-3'-UTR saturation experiment (**Figure 25**) was transformed by the scatchard plot method (**Table 8**). The quantity of **[ Protein Bound ] / ( [ RNA total ] x [ Protein Free ] )** was plotted against **[ Protein Bound ] / [ RNA total ] .** A best fit line and its respective linear equation was generated by Microsoft Excel to minimize its variance from each data point. The dissociation constant of interaction was deduced from the slope *(figure printed on the next page).*

**Figure 28. Scatchard Plot of interaction between La protein and 3'-UTR wild type probe.**

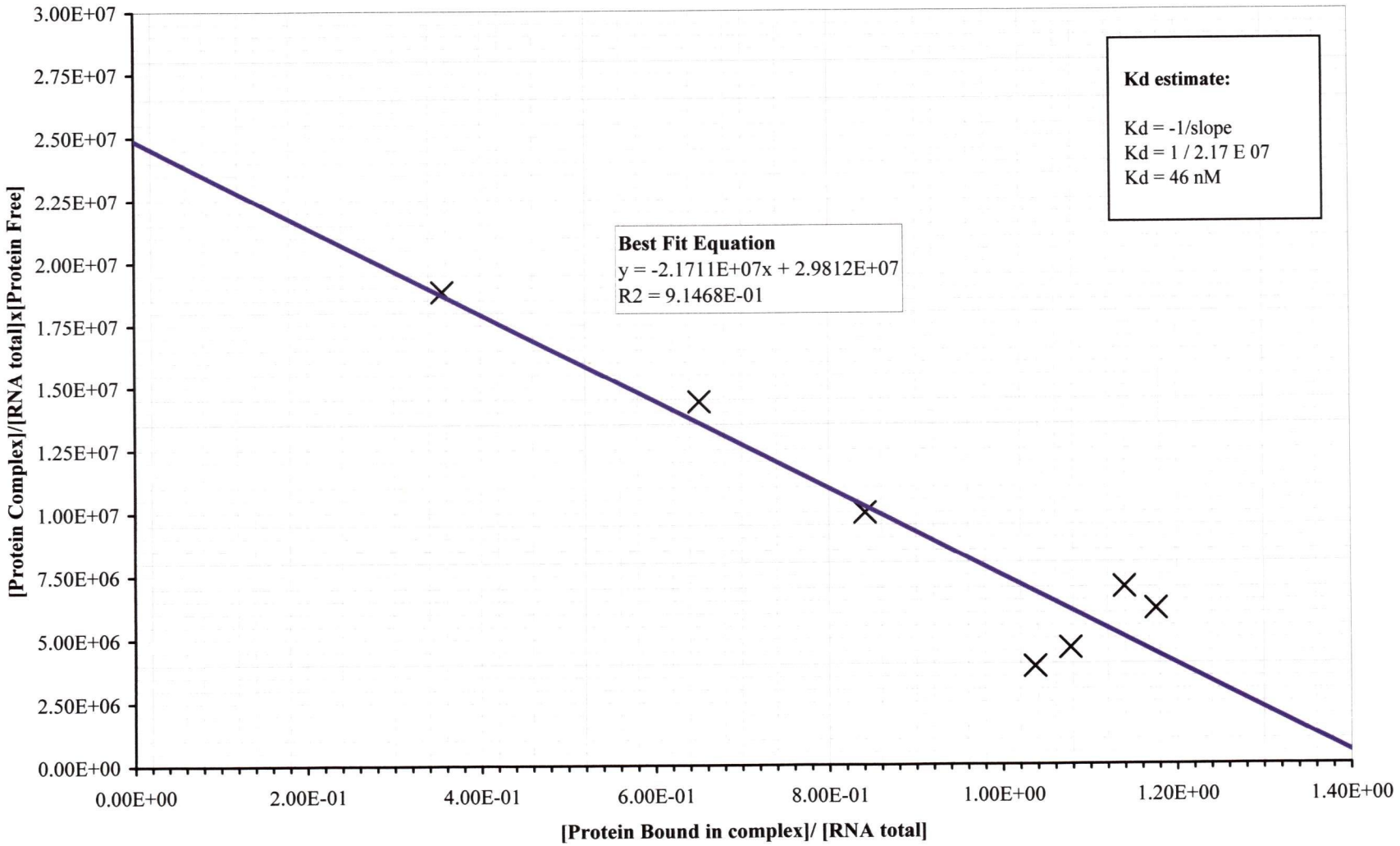

The apparent dissociation constant (Kd) and stoichiometry of interaction were deduced from the scatchard plots. The Kd is calculated from the slope of the curve (Kd= -1/slope) while the stoichiometry of interaction is reported by the X-intercept. In other words, the scatchard plot derived these two quantities by calculations involving all the data points in each of the experiment. From the slope of the best fit lines the Kd for the 3'-UTR was estimated to be 46 nM ($4.6x10^{-8}$ M, **Figure 28**). In general an experimental Kd value of 1-100 nM reflects a moderate to strong interaction. Whether the interaction is physiologically significant will depend on the concentration of the reactants in a cellular environment.

## 5.3 DISCUSSION

The La autoantigen was initially identified in patients suffering from autoimmune disorders such as systemic [223] and Sjogren's syndrome [7]. It is now understood that the La autoantigen mainly functions in the synthesis, termination and release of polymerase III transcripts. In normal cellular environments, La has also been reported to interact with the U-rich 5' regions of ribosomal mRNAs *in vitro* and to stimulate their *in vivo* translation in a Xenopus tissue culture system [89,266]. A uridine-rich sequence is also present in the CVB3 IRES sequence (**Figure 9**). In our experiments, by comparing cross-competition from the 5'-UTR sequences, the La autoantigen appears to bind most strongly to the sequence nt 210-529. The presence of a major tRNA-like stem loop in this region (nt 210-481, **Figure 9**) is consistent with the tRNA processing function of the protein. This sequence, although not as critical as the core IRES in determining translation initiation of the virus [349], may have served as an important site for the recognition of the CVB3 RNA by the La autoantigen.

***Role of secondary structures in the interaction of La with the 5'-UTR probes.***

Interaction of La with the three 5'-UTR probes were demonstrated by UV cross-linking between labeled probes and purified La protein (**Figure 23**). Although the La autoantigen appears to bind to all three probes of the 5'-UTR, we have not observed a common primary RNA sequence within the three 5'-UTR probes. Thus, interaction of the La protein with CVB3 5'-UTR is likely dependent on RNA secondary structures. This postulation is also supported by the observation that pre-heating the sequence nt 1-209 was required for detecting the probe-La complex formation with the nt 1-209. Heating the probe at 95 °C prior to the 10-minute

incubation at 37 °C would have allowed the probe RNA to transit from a denatured state (at 95 °C) to the native state (37°C). Thus, the transition may have provided intermediate secondary structure(s) that are optimal to the binding of the La protein. In a cellular environment, factors such as eIF4A and eIF4B normally help resolve and modify the high-order RNA structures, thereby facilitating efficient protein binding for translation initiation. My experiment on UV cross-linking of HeLa cell proteins (lysate) has shown that the proteins binding to nt 1-209 are similar in size to eIF4A and eIF4B (**Table 6**). However, when using the purified recombinant La protein in UV cross-linking with the 5'-UTR probes, no such eIF factors were present. In other words, the apparent low affinity of this sequence towards the La protein as observed by our experiment is likely due to the lack of other chaperone molecules that helps optimize the RNA structure for protein interaction.

***Functional significance of the La protein-5'-UTR interaction.***

Reflecting on the findings that the La protein can associate with the 40S ribosomal subunits (**Chapter I**), my data suggests that the La autoantigen – CVB3 5'-UTR interaction stimulates internal translation initiation of the CVB3 genome by forming a pre-translation initiation complex. This hypothesis is supported by the observation that the La autoantigen binds to the IRES of EMCV and stimulates translation initiation, and that La protein interacts with multiple sites on the hepatitis C virus RNA [5]. My findings on the La autoantigen and 5'-UTR binding were accepted for publication in the Virus Research [80]. At the same time when my work was being published, Ray et.al. [281] also reported a stimulatory effect of the La protein in a dose dependent manner on CVB3 IRES, although the mechanism of stimulation was not investigated.

This stimulatory effect of the La protein has thus verified the functional significance of the protein-CVB3 UTR interactions that I have observed.

***Interaction of La protein with the 3'-UTR did not depend on tertiary structures.***

In addition, data from the 3'-UTR UV cross-linking experiments (**Chapter IV**) suggest that a 52 kDa protein may bind to the 3'-UTR, a process that is independent of mutations and the poly-(A) sequence. Thus, the binding site and / or RNA structure that this 52 kDa protein recognizes is located within the actual 3'-UTR sequence. The 52 kDa La protein is subsequently confirmed to bind to the 5'- and 3'- UTR. The La-3'-UTR interaction is unlikely to depend on the 3'-UTR tertiary structures, because the 3'-UTR mutant RNAs, which do not possess the wild type tertiary structures, also competed for the interaction with the La protein. Using the saturation plot and the scatchard plot, I have determined the apparent dissociation constant. The results are discussed below.

***Affinity of the La protein – 3'-UTR interaction.***

The La protein-3'-UTR interaction was characterized by the scatchard plot method. The apparent Kd value is estimated to be significant (46 nM). In consideration of the previously reported effect of the 3'-UTR on CVB3 replication, my data suggests the La-3'-UTR interaction may have functional implications in the overall process of viral replication. In this respect, the interaction of the La protein with the minus-strand of the vesicular stomatitis virus (VSV) RNA has recently be reported to stimulate viral replication [337,338]. This finding suggests the potential function of La protein in viral RNA transcription. The potential roles of La-3'-UTR interaction in CVB3 replication may be highlighted by two separate events: 1) transcription of viral RNA

from a template; 2) expression of functional viral proteases and other mature non-structural proteins from the genome, and hence the amount of replication complex that is available to perform the RNA-dependent RNA transcription. The first event is directly related to the 3'-UTR sequence. As discussed in the introduction, the picornaviral 3'-UTR sequence serves as the anchoring point of the RNA-dependent RNA transcription complex. Whether the La-3'-UTR interaction may serve to facilitate template transcription remains unknown. Thus, as an extension of my current findings, it would be interesting to test for potential interactions between the La protein and the viral 3D polymerase. The second event is in fact highly dependent on the viral RNA translation initiation. As the viral replication complex is composed of viral and host proteins, sufficient expression of viral proteins would affect the rate of viral replication. At this point it is worth noting that host proteins such as PTB have been suggested to serve dual roles in the translation and RNA replication of the poliovirus (discussed in the Introduction). Considering my observation that the La protein can interact with both the CVB3 5' and 3'-UTR; it is reasonable to hypothesize that the La-UTR interactions may serve in both the viral translation and transcription processes. Consequently, this raises the question of whether the CVB3 3'-UTR may also co-operate with the 5'-UTR in promoting viral translation and or replication. To date, there is no data that suggest the participation of the CVB3 3'-UTR in viral translation initiation. Findings by Melchers et.al. [229] seem to suggest that the transcription mediated by the CVB3 3'-UTR and the CVB3 translation were two discrete processes [229]. However, Melchers' experiments were designed to specifically discover determinants of viral replication, not translation initiation. Also, the lack of participation of the tertiary mutants at nt 7391/2 and 7352/3 in the CVB3 translation initiation does not exclude other sites within the 3'-UTR in regulating viral translation. At the same time, data from the HCV system seem to

support a functional role of the 3'-UTR in directly stimulating viral translation [241]. In short, further investigation into the role of the 3'-UTR in promoting picornaviral translation initiation will reveal important mechanistic data on the subject.

***Circularization of CVB3 RNA.***

In the mammalian and yeast systems, the concept of circularized mRNA during translation has gained wide acceptance [334]. Synergism between eIF4G, poly-(A) and poly-(A) tail binding proteins in stimulating translation initiation has been a focus of many studies. Circularization of the poliovirus RNA was recently demonstrated by Herold and Andino [139]. In brief, long-range interactions between protein and PV UTRs complexes were shown to be necessary for RNA replication. The authors also demonstrated that the initiation of negative strand RNA synthesis requires a 3' poly-(A) tail, which also echoes my findings with respect to the importance of the CVB3 poly-(A) tail in recruiting host protein interactions. The PV 5' and 3'-UTR bridge is formed when the 5'-UTR RNP complex interacts with the poly-(A) binding protein bound to the 3' poly-(A) tail, essentially circularizing the viral genome and this process is required for the initiation of negative strand RNA synthesis. RNA circularization may be a general mechanism for replication of positive strand RNA viruses. Reflecting on these findings, my data does not directly support a model of circularized RNA for the CVB3 viral translation and/or replication process. In contrast to PTB protein which contains 4 RRMs and has been demonstrated to bind to multiple sites in the 5'-UTR of other viral RNAs (Introduction, chapter I), La protein only possesses one true RRM. Thus, it is likely that a La protein may not interact simultaneously with multiple RNA sites on the CVB3 5' and 3'-UTRs. Data from my dual-stage UV cross-linking experiments suggested that while the La protein may interact with either of the

UTR sequences, only one of the UTR may occupy the protein at a time. Circularization of a CVB3 genomic RNA by one molecule of La protein is unlikely, although under the experimental conditions the possibility of protein dimerization could not be examined. At the same time, it is also important to realize that recent findings demonstrated the dimerization of La protein and the consequential enhancement of translation. Thus the question of whether a multiple La protein molecules interacting with the 5'-UTR and the 3'-UTR to form a circularized complex during viral translation and replication remains a possibility.

***Possible dimerization of La protein-UTR complexes.***

Protein-RNA UV cross-linking experiments have been used in other RNA studies. Throughout my investigation, I have experimented with different buffers and reaction conditions. Data presented in my results were optimized for the best band patterns, and the same patterns were reproducible in at least 3 independent experiments with different batches of radiolabeled UTR probes and protein extracts. During my trial experiments, I have noticed that the use of > 1μg La protein in a reaction with total volume exceeding 30 μl at times can result in the detection of labeled protein complexes with MW of approximately 100+ kDa. These data were not included in my analysis because the detections were not always reproducible. However, since only one pure protein (recombinant La protein) was used in these reactions, the only logical explanation for observing the 100+ kDa bands were due to the dimerized La protein-probe complex. This is a reasonable preliminary evidence to indicate that La protein-UTR complexes may dimerize under specific conditions, possibly leading to the circularization of the CVB3 genome RNA. Relevant to the potential La protein-mediated RNA circularization is the observation that the dimerization of the La protein can stimulate viral translation, although the

mechanism of such is still a mystery [88]. Thus, my current observations provide a molecular basis for the synergism of dimerization: Multiple copies of the La protein may interact with several sites in the 5'-UTR and 3'-UTR; dimerization / multimerization of the La protein can result in circularized protein-RNA complexes which serve to stimulate translation initiation.

To demonstrate the La protein facilitates CVB3 RNA circularization would be a significant step towards understanding the mechanism of CVB3 pathogenesis. The standard models of mRNA and RNA circularization in yeast / eukaryotic / other viral systems, rest on the interaction of eIF4G and PABP, bringing the 5' and 3' ends of the RNA closed together to form a loop. This model, however, can not be applied directly to the CVB3 or poliovirus system. In a CVB3 infection, the eIF4G carboxyl domain is cleaved by the viral protease. This cleavage will remove the domain of PABP interaction on the eIF4G and thus disables the interaction of the two and inhibits the circularization process. If circularization does occur with the CVB3 RNA, additional 5'-3' bridging molecules are thus required. To this end, the La protein can be the key alternative molecule in mediating RNA circularization.

Circularization of the viral RNA would have two major theoretical advantages to the virus. Firstly, without the proper cap structure and with the extensive RNA secondary structure in the 5'-UTR, the CVB3 genome may not compete favorably against host mRNA for the standard translation apparatus. In this regard, the circularized complex confers improved efficiency to the viral translation by facilitating repeated rounds of protein expression, eliminating the need to recruit and re-assemble a new translation initiation complex at the 5' end. The advantage of this process may be most significant during early infection when very limited

number of viral RNA must compete with the vast majority of capped mRNA for translation. Secondly, replication of the viral RNA occurs late in the viral cycle. In a HeLa cell culture environment this occurs typically in a two-hour time frame, from 7-9 hrs p.i. (cell lysis), when most host protein synthesis has been inhibited. It is conceivable that rapid viral RNA transcription is necessary to produce the progeny genome and allow packaging into the virions. A circularized complex, again, may assist and enhance the efficiency of this process. Although this is still conjecture, the La protein may be an important factor that helps the overall viral pathogenesis by facilitating efficient translation and transcription.

***Method developments and experimental limitations.***

Throughout my investigations, I have optimized and refined parameters related to the UV cross-linking experiments. Significant progress has been made to improve sensitivity, reproducibility and resolution of the technique in detecting protein interactions. Of note, the use of competitor RNAs in the HeLa cell experiment was successful to detect differential affinities of the protein-probe interactions (**Chapter IV**). This has led to two important developments in my subsequent studies. Firstly, given that a protein-RNA interaction is observed by the UV cross-linking technique, it is important to determine the *specificity* (e.g. by competition between yeast tRNA and self RNAs) and the *affinity* (e.g. by how the band intensity changes in response to the doses of competitor). These two variables would be important in characterizing the significance of each protein-UTR interaction. Secondly, the sensitivity of my current UV cross-linking procedure was suitable for revealing such differences. The development of a method to quantify the degree of complex formation in the UV cross-linking experiments would greatly improve my ability to characterize the interaction.

To this end, I have modeled the La protein-UTR interaction by a two-molecule-interaction equilibrium. This model of interaction is supported by the saturation assay that each La protein appears to interact with one molecule of the 3'-UTR probe. Consequently, using the scatchard plot transformation, the Kd of the interaction was estimated and the value was concluded as an apparent value because of several reasons: 1) the concentration of the complex was estimated indirectly from the amount of radioactive protein-probe complex. Variables and uncertainties in the measurement of radioactivity thus impose a limitation in the actual estimate of the amount of protein complex. 2) the reaction was executed in an in vitro condition which does not necessarily reflect the physiological concentration of the reactants (e.g. La protein and viral RNA at different stages of the infection in a cytoplasmic environment). Thus, while the apparent Kd value does suggest a significant interaction between the protein and the RNA, the functional implications in the CVB3 pathogenesis remains to be verified. Importantly, my approach in the characterization of the La protein-UTR interactions has provided an example of how the specificity and affinity of other host proteins - CVB3 UTR interactions may be investigated.

Finally, adaptation of the dual-stage UV cross-linking provided a means to extend the UV cross-linking technique to assess whether concurrent binding of La protein to the 5' and 3'-UTR was feasible. Although highly reproducible, I have observed that the dual stage UV cross-linking procedure imposed a reduced resolution of protein-complex on the SDS-PAGE: the bands in **Figure 27** were not as discrete as those observed in **Figure 18** (one stage UV cross linking between HeLa cell protein lysate and the 5'-UTR probes) and some level of protein

degradation was observed. The cause of reduced resolution can not be definitively identified, but it may be related to prolonged protein–RNA incubations and manipulations: both the labeled probe and the recombinant La protein are susceptible to heat degradation; the small volume of reaction (necessitated by the optimized UV cross-linking procedure) could suffer changes in volume as a result of evaporation during the extended period of UV light exposure and or incubation, leading to changes in salt concentration and pH of the reaction.

# CHAPTER VI CONCLUSION AND FUTURE DIRECTIONS.

In the course of my graduate program, I have had the opportunity to investigate the molecular aspects of protein-UTR interactions. Prior to the commencement of my studies, there were several interesting publications which described determinants of CVB3 tropism and viral replication. These determinants included specific nucleotide sequences that do not encode for functional proteins. The molecular effectors and mechanisms of CVB3 tissue tropism were unknown. Limited work was published in the investigation of protein-UTR interactions with other related viruses. My study made the first attempt to verify protein-CVB3 UTR interactions and identified targets that are worth further investigations.

## 6.1 Conclusions and scientific contributions.

By using molecular techniques, such as PCR based cloning and mutation, mobility shift assay, UV cross-linking assay, recombinant protein expression and purification, *in situ* hybridization, and modeling of the protein–RNA interaction by a chemical equilibrium, I have investigated specific protein-CVB3 UTR interactions from the perspective of viral pathogenesis. The interactions of the La protein with the 5' and 3'-UTR is verified and further characterized. A summary of the important findings and contributions to scientific knowledge are listed below:

1. ISH indicates a strong resistance of the A/J mouse kidney towards CVB3 infection. In addition, the endocrine and exocrine pancreas cell types exhibit contrasting susceptibilities to CVB3 infection.

2. A specific 28 kDa protein interaction with the CVB3 5'-UTR antisense sequence of the nt 210-529 correlates with the resistance to viral infection in the kidney, liver and the 10-week-old heart, as compared to other organs.

3. Fourteen HeLa cell proteins specifically bind the CVB3 5'-UTR sequences. Molecular weights of six of these proteins resemble that of the eIF4A, 4B, 4G, DAP5, La protein and PTB, respectively.

4. Specific interactions of certain HeLa cell protein with the 3'-UTR is dependent on the presence of the poly-(A) tail sequence.

5. Two HeLa cell proteins, 22 and 24 kDa in sizes, interact with the antisense sequence of the mutated 3'-UTRs and such interactions correlate with their respective inhibitory function on virus replication.

6. The La protein may interact with multiple sites of the CVB3 5'-UTR. Binding affinity is the highest in the nt 210-529, followed by the nt 530-630 and nt 1-209.

7. The La protein also interacts with the CVB3 3'-UTR. The interaction is not dependent on the 3'-UTR tertiary structures.

8. Apparent Kd of the La protein-3'-UTR interaction has been determined to be 46 nM.

9. Interaction of the La protein with either the CVB3 5'-UTR or the 3'-UTR is mutually exclusive.

10. Concurrent binding of both UTRs to the La protein is not supported by my observations. However, based on the ability of the protein to dimerize, the circularization of the CVB3 RNA by La protein remains a possibility.

One of the significant contributions of my work is the discovery of many specific protein interactions with the CVB3 5' and 3'-UTR, some of which correlate to the CVB3 tissue tropism. A few of these interactions resemble known eukaryotic translation initiation factors, while other novel proteins require further sequence identification and biochemical characterization. My work on the La protein-CVB3 UTR interaction has provided an initial attempt to study protein-UTR interactions based on the UV cross-linking and the purified recombinant protein methods.

## 6.2 Strategies for future directions

To further investigate the identities of the important UTR-binding proteins, I propose to perform experiments in the following directions:

1. To identify the amino acid sequence of the UTR-binding proteins that are potentially important in CVB3 susceptible and resistant cell types, by the methods of immunoprecipitation, recombinant protein expression, and other proteomics techniques.
2. To identify the protein binding sites on the 5' and 3'-UTR by foot-printing assays.

To achieve the above directions, I have initiated experiments by three major techniques: the Laser capture microdissection (LCM), two dimensional polyacrylamide gel electrophoresis (2D PAGE) and Mass spectrometry (MS).

***To separate the endocrine and exocrine cell types by LCM***

An important ISH observation was the contrasting susceptibility of the endocrine and exocrine cell types. Currently, there is no satisfactory explanation for the difference in susceptibility of these two cell types. While receptor expression may account for such, it is also probable that specific cytoplasmic UTR-binding proteins that may either enhance or inhibit the CVB3 pathogenesis in the respective cell types. In this regard, investigation of the UTR binding proteins in the two respective cell types will be important to understand the mechanism of CVB3 tropism. To achieve this objective, the laser capture microdissection (LCM) is ideal for isolating these two pancreatic cell types. A flow chart describing the general LCM approach is listed in **Figure 29.** In brief, frozen tissue sections are placed under a normal optical microscope. Capturing of the specific cells involves the use of an adhesive plastic material (cap) which is placed between the lens and the frozen tissue section. When stimulated by a laser light, this cap extends to physically contact the laser-targeted cells. The cells then adhere to the cap for removal. Preliminary data of isolating the A/J mouse endocrine / exocrine cell types by the LCM method were demonstrated in **Figure 30**. Following isolation, the exocrine and endocrine cell types can be studied independently for their differences in UTR-binding proteins.

**Figure 29. General strategy for LCM procedure.**

Laser Capture Microdissection (LCM) Process. Image courtesy of Arcturus.

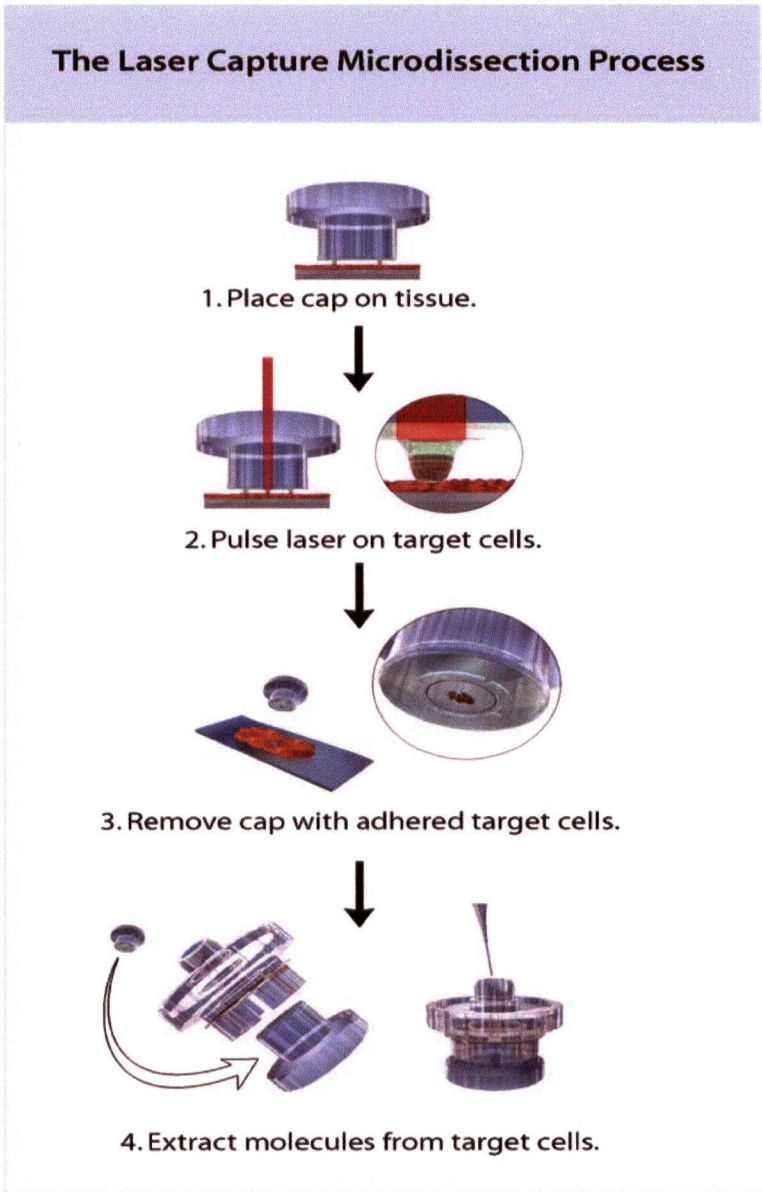

**Figure 30. LCM separation of endocrine and exocrine cells.**
A/J mouse pancreas was flash frozen, section at 8mm thickness, embedded in paraffin and stored at -80 °C. LCM was performed to remove the endocrine cell types.

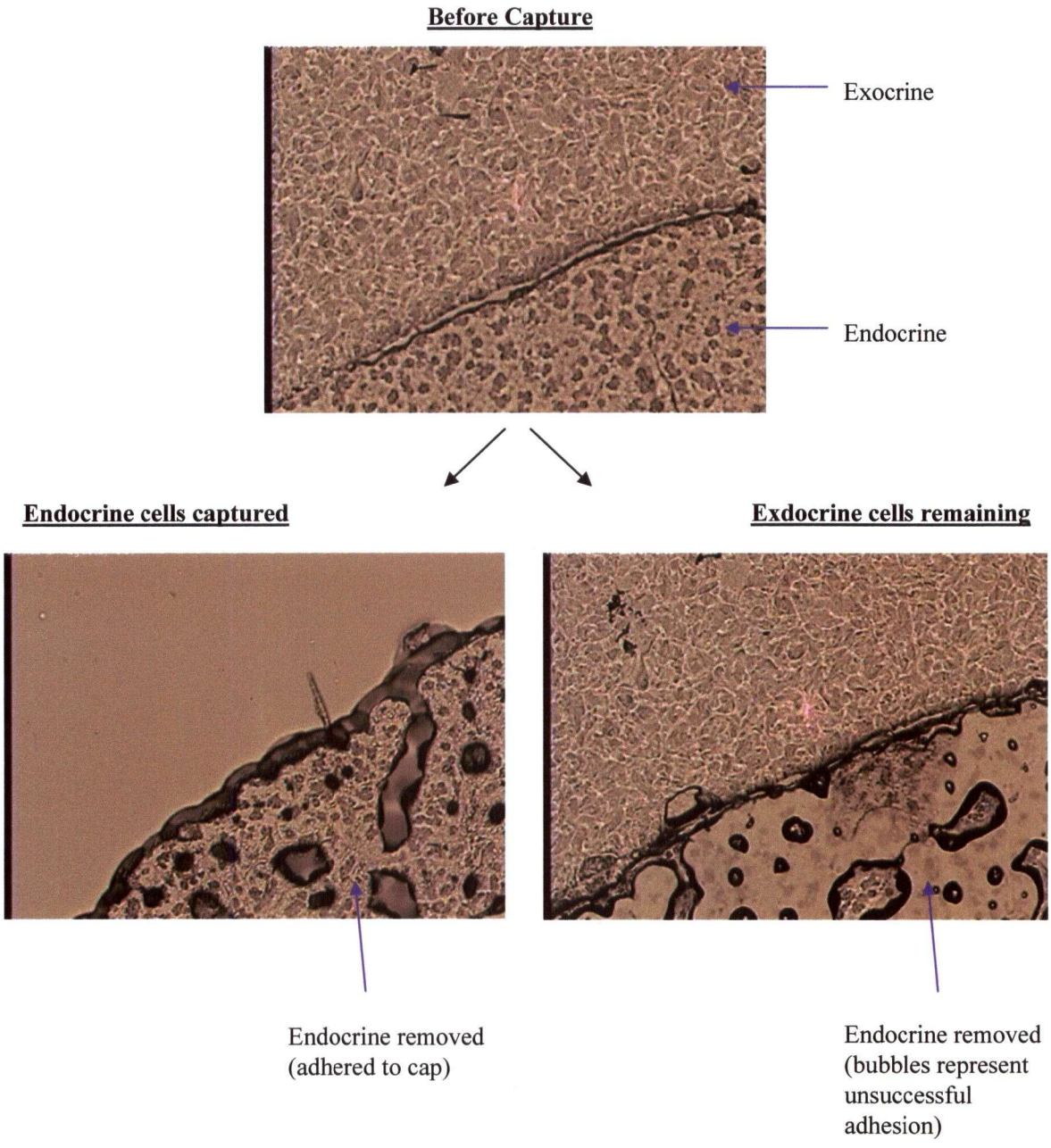

***To sequence identify UTR binding proteins by 2D PAGE and Mass Spectrometry (MS)***

The use of 2D PAGE enable protein isolation first by their isoelectric points (pI values) and then by MWs. This allows greater resolution of the numerous proteins in a lysate than the 1D PAGE. My initial attempts of protein separation were highly reproducible (**Figure 31**) with good resolutions. Samples of 5'-UTR (IRES sequence) cross-linked HeLa cell lysate was compared to non-cross-linked lysates. Specific differences in the migration of proteins indicated proteins that are bound to the respective UTR sequence. Thus, proteins of interest can be subsequently identified: Protein on the 2D PAGE can be removed, trypsinized and the sequence identity can be analyzed by the Matrix assisted laser desorption/ionization mass spectrometry (MALDI-MS) method. Of note, unique proteins such as the p28 from the kidney (which bound to the nt 210-529) and the 22/24 kDa doublets (which bound to the 3'-UTR sequence) can be specifically traced on the 2D gel by the corresponding molecular weights. Direct isolation and identification of these proteins would thus be possible.

***To verify UTR-protein interactions by standard molecular techniques***

Following the sequence identification from 2D PAGE/MS experiments, verification of the interaction would be necessary. This can be achieved by traditional molecular techniques such as immunoprecipitation and recombinant protein expressions. Also, literature search and analysis of the upstream/ downstream molecules of the identified proteins will provide important information with respect to the mechanism of how the interaction with the CVB3 UTRs can lead to specific pathogenic functions.

**Figure 31. 2D PAGE separation of UTR-binding proteins from HeLa cell.**

Non-labeled 5' UTR RNA nt 530-630 was UV cross-linked to HeLa cell lysate (right panel). As a control, HeLa cell lysate was also UV cross-linked without the presence of the 5' UTR RNA (left panel). The two lysates were analyzed by 2D PAGE, from pI 3-11 (horizontal dimension) and MW 250 kDa to 5 kDa (vertical dimension). The distribution of proteins on both gels are highly similar, thus demonstrating the consistency of the 2D PAGE experiment. Individual protein spots that appear shifted as a result of protein-RNA interactions are outlined (blue dotted lines). These are targets that requires further identification and verification.

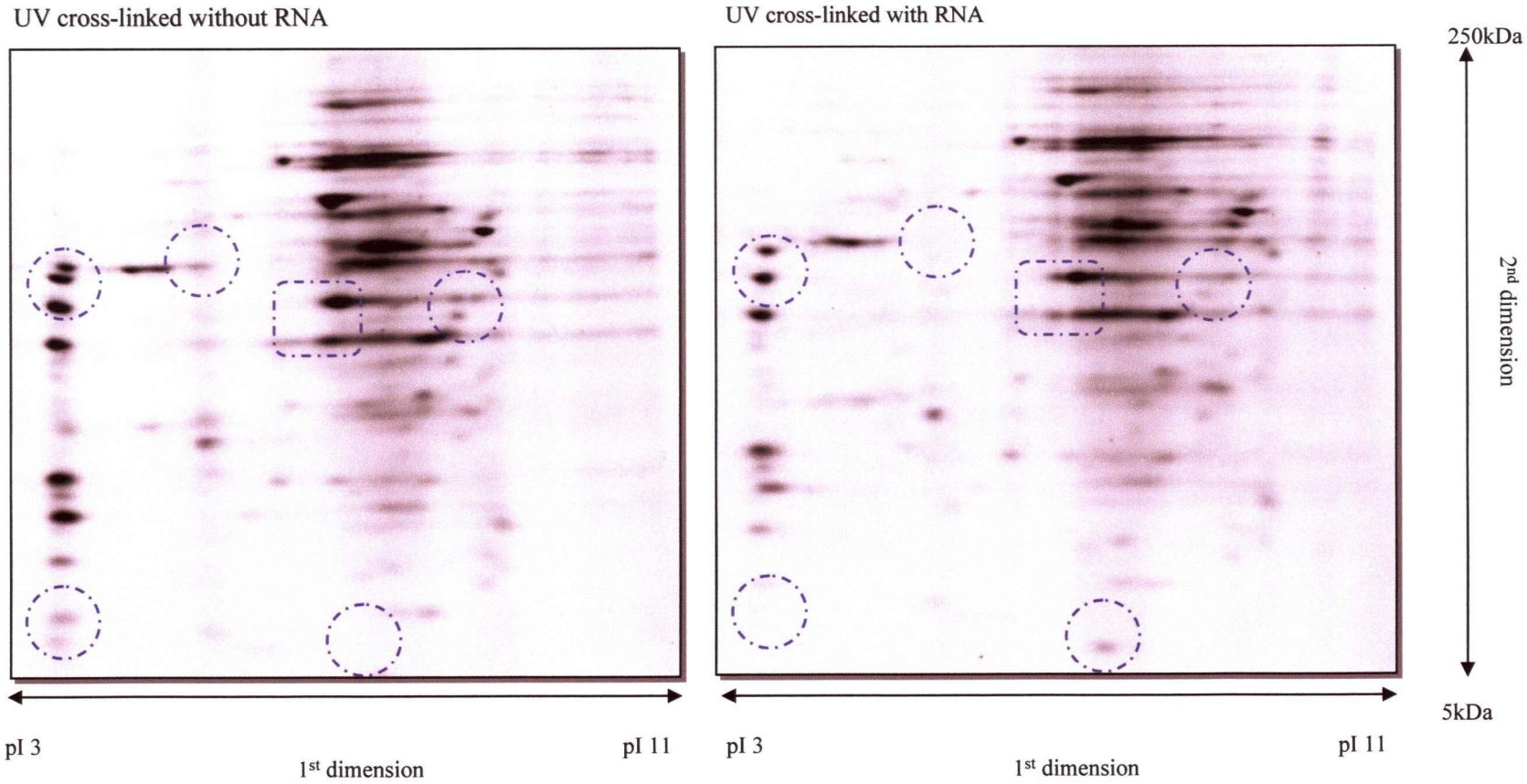

***To enhance the biochemical analysis of protein-RNA interaction by large format SDS-PAGE***

A short coming of my biochemical analysis of the La –UTR interaction was in the calculation of the apparent dissociation constant (apparent Kd). The amount of protein-UTR complex in my calculations was estimated by a conversion from radioactivity count. The conversion assumed a linear relationship between complex formation and radioactivity, and depends on the estimated cpm count of the saturation of the La protein by RNA probes. This assumption is largely valid based on the the principle of chemical equilibrium but remains an indirect measurement of the complex-concentration. Factors such as the efficiency of UV cross-linking and radioactivity detection can incur uncertainties in the calculation process. Thus, in order to derive a more realistic (non-apparent) Kd value, I propose to perform the experiments based on large format (30 cm+) 1D SDS-PAGE. The increase in gel dimension would allow extended electrophoresis time to completely separate the labeled complex from RNase A-digested probe sequences, but retaining both in the gel. Throughout my investigation, small format SDS PAGE (12 cm) was used. While sufficient to resolve the protein-RNA complexes and MW of UTR binding proteins, RNase A-digested probes usually exit the gel rapidly. These RNase A digested probe sequences represent excess probe sequences that did not react with the protein. The large format gel would retain these RNase A-digested products in the lower part of the gel and thus allow quantification of the total radioactivity. By measuring radioactivities of the protein-UTR complex, the non-protein bound radioactive ribonucleotides and the initial activity at the beginning of the reaction, I can obtain a direct estimate of the ratio of complex formation in relation to the input quantities (amount of protein and specific radioactivity of the labeled probe). This can avoid assumptions that were made in my calculations. The approach

should be technically feasible and requires only optimizations to ensure reproducibility without significant modification of the interaction procedures.

## 6.3 Final remarks

In summary, by identifying novel UTR-protein interactions and their potential correlations with CVB3 infectivity over the course of my graduate studies, I have provided interesting and testable protein targets for further investigations. In the course of CVB3 infection, molecular mechanisms of the viral translation and transcription are fundamental processes that lead to a variety of pathologic observations and systemic illnesses. Further investigation of the protein-UTR interactions by the use of high throughput proteomics technologies will allow us to gain a much better understanding of how molecular events in the translation and transcription of the CVB3 genome can account for the CVB3 specific pathological phenotypes. The knowledge can significantly advance the design of CVB3 specific interventions.

# CHAPTER VII MATERIALS AND METHODS

## 7.1 Plasmid construction.

PCR reactions were performed to amplify DNA fragments corresponding to the various 5' and 3'-UTRs. The respective primers are listed in **Table 7**. The amplified DNA fragments were cloned directly into the dual promoter T/A vector (*Invitrogen*) as per manufacturer's instruction. Cloned sequences and their orientations with respect to the RNA polymerase promoter on the vector were verified by DNA sequencing.

## 7.2 In vitro transcription.

Prior to transcription, plasmid templates were linearized and purified by phenol/chloroform extraction and ethanol precipitation. RNAs of the three cloned sequences were synthesized by *in vitro* transcription using 1 μg of linearized plasmids and the appropriate RNA polymerase in the presence of [α-$^{32}$P]UTP or [α-$^{32}$P]CTP (3,000 Ci / mmol, Amersham) as per manufacturer's instruction. Non-radioactive labeled RNA was also synthesized, and served as specific competitors in the mobility shift and UV cross-linking experiments. RNA transcripts were purified by RNase-free DNase I digestion, phenol/chloroform extractions and ethanol precipitation at - 80 °C. The integrity and purity of RNA were verified either on a 1.5% formaldehyde-containing agarose gel (for non-radioactive transcripts) or autoradiography with 6 % SDS-PAGE ([α-$^{32}$P] UTP labeled transcripts). Non-labeled transcripts were quantified by spectrophotometry and radioactive transcripts were adjusted to a specific activity of 1 x $10^7$ – 1 x $10^8$ cpm / μg.

**Table 7a. 5'-UTR construction**

Primers used for construction of plasmids of the 5'-UTR. Primer sequences are presented in a 5' → 3' format.

| Cloned Sequence | 5' primer | 3' primer | PCR temperature |
|---|---|---|---|
| (5'-UTR) | | | |
| nt 1-209 | 5'-TTAAAACAGCCTG-3' | 5'-GTGAGCAGTCTA-3' | 63 °C |
| nt 210-529 | 5'-CGCGGTTGAAG-3' | 5'-GAGTTGCCCGTTA-3' | 53 °C |
| nt 530-630 | 5'-CTGCAGCGGAA-3' | 5'-ATCCAATAGCT-3' | 47 °C |

**Table 7b.** Primers used in the PCR generation of the wild-type and mutant CVB3 3'-UTR DNA. Mutated nucleotides are in bold and underlined. The Sal I site is included after the poly-(A) tail (33 T sequences on primers) to allow exact linearization during in vitro transcription. The indicated PCR temperatures were experimentally determined.

| Primers | Sequence (5' to 3') | PCR temp. (°C) |
|---|---|---|
| **Clone:** | **Wild type 3'-UTR with poly A tail (WT)** | |
| 5′ primer | TTAGA GACAA TTTG | 55′C |
| 3′ primer | TGCGG TCGAC TTTTT TTTTT TTTTT TTTTT TTTTT TTTTT CGCAC CGAAT GCGGA GAATT | |
| **Wild type 3'-UTR without poly A tail (dA)** | | |
| 5′ primer | TTAGA GACAA TTTG | 52′C |
| 3′ primer | CGCAC CGAAT GCGGA GAATT | |
| **Mutant 3'-UTR at nt 7352 and 7353 (Y)** | | |
| 5′ primer | TTAGA GACAA TTTGA AATAA TTTAG ATTGG CTTAA CCCTA CTGTG CTAAC C**cc**AC CAGAT AACGG | 48′C |
| 3′ primer | TGCGG TCGAC TTTTT TTTTT TTTTT TTTTT TTTTT TTTTT CGCAC CGAAT GCGGA GAATT | |

**Table 7 continued**

**Mutant 3'-UTR at nt 7391 and 7392 (X)**

| | | |
|---|---|---|
| 5′ primer | TTAGA GACAA TTTG | 48′C |
| 3′ primer | TGCGG TCGAC TTTTT TTTTT TTTTT TTTTT TTTTT TTTTT CGCAC CG**cc**T GCGGA GAATT | |

**Complementary mutant 3'-UTR at both nt 7352-3 and 7391-2 (XY)**

| | | |
|---|---|---|
| 5′ primer | TTAGA GACAA TTTGA AATAA TTTAG ATTGG CTTAA CCCTA CTGTG CTAAC C**cc**AC CAGAT AACGG | 48′C |
| 3′ primer | TGCGG TCGAC TTTTT TTTTT TTTTT TTTTT TTTTT TTTTT CGCAC CG**cc**T GCGGA GAATT | |

**Deletion mutant 3'-UTR from nt 7390 to 7396 (dX)**

| | | |
|---|---|---|
| 5′ primer | TTAGA GACAA TTTG | 47′C |
| 3′ primer | TGCGG TCGAC TTTTT TTTTT TTTTT TTTTT TTTTT TTTTT CGC-- ----- GCGGA GAATT | |

## 7.3 Preparation of HeLa cell extracts.

HeLa cells (ATCC) were grown in Eagle's minimal essential medium supplemented with 10% fetal bovine serum. Cells were harvested mechanically at approximately 95% confluency, washed 2x with PBS and incubated with lysis buffer (50 mM Tris-HCl pH 7.4, 150mM NaCl, 1% Triton, 0.1 % SDS, 0.5 % Na Deoxycholate, 10 mM EDTA) for 10 min. Cell lysates were dialyzed against buffer A [90 mM KOAc, 1.5 mM $Mg(OAc)_2$, 1 mM dithiothreitol (DDT), 10 mM HEPES, pH 7.6] for 12 hrs at 4 °C. Protein concentration was determined by spectrophotometry using the Bradford protein assay kit (Bio-Rad). The concentration of the protein extracts was adjusted to 20 μg / μl. The extract was used directly for RNA-protein interaction assays or stored in aliquots at –80 °C until use.

## 7.4 Preparation of lysates from A/J mouse organs.

4- and 10-week-old non-infected A/J mice were sacrificed and internal organs (heart, kidney, brain, liver, spleen and pancreas) were flash frozen by immersion in liquid nitrogen. Protein extracts were prepared by the method of Correia et al.. Approximately 0.5 g of organ tissue is rapidly triturated with a pestle and mortar. One ml of the solubilization buffer [10 mM Hepes (pH 1.9), 10 mM KCl, 0.1 mM EDTA, 0.1 mM EGTA, 1 mM dithiothreitol (DTT), 0.5 mM phenylmethylsulfonyl fluoride (PMSF) and 0.1 % v/v leupeptin] is added to the powdered tissue. The mixture was then homogenized by 10 strokes in a Dounce manual tissue grinder with 20 μl of Nonidet P40 (NP-40), and left on ice for 15 min. The mixture was further homogenized by 5 strokes before centrifuging at 1000 x g for 5 min. The bottom fraction was washed three times with 1 ml of solubilization buffer with 0.5% NP-40. The remaining pellet was resuspended in 200 μl of storage buffer [20 mM Hepes (pH 7.9), 400 mM NaCl, 1.0 mM EDTA,

1.0 mM EGTA, 1.0 mM DTT, 1.0 mM PMSF, 10% glycerol and 0.1% leupeptin]. The suspension was then incubated on ice for 30 min and centrifuged at 12000 x g for 5 min. The supernatant was then aliquoted in 50 µl and stored at -80 °C. The aliquots contained ~ 400 µg protein and were used directly for RNA-protein interaction assays or stored in aliquots at -80 °C until use.

## 7.5 RNA mobility shift assays.

All RNA-protein interactions were carried out in a total volume of 20 µl. Five µl of binding buffer (2.5 mM KCl, 10 mM HEPES, 2 mM $MgCl_2$, 0.1 mM EDTA, 2 mM DTT, 5 □g heparin and 3.8 % glycerol), 500 ng (~5 x $10^6$ cpm) of radioactive probe and 20 µg of HeLa cell extract were incubated for 15 min at 37 °C. In competition assays, either an unlabeled form of the probe RNA (self competitor) or yeast tRNA was incubated with cell extracts for 5 min prior to adding radioactive probes. Unlabeled yeast tRNA (*Sigma*) was used as a non-specific competitor because it was not homologous to the viral RNA sequences but contained similar stem-loop structures. Protein-RNA mixes were analyzed by electrophoresis through a 4 % non-denaturing polyacrylamide gel. After drying the gel, radioactivity was visualized by autoradiography.

## 7.6 UV cross-linking experiments.

Reactions were carried out in a total volume of 20 µl containing 5 µl of binding buffer (see above). Unless otherwise indicated, 500 ng of labeled transcripts (5 x $10^6$ cpm) was incubated with 10 µg of HeLa cell extracts or 10 µg organ lysates at 37 °C for 15 min. Competitor RNAs were added five min. before adding radioactive probes, at indicated molar

excess ratios. The reaction mixtures were kept on ice and UV cross-linked (*Stratagene 2400*) for 25 min at a distance of 3 cm from the UV bulb. Total UV energy applied was 22.5kJ. After UV-irradiation, all samples were treated with 200 ng of RNase A at 37 °C for 20 min. As control, a reaction not treated with UV irradiation was digested with RNase A. Protein-probe complexes were then analyzed under reducing conditions by 9 % SDS-PAGE. The gels were fixed in a solution containing 15 % methanol and 20 % acetic acid for 10 min and dried on Whatman paper. The dried gel-paper was overlaied with autoradiograph film to image the protein-probe complex. MWs of probe-protein complexes were determined by comparing against simultaneously loaded protein markers. Additional modifications to the above core procedures were described in the respective results sections.

## 7.7 Virus, animal and tissue processing.

CVB3 was generously provided by Dr. Reinhard Kandolf (University of Tübingen, Germany). The full length cDNA sequence of the virus is listed in **section 7.11**. Virus was propagated in HeLa cell monolayers in modified Eagle's medium (MEM) containing 10% fetal bovine serum (FBS) and 50 μg / ml gentamycin (Gibco, Grand Island, NY) at 37 °C in a humidified 5% $CO_2$ atmosphere. When 70-90% of the cell monolayer showed viral cytopathic effects, flasks were frozen-thawed three times. Large cellular debris was removed by centrifugation at 2000 x g. Viral titers in the supernatant were determined by plaque assays. Dilutions of this supernatant were used for inoculation of mice. Inbred adolescent and young adult A/J [H-$2^a$] mice (Jackson Laboratory, Bar Harbor, ME), 4 and 10 weeks of age, respectively, were infected with coxsackievirus B3 ($10^5$ pfu) or sham-infected with PBS intra-peritoneally, and euthanized by $CO_2$ narcosis on day 4 post infection (p.i.). Fresh tissue was

taken from heart, kidney, brain, liver, spleen and pancreas for fixation in 4% paraformaldehyde, paraffin-embedding, and histological sectioning for histopathological staining and *in situ* hybridization (ISH) of viral genome. Two 3-mm thick tissue slices of each organ were obtained per animal at sacrifice. Slices from the heart included left and right ventricular myocardium at the mid-cavity level of the ventricular free walls and ventricular septum. A portion of each tissue was archived for plaque assay, immediately frozen in liquid nitrogen and stored at – 80 °C.

## 7.8 In situ hybridization.

CVB3 specific riboprobes were prepared by *in vitro* transcription of full length CVB3 cDNAs containing Sp6 and T7 promoters. These riboprobes were of the antisense sequence and labeled with digoxigenin-11-5'-triphosphate (DIG-11-UTP, Boehringer Mannheim, Laval, PQ). ISH was performed according to the procedures as previously described [70]. Briefly, tissue sections were formaldehyde-fixed, alcohol-dehydrated, xylene-cleared, paraffin-embedded, cut at 4-micron thickness, mounted on silanated slides and dried overnight at 60 °C to ensure proper continuous adhesion of the sections during processing. Slides were deparaffinized, rehydrated and permeabilized with proteinase K. The hybridization solution contained a digoxigenin-labeled, viral strand specific riboprobe (antisense strand, nt 888-7399), 50% deionized formamide, 10 mM Tris-HCl (pH7.4), 1 mM EDTA, rabbit liver t-RNA 200 μg/ml, 600 mM NaCl, 10 mM dithiothreitol, 0.02% polyvinylpyrrolidone, 0.02% ficoll, 0.02% bovine serum albumin, 0.1% SDS. Twenty μl of hybridization mixture was applied to each slide, then the siliconized coverslips were mounted and sealed with rubber cement. Hybridization was allowed to proceed at 42 °C for 24 h. Post-hybridization washing was followed by blocking with 2% lamb serum. Anti-digoxigenin-AP-Fab fragments (Boehringer Mannheim, Laval, PQ) were then

applied to each slide (1:500 diluted, 150 µl per section) and incubated at 37 °C for 30 min. Sigma Fast BCIB/NBT buffered substrate tablet was used as colour substrate for the detection of alkaline phosphatase activity. Two tablets were dissolved in 300 ml of distilled water for the incubation of slides at 37 °C with very slow shaking. The colour usually developed in 24 h. Slides were subsequently counterstained with carmalum and examined quantitatively for reaction product by light microscopy.

## 7.9 Protein purification.

I have modified the original pGEX-La protein purification procedures to achieve optimal purity and yield. Each 100ml of the transformed *E. coli* (BL21 DE3) cell was induced at mid-log phase by Isopropyl-β-D-thiogalactopyranoside (IPTG, final concentration 0.1 mM) and allowed to grow at 26 °C for another 20 hrs. During purification, cell lysate / protein samples were kept on ice at all times to prevent thermal degradation of the La protein. Induced cells were collected by swing bucket centrifugation at 4 °C at 3,500 rpm for 15 min. Higher centrifugation speeds results in cell pellets that appear resistant to sonication and produce frothy cell lysates. The 100ml culture was centrifuged in four equal volumes to ensure efficient precipitation. Each of the four cell pellets were resuspended in 5 ml phosphate saline buffer (PBS, pH7.0), exposed to two freeze-thaw (-80 °C to 4 °C) cycles, followed by five 1-min 50% output sonication (SONEX). A straw colored clear solution indicated optimal cell lysis. Cloudiness of the lysate may result from cells resistant to lysis and in this scenario, addition of 1% volume triton X-100 should clear the solution in about 20 min. The final lysate was centrifuged at 4,000 rpm for 5 min to remove cellular debris. Each of the 5 ml supernatant was treated with 150 ul 50%

glutathione sepharose 4B beads (*Pharmacia Biotech*) at 4 °C for 1 to 3 hrs, in narrow diameter (1 cm) 15 ml Falcon tubes. The tubes were laid flat to maximize the interaction surface area between the beads and proteins. This resulted in noticeable increase in final yield. After incubation, the lysate was centrifuged at 3,000 rpm for 10 min and the pelleted beads were washed with 10 ml PBS. Five washes were repeated. Finally, 5 units of thrombin were added to the washed beads together with 100 to 200 µl PBS. This quantity of thrombin was insignificant and not detectable on SDS PAGE by coomassie blue staining. Cleavage of the La protein from the GST-coupled sepharose beads were allowed to occur at 4 °C for 2-5 hrs, followed by a centrifugation at 2500 rpm for 5 min. The supernatant was tested for protein concentration and purity by the Bradford assay and 10 % SDS-PAGE, respectively. To obtain the non-cleaved form of the GST-La recombinant protein, the washed beads were treated with the standard Glutathione elution buffer (Pharmacia).

## 7.10 Estimation of the apparent Kd and stoichiometry of La-UTR interaction

The apparent dissociation constants of interaction between the La protein and the 5' or 3'-UTR labeled RNA were determined by saturation experiments and the subsequent scatchard plot transformation of data. The two quantities allow a biochemical assessment of the physiological significance of the La-UTR interactions.

To characterize the interaction between the La protein and the UTR RNA, I have modeled the interaction by the following equilibrium equation:

$$\text{La protein + RNA probe} \underset{\text{Kd}}{\overset{\text{Ka}}{\rightleftharpoons}} \text{Protein-RNA complex}$$

This equilibrium was studied by a simple saturation experiment: I have used a fixed amount of La protein in each of the reactions (initial concentration: $3.27 \times 10^{-7}$ M) while the amount of radiolabeled RNA was increased until complex formation was saturated. The ratios of interaction was listed in **Table 8**. Saturation was observed in reactions where labeled-RNA probe was in large excess over protein. At such large probe-excess condition, the equilibrium of the protein-probe interaction was driven forward to form products and thus, it was reasonably accurate to assume that the final amount of protein-probe complex was the same as the initial amount of La protein used in the reactions. The cpm count of complex at saturation was estimated from graph (the plateau level). This maximum cpm count at saturation was equated to the initial concentration of La protein used in the reactions. Hence, the concentration of complex at other points in the same experiment was calculated from its radioactivity. The background radioactivity (~250 cpm) was subtracted from all values. The calculation was achieved with the assumption that the radioactivity recovered bears a linear relationship to the amount of protein-probe complex. The equation used is listed below:

$$[\text{Bound complex}] = \frac{(\text{CPM of complex} - \text{background})}{(\text{Max. CPM} - \text{background})} \times [\text{total La protein}]$$

After calculating the concentration of complex of each reaction, I generated the corresponding scatchard plot according to the standard scatchard equation:

$$\frac{\text{Bound complex / total RNA}}{\text{Free proteins}} = \text{Ka}\left(\text{N} - \frac{\text{Bound complex}}{\text{Total RNA}}\right)$$

Where N denotes the molecular ratio of interaction.

The concentrations of the total RNA were given by the amount of probe added in each reaction. The concentrations of the bound complex were calculated by the above mentioned assumptions. The concentration of free proteins was calculated by subtracting the amount of bound complex from the amount of total protein. Data processing was programmed on a Microsoft excel work sheet and the calculated values were manually checked for accuracy. The values of [bound complex / (total RNA x free proteins)] were plotted on the Y axis and the values of [Bound complex / total RNA] were plotted on the X axis. From this plot, I calculated the apparent Kd of the interactions.

The standard Scatchard plot for a one to one molecular interaction is a linear graph in the general form of Y = MX + C where M is the slope of the curve and corresponds to the (-Ka) value. Ka is the association constant which is the inverse of Kd.

$$\frac{\text{Bound complex / total RNA}}{\text{Free proteins}} = -\text{Ka}\left(\frac{\text{Bound complex}}{\text{Total RNA}}\right) + \text{Ka (N)}$$

*Which is in the form of:*

$$Y = M(X) + C$$

Similar Scatchard plot analyses have been used in other single substrate-interaction studies such as the poliovirus receptor-virion interactions [12]. By transforming the data of the saturation curve into a standard scatchard plot, I have determined the apparent dissociation constant (Kd) of the La protein- 3'-UTR interaction. All data was organized, processed and plotted using Microsoft Excel.

**Table 8.** Conditions of reactions in the saturation experiment. Wild-type probe RNA was transcribed by in vitro isotope labeling. Concentrations of protein and RNA were measured by the Bradford assay and spectrophotometry, respectively. A fixed amount of La protein was used in each experiment to limit the maximum amount of complex formation.

| | Wild type Probe RNA | | Recombinant La protein | | Buffer Volume | DepC $H_2O$ | Total Rxn Volume |
|---|---|---|---|---|---|---|---|
| Rxn No. | (µl) | Conc (ng/ µl) | (µl) | Conc (ng/ µl) | (µl) | (µl) | (µl) |
| 1 | 1.0 | 40 | 1 | 245 | 4 | 10.0 | 16 |
| 2 | 1.5 | 40 | 1 | 245 | 4 | 9.5 | 16 |
| 3 | 2.0 | 40 | 1 | 245 | 4 | 9.0 | 16 |
| 4 | 2.5 | 40 | 1 | 245 | 4 | 8.5 | 16 |
| 5 | 5.0 | 40 | 1 | 245 | 4 | 6.0 | 16 |
| 6 | 1.5 | 200 | 1 | 245 | 4 | 9.5 | 16 |
| 7 | 3.0 | 200 | 1 | 245 | 4 | 8.0 | 16 |

## 7.11 Calculations of the Scatchard Plot transformation

**Table 9. Scatchard Plot transformation of data from saturation plot for the La-3'-UTR interaction.**

The amount of protein-UTR complex is estimated from the cpm count obtained in each reaction. The initial concentrations of La protein and probe RNA are calculated from the input conditions (**Table 8**). The saturation point is estimated from **Figure 25** (9600cpm). Using this information, the % of protein engaged in complex formation with the RNA probe is estimated, and hence the concentration (apparent) of the protein-UTR complex is calculated. Molecular weights of the La protein and the 3'-UTR wild type probe is listed.

| RNA mole | RNA conc (M) | CPM Count of complex | % Protein in complex [ CPM - Background ] / [Max cpm] | protein mole (limited) | Protein Conc (initial) | Protein in Complex | Protein Free | **Protein Bound / RNA total** | **Protein Bound / (RNA totalxProtein Free)** |
|---|---|---|---|---|---|---|---|---|---|
| 9.23E-13 | 5.77E-08 | 1506 | 81.71% | 5.23E-12 | 3.27E-07 | 5.98E-08 | 2.67E-07 | **1.04E+00** | **3.88E+06** |
| 1.38E-12 | 8.65E-08 | 2487 | 71.49% | 5.23E-12 | 3.27E-07 | 9.32E-08 | 2.34E-07 | **1.08E+00** | **4.61E+06** |
| 1.85E-12 | 1.15E-07 | 3733 | 58.51% | 5.23E-12 | 3.27E-07 | 1.36E-07 | 1.91E-07 | **1.18E+00** | **6.15E+06** |
| 2.31E-12 | 1.44E-07 | 4575 | 49.74% | 5.23E-12 | 3.27E-07 | 1.64E-07 | 1.63E-07 | **1.14E+00** | **7.01E+06** |
| 4.61E-12 | 2.88E-07 | 6875 | 25.78% | 5.23E-12 | 3.27E-07 | 2.43E-07 | 8.43E-08 | **8.41E-01** | **9.98E+06** |
| 6.92E-12 | 4.33E-07 | 8022 | 13.83% | 5.23E-12 | 3.27E-07 | 2.82E-07 | 4.52E-08 | **6.51E-01** | **1.44E+07** |
| 1.38E-11 | 8.65E-07 | 8795 | 5.78% | 5.23E-12 | 3.27E-07 | 3.08E-07 | 1.89E-08 | **3.56E-01** | **1.88E+07** |

| | | | | | |
|---|---|---|---|---|---|
| La protein | 46837 | g/mol | 3'-UTR + 33pA | 43337 | g/mol |

## REFERENCES


1. 1983. A critical appraisal of viral taxonomy *In* R. E. F. Matthews (ed.), CRC Press, Boca Raton, Fl., USA.

2. **Agol, V. I.** 1991. The 5'-untranslated region of picornaviral genomes. Adv. Virus Res. **40**:103-180.

3. **Aldabe, R., E. Feduchi, I. Novoa, and L. Carrasco**. 1995. Expression of poliovirus 2Apro in mammalian cells: effects on translation. FEBS Lett. **377**:1-5.

4. **Aldabe, R., A. Irurzun, and L. Carrasco**. 1997. Poliovirus protein 2BC increases cytosolic free calcium concentrations. J. Virol. **71**:6214-6217.

5. **Ali, N. and A. Siddiqui**. 1997. The La antigen binds 5' noncoding region of the hepatitis C virus RNA in the context of the initiator AUG codon and stimulates internal ribosome entry site-mediated translation. Proc. Natl. Acad. Sci. U. S. A **94**:2249-2254.

6. **Allaire, M., M. M. Chernaia, B. A. Malcolm, and M. N. James**. 1994. Picornaviral 3C cysteine proteinases have a fold similar to chymotrypsin-like serine proteinases. Nature **369**:72-76.

7. **Alspaugh, M. A. and E. M. Tan**. 1975. Antibodies to cellular antigens in Sjogren's syndrome. J. Clin. Invest **55**:1067-1073.

8. **Andino, R., N. Boddeker, D. Silvera, and A. V. Gamarnik**. 1999. Intracellular determinants of picornavirus replication. Trends Microbiol. **7**:76-82.

9. **Andino, R., G. E. Rieckhof, P. L. Achacoso, and D. Baltimore**. 1993. Poliovirus RNA synthesis utilizes an RNP complex formed around the 5'-end of viral RNA. EMBO J. **12**:3587-3598.

10. **Andino, R., G. E. Rieckhof, and D. Baltimore**. 1990. A functional ribonucleoprotein complex forms around the 5' end of poliovirus RNA. Cell **63**:369-380.

11. **Archard, L. C., P. J. Richardson, E. G. Olsen, V. Dubowitz, C. Sewry, and N. E. Bowles**. 1987. The role of Coxsackie B viruses in the pathogenesis of myocarditis, dilated cardiomyopathy and inflammatory muscle disease. Biochem. Soc. Symp. **53**:51-62.

12. **Arita, M., S. Koike, J. Aoki, H. Horie, and A. Nomoto**. 1998. Interaction of poliovirus with its purified receptor and conformational alteration in the virion. J. Virol. **72**:3578-3586.

13. **Arnaud, E., C. Touriol, C. Boutonnet, M. C. Gensac, S. Vagner, H. Prats, and A. C. Prats**. 1999. A new 34-kilodalton isoform of human fibroblast growth factor 2 is cap

dependently synthesized by using a non-AUG start codon and behaves as a survival factor. Mol. Cell Biol. **19**:505-514.

14. **Arnold, E., M. Luo, G. Vriend, M. G. Rossmann, A. C. Palmenberg, G. D. Parks, M. J. Nicklin, and E. Wimmer**. 1987. Implications of the picornavirus capsid structure for polyprotein processing. Proc. Natl. Acad. Sci. U. S. A **84**:21-25.

15. **Atkinson, M. A., M. A. Bowman, L. Campbell, B. L. Darrow, D. L. Kaufman, and N. K. Maclaren**. 1994. Cellular immunity to a determinant common to glutamate decarboxylase and coxsackie virus in insulin-dependent diabetes. J. Clin. Invest **94**:2125-2129.

16. **Attal, J., M. C. Theron, S. Rival, C. Puissant, and L. M. Houdebine**. 2000. The efficiency of different IRESs (internal ribosomes entry site) in monocistronic mRNAS. Mol. Biol. Rep. **27**:21-26.

17. **Bachmann, M., H. Althoff, H. Troster, C. Selenka, D. Falke, and W. E. Muller**. 1992. Translocation of the nuclear autoantigen La to the cell surface of herpes simplex virus type 1 infected cells. Autoimmunity **12**:37-45.

18. **Bachmann, M., S. Chang, A. Bernd, W. Mayet, K. H. Meyer zum Buschenfelde, and W. E. Muller**. 1991. Translocation of the nuclear autoantigen La to cell surface: assembly and disassembly with the extracellular matrix. Autoimmunity **9**:99-107.

19. **Bachmann, M., H. Deister, A. Pautz, J. Laubinger, M. Schmitz, D. Falke, J. Podlech, and D. Grolz**. 1998. The human autoantigen La/SS-B accelerates herpes simplex virus type 1 replication in transfected mouse 3T3 cells. Clin. Exp. Immunol. **112**:482-489.

20. **Bachmann, M., D. Grolz, H. Bartsch, R. R. Klein, and H. Troster**. 1997. Analysis of expression of an alternative La (SS-B) cDNA and localization of the encoded N- and C-terminal peptides. Biochim. Biophys. Acta **1356**:53-63.

21. **Bachmann, M., H. C. Schroder, D. Falke, and W. E. Muller**. 1988. Alteration of the intracellular localization of the La protein compared with the localization of U snRNPs. Cell Biol. Int. Rep. **12**:765-789.

22. **Back, S. H., Y. K. Kim, W. J. Kim, S. Cho, H. R. Oh, J. E. Kim, and S. K. Jang**. 2002. Translation of polioviral mRNA is inhibited by cleavage of polypyrimidine tract-binding proteins executed by polioviral 3C(pro). J. Virol. **76**:2529-2542.

23. **Badorff, C., N. Berkely, S. Mehrotra, J. W. Talhouk, R. E. Rhoads, and K. U. Knowlton**. 2000. Enteroviral protease 2A directly cleaves dystrophin and is inhibited by a dystrophin-based substrate analogue. J. Biol. Chem. **275**:11191-11197.

24. **Badorff, C., B. Fichtlscherer, R. E. Rhoads, A. M. Zeiher, A. Muelsch, S. Dimmeler, and K. U. Knowlton**. 2000. Nitric oxide inhibits dystrophin proteolysis by coxsackieviral protease 2A through S-nitrosylation: A protective mechanism against enteroviral cardiomyopathy. Circulation **102**:2276-2281.

25. **Badorff, C., G. H. Lee, and K. U. Knowlton**. 2000. Enteroviral cardiomyopathy: bad news for the dystrophin-glycoprotein complex. Herz **25**:227-232.

26. **Badorff, C., G. H. Lee, B. J. Lamphear, M. E. Martone, K. P. Campbell, R. E. Rhoads, and K. U. Knowlton**. 1999. Enteroviral protease 2A cleaves dystrophin: evidence of cytoskeletal disruption in an acquired cardiomyopathy. Nat. Med. **5**:320-326.

27. **Baltimore, D., A. Huang, K. F. Manly, D. Rekosh, and M. Stampfer**. 1971. The synthesis of protein by mammalian RNA viruses. In: strategy of the viral genome. Ciba Found. Symp.101-110.

28. **Barbaro, G., G. Di Lorenzo, B. Grisorio, and G. Barbarini**. 1998. Incidence of dilated cardiomyopathy and detection of HIV in myocardial cells of HIV-positive patients. Gruppo Italiano per lo Studio Cardiologico dei Pazienti Affetti da AIDS. N. Engl. J. Med. **339**:1093-1099.

29. **Barco, A., E. Feduchi, and L. Carrasco**. 2000. Poliovirus protease 3C(pro) kills cells by apoptosis. Virology **266**:352-360.

30. **Barton, D. J., E. P. Black, and J. B. Flanegan**. 1995. Complete replication of poliovirus in vitro: preinitiation RNA replication complexes require soluble cellular factors for the synthesis of VPg-linked RNA. J. Virol. **69**:5516-5527.

31. **Beijerinck, M. W.** 1898. Concerning a contagium vivum fluidum as a cause of the spot-disease of tobacco leaves. Verh. Akad Wetensch, Amsterdam II **6**:3-21.

32. **Belsham, G. J. and N. Sonenberg**. 1996. RNA-protein interactions in regulation of picornavirus RNA translation. Microbiol. Rev. **60**:499-511.

33. **Belsham, G. J., G. M. McInerney, and N. Ross-Smith**. 2000. Foot-and-Mouth Disease Virus 3C Protease Induces Cleavage of Translation Initiation Factors eIF4A and eIF4G within Infected Cells. The Journal of Virology **74**:272-280.

34. **Bergelson, J. M., M. Chan, K. R. Solomon, N. F. St John, H. Lin, and R. W. Finberg**. 1994. Decay-accelerating factor (CD55), a glycosylphosphatidylinositol-anchored complement regulatory protein, is a receptor for several echoviruses. Proc. Natl. Acad. Sci. U. S. A **91**:6245-6249.

35. **Bergelson, J. M., J. A. Cunningham, G. Droguett, E. A. Kurt-Jones, A. Krithivas, J. S. Hong, M. S. Horwitz, R. L. Crowell, and R. W. Finberg**. 1997. Isolation of a common receptor for Coxsackie B viruses and adenoviruses 2 and 5. Science **275**:1320-1323.

36. **Bergelson, J. M., A. Krithivas, L. Celi, G. Droguett, M. S. Horwitz, T. Wickham, R. L. Crowell, and R. W. Finberg**. 1998. The murine CAR homolog is a receptor for coxsackie B viruses and adenoviruses. J. Virol. **72**:415-419.

37. **Bergelson, J. M., J. G. Mohanty, R. L. Crowell, N. F. St John, D. M. Lublin, and R. W. Finberg**. 1995. Coxsackievirus B3 adapted to growth in RD cells binds to decay-accelerating factor (CD55). J. Virol. **69**:1903-1906.

38. **Berstein, H. D. and D. Baltimore**. 1988. Poliovirus mutant that contains a cold-sensitive defect in viral RNA synthesis. J. Virol. **62**:2922-2928.

39. **Bialik, S., V. L. Cryns, A. Drincic, S. Miyata, A. L. Wollowick, A. Srinivasan, and R. N. Kitsis**. 1999. The mitochondrial apoptotic pathway is activated by serum and glucose deprivation in cardiac myocytes. Circ. Res. **85**:403-414.

40. **Bienz, K., D. Egger, Y. Rasser, and W. Bossart**. 1983. Intracellular distribution of poliovirus proteins and the induction of virus-specific cytoplasmic structures. Virology **131**:39-48.

41. **Bienz, K., D. Egger, M. Troxler, and L. Pasamontes**. 1990. Structural organization of poliovirus RNA replication is mediated by viral proteins of the P2 genomic region. J. Virol. **64**:1156-1163.

42. **Birch, G. M., T. Black, S. K. Malcolm, M. T. Lai, R. E. Zimmerman, and S. R. Jaskunas**. 1995. Purification of recombinant human rhinovirus 14 3C protease expressed in Escherichia coli. Protein Expr. Purif. **6**:609-618.

43. **Black, A. C., J. Luo, S. Chun, A. Bakker, J. K. Fraser, and J. D. Rosenblatt**. 1996. Specific binding of polypyrimidine tract binding protein and hnRNP A1 to HIV-1 CRS elements. Virus Genes **12**:275-285.

44. **Black, A. C., J. Luo, C. Watanabe, S. Chun, A. Bakker, J. K. Fraser, J. P. Morgan, and J. D. Rosenblatt**. 1995. Polypyrimidine tract-binding protein and heterogeneous nuclear ribonucleoprotein A1 bind to human T-cell leukemia virus type 2 RNA regulatory elements. J. Virol. **69**:6852-6858.

45. **Blackwell, J. L. and M. A. Brinton**. 1997. Translation elongation factor-1 alpha interacts with the 3' stem-loop region of West Nile virus genomic RNA. J. Virol. **71**:6433-6444.

46. **Blyn, L. B., J. S. Towner, B. L. Semler, and E. Ehrenfeld**. 1997. Requirement of poly(rC) binding protein 2 for translation of poliovirus RNA. J. Virol. **71**:6243-6246.

47. **Bonneau, A. M. and N. Sonenberg**. 1987. Involvement of the 24-kDa cap-binding protein in regulation of protein synthesis in mitosis. J. Biol. Chem. **262**:11134-11139.

48. **Borman, A. and R. J. Jackson**. 1992. Initiation of translation of human rhinovirus RNA: mapping the internal ribosome entry site. Virology **188**:685-696.

49. **Borman, A. M., J. L. Bailly, M. Girard, and K. M. Kean**. 1995. Picornavirus internal ribosome entry segments: comparison of translation efficiency and the requirements for optimal internal initiation of translation in vitro. Nucleic Acids Res. **23**:3656-3663.

50. **Borman, A. M., F. G. Deliat, and K. M. Kean**. 1994. Sequences within the poliovirus internal ribosome entry segment control viral RNA synthesis. EMBO J. **13**:3149-3157.

51. **Borman, A. M., P. Le Merciea, M. Girard, and K. M. Kean**. 1997. Comparison of picornaviral IRES-driven internal initiation of translation in cultured cells of different origins. Nucleic Acids Res. **25**:932.

52. **Borman, A. M., Y. M. Michel, C. E. Malnou, and K. M. Kean**. 2002. Free poly(A) stimulates capped mRNA translation in vitro through the eIF4G-poly(A)-binding protein interaction. J. Biol. Chem. **277**:36818-36824.

53. **Bouchard, M. J., D. H. Lam, and V. R. Racaniello**. 1995. Determinants of attenuation and temperature sensitivity in the type 1 poliovirus Sabin vaccine. J. Virol. **69**:4972-4978.

54. **Bovee, M. L., B. J. Lamphear, R. E. Rhoads, and R. E. Lloyd**. 1998. Direct cleavage of elF4G by poliovirus 2A protease is inefficient in vitro. Virology **245**:241-249.

55. **Bowles, N. E., V. Dubowitz, C. A. Sewry, and L. C. Archard**. 1987. Dermatomyositis, polymyositis, and Coxsackie-B-virus infection. Lancet **1**:1004-1007.

56. **Bowles, N. E., J. Ni, F. Marcus, and J. A. Towbin**. 2002. The detection of cardiotropic viruses in the myocardium of patients with arrhythmogenic right ventricular dysplasia/cardiomyopathy. J. Am. Coll. Cardiol. **39**:892-895.

57. **Brunet, A. and J. Pouyssegur**. 1997. Mammalian MAP kinase modules: how to transduce specific signals. Essays Biochem. **32**:1-16.

58. **Butterworth, B. E., E. J. Shimshick, and F. H. Yin**. 1976. Association of the polioviral RNA polymerase complex with phospholipid membranes. J. Virol. **19**:457-466.

59. **Caliguiri, L. A. and I. Tamm**. 1970. Characterization of poliovirus-specific structures associated with cytoplasmic membranes. Virology **42**:112-122.

60. **Cameron-Wilson, C. L., Y. A. Pandolfino, H. Y. Zhang, B. Pozzeto, and L. C. Archard**. 1998. Nucleotide sequence of an attenuated mutant of coxsackievirus B3 compared with the cardiovirulent wildtype: assessment of candidate mutations by analysis of a revertant to cardiovirulence. Clin. Diagn. Virol. **9**:99-105.

61. **Carson, S. D., N. N. Chapman, and S. M. Tracy**. 1997. Purification of the putative coxsackievirus B receptor from HeLa cells. Biochem. Biophys. Res. Commun. **233**:325-328.

62. **Carson, S. D., J. T. Hobbs, S. M. Tracy, and N. M. Chapman**. 1999. Expression of the coxsackievirus and adenovirus receptor in cultured human umbilical vein endothelial cells: regulation in response to cell density. J. Virol. **73**:7077-7079.

63. **Carter, M. S. and P. Sarnow**. 2000. Distinct mRNAs that encode La autoantigen are differentially expressed and contain internal ribosome entry sites. J. Biol. Chem. **275**:28301-28307.

64. Carthy, C. Pathogenesis of coxsackievirus B3 induced myocarditis and systemic disease: viral localization, direct injury and activation of host cell death machinery. 2002.
Ref Type: Thesis/Dissertation

65. **Carthy, C. M., D. J. Granville, H. Jiang, J. G. Levy, C. M. Rudin, C. B. Thompson, B. M. McManus, and D. W. Hunt**. 1999. Early release of mitochondrial cytochrome c and expression of mitochondrial epitope 7A6 with a porphyrin-derived photosensitizer: Bcl-2 and Bcl-xL overexpression do not prevent early mitochondrial events but still depress caspase activity. Lab Invest **79**:953-965.

66. **Carthy, C. M., D. J. Granville, K. A. Watson, D. R. Anderson, J. E. Wilson, D. Yang, D. W. Hunt, and B. M. McManus**. 1998. Caspase activation and specific cleavage of substrates after coxsackievirus B3-induced cytopathic effect in HeLa cells. J. Virol. **72**:7669-7675.

67. **Carthy, C. M., B. Yanagawa, H. Luo, D. J. Granville, D. Yang, P. Cheung, C. Cheung, M. Esfandiarei, C. M. Rudin, C. B. Thompson, D. W. Hunt, and B. M. McManus**. 2003. Bcl-2 and Bcl-xL overexpression inhibits cytochrome c release, activation of multiple caspases, and virus release following coxsackievirus B3 infection. Virology **313**:147-157.

68. **Carthy, C. M., D. Yang, D. R. Anderson, J. E. Wilson, and B. M. McManus**. 1997. Myocarditis as systemic disease: new perspectives on pathogenesis. Clin. Exp. Pharmacol. Physiol **24**:997-1003.

69. **Chambers, J. C. and J. D. Keene**. 1985. Isolation and analysis of cDNA clones expressing human lupus La antigen. Proc. Natl. Acad. Sci. U. S. A **82**:2115-2119.

70. **Chambers, J. C., M. G. Kurilla, and J. D. Keene**. 1983. Association between the 7 S RNA and the lupus La protein varies among cell types. J. Biol. Chem. **258**:11438-11441.

71. **Chan, Y. L., R. Gutell, H. F. Noller, and I. G. Wool**. 1984. The nucleotide sequence of a rat 18 S ribosomal ribonucleic acid gene and a proposal for the secondary structure of 18 S ribosomal ribonucleic acid. J. Biol. Chem. **259**:224-230.

72. **Chang, Y. N., D. J. Kenan, J. D. Keene, A. Gatignol, and K. T. Jeang**. 1994. Direct interactions between autoantigen La and human immunodeficiency virus leader RNA. J. Virol. **68**:7008-7020.

73. **Chapman, N. M., A. Ragland, J. S. Leser, K. Hofling, S. Willian, B. L. Semler, and S. Tracy**. 2000. A group B coxsackievirus/poliovirus 5' nontranslated region chimera can act as an attenuated vaccine strain in mice. J. Virol. **74**:4047-4056.

74. **Chapman, N. M., J. R. Romero, M. A. Pallansch, and S. Tracy**. 1997. Sites other than nucleotide 234 determine cardiovirulence in natural isolates of coxsackievirus B3. J. Med. Virol. **52**:258-261.

75. **Chapman, N. M., Z. Tu, S. Tracy, and C. J. Gauntt**. 1994. An infectious cDNA copy of the genome of a non-cardiovirulent coxsackievirus B3 strain: its complete sequence analysis and comparison to the genomes of cardiovirulent coxsackieviruses. Arch. Virol. **135**:115-130.

76. **Chappell, S. A., G. M. Edelman, and V. P. Mauro**. 2000. A 9-nt segment of a cellular mRNA can function as an internal ribosome entry site (IRES) and when present in linked multiple copies greatly enhances IRES activity. Proc. Natl. Acad. Sci. U. S. A **97**:1536-1541.

77. **Chappell, S. A., G. C. Owens, and V. P. Mauro**. 2001. A 5' Leader of Rbm3, a Cold Stress-induced mRNA, Mediates Internal Initiation of Translation with Increased Efficiency under Conditions of Mild Hypothermia. J. Biol. Chem. **276**:36917-36922.

78. **Charriaut-Marlangue, C. and Y. Ben Ari**. 1995. A cautionary note on the use of the TUNEL stain to determine apoptosis. Neuroreport **7**:61-64.

79. **Chen, L., Y. Lin, C. Liao, C. Lin, Y. Huang, C. Yeh, S. Lai, J. Jan, and C. Chin**. 1996. Generation and characterization of organ-tropism mutants of japanese encephalitis virus in vivo and in vitro. Virology **223**:79-88.

80. **Cheung, P., M. Zhang, J. Yuan, D. Chau, B. Yanagawa, and B. McManus**. 2002. Specific interactions of HeLa cell proteins with coxsackievirus B3 RNA: La autoantigen binds differentially to multiple sites within the 5' untranslated region. (IN PRESS). Virus Research **(IN PRESS)**.

81. **Cheung, P., B. Yanagawa, H. Zhang, A. Wang, H. Luo, M. Esfandiarei, A. Saurez, J. Wilson, C. Carthy, B. McManus, and B. Yang**. 2001. Molecular Mechanisms of Cardiovirulence and Host Cell Responses in Coxsackievirus B3 induced Myocarditis. Recent Research Developments in Virology **3**:427-454.

82. **Clark, M. E., P. M. Lieberman, A. J. Berk, and A. Dasgupta**. 1993. Direct cleavage of human TATA-binding protein by poliovirus protease 3C in vivo and in vitro. Mol. Cell Biol. **13**:1232-1237.

83. **Clarkson, N. A., R. Kaufman, D. M. Lublin, T. Ward, P. A. Pipkin, P. D. Minor, D. J. Evans, and J. W. Almond**. 1995. Characterization of the echovirus 7 receptor: domains of CD55 critical for virus binding. J. Virol. **69**:5497-5501.

84. **Coldwell, M. J., S. A. Mitchell, M. Stoneley, M. MacFarlane, and A. E. Willis**. 2000. Initiation of Apaf-1 translation by internal ribosome entry. Oncogene **19**:899-905.

85. **Couderc, T., N. Guedo, V. Calvez, I. Pelletier, J. Hogle, F. Colbere-Garapin, and B. Blondel**. 1994. Substitutions in the capsids of poliovirus mutants selected in human

neuroblastoma cells confer on the Mahoney type 1 strain a phenotype neurovirulent in mice. J. Virol. **68**:8386-8391.

86. **Coyne, K. E., S. E. Hall, S. Thompson, M. A. Arce, T. Kinoshita, T. Fujita, D. J. Anstee, W. Rosse, and D. M. Lublin**. 1992. Mapping of epitopes, glycosylation sites, and complement regulatory domains in human decay accelerating factor. J. Immunol. **149**:2906-2913.

87. **Craig, A. W., A. Haghighat, A. T. Yu, and N. Sonenberg**. 1998. Interaction of polyadenylate-binding protein with the eIF4G homologue PAIP enhances translation. Nature **392**:520-523.

88. **Craig, A. W., Y. V. Svitkin, H. S. Lee, G. J. Belsham, and N. Sonenberg**. 1997. The La autoantigen contains a dimerization domain that is essential for enhancing translation. Mol. Cell Biol. **17**:163-169.

89. **Crosio, C., P. P. Boyl, F. Loreni, P. Pierandrei-Amaldi, and F. Amaldi**. 2000. La protein has a positive effect on the translation of TOP mRNAs in vivo. Nucleic Acids Res. **28**:2927-2934.

90. **D'Ambrosio, A., G. Patti, A. Manzoli, G. Sinagra, A. Di Lenarda, F. Silvestri, and G. Di Sciascio**. 2001. The fate of acute myocarditis between spontaneous improvement and evolution to dilated cardiomyopathy: a review. Heart **85**:499-504.

91. **Dalldorf, G. and G. M. Sickles**. 1948. An unidentified filterable agent isolated from the feces of children with paralysis. Science **108**:61-62.

92. **Das, S., D. J. Kenan, D. Bocskai, J. D. Keene, and A. Dasgupta**. 1996. Sequences within a small yeast RNA required for inhibition of internal initiation of translation: interaction with La and other cellular proteins influences its inhibitory activity. J. Virol. **70**:1624-1632.

93. **Davis, L. S., S. S. Patel, J. P. Atkinson, and P. E. Lipsky**. 1988. Decay-accelerating factor functions as a signal transducing molecule for human T cells. J. Immunol. **141**:2246-2252.

94. **Day, S. P., P. Murphy, E. A. Brown, and S. M. Lemon**. 1992. Mutations within the 5' nontranslated region of hepatitis A virus RNA which enhance replication in BS-C-1 cells. J. Virol. **66**:6533-6540.

95. **de Jong, A. S., I. W. Schrama, P. H. Willems, J. M. Galama, W. J. Melchers, and F. J. van Kuppeveld**. 2002. Multimerization reactions of coxsackievirus proteins 2B, 2C and 2BC: a mammalian two-hybrid analysis. J. Gen. Virol. **83**:783-793.

96. **De, B. P., S. Gupta, H. Zhao, J. A. Drazba, and A. K. Banerjee**. 1996. Specific interaction in vitro and in vivo of glyceraldehyde-3-phosphate dehydrogenase and LA protein with cis-acting RNAs of human parainfluenza virus type 3. J. Biol. Chem. **271**:24728-24735.

97. **Dec, G. W., Jr., I. F. Palacios, J. T. Fallon, H. T. Aretz, J. Mills, D. C. Lee, and R. A. Johnson**. 1985. Active myocarditis in the spectrum of acute dilated cardiomyopathies. Clinical features, histologic correlates, and clinical outcome. N. Engl. J. Med. **312**:885-890.

98. **Dever, T. E., M. J. Glynias, and W. C. Merrick**. 1987. GTP-binding domain: three consensus sequence elements with distinct spacing. Proc. Natl. Acad. Sci. U. S. A **84**:1814-1818.

99. **Dildine, S. L. and B. L. Semler**. 1992. Conservation of RNA-protein interactions among picornaviruses. J. Virol. **66**:4364-4376.

100. **Duggal, R., A. Cuconati, M. Gromeier, and E. Wimmer**. 1997. Genetic recombination of poliovirus in a cell-free system. Proc. Natl. Acad. Sci. U. S. A **94**:13786-13791.

101. **Dunn, J. J., S. S. Bradrick, N. M. Chapman, S. M. Tracy, and J. R. Romero**. 2003. The stem loop II within the 5' nontranslated region of clinical coxsackievirus B3 genomes determines cardiovirulence phenotype in a murine model. J. Infect. Dis. **187**:1552-1561.

102. **Dunn, J. J., N. M. Chapman, S. Tracy, and J. R. Romero**. 2000. Genomic determinants of cardiovirulence in coxsackievirus B3 clinical isolates: localization to the 5' nontranslated region. J. Virol. **74**:4787-4794.

103. **Evan, G. I. and T. D. Littlewood**. 1993. The role of c-myc in cell growth. Curr. Opin. Genet. Dev. **3**:44-49.

104. **Evans, A. S.** 1982. Epidemiology and Control Viral infections of humans. Plenum, New York.

105. **Evans, D. J. and J. W. Almond**. 1998. Cell receptors for picornaviruses as determinants of cell tropism and pathogenesis. Trends Microbiol. **6**:202.

106. **Falk, M. M., P. R. Grigera, I. E. Bergmann, A. Zibert, G. Multhaup, and E. Beck**. 1990. Foot-and-mouth disease virus protease 3C induces specific proteolytic cleavage of host cell histone H3. J. Virol. **64**:748-756.

107. **Fitch, W.** 1977. On the problem of discovering the most parsimonious tree. Am Naturalist **111**:223-257.

108. **Fricks, C. E. and J. M. Hogle**. 1990. Cell-induced conformational change in poliovirus: externalization of the amino terminus of VP1 is responsible for liposome binding. J. Virol. **64**:1934-1945.

109. **Fuster, V., B. J. Gersh, E. R. Giuliani, A. J. Tajik, R. O. Brandenburg, and R. L. Frye**. 1981. The natural history of idiopathic dilated cardiomyopathy. Am J. Cardiol. **47**:525-531.

110. **Galy, B.** 2000. IRES elements: fine-tuning of gene expression at the translational level. Trends Biochem. Sci. **25**:426.

111. **Gamarnik, A. V. and R. Andino**. 1996. Replication of poliovirus in Xenopus oocytes requires two human factors. EMBO J. **15**:5988-5998.

112. **Gamarnik, A. V. and R. Andino**. 1997. Two functional complexes formed by KH domain containing proteins with the 5' noncoding region of poliovirus RNA. RNA. **3**:882-892.

113. **Gan, W., M. LaCelle, and R. E. Rhoads**. 1998. Functional characterization of the internal ribosome entry site of eIF4G mRNA. J. Biol. Chem. **273**:5006-5012.

114. **Gauntt, C., E. Godney, C. Lutton, H. Arizipe, N. Chapman, S. Tracy, G. Revtyak, A. Valente, and M. Rozek**. 1989. Mechanisms of coxsackievirus induced acute myocarditis in the mouse, p. 161-182. *In* L. De la Maza and E. Peterson (eds.), Medical Virology. Lawrence Erlbaum Associates, Hellsdale, N.J.

115. **Gauntt, C. J. and M. A. Pallansch**. 1996. Coxsackievirus B3 clinical isolates and murine myocarditis. Virus Res. **41**:89-99.

116. **Gingras, A. C., B. Raught, and N. Sonenberg**. 1999. eIF4 initiation factors: effectors of mRNA recruitment to ribosomes and regulators of translation. Annu. Rev. Biochem. **68**:913-963.

117. **Glass, M. J., X. Y. Jia, and D. F. Summers**. 1993. Identification of the hepatitis A virus internal ribosome entry site: in vivo and in vitro analysis of bicistronic RNAs containing the HAV 5' noncoding region. Virology **193**:842-852.

118. **Godman, G. C., H. Bunting, and J. L. Melnick**. 1952. The histopathology of coxsackievirus infection in mice. I. Morphologic observations with four different viral types. Am. J. Pathol. **28**:223-257.

119. **Goldstaub, D., A. Gradi, Z. Bercovitch, Z. Grosmann, Y. Nophar, S. Luria, N. Sonenberg, and C. Kahana**. 2000. Poliovirus 2A protease induces apoptotic cell death. Mol. Cell Biol. **20**:1271-1277.

120. **Goss, D. J., S. E. Carberry, T. E. Dever, W. C. Merrick, and R. E. Rhoads**. 1990. A fluorescence study of the interaction of protein synthesis initiation factors 4A, 4E, and 4F with mRNA and oligonucleotide analogs. Biochim. Biophys. Acta **1050**:163-166.

121. **Gottlieb, E. and J. A. Steitz**. 1989. Function of the mammalian La protein: evidence for its action in transcription termination by RNA polymerase III. EMBO J. **8**:851-861.

122. **Gottlieb, E. and J. A. Steitz**. 1989. The RNA binding protein La influences both the accuracy and the efficiency of RNA polymerase III transcription in vitro. EMBO J. **8**:841-850.

123. **Gradi, A., H. Imataka, Y. V. Svitkin, E. Rom, B. Raught, S. Morino, and N. Sonenberg**. 1998. A novel functional human eukaryotic translation initiation factor 4G. Mol. Cell Biol. **18**:334-342.

124. **Gradi, A., Y. V. Svitkin, H. Imataka, and N. Sonenberg**. 1998. Proteolysis of human eukaryotic translation initiation factor eIF4GII, but not eIF4GI, coincides with the shutoff of host protein synthesis after poliovirus infection. Proc. Natl. Acad. Sci. U. S. A **95**:11089-11094.

125. **Grasl-Kraupp, B., B. Ruttkay-Nedecky, H. Koudelka, K. Bukowska, W. Bursch, and R. Schulte-Hermann**. 1995. In situ detection of fragmented DNA (TUNEL assay) fails to discriminate among apoptosis, necrosis, and autolytic cell death: a cautionary note. Hepatology **21**:1465-1468.

126. **Grist, N. R. and D. Reid**. 1993. Epidemiology of viral infections of the heart, p. 23-30. *In* J.E.Banatvala (ed.), Viral Infections of teh Heart. Edward Arnold, London.

127. **Gromeier, M., B. Bossert, M. Arita, A. Nomoto, and E. Wimmer**. 1999. Dual stem loops within the poliovirus internal ribosomal entry site control neurovirulence. J. Virol. **73**:958-964.

128. **Gromeier, M., S. Mueller, D. Solecki, B. Bossert, G. Bernhardt, and E. Wimmer**. 1997. Determinants of poliovirus neurovirulence. J. Neurovirol. **3 Suppl 1**:S35-S38.

129. **Gutierrez, A. L., M. Denova-Ocampo, V. R. Racaniello, and R. M. del Angel**. 1997. Attenuating mutations in the poliovirus 5' untranslated region alter its interaction with polypyrimidine tract-binding protein. J. Virol. **71**:3826-3833.

130. **Gutierrez-Escolano, A. L., Z. U. Brito, R. M. del Angel, and X. Jiang**. 2000. Interaction of cellular proteins with the 5' end of Norwalk virus genomic RNA. J. Virol. **74**:8558-8562.

131. **Gutierrez-Escolano, L. and R. M. del Angel**. 1996. Nuclear proteins bind to poliovirus 5' untranslated region. Arch. Med. Res. **27**:413-419.

132. **Haller, A. A. and B. L. Semler**. 1995. Stem-loop structure synergy in binding cellular proteins to the 5' noncoding region of poliovirus RNA. Virology **206**:923-934.

133. **Harris, K. S., S. R. Reddigari, M. J. Nicklin, T. Hammerle, and E. Wimmer**. 1992. Purification and characterization of poliovirus polypeptide 3CD, a proteinase and a precursor for RNA polymerase. J. Virol. **66**:7481-7489.

134. **Harris, K. S., W. Xiang, L. Alexander, W. S. Lane, A. V. Paul, and E. Wimmer**. 1994. Interaction of poliovirus polypeptide 3CDpro with the 5' and 3' termini of the poliovirus genome. Identification of viral and cellular cofactors needed for efficient binding. J. Biol. Chem. **269**:27004-27014.

135. **Hellen, C. U., T. V. Pestova, M. Litterst, and E. Wimmer**. 1994. The cellular polypeptide p57 (pyrimidine tract-binding protein) binds to multiple sites in the poliovirus 5' nontranslated region. J. Virol. **68**:941-950.

136. **Hellen, C. U., G. W. Witherell, M. Schmid, S. H. Shin, T. V. Pestova, A. Gil, and E. Wimmer**. 1993. A cytoplasmic 57-kDa protein that is required for translation of picornavirus RNA by internal ribosomal entry is identical to the nuclear pyrimidine tract-binding protein. Proc. Natl. Acad. Sci. U. S. A **90**:7642-7646.

137. **Hellen, C. U. T. and E. Wimmer**. 1995. Enterovirus Genetics, p. 25-72. *In* H. A. Robart (ed.), Human Enterovirus Infections. ASM Press, Washinton, D.C.

138. **Henis-Korenblit, S., N. L. Strumpf, D. Goldstaub, and A. Kimchi**. 2000. A novel form of DAP5 protein accumulates in apoptotic cells as a result of caspase cleavage and internal ribosome entry site-mediated translation. Mol. Cell Biol. **20**:496-506.

139. **Herold, J. and R. Andino**. 2001. Poliovirus RNA replication requires genome circularization through a protein-protein bridge. Mol. Cell **7**:581-591.

140. **Holcik, M., H. Gibson, and R. G. Korneluk**. 2001. XIAP: apoptotic brake and promising therapeutic target. Apoptosis. **6**:253-261.

141. **Holcik, M. and R. G. Korneluk**. 2000. Functional characterization of the X-linked inhibitor of apoptosis (XIAP) internal ribosome entry site element: role of La autoantigen in XIAP translation. Mol. Cell Biol. **20**:4648-4657.

142. **Holcik, M., C. Yeh, R. G. Korneluk, and T. Chow**. 2000. Translational upregulation of X-linked inhibitor of apoptosis (XIAP) increases resistance to radiation induced cell death. Oncogene **19**:4174-4177.

143. **Honda, M., S. Kaneko, E. Matsushita, K. Kobayashi, G. A. Abell, and S. M. Lemon**. 2000. Cell cycle regulation of hepatitis C virus internal ribosomal entry site-directed translation. Gastroenterology **118**:152-162.

144. **Huber, S. A. and B. Pfaeffle**. 1994. Differential Th1 and Th2 cell responses in male and female BALB/c mice infected with coxsackievirus group B type 3. J. Virol. **68**:5126-5132.

145. **Huez, I., S. Bornes, D. Bresson, L. Creancier, and H. Prats**. 2001. New vascular endothelial growth factor isoform generated by internal ribosome entry site-driven CUG translation initiation. Mol. Endocrinol. **15**:2197-2210.

146. **Hunt, S. L., J. J. Hsuan, N. Totty, and R. J. Jackson**. 1999. unr, a cellular cytoplasmic RNA-binding protein with five cold-shock domains, is required for internal initiation of translation of human rhinovirus RNA. Genes Dev. **13**:437-448.

147. **Hunt, S. L. and R. J. Jackson**. 1999. Polypyrimidine-tract binding protein (PTB) is necessary, but not sufficient, for efficient internal initiation of translation of human rhinovirus-2 RNA. RNA. **5**:344-359.

148. **Hunt, S. L., A. Kaminski, and R. J. Jackson**. 1993. The influence of viral coding sequences on the efficiency of internal initiation of translation of cardiovirus RNAs. Virology **197**:801-807.

149. **Ida-Hosonuma, M., T. Iwasaki, C. Taya, Y. Sato, J. Li, N. Nagata, H. Yonekawa, and S. Koike**. 2002. Comparison of neuropathogenicity of poliovirus in two transgenic mouse strains expressing human poliovirus receptor with different distribution patterns. J. Gen. Virol. **83**:1095-1105.

150. **Iizuka, N., M. Kohara, K. Hagino-Yamagishi, S. Abe, T. Komatsu, K. Tago, M. Arita, and A. Nomoto**. 1989. Construction of less neurovirulent polioviruses by introducing deletions into the 5' noncoding sequence of the genome. J. Virol. **63**:5354-5363.

151. **Imataka, H., A. Gradi, and N. Sonenberg**. 1998. A newly identified N-terminal amino acid sequence of human eIF4G binds poly(A)-binding protein and functions in poly(A)-dependent translation. EMBO J. **17**:7480-7489.

152. **Irie-Sasaki, J., T. Sasaki, W. Matsumoto, A. Opavsky, M. Cheng, G. Welstead, E. Griffiths, C. Krawczyk, C. D. Richardson, K. Aitken, N. Iscove, G. Koretzky, P. Johnson, P. Liu, D. M. Rothstein, and J. M. Penninger**. 2001. CD45 is a JAK phosphatase and negatively regulates cytokine receptor signalling. Nature **409**:349-354.

153. **Isoyama, T., N. Kamoshita, K. Yasui, A. Iwai, K. Shiroki, H. Toyoda, A. Yamada, Y. Takasaki, and A. Nomoto**. 1999. Lower concentration of La protein required for internal ribosome entry on hepatitis C virus RNA than on poliovirus RNA. J. Gen. Virol. **80 ( Pt 9)**:2319-2327.

154. **Ito, T. and M. M. Lai**. 1997. Determination of the secondary structure of and cellular protein binding to the 3'-untranslated region of the hepatitis C virus RNA genome. J. Virol. **71**:8698-8706.

155. **Ivanoff, L. A., T. Towatari, J. Ray, B. D. Korant, and S. R. Petteway, Jr.** 1986. Expression and site-specific mutagenesis of the poliovirus 3C protease in Escherichia coli. Proc. Natl. Acad. Sci. U. S. A **83**:5392-5396.

156. **Jackson, R. J. and A. Kaminski**. 1995. Internal initiation of translation in eukaryotes: the picornavirus paradigm and beyond. RNA. **1**:985-1000.

157. **Jaramillo, M., T. E. Dever, W. C. Merrick, and N. Sonenberg**. 1991. RNA unwinding in translation: assembly of helicase complex intermediates comprising eukaryotic initiation factors eIF-4F and eIF-4B. Mol. Cell Biol. **11**:5992-5997.

158. **Jin, O., M. J. Sole, J. W. Butany, W. K. Chia, P. R. McLaughlin, P. Liu, and C. C. Liew**. 1990. Detection of enterovirus RNA in myocardial biopsies from patients with myocarditis and cardiomyopathy using gene amplification by polymerase chain reaction. Circulation **82**:8-16.

159. **Johannes, G. and P. Sarnow**. 1998. Cap-independent polysomal association of natural mRNAs encoding c-myc, BiP, and eIF4G conferred by internal ribosome entry sites. RNA. **4**:1500-1513.

160. **Johannes, G. and P. Sarnow**. 1998. Cap-independent polysomal association of natural mRNAs encoding c-myc, BiP, and eIF4G conferred by internal ribosome entry sites. RNA. **4**:1500-1513.

161. **Jore, J., B. De Geus, R. J. Jackson, P. H. Pouwels, and B. E. Enger-Valk**. 1988. Poliovirus protein 3CD is the active protease for processing of the precursor protein P1 in vitro. J. Gen. Virol. **69 ( Pt 7)**:1627-1636.

162. **Joshi, R. L., J. M. Ravel, and A. L. Haenni**. 1986. Interaction of turnip yellow mosaic virus Val-RNA with eukaryotic elongation factor EF-1 [alpha]. Search for a function. EMBO J. **5**:1143-1148.

163. **Kaminski, A., M. T. Howell, and R. J. Jackson**. 1990. Initiation of encephalomyocarditis virus RNA translation: the authentic initiation site is not selected by a scanning mechanism. EMBO J. **9**:3753-3759.

164. **Kaminski, A., S. L. Hunt, J. G. Patton, and R. J. Jackson**. 1995. Direct evidence that polypyrimidine tract binding protein (PTB) is essential for internal initiation of translation of encephalomyocarditis virus RNA. RNA. **1**:924-938.

165. **Kaminski, A. and R. J. Jackson**. 1998. The polypyrimidine tract binding protein (PTB) requirement for internal initiation of translation of cardiovirus RNAs is conditional rather than absolute. RNA. **4**:626-638.

166. **Kandolf, R.** 1995. [The molecular pathogenesis of enterovirus myocarditis. Virus persistence and chronic inflammation]. Internist (Berl) **36**:430-438.

167. **Kandolf, R., K. Klingel, H. Mertsching, A. Canu, C. Hohenadl, R. Zell, B. Y. Reimann, A. Heim, B. M. McManus, A. K. Foulis, and .** 1991. Molecular studies on enteroviral heart disease: patterns of acute and persistent infections. Eur. Heart J. **12 Suppl D**:49-55.

168. **Karnauchow, T. M., D. L. Tolson, B. A. Harrison, E. Altman, D. M. Lublin, and K. Dimock**. 1996. The HeLa cell receptor for enterovirus 70 is decay-accelerating factor (CD55). J. Virol. **70**:5143-5152.

169. **Kaufman, D. L., M. G. Erlander, M. Clare-Salzler, M. A. Atkinson, N. K. Maclaren, and A. J. Tobin**. 1992. Autoimmunity to two forms of glutamate decarboxylase in insulin-dependent diabetes mellitus. J. Clin. Invest **89**:283-292.

170. **Kean, K. M., H. Agut, O. Fichot, E. Wimmer, and M. Girard**. 1988. A poliovirus mutant defective for self-cleavage at the COOH-terminus of the 3C protease exhibits secondary processing defects. Virology **163**:330-340.

171. **Kim, J. H., B. Hahm, Y. K. Kim, M. Choi, and S. K. Jang**. 2000. Protein-protein interaction among hnRNPs shuttling between nucleus and cytoplasm. J. Mol. Biol. **298**:395-405.

172. **Kim, Y. K., S. H. Back, J. Rho, S. H. Lee, and S. K. Jang**. 2001. La autoantigen enhances translation of BiP mRNA. Nucleic Acids Res. **29**:5009-5016.

173. **Kim, Y. K., B. Hahm, and S. K. Jang**. 2000. Polypyrimidine tract-binding protein inhibits translation of bip mRNA. J. Mol. Biol. **304**:119-133.

174. **Kim, Y. K. and S. K. Jang**. 1999. La protein is required for efficient translation driven by encephalomyocarditis virus internal ribosomal entry site. J. Gen. Virol. **80 ( Pt 12)**:3159-3166.

175. **Kim, Y. U., T. Kinoshita, H. Molina, D. Hourcade, T. Seya, L. M. Wagner, and V. M. Holers**. 1995. Mouse complement regulatory protein Crry/p65 uses the specific mechanisms of both human decay-accelerating factor and membrane cofactor protein. J. Exp. Med. **181**:151-159.

176. **King, A. M. Q., F. Brown, P. Christian, T. Hovi, T. Hyypia, N. J. Knowles, S. M. Lemon, P. D. Minor, A. C. Palmenberg, T. Skern, and G. Stanway**. 1999. Picornaviridae *In* M. H. V. Van REgenmortel, C. M. Fauquet, and D. H. L. e. al. Bishop (eds.), Virus Toxonomy. New York.

177. **Kishimoto, C., H. Kawamata, S. Sakai, H. Shinohara, and H. Ochiai**. 2000. Role of MIP-2 in coxsackievirus B3 myocarditis. J. Mol. Cell Cardiol. **32**:631-638.

178. **Kishimoto, C., H. Takada, Y. Hiraoka, H. Shinohara, and M. Kitazawa**. 2000. Protection against murine coxsackievirus B3 myocarditis by T cell vaccination. J. Mol. Cell Cardiol. **32**:2269-2277.

179. **Kishimoto, C., H. Takada, H. Kawamata, M. Umatake, and H. Ochiai**. 2001. Immunoglobulin treatment prevents congestive heart failure in murine encephalomyocarditis viral myocarditis associated with reduction of inflammatory cytokines. J. Pharmacol. Exp. Ther. **299**:645-651.

180. **Kishimoto, C., N. Takamatsu, H. Kawamata, H. Shinohara, and H. Ochiai**. 2000. Immunoglobulin treatment ameliorates murine myocarditis associated with reduction of neurohumoral activity and improvement of extracellular matrix change. J. Am. Coll. Cardiol. **36**:1979-1984.

181. **Kishimoto, C., K. A. Thorp, and W. H. Abelmann**. 1990. Immunosuppression with high doses of cyclophosphamide reduces the severity of myocarditis but increases the mortality in murine Coxsackievirus B3 myocarditis. Circulation **82**:982-989.

182. **Kitamura, N., B. L. Semler, P. G. Rothberg, G. R. Larsen, C. J. Adler, A. J. Dorner, E. A. Emini, R. Hanecak, J. J. Lee, W. S. van der, C. W. Anderson, and E. Wimmer**. 1981. Primary structure, gene organization and polypeptide expression of poliovirus RNA. Nature **291**:547-553.

183. **Klingel, K., C. Hohenadl, A. Canu, M. Albrecht, M. Seemann, G. Mall, and R. Kandolf**. 1992. Ongoing enterovirus-induced myocarditis is associated with persistent heart muscle infection: quantitative analysis of virus replication, tissue damage, and inflammation. Proc. Natl. Acad. Sci. U. S. A **89**:314-318.

184. **Klingel, K., P. Rieger, G. Mall, H. C. Selinka, M. Huber, and R. Kandolf**. 1998. Visualization of enteroviral replication in myocardial tissue by ultrastructural in situ hybridization: identification of target cells and cytopathic effects. Lab Invest **78**:1227-1237.

185. **Klingel, K., S. Stephan, M. Sauter, R. Zell, B. M. McManus, B. Bultmann, and R. Kandolf**. 1996. Pathogenesis of murine enterovirus myocarditis: virus dissemination and immune cell targets. J. Virol. **70**:8888-8895.

186. **Kockx, M. M., J. Muhring, M. W. Knaapen, and G. R. de Meyer**. 1998. RNA synthesis and splicing interferes with DNA in situ end labeling techniques used to detect apoptosis. Am J. Pathol. **152**:885-888.

187. **Kolupaeva, V. G., C. U. Hellen, and I. N. Shatsky**. 1996. Structural analysis of the interaction of the pyrimidine tract-binding protein with the internal ribosomal entry site of encephalomyocarditis virus and foot-and-mouth disease virus RNAs. RNA. **2**:1199-1212.

188. **Kolupaeva, V. G., T. V. Pestova, C. U. Hellen, and I. N. Shatsky**. 1998. Translation eukaryotic initiation factor 4G recognizes a specific structural element within the internal ribosome entry site of encephalomyocarditis virus RNA. J. Biol. Chem. **273**:18599-18604.

189. **Kozak, M.** 2001. New ways of initiating translation in eukaryotes? Mol Cell Biol. **21**:1899-1907.

190. **Krausslich, H. G. and E. Wimmer**. 1988. Viral proteinases. Annu. Rev. Biochem. **57**:701-754.

191. **Kuge, S. and A. Nomoto**. 1987. Construction of viable deletion and insertion mutants of the Sabin strain of type 1 poliovirus: function of the 5' noncoding sequence in viral replication. J. Virol. **61**:1478-1487.

192. **Lama, J., A. V. Paul, K. S. Harris, and E. Wimmer**. 1994. Properties of purified recombinant poliovirus protein 3aB as substrate for viral proteinases and as co-factor for RNA polymerase 3Dpol. J. Biol. Chem. **269**:66-70.

193. **Lama, J., M. A. Sanz, and P. L. Rodriguez**. 1995. A role for 3AB protein in poliovirus genome replication. J. Biol. Chem. **270**:14430-14438.

194. **Lamphear, B. J., R. Kirchweger, T. Skern, and R. E. Rhoads**. 1995. Mapping of functional domains in eukaryotic protein synthesis initiation factor 4G (eIF4G) with picornaviral proteases. Implications for cap-dependent and cap-independent translational initiation. J. Biol. Chem. **270**:21975-21983.

195. **Lamphear, B. J., R. Yan, F. Yang, D. Waters, H. D. Liebig, H. Klump, E. Kuechler, T. Skern, and R. E. Rhoads**. 1993. Mapping the cleavage site in protein synthesis initiation factor eIF-4 gamma of the 2A proteases from human Coxsackievirus and rhinovirus. J. Biol. Chem. **268**:19200-19203.

196. **Lazarus, L. H. and R. Barzilai**. 1974. Association of foot-and-mouth disease virus replicase with RNA template and cytoplasmic membranes. J. Gen. Virol. **23**:213-218.

197. **Lee, C., E. Maull, N. Chapman, S. Tracy, and C. Gauntt**. 1997. Genomic regions of coxsackievirus B3 associated with cardiovirulence. J. Med. Virol. **52**:341-347.

198. **Lee, C., E. Maull, N. Chapman, S. Tracy, J. Wood, and C. Gauntt**. 1997. Generation of an infectious cDNA of a highly cardiovirulent coxsackievirus B3(CVB3m) and comparison to other infectious CVB3 cDNAs. Virus Res. **50**:225-235.

199. **Lee, G. H., C. Badorff, and K. U. Knowlton**. 2000. Dissociation of sarcoglycans and the dystrophin carboxyl terminus from the sarcolemma in enteroviral cardiomyopathy. Circ. Res. **87**:489-495.

200. **Lemon, S. M.** 1985. Type A viral hepatitis. New developments in an old disease. N. Engl. J. Med. **313**:1059-1067.

201. **Li, J. P. and D. Baltimore**. 1990. An intragenic revertant of a poliovirus 2C mutant has an uncoating defect. J. Virol. **64**:1102-1107.

202. **Liebig, H. D., E. Ziegler, R. Yan, K. Hartmuth, H. Klump, H. Kowalski, D. Blaas, W. Sommergruber, L. Frasel, B. Lamphear, and .** 1993. Purification of two picornaviral 2A proteinases: interaction with eIF-4 gamma and influence on in vitro translation. Biochemistry **32**:7581-7588.

203. **Lin, C. H. and J. G. Patton**. 1995. Regulation of alternative 3' splice site selection by constitutive splicing factors. RNA. **1**:234-245.

204. **Ling, J., S. J. Morley, V. M. Pain, W. F. Marzluff, and D. R. Gallie**. 2002. The histone 3'-terminal stem-loop-binding protein enhances translation through a functional and physical interaction with eukaryotic initiation factor 4G (eIF4G) and eIF3. Mol. Cell Biol. **22**:7853-7867.

205. **Liu, P., K. Aitken, Y. Y. Kong, M. A. Opavsky, T. Martino, F. Dawood, W. H. Wen, I. Kozieradzki, K. Bachmaier, D. Straus, T. W. Mak, and J. M. Penninger**. 2000. The

tyrosine kinase p56lck is essential in coxsackievirus B3-mediated heart disease. Nat. Med. **6**:429-434.

206. **Liu, P. P. and J. W. Mason**. 2001. Advances in the understanding of myocarditis. Circulation **104**:1076-1082.

207. **Liu, Z., C. M. Carthy, P. Cheung, L. Bohunek, J. E. Wilson, B. M. McManus, and D. Yang**. 1999. Structural and functional analysis of the 5' untranslated region of coxsackievirus B3 RNA: In vivo translational and infectivity studies of full-length mutants. Virology **265**:206-217.

208. **Lloyd, R. E., H. G. Jense, and E. Ehrenfeld**. 1987. Restriction of translation of capped mRNA in vitro as a model for poliovirus-induced inhibition of host cell protein synthesis: relationship to p220 cleavage. J. Virol. **61**:2480-2488.

209. **Lomakin, I. B., C. U. Hellen, and T. V. Pestova**. 2000. Physical association of eukaryotic initiation factor 4G (eIF4G) with eIF4A strongly enhances binding of eIF4G to the internal ribosomal entry site of encephalomyocarditis virus and is required for internal initiation of translation. Mol. Cell Biol. **20**:6019-6029.

210. **Lopez, d. Q., E. Lafuente, and E. Martinez-Salas**. 2001. IRES interaction with translation initiation factors: functional characterization of novel RNA contacts with eIF3, eIF4B, and eIF4GII. RNA. **7**:1213-1226.

211. **Lowenstein, C. J., S. L. Hill, A. Lafond-Walker, J. Wu, G. Allen, M. Landavere, N. R. Rose, and A. Herskowitz**. 1996. Nitric oxide inhibits viral replication in murine myocarditis. J. Clin. Invest **97**:1837-1843.

212. **Lublin, D. M. and J. P. Atkinson**. 1989. Decay-accelerating factor: biochemistry, molecular biology, and function. Annu. Rev. Immunol. **7**:35-58.

213. **Macejak, D. G. and P. Sarnow**. 1991. Internal initiation of translation mediated by the 5' leader of a cellular mRNA. Nature **353**:90-94.

214. **Majno, G. and I. Joris**. 1995. Apoptosis, oncosis, and necrosis. An overview of cell death. Am J. Pathol. **146**:3-15.

215. **Malcolm, B. A.** 1995. The picornaviral 3C proteinases: cysteine nucleophiles in serine proteinase folds. Protein Sci. **4**:1439-1445.

216. **Martin, A. B., S. Webber, F. J. Fricker, R. Jaffe, G. Demmler, D. Kearney, Y. H. Zhang, J. Bodurtha, B. Gelb, J. Ni, and .** 1994. Acute myocarditis. Rapid diagnosis by PCR in children. Circulation **90**:330-339.

217. **Martinez-Salas, E., J. C. Saiz, M. Davila, G. J. Belsham, and E. Domingo**. 1993. A single nucleotide substitution in the internal ribosome entry site of foot-and-mouth disease virus leads to enhanced cap-independent translation in vivo. J. Virol. **67**:3748-3755.

218. **Martino, T. A., P. Liu, M. Petric, and M. J. Sale**. 1995. Enteroviral Myocarditis and Dilated Cardiomyopathy: A review of clinical and experimental studies, p. 291-351. *In* H. A. Rotbart (ed.), Human Enterovirus. Plenum Press, New York.

219. **Martino, T. A., P. Liu, and M. J. Sole**. 1994. Viral infection and the pathogenesis of dilated cardiomyopathy. Circ. Res. **74**:182-188.

220. **Martino, T. A., M. Petric, H. Weingartl, J. M. Bergelson, M. A. Opavsky, C. D. Richardson, J. F. Modlin, R. W. Finberg, K. C. Kain, N. Willis, C. J. Gauntt, and P. P. Liu**. 2000. The coxsackie-adenovirus receptor (CAR) is used by reference strains and clinical isolates representing all six serotypes of coxsackievirus group B and by swine vesicular disease virus. Virology **271**:99-108.

221. **Matsumori, A., C. Yutani, Y. Ikeda, S. Kawai, and S. Sasayama**. 2000. Hepatitis C virus from the hearts of patients with myocarditis and cardiomyopathy. Lab Invest **80**:1137-1142.

222. **Matthews, D. A., W. W. Smith, R. A. Ferre, B. Condon, G. Budahazi, W. Sisson, J. E. Villafranca, C. A. Janson, H. E. McElroy, C. L. Gribskov, and .** 1994. Structure of human rhinovirus 3C protease reveals a trypsin-like polypeptide fold, RNA-binding site, and means for cleaving precursor polyprotein. Cell **77**:761-771.

223. **Mattioli, M. and M. Reichlin**. 1974. Heterogeneity of RNA protein antigens reactive with sera of patients with systemic lupus erythematosus. Description of a cytoplasmic nonribosomal antigen. Arthritis Rheum. **17**:421-429.

224. **Mbida, A. D., B. Pozzetto, O. G. Gaudin, F. Grattard, J. C. Le Bihan, Y. Akono, and A. Ros**. 1992. A 44,000 glycoprotein is involved in the attachment of echovirus-11 onto susceptible cells. Virology **189**:350-353.

225. **McBride, A. E., A. Schlegel, and K. Kirkegaard**. 1996. Human protein Sam68 relocalization and interaction with poliovirus RNA polymerase in infected cells. Proc. Natl. Acad. Sci. U. S. A **93**:2296-2301.

226. **McManus, B. M., L. H. Chow, J. E. Wilson, D. R. Anderson, J. M. Gulizia, C. J. Gauntt, K. E. Klingel, K. W. Beisel, and R. Kandolf**. 1993. Direct myocardial injury by enterovirus: a central role in the evolution of murine myocarditis. Clin. Immunol. Immunopathol. **68**:159-169.

227. **Medof, M. E., D. M. Lublin, V. M. Holers, D. J. Ayers, R. R. Getty, J. F. Leykam, J. P. Atkinson, and M. L. Tykocinski**. 1987. Cloning and characterization of cDNAs encoding the complete sequence of decay-accelerating factor of human complement. Proc. Natl. Acad. Sci. U. S. A **84**:2007-2011.

228. **Meerovitch, K., Y. V. Svitkin, H. S. Lee, F. Lejbkowicz, D. J. Kenan, E. K. Chan, V. I. Agol, J. D. Keene, and N. Sonenberg**. 1993. La autoantigen enhances and corrects aberrant translation of poliovirus RNA in reticulocyte lysate. J. Virol. **67**:3798-3807.

229. **Melchers, W. J., J. G. Hoenderop, H. J. Bruins Slot, C. W. Pleij, E. V. Pilipenko, V. I. Agol, and J. M. Galama**. 1997. Kissing of the two predominant hairpin loops in the coxsackie B virus 3' untranslated region is the essential structural feature of the origin of replication required for negative-strand RNA synthesis. J. Virol. **71**:686-696.

230. **Mena, I., C. Fischer, J. R. Gebhard, C. M. Perry, S. Harkins, and J. L. Whitton**. 2000. Coxsackievirus infection of the pancreas: evaluation of receptor expression, pathogenesis, and immunopathology. Virology **271**:276-288.

231. **Merrick, W. C. and J. W. B. Hershey**. 1996. The Pathway and mechanism of eukaryotic protein synthesis, p. 31-69. *In* J. W. B. e. al. Hershey (ed.), Trnaslational Control. Cold Spring Harbor laboratory Press.

232. **Merrick, W. C.** 1992. Mechanism and regulation of eukaryotic protein synthesis. Microbiol. Rev. **56**:291-315.

233. **Methot, N., G. Pickett, J. D. Keene, and N. Sonenberg**. 1996. In vitro RNA selection identifies RNA ligands that specifically bind to eukaryotic translation initiation factor 4B: the role of the RNA remotif. RNA. **2**:38-50.

234. **Michel, Y. M., D. Poncet, M. Piron, K. M. Kean, and A. M. Borman**. 2000. Cap-Poly(A) synergy in mammalian cell-free extracts. Investigation of the requirements for poly(A)-mediated stimulation of translation initiation. J. Biol. Chem. **275**:32268-32276.

235. **Mirmomeni, M. H., P. J. Hughes, and G. Stanway**. 1997. An RNA tertiary structure in the 3' untranslated region of enteroviruses is necessary for efficient replication. Journal of Virology **71**:2370.

236. **Mitchell, S. A., E. C. Brown, M. J. Coldwell, R. J. Jackson, and A. E. Willis**. 2001. Protein factor requirements of the Apaf-1 internal ribosome entry segment: roles of polypyrimidine tract binding protein and upstream of N-ras. Mol. Cell Biol. **21**:3364-3374.

237. **Miyashita, K., J. Okunishi, R. Utsumi, S. Tagiri, K. Hotta, T. Komano, T. Tamura, and N. Satoh**. 1996. Cleavage specificity of coxsackievirus 3C proteinase for peptide substrate (2): Importance of the P2 and P4 residues. Biosci. Biotechnol. Biochem. **60**:1528-1529.

238. **Miyashita, K., R. Utsumi, T. Utsumi, T. Komao, and N. Satoh**. 1995. Mutational Analysis of the putative substrate-binding site of 3C proteinase of coxsackievirus b3. Biosci. Biotechnol. Biochem. **59**:121-122.

239. **Muckelbauer, J. K., M. Kremer, I. Minor, G. Diana, F. J. Dutko, J. Groarke, D. C. Pevear, and M. G. Rossmann**. 1995. The structure of coxsackievirus B3 at 3.5 A resolution. Structure. **3**:653-667.

240. **Muckelbauer, J. K. and M. G. Rossmann**. 1997. The structure of coxsackievirus B3. Curr. Top. Microbiol. Immunol. **223**:191-208.

241. **Murakami, K., M. Abe, T. Kageyama, N. Kamoshita, and A. Nomoto**. 2001. Down-regulation of translation driven by hepatitis C virus internal ribosomal entry site by the 3' untranslated region of RNA. Arch. Virol. **146**:729-741.

242. **Nagai, Y.** 1995. Virus activation by host proteinases. Microbiol. Immunol. **39**:1-9.

243. **Nakamura, H., T. Yamamoto, T. Yamamura, F. Nakao, S. Umemoto, T. Shintaku, K. Yamaguchi, P. Liu, and M. Matsuzaki**. 1999. Repetitive coxsackievirus infection induces cardiac dilatation in post-myocarditic mice. Jpn. Circ. J. **63**:794-802.

244. **Nanbru, C., I. Lafon, S. Audigier, M. C. Gensac, S. Vagner, G. Huez, and A. C. Prats**. 1997. Alternative translation of the proto-oncogene c-myc by an internal ribosome entry site. J. Biol. Chem. **272**:32061-32066.

245. **Nattel, S. and D. Li**. 2000. Ionic remodeling in the heart: pathophysiological significance and new therapeutic opportunities for atrial fibrillation. Circ. Res. **87**:440-447.

246. **Nichol, S.** 1996. RNA viruses. Life on the edge of catastrophe. Nature **384**:218-219.

247. **Nicholson, R., J. Pelletier, S. Y. Le, and N. Sonenberg**. 1991. Structural and functional analysis of the ribosome landing pad of poliovirus type 2: in vivo translation studies. J. Virol. **65**:5886-5894.

248. **Nicholson-Weller, A. and C. E. Wang**. 1994. Structure and function of decay accelerating factor CD55. J. Lab Clin. Med. **123**:485-491.

249. **Nomoto, A., S. Koike, and J. Aoki**. 1994. Tissue tropism and species specificity of poliovirus infection. Trends Microbiol. **2**:47-51.

250. **Nomoto, A., K. Tsukiyama-Kohara, and M. Kohara**. 1995. Mechanism of translation initiation on hepatitis C virus RNA. Princess Takamatsu Symp. **25**:111-119.

251. **O'Connell, J. B.** The role of myocarditis in end-stage dilated cardiomyopathy. Texas Heart Institute Journal **14**, 268-275. 1987.

252. **Ohlmann, T., M. Rau, S. J. Morley, and V. M. Pain**. 1995. Proteolytic cleavage of initiation factor eIF-4 gamma in the reticulocyte lysate inhibits translation of capped mRNAs but enhances that of uncapped mRNAs. Nucleic Acids Res. **23**:334-340.

253. **Ohndorf, U. M., C. Steegborn, R. Knijff, and P. Sondermann**. 2001. Contributions of the individual domains in human La protein to its RNA 3'-end binding activity. J. Biol. Chem. **276**:27188-27196.

254. **Ono, K., A. Matsumori, T. Shioi, Y. Furukawa, and S. Sasayama**. 1998. Cytokine gene expression after myocardial infarction in rat hearts: possible implication in left ventricular remodeling. Circulation **98**:149-156.

255. **Opavsky, M. A., J. Penninger, K. Aitken, W. H. Wen, F. Dawood, T. Mak, and P. Liu**. 1999. Susceptibility to myocarditis is dependent on the response of alphabeta T lymphocytes to coxsackieviral infection. Circ. Res. **85**:551-558.

256. **Page, G. S., A. G. Mosser, J. M. Hogle, D. J. Filman, R. R. Rueckert, and M. Chow**. 1988. Three-dimensional structure of poliovirus serotype 1 neutralizing determinants. J. Virol. **62**:1781-1794.

257. **Palmenberg, A. C.** 1990. Proteolytic processing of picornaviral polyprotein. Annu. Rev. Microbiol. **44**:603-623.

258. **Palmenberg, A. C., E. M. Kirby, M. R. Janda, N. L. Drake, G. M. Duke, K. F. Potratz, and M. S. Collett**. 1984. The nucleotide and deduced amino acid sequences of the encephalomyocarditis viral polyprotein coding region. Nucleic Acids Res. **12**:2969-2985.

259. **Pardigon, N. and J. H. Strauss**. 1996. Mosquito homolog of the La autoantigen binds to Sindbis virus RNA. J. Virol. **70**:1173-1181.

260. **Paul, A. V., X. Cao, K. S. Harris, J. Lama, and E. Wimmer**. 1994. Studies with poliovirus polymerase 3Dpol. Stimulation of poly(U) synthesis in vitro by purified poliovirus protein 3AB. J. Biol. Chem. **269**:29173-29181.

261. **Paul, A. V., A. Molla, and E. Wimmer**. 1994. Studies of a putative amphipathic helix in the N-terminus of poliovirus protein 2C. Virology **199**:188-199.

262. **Pause, A. and N. Sonenberg**. 1992. Mutational analysis of a DEAD box RNA helicase: the mammalian translation initiation factor eIF-4A. EMBO J. **11**:2643-2654.

263. **Peck, M. L. and D. Herschlag**. 1999. Effects of oligonucleotide length and atomic composition on stimulation of the ATPase activity of translation initiation factor elF4A. RNA. **5**:1210-1221.

264. **Peek, R., G. J. Pruijn, and W. J. Van Venrooij**. 1996. Interaction of the La (SS-B) autoantigen with small ribosomal subunits. Eur. J. Biochem. **236**:649-655.

265. **Pelham, H. R.** 1978. Translation of encephalomyocarditis virus RNA in vitro yields an active proteolytic processing enzyme. Eur. J. Biochem. **85**:457-462.

266. **Pellizzoni, L., B. Cardinali, N. Lin-Marq, D. Mercanti, and P. Pierandrei-Amaldi**. 1996. A Xenopus laevis homologue of the La autoantigen binds the pyrimidine tract of the 5' UTR of ribosomal protein mRNAs in vitro: implication of a protein factor in complex formation. J. Mol. Biol. **259**:904-915.

267. **Perez, I., C. H. Lin, J. G. McAfee, and J. G. Patton**. 1997. Mutation of PTB binding sites causes misregulation of alternative 3' splice site selection in vivo. RNA. **3**:764-778.

268. **Perez, I., J. G. McAfee, and J. G. Patton**. 1997. Multiple RRMs contribute to RNA binding specificity and affinity for polypyrimidine tract binding protein. Biochemistry **36**:11881-11890.

269. **Perez, L. and L. Carrasco**. 1992. Lack of direct correlation between p220 cleavage and the shut-off of host translation after poliovirus infection. Virology **189**:178-186.

270. **Pestova, T. V., C. U. Hellen, and E. Wimmer**. 1991. Translation of poliovirus RNA: role of an essential cis-acting oligopyrimidine element within the 5' nontranslated region and involvement of a cellular 57-kilodalton protein. J. Virol. **65**:6194-6204.

271. **Pestova, T. V., I. N. Shatsky, and C. U. Hellen**. 1996. Functional dissection of eukaryotic initiation factor 4F: the 4A subunit and the central domain of the 4G subunit are sufficient to mediate internal entry of 43S preinitiation complexes. Mol. Cell Biol. **16**:6870-6878.

272. **Petrik, J., H. Parker, and G. J. Alexander**. 1999. Human hepatic glyceraldehyde-3-phosphate dehydrogenase binds to the poly(U) tract of the 3' non-coding region of hepatitis C virus genomic RNA. J. Gen. Virol. **80 ( Pt 12)**:3109-3113.

273. **Pilipenko, E. V., A. P. Gmyl, S. V. Maslova, E. V. Khitrina, and V. I. Agol**. 1995. Attenuation of Theiler's murine encephalomyelitis virus by modifications of the oligopyrimidine/AUG tandem, a host-dependent translational cis element. J. Virol. **69**:864-870.

274. **Pincus, S. E., D. C. Diamond, E. A. Emini, and E. Wimmer**. 1986. Guanidine-selected mutants of poliovirus: mapping of point mutations to polypeptide 2C. J. Virol. **57**:638-646.

275. **Pincus, S. E. and E. Wimmer**. 1986. Production of guanidine-resistant and -dependent poliovirus mutants from cloned cDNA: mutations in polypeptide 2C are directly responsible for altered guanidine sensitivity. J. Virol. **60**:793-796.

276. **Pogue, G. P., J. Hofmann, R. Duncan, J. M. Best, J. Etherington, R. D. Sontheimer, and H. L. Nakhasi**. 1996. Autoantigens interact with cis-acting elements of rubella virus RNA. J. Virol. **70**:6269-6277.

277. **Poole, T. L., C. Wang, R. A. Popp, L. N. Potgieter, A. Siddiqui, and M. S. Collett**. 1995. Pestivirus translation initiation occurs by internal ribosome entry. Virology **206**:750-754.

278. **Porter, A. G.** 1993. Picornavirus nonstructural proteins: emerging roles in virus replication and inhibition of host cell functions. J. Virol. **67**:6917-6921.

279. **Pyronnet, S., L. Pradayrol, and N. Sonenberg**. 2000. A cell cycle-dependent internal ribosome entry site. Mol. Cell **5**:607-616.

280. **Ramsingh, A., A. Hixson, B. Duceman, and J. Slack**. 1990. Evidence suggesting that virulence maps to the P1 region of the coxsackievirus B4 genome. J. Virol. **64**:3078-3081.

281. **Ray, P. S. and S. Das**. 2002. La autoantigen is required for the internal ribosome entry site-mediated translation of Coxsackievirus B3 RNA. Nucleic Acids Res. **30**:4500-4508.

282. **Reetoo, K. N., S. A. Osman, S. J. Illavia, C. L. Cameron-Wilson, J. E. Banatvala, and P. Muir**. 2000. Quantitative analysis of viral RNA kinetics in coxsackievirus B3-induced murine myocarditis: biphasic pattern of clearance following acute infection, with persistence of residual viral RNA throughout and beyond the inflammatory phase of disease. J. Gen. Virol. **81**:2755-2762.

283. **Reynolds, J. E., A. Kaminski, H. J. Kettinen, K. Grace, B. E. Clarke, A. R. Carroll, D. J. Rowlands, and R. J. Jackson**. 1995. Unique features of internal initiation of hepatitis C virus RNA translation. EMBO J. **14**:6010-6020.

284. **Rinehart, J. E., R. M. Gomez, and R. P. Roos**. 1997. Molecular determinants for virulence in coxsackievirus B1 infection. J. Virol. **71**:3986-3991.

285. **Roelvink, P. W., A. Lizonova, J. G. Lee, Y. Li, J. M. Bergelson, R. W. Finberg, D. E. Brough, I. Kovesdi, and T. J. Wickham**. 1998. The coxsackievirus-adenovirus receptor protein can function as a cellular attachment protein for adenovirus serotypes from subgroups A, C, D, E, and F. J. Virol. **72**:7909-7915.

286. **Rogers, G. W., Jr., N. J. Richter, and W. C. Merrick**. 1999. Biochemical and kinetic characterization of the RNA helicase activity of eukaryotic initiation factor 4A. J Biol. Chem. **274**:12236-12244.

287. **Rohll, J. B., N. Percy, R. Ley, D. J. Evans, J. W. Almond, and W. S. Barclay**. 1994. The 5'-untranslated regions of picornavirus RNAs contain independent functional domains essential for RNA replication and translation. J. Virol. **68**:4384-4391.

288. **Rombaut, B., A. Boeye, M. Ferguson, P. D. Minor, A. Mosser, and R. Rueckert**. 1990. Creation of an antigenic site in poliovirus type 1 by assembly of 14 S subunits. Virology **174**:305-307.

289. **Ryan, M. D. and M. Flint**. 1997. Virus-encoded proteinases of the picornavirus super-group. J. Gen. Virol. **78 ( Pt 4)**:699-723.

290. **Sachs, A. B., P. Sarnow, and M. W. Hentze**. 1997. Starting at the beginning, middle, and end: translation initiation in eukaryotes. Cell **89**:831-838.

291. **Saleh, L., R. C. Rust, R. Fullkrug, E. Beck, G. Bassili, K. Ochs, and M. Niepmann**. 2001. Functional interaction of translation initiation factor eIF4G with the foot-and-mouth disease virus internal ribosome entry site. J. Gen. Virol. **82**:757-763.

292. **Sandoval, I. V. and L. Carrasco**. 1997. Poliovirus infection and expression of the poliovirus protein 2B provoke the disassembly of the Golgi complex, the organelle target for the antipoliovirus drug Ro-090179. J. Virol. **71**:4679-4693.

293. **Saura, M., C. Zaragoza, A. McMillan, R. A. Quick, C. Hohenadl, J. M. Lowenstein, and C. J. Lowenstein**. 1999. An antiviral mechanism of nitric oxide: inhibition of a viral protease. Immunity. **10**:21-28.

294. **Schultz, D. E., C. C. Hardin, and S. M. Lemon**. 1996. Specific interaction of glyceraldehyde 3-phosphate dehydrogenase with the 5'-nontranslated RNA of hepatitis A virus. J. Biol. Chem. **271**:14134-14142.

295. **Seipelt, J., A. Guarne, E. Bergmann, M. James, W. Sommergruber, I. Fita, and T. Skern**. 1999. The structures of picornaviral proteinases. Virus Res. **62**:159-168.

296. **Shafren, D. R., R. C. Bates, M. V. Agrez, R. L. Herd, G. F. Burns, and R. D. Barry**. 1995. Coxsackieviruses B1, B3, and B5 use decay accelerating factor as a receptor for cell attachment. J. Virol. **69**:3873-3877.

297. **Shafren, D. R., D. J. Dorahy, S. J. Greive, G. F. Burns, and R. D. Barry**. 1997. Mouse cells expressing human intercellular adhesion molecule-1 are susceptible to infection by coxsackievirus A21. J. Virol. **71**:785-789.

298. **Shafren, D. R., D. J. Dorahy, R. A. Ingham, G. F. Burns, and R. D. Barry**. 1997. Coxsackievirus A21 binds to decay-accelerating factor but requires intercellular adhesion molecule 1 for cell entry. J. Virol. **71**:4736-4743.

299. **Shafren, D. R., D. T. Williams, and R. D. Barry**. 1997. A decay-accelerating factor-binding strain of coxsackievirus B3 requires the coxsackievirus-adenovirus receptor protein to mediate lytic infection of rhabdomyosarcoma cells. J. Virol. **71**:9844-9848.

300. **Shenoy-Scaria, A. M., J. Kwong, T. Fujita, M. W. Olszowy, A. S. Shaw, and D. M. Lublin**. 1992. Signal transduction through decay-accelerating factor. Interaction of glycosyl-phosphatidylinositol anchor and protein tyrosine kinases p56lck and p59fyn 1. J. Immunol. **149**:3535-3541.

301. **Shiroki, K., T. Isoyama, S. Kuge, T. Ishii, S. Ohmi, S. Hata, K. Suzuki, Y. Takasaki, and A. Nomoto**. 1999. Intracellular redistribution of truncated La protein produced by poliovirus 3Cpro-mediated cleavage. J. Virol. **73**:2193-2200.

302. **Sommergruber, W., G. Casari, F. Fessl, J. Seipelt, and T. Skern**. 1994. The 2A proteinase of human rhinovirus is a zinc containing enzyme. Virology **204**:815-818.

303. **Sonenberg, N.** 1988. Cap-binding proteins of eukaryotic messenger RNA: functions in initiation and control of translation. Prog. Nucleic Acid Res. Mol. Biol. **35**:173-207.

304. **Song, W. C., C. Deng, K. Raszmann, R. Moore, R. Newbold, J. A. McLachlan, and M. Negishi**. 1996. Mouse decay-accelerating factor: selective and tissue-specific

induction by estrogen of the gene encoding the glycosylphosphatidylinositol-anchored form. J. Immunol. **157**:4166-4172.

305. **Spicer, A. P., M. F. Seldin, and S. J. Gendler**. 1995. Molecular cloning and chromosomal localization of the mouse decay-accelerating factor genes. Duplicated genes encode glycosylphosphatidylinositol-anchored and transmembrane forms. J. Immunol. **155**:3079-3091.

306. **Sprengart, M. L., H. P. Fatscher, and E. Fuchs**. 1990. The initiation of translation in E. coli: apparent base pairing between the 16srRNA and downstream sequences of the mRNA. Nucleic Acids Res. **18**:1719-1723.

307. **Stanway, G. and T. Hyypia**. 1999. Parechoviruses. J. Virol. **73**:5249-5254.

308. **Stoneley, M., S. A. Chappell, C. L. Jopling, M. Dickens, M. MacFarlane, and A. E. Willis**. 2000. c-Myc protein synthesis is initiated from the internal ribosome entry segment during apoptosis. Mol. Cell Biol. **20**:1162-1169.

309. **Stoneley, M., T. Subkhankulova, J. P. Le Quesne, M. J. Coldwell, C. L. Jopling, G. J. Belsham, and A. E. Willis**. 2000. Analysis of the c-myc IRES; a potential role for cell-type specific trans-acting factors and the nuclear compartment. Nucleic Acids Res. **28**:687-694.

310. **Svitkin, Y. V., A. Gradi, H. Imataka, S. Morino, and N. Sonenberg**. 1999. Eukaryotic initiation factor 4GII (eIF4GII), but not eIF4GI, cleavage correlates with inhibition of host cell protein synthesis after human rhinovirus infection. J. Virol. **73**:3467-3472.

311. **Svitkin, Y. V., H. Imataka, K. Khaleghpour, A. Kahvejian, H. D. Liebig, and N. Sonenberg**. 2001. Poly(A)-binding protein interaction with eIF4G stimulates picornavirus IRES-dependent translation. RNA. **7**:1743-1752.

312. **Svitkin, Y. V., K. Meerovitch, H. S. Lee, J. N. Dholakia, D. J. Kenan, V. I. Agol, and N. Sonenberg**. 1994. Internal translation initiation on poliovirus RNA: further characterization of La function in poliovirus translation in vitro. J. Virol. **68**:1544-1550.

313. **Svitkin, Y. V., A. Pause, and N. Sonenberg**. 1994. La autoantigen alleviates translational repression by the 5' leader sequence of the human immunodeficiency virus type 1 mRNA. J. Virol. **68**:7001-7007.

314. **Takegami, T., R. J. Kuhn, C. W. Anderson, and E. Wimmer**. 1983. Membrane-dependent uridylylation of the genome-linked protein VPg of poliovirus. Proc. Natl. Acad. Sci. U. S. A **80**:7447-7451.

315. **Takegami, T., B. L. Semler, C. W. Anderson, and E. Wimmer**. 1983. Membrane fractions active in poliovirus RNA replication contain VPg precursor polypeptides. Virology **128**:33-47.

316. **Tesar, M. and O. Marquardt**. 1990. Foot-and-mouth disease virus protease 3C inhibits cellular transcription and mediates cleavage of histone H3. Virology **174**:364-374.

317. **Tobin, G. J., D. C. Young, and J. B. Flanegan**. 1989. Self-catalyzed linkage of poliovirus terminal protein VPg to poliovirus RNA. Cell **59**:511-519.

318. **Tomko, R. P., R. Xu, and L. Philipson**. 1997. hCar and mCAR: The human and mouse cellular receptors for subgroup C adenovirus and group B coxsackieviruses. Proc. Natl. Acad. Sci. U. S. A **94**:3356.

319. **Towbin, J. A., K. R. Bowles, and N. E. Bowles**. 1999. Etiologies of cardiomyopathy and heart failure. Nat. Med. **5**:266-267.

320. **Toyoda, H., N. Koide, M. Kamiyama, K. Tobita, K. Mizumoto, and N. Imura**. 1994. Host factors required for internal initiation of translation on poliovirus RNA. Arch. Virol. **138**:1-15.

321. **Tracy, S., V. Wiegand, B. McManus, C. Gauntt, M. Pallansch, M. Beck, and N. Chapman**. 1990. Molecular approaches to enteroviral diagnosis in idiopathic cardiomyopathy and myocarditis. J. Am. Coll. Cardiol. **15**:1688-1694.

322. **Trump, B. F., I. K. Berezesky, S. H. Chang, and P. C. Phelps**. 1997. The pathways of cell death: oncosis, apoptosis, and necrosis. Toxicol. Pathol. **25**:82-88.

323. **Tu, Z., N. M. Chapman, G. Hufnagel, S. Tracy, J. R. Romero, W. H. Barry, L. Zhao, K. Currey, and B. Shapiro**. 1995. The cardiovirulent phenotype of coxsackievirus B3 is determined at a single site in the genomic 5' nontranslated region. J. Virol. **69**:4607-4618.

324. **Ukimura, A., H. Deguchi, Y. Kitaura, S. Fujioka, M. Hirasawa, K. Kawamura, and K. Hirai**. 1997. Intracellular viral localization in murine coxsackievirus-B3 myocarditis. Ultrastructural study by electron microscopic in situ hybridization. Am. J. Pathol. **150**:2061-2074.

325. **Vagner, S., M. C. Gensac, A. Maret, F. Bayard, F. Amalric, H. Prats, and A. C. Prats**. 1995. Alternative translation of human fibroblast growth factor 2 mRNA occurs by internal entry of ribosomes. Mol. Cell Biol. **15**:35-44.

326. **van Kuppeveld, F. J., J. M. Galama, J. Zoll, and W. J. Melchers**. 1995. Genetic analysis of a hydrophobic domain of coxsackie B3 virus protein 2B: a moderate degree of hydrophobicity is required for a cis-acting function in viral RNA synthesis. J. Virol. **69**:7782-7790.

327. **van Kuppeveld, F. J., P. J. van den Hurk, d. van, V, J. M. Galama, and W. J. Melchers**. 1997. Chimeric coxsackie B3 virus genomes that express hybrid coxsackievirus-poliovirus 2B proteins: functional dissection of structural domains involved in RNA replication. J. Gen. Virol. **78 ( Pt 8)**:1833-1840.

328. **Waggoner, S. and P. Sarnow**. 1998. Viral ribonucleoprotein complex formation and nucleolar-cytoplasmic relocalization of nucleolin in poliovirus-infected cells. J. Virol. **72**:6699-6709.

329. **Walter, B. L., J. H. Nguyen, E. Ehrenfeld, and B. L. Semler**. 1999. Differential utilization of poly(rC) binding protein 2 in translation directed by picornavirus IRES elements. RNA. **5**:1570-1585.

330. **Wang, A., P. K. Cheung, H. Zhang, C. M. Carthy, L. Bohunek, J. E. Wilson, B. M. McManus, and D. Yang**. 2001. Specific inhibition of coxsackievirus B3 translation and replication by phosphorothioate antisense oligodeoxynucleotides. Antimicrob. Agents Chemother. **45**:1043-1052.

331. **Wang, Q. M.** 1999. Protease inhibitors as potential antiviral agents for the treatment of picornaviral infections. Prog. Drug Res. **52**:197-219.

332. **Wang, X. and J. M. Bergelson**. 1999. Coxsackievirus and adenovirus receptor cytoplasmic and transmembrane domains are not essential for coxsackievirus and adenovirus infection. J. Virol. **73**:2559-2562.

333. **Wee, L., P. Liu, L. Penn, J. W. Butany, P. R. McLaughlin, M. J. Sole, and C. C. Liew**. 1992. Persistence of viral genome into late stages of murine myocarditis detected by polymerase chain reaction. Circulation **86**:1605-1614.

334. **Wells, S. E., P. W. Hillner, R. D. Vale, and A. B. Sachs**. 1998. Circularization of mRNA by eukaryotic translational initiation factors. Mol. Cell **2**:140.

335. **West, M. J., M. Stoneley, and A. E. Willis**. 1998. Translational induction of the c-myc oncogene via activation of the FRAP/TOR signalling pathway. Oncogene **17**:769-780.

336. **Why, H. J., B. T. Meany, P. J. Richardson, E. G. Olsen, N. E. Bowles, L. Cunningham, C. A. Freeke, and L. C. Archard**. 1994. Clinical and prognostic significance of detection of enteroviral RNA in the myocardium of patients with myocarditis or dilated cardiomyopathy. Circulation **89**:2582-2589.

337. **Wilusz, J. and J. D. Keene**. 1984. Interactions of plus and minus strand leader RNAs of the New Jersey serotype of vesicular stomatitis virus with the cellular La protein. Virology **135**:65-73.

338. **Wilusz, J., M. G. Kurilla, and J. D. Keene**. 1983. A host protein (La) binds to a unique species of minus-sense leader RNA during replication of vesicular stomatitis virus. Proc. Natl. Acad. Sci. U. S. A **80**:5827-5831.

339. **Wimmer, E., C. U. Hellen, and X. Cao**. 1993. Genetics of poliovirus. Annu. Rev. Genet. **27**:353-436.

340. **Woodruff, J. F.** 1980. Viral myocarditis. A review. Am. J. Pathol. **101**:425-484.

341. **Wyatt, H. V.** 1979. Poliomyelitis in the fetus and the newborn. A comment on the new understanding of the pathogenesis. Clin. Pediatr. (Phila) **18**:33-38.

342. **Xu, R. and R. L. Crowell**. 1996. Expression and distribution of the receptors for coxsackievirus B3 during fetal development of the Balb/c mouse and of their brain cells in culture. Virus Res. **46**:157-170.

343. **Xu, R., J. G. Mohanty, and R. L. Crowell**. 1995. Receptor proteins on newborn Balb/c mouse brain cells for coxsackievirus B3 are immunologically distinct from those on HeLa cells. Virus Res. **35**:323-340.

344. **Yalamanchili, P., U. Datta, and A. Dasgupta**. 1997. Inhibition of host cell transcription by poliovirus: cleavage of transcription factor CREB by poliovirus-encoded protease 3Cpro. J. Virol. **71**:1220-1226.

345. **Yalamanchili, P., K. Harris, E. Wimmer, and A. Dasgupta**. 1996. Inhibition of basal transcription by poliovirus: a virus- encoded protease (3Cpro) inhibits formation of TBP-TATA box complex in vitro. J. Virol. **70**:2922-2929.

346. **Yalamanchili, P., K. Weidman, and A. Dasgupta**. 1997. Cleavage of transcriptional activator Oct-1 by poliovirus encoded protease 3Cpro. Virology **239**:176-185.

347. **Yanagawa, B., O. B. Spiller, J. Choy, H. Luo, P. Cheung, H. M. Zhang, I. G. Goodfellow, D. J. Evans, A. Suarez, D. Yang, and B. M. McManus**. 2003. Coxsackievirus B3-associated myocardial pathology and viral load reduced by recombinant soluble human decay-accelerating factor in mice. Lab Invest **83**:75-85.

348. **Yang, D., P. Cheung, Y. Sun, J. Yuan, H. Zhang, C. M. Carthy, D. R. Anderson, L. Bohunek, J. E. Wilson, and B. M. McManus**. 2003. A shine-dalgarno-like sequence mediates in vitro ribosomal internal entry and subsequent scanning for translation initiation of coxsackievirus B3 RNA. Virology **305**:31-43.

349. **Yang, D., J. E. Wilson, D. R. Anderson, L. Bohunek, C. Cordeiro, R. Kandolf, and B. M. McManus**. 1997. In vitro mutational and inhibitory analysis of the cis-acting translational elements within the 5' untranslated region of coxsackievirus B3: potential targets for antiviral action of antisense oligomers. Virology **228**:63-73.

350. **Yang, D., J. Yu, Z. Luo, C. M. Carthy, J. E. Wilson, Z. Liu, and B. M. McManus**. 1999. Viral myocarditis: identification of five differentially expressed genes in coxsackievirus B3-infected mouse heart. Circ. Res. **84**:704-712.

351. Yang, DC., Zhang, M. H, Cheung, P., Yuan, J., Yanagawa, B., Chau, D., Luo, H., Wilson, J., and McManus, B. Coxsackieviru B3 protease 2A and 3C induce cell death through apoptosis. 21st ASV annual meeting, University of Kentucky, USA . 2002.
Ref Type: Abstract

352. **Yi, M., D. E. Schultz, and S. M. Lemon**. 2000. Functional significance of the interaction of hepatitis A virus RNA with glyceraldehyde 3-phosphate dehydrogenase

(GAPDH): opposing effects of GAPDH and polypyrimidine tract binding protein on internal ribosome entry site function. J. Virol. **74**:6459-6468.

353. **Yu, S. F. and R. E. Lloyd**. 1991. Identification of essential amino acid residues in the functional activity of poliovirus 2A protease. Virology **182**:615-625.

354. **Zaragoza, C., C. J. Ocampo, M. Saura, A. McMillan, and C. J. Lowenstein**. 1997. Nitric oxide inhibition of coxsackievirus replication in vitro. J. Clin. Invest **100**:1760-1767.

355. **Zhang, H. M., P. Cheung, B. Yanagawa, B. M. McManus, and D. C. Yang**. 2003. BNips: A group of pro-apoptotic proteins in the Bcl-2 family. Apoptosis. **8**:229-236.

356. **Zhang, H. M., B. Yanagawa, P. Cheung, H. Luo, J. Yuan, D. Chau, A. Wang, L. Bohunek, J. E. Wilson, B. M. McManus, and D. Yang**. 2002. Nip21 gene expression reduces coxsackievirus B3 replication by promoting apoptotic cell death via a mitochondria-dependent pathway. Circ. Res. **90**:1251-1258.

357. **Zhang, H. M., J. Yuan, P. Cheung, H. Luo, B. Yanagawa, D. Chau, N. S. Tozy, B. Wong, J. Zhang, J. E. Wilson, B. M. McManus, and D. Yang**. 2003. Over-expression of interferon-gamma -inducible GTPase inhibits coxsackievirus B3-induced apoptosis Through the activation of the PI3-K/Akt pathway and inhibition of viral replication. J. Biol. Chem.

358. **Zhang, H. Y., G. E. Yousef, L. Cunningham, N. W. Blake, X. Ouyang, T. A. Bayston, R. Kandolf, and L. C. Archard**. 1993. Attenuation of a reactivated cardiovirulent coxsackievirus B3: The 5'-nontranslated region does not contain major attenuation determinants. J. Med. Virol. **41**:129-137.

359. **Ziegler, E., A. M. Borman, F. G. Deliat, H. D. Liebig, D. Jugovic, K. M. Kean, T. Skern, and E. Kuechler**. 1995. Picornavirus 2A proteinase-mediated stimulation of internal initiation of translation is dependent on enzymatic activity and the cleavage products of cellular proteins. Virology **213**:549-557.

360. **Ziegler, E., A. M. Borman, R. Kirchweger, T. Skern, and K. M. Kean**. 1995. Foot-and-mouth disease virus Lb proteinase can stimulate rhinovirus and enterovirus IRES-driven translation and cleave several proteins of cellular and viral origin. J. Virol. **69**:3465-3474.